TESLA - COLLABORATION

Transparencies from **the TTF Coupler Meeting, Saclay, October 19-20, 1998**

Editor: S. Chel, C. Travier

CEA Saclay

November 1998, TESLA 98-28

TTF coupler meeting
Saclay, October 19-20, 1998

Editor : S. Chel, C. Travier
CEA Saclay

Agenda

Monday 19th October

9 :30	Opening - scope of the meeting	B. Aune (Saclay)
9 :45	Status of input coupler TTF2 and TTF3	W.D. Möller(DESY)
10 :30	coffee break	
11 :00	Variable coupling by stub tuner	B. Dwersteg (DESY)
11 :20	open discussion : should the coupler be tunable ?	
12 :30	Lunch	
14 :00	New cryostat design. Implication on coupler design	C. Pagani (Milan)
14 :45	open discussion : should the coupler be rigid ?	
15 :30	Status of WG coupler activity at DESY	V. Kaljuzhny (DESY)
16 :00	open discussion :	
	where is our present understanding of limits of existing couplers, new ideas ?	
	TM010 mode waveguide window	A. Zavadtsev (DESY)
16 :45	Coffee break	
17 :00	Status of superstructure studies	J. Sekutowicz (DESY)
17 :20	open discussion : specification for superstructure coupler	
	WG vs. Coax, ...	
	fabrication experience, brazing, ceramics	
	Cu coating, ...	
	Coaxial coupler for superstructures	D. Proch (DESY)

Tuesday, October 20th

9 :30	Saclay/Orsay test bench	M.Desmons (Saclay)
10 :00	Test results	C. Travier (Saclay)
11 :00	Coffee break	
11 :30	Traveling wave window design	C. Travier (Saclay)
12 :00	Polarized transition	P. Lepercq (LAL)
12 :30	Lunch	
14 :00	Coupler test bench visit	
15 :00	Multipactor simulation	D. Proch (DESY)
15 :20	TiN coating studies	S. Chel (Saclay)
15 :40	open discussion	
	-what will be done next at DESY, Saclay ?	
	-subject of possible cooperation	
	-important items not under investigation	
	-are there outside activities of interest for us ?	
18 : 00	end of meeting	

Meeting conclusions

This coupler workshop held in Saclay on October 19th and 20th was meant to have an update on the work concerning input power couplers related to the TESLA project. The last such review was done more than 2 years ago at DESY (may 29th and 30th, TESLA note 96-09). The presentations included a status of TTF couplers production, processing and operation status, several talks about future coupler related to new cryostat design and superstructures. The status of the Saclay/Orsay coupler development was also presented including test results and design of new components. A large space was given to open discussions concerning questions like : should the coupler be tunable, rigid, waveguide or coax, ... ?

1) Main results

The high power test of TTF2 couplers have shown that this coupler can sustain high power (up to 1.8 MW), and that the multipactor can be processed. The TTF3 coupler has the same cold part as the TTF2 coupler but has a different waveguide to coax transition that includes a cylindrical window, allowing to suppress the expensive warm waveguide window. Experiment and simulations have shown that the present design of cylindrical window is multipactor free.

The recent test of the $\lambda/2$ window at Saclay indicates that this window can also sustain high power (1 MW, limited by klystron power), both at room temperature and 80 K. Here too, the window is multipactor free.

2) Tunability and flexibility of the coupler

An important discussion was conducted on the question of the necessity of a tunable coupler. The different reasons that could demand for a change in the Qext were reviewed :

- cavity fabrication errors : it is estimated from present experience that this necessitates at most a tunability of $\pm$ 25%, that can be obtained with the waveguide three stubs transformer.
- change of current or gradient : the fixed Qext leads to an over power consumption if the current or gradient are not the nominal ones. This is OK since the machine is supposed to operate at nominal parameters.
- bad cavities : if a cavity becomes much worse then the others in the cryomodule, it will be detuned.

From these considerations, it can be concluded that the tunability of the coupler itself is not necessary. A stub tuner placed at the rectangular, warm waveguide will adjust phase and coupling at the cost of some overvoltage in the coax-line. However, it would be important to conduct a detailed reflection on the implication of this choice.
It was then noted that for the present cryostat and coupler design (TTF3) going to fixed Qext coupler will not make much savings. One can only save the tuning system, since the bellows are necessary for compensating thermal shrinkage.

With the new cryostat design for TTF module 5 and higher, the coupler do not need to compensate for this thermal shrinkage, since the cavities can slide on their support. In this

case, the coupler can be rigid. Its connection to the cryostat should however provide for a $\pm$ 2 mm error to take into account mechanical tolerances. This can be obtained on the warm part of the coupler at the level of its connection to the cryostat, so that the RF conductor can be completely free of bellows. The other condition to allow such scheme, is to find a way to limit the forces applied to the coupler (or the cavity coupler port) by the cavities or helium pipes bellows to 5 kg.

3) Remaining questions

Several questions were discussed but remained unanswered with present knowledge.

- should the superstructure include 4 or 8 cavities, and consequently, what is the necessary power demanded to the coupler. It was however shown, that the peak power demanded for HPP in the case of 4*7 cells cavities superstructure, can be reduced to 1.6 times the peak power needed for one 9 cell cavity by detuning the sub-units, and not 3.1 as for a tuned superstructure.
- should the coupler for superstructure be coax or waveguide ?
- are cavity electrons and radiation really damageable for coupler window in the case of TESLA ? Do we need to shield the window surface against direct sight from the beam ?
- though with our present operating experience, there are no convincing argument to give up the 2 window design, someone raised the question whether two was really necessary ?
- for the processing of the coupler, several questions were raised and would need more investigation :
  - is there an effect of temperature ?
  - what is the level of tolerable activity ? (at present it seems that Saclay allows much more activity than DESY during processing. It would be good to compare with more detail the processing procedures, interlock levels, etc..
  - effect of bias ?
  - what are the gas desorbed during processing ? It would be good to do the RGA ? It was reported by DESY that storing coupler parts in plastic bags increases multipactor of these components.
  - can we use gas discharge during processing ?

4) Collaboration

In conclusion, it was decided that a tighter collaboration should take place between Saclay/Orsay and DESY. This collaboration would include :

- regular meetings (the next one was fixed in April 1999 at DESY)
- visits of individuals to participate to the work (e.g. processing) in the other lab
- establish a common database (e.g. ceramic properties)
- TiN coating
- multipacting calculations (e.g. the $\lambda/2$ window will be calculated with Helsinki code)

List of participants

DESY

Bernhard Dwersteg
Serguei Iariguine
Valentin Kaljuzhny
Lutz Lilje
Jerzy Lorkiewicz
Cornelius Martens
Wolf-Dietrich Moeller
Dieter Proch
Jacek Sekutowicz
Alexandre Zavadtsev

INFN Milan

Carlo Pagani

LAL Orsay

Jean-Claude Bourdon
Terry Garvey
Laurent Grandsire
Bernard Jacquemard
Joel Leduff
Pierre Lepercq
Guy Macé
Jean Marini
Roger Panvier

IPN Orsay

Thomas Junquera
Jean Lesrel

CEA Saclay

Bernard Aune
Stéphane Chel
Michel Desmons
Michel Juillard

STATUS OF INPUT COUPLER TTF 2 AND TTF 3

WOLF - DIETRICH MÖLLER
DESY, Hamburg

W.D. Möller, TTF coupler meeting, Saclay, October 19-20, 1998

STATUS OF INPUT COUPLER TTF 2 AND TTF 3

TTF COUPLER MEETING
SACLAY, OCT. 19- 20, 1998

WOLF - DIETRICH MÖLLER
DESY, Hamburg

1. Specification for TTF Couplers
2. The Prototype Couplers FNAL 1 and TTF 1
3. Problems of the Prototypes and Requirements for Improvement
4. Design TTF 2 and TTF 3
5. Test Results of the TTF 2 Coupler on Test Stand
6. Problems with the TTF 2 Coupler
7. Production Status

1. Specification for TTF Couplers

-1.3 GHz
-pulsed operation, 1.33 msec pulse length, 800 μsec flat top with beam
-maximal operation power: 210 kW
-peak power capability up to 1 MW for High Power Processing in situ
at reduced pulse length (500 μsec) and repetition rate (1 Hz)
-Qext between 10^6 and 10^7
-sufficient diagnostic system for interlock and monitoring
-transverse flexibility up to 15 mm
-two windows for clean cavity assembly and safety reasons

2. The Prototype Couplers FNAL 1 and TTF 1

2.1. Prototype production:

FNAL delivered 15 complete couplers:
-5 couplers assembled at module 1
-2 couplers assembled at booth capture cavities at DESY and FNAL
8 couplers under assembly at module 2

DESY produced 3 couplers TTF 1:
-all assembled at module 1

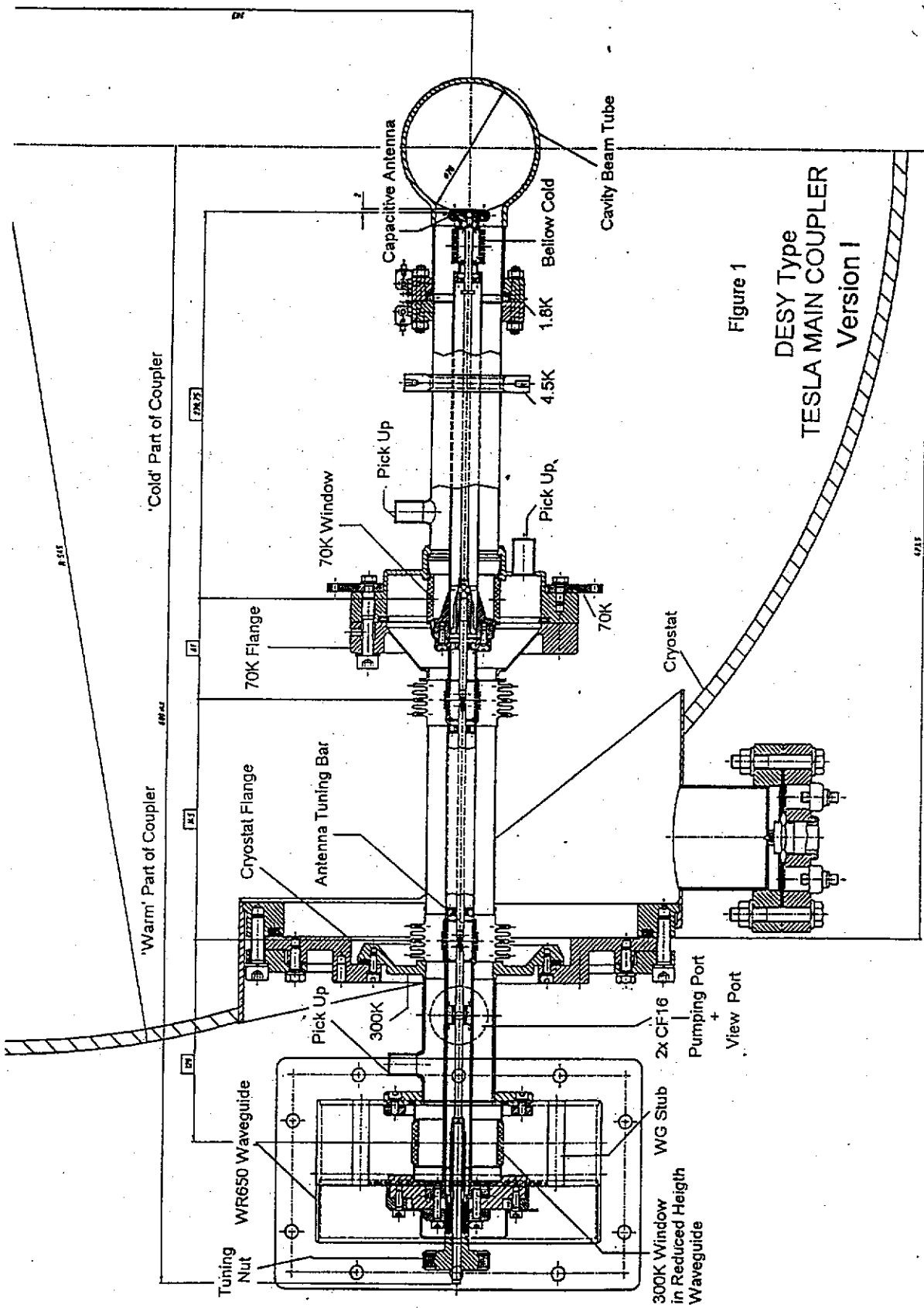
Figure 1
DESY Type
TESLA MAIN COUPLER
Version I
'Cold' Part of Coupler
'Warm' Part of Coupler
Capacitive Antenna
Cavity Beam Tube
Below Cold
1.8K
4.5K
Pick Up
Pick Up
70K Window
70K
70K Flange
Cryostat
Cryostat Flange
Antenna Tuning Bar
Pick Up
300K
2x CF16
Pumping Port
+
View Port
WR650 Waveguide
WG Stub
Tuning
Nut
300K Window
in Reduced Heigth
Waveguide

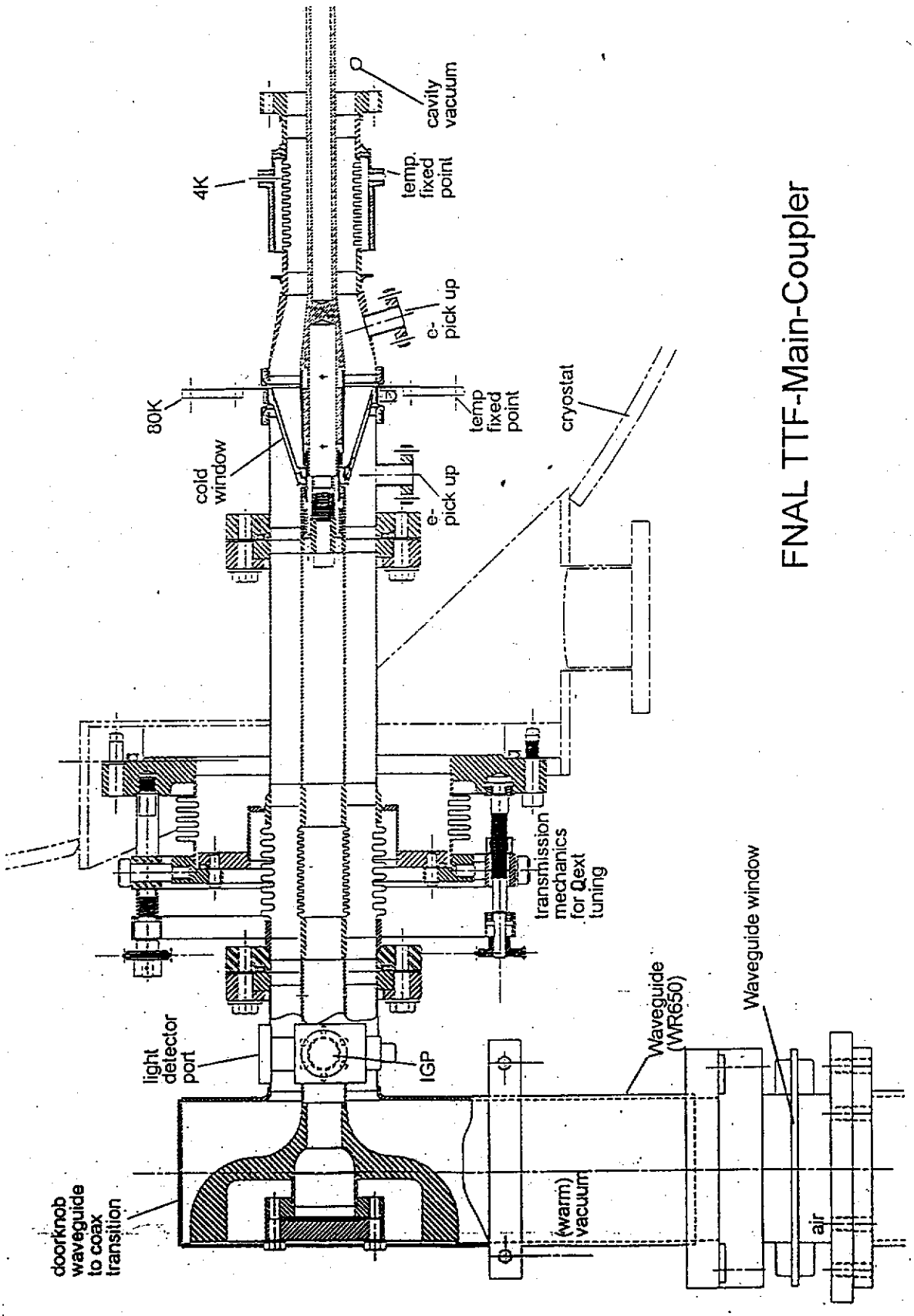

W.D. Möller, TTF coupler meeting, Saclay, October 19-20, 1998

2.2. Diagnostic system:

-pressure at cavity and coupler vacuum
-several electron pick ups in both vacua
-photomultiplier at coupler vacuum
-photodiode on air side of RT window
-Pt 1000 temperature sensor on 70 K window
-infrared temperature sensor for RT window

2.3. Assembly:

-cold coupler (70K window) onto the cavity in clean room class 10
-warm parts 'dirty' in the TTF hall

2.4. Processing Procedure:

Cycle the power from low to high values, starting with short pulses (20 μsec). After reaching the specified power value double the pulse length and start again at low power.

Processing was necessary for each operation type like cavity off / on resonance,coupler warm / cold and after each assembly / disassembly.

The processing time was different for each individual coupler: 3 days to more than a week, typical less than 1 week.

2.5. Processing of Prototypes:

on coupler test stand:
2 FNAL couplers and 3 TTF 1 couplers

on horizontal test cryostat together with the cavity:
7 cavities of module 1, (schedule problems)
5 cavities of module 2 (schedule problems)
(due to late delivery of the warm FNAL couplers parts the tests where performed with the same warm coax, wave guide and wave guide window)

on module 1:
all FNAL warm coupler parts were processed the first time on the module (max. power = 400 kW)

on module 2:
not jet ready assembled

2.6. Experience:

All couplers reached the specified values (TTF 1 after assembling of a redesigned warm window).
Operation on capture cavities and module 1 was without problems (nearly no interlock events due to the couplers). Limitations only by the cavity performances.
High Power Processing in situ could be done only up to 400 kW per coupler at the module.

3. Problems of Prototypes and Requirements for Improvement

3.1. Problems:

production:

-copper plating on bellows and weldings (FNAL)
-gray clouds on the ceramics after brazing
-Philips wave guide window not more available, new other wave guide windows are very expensive

assembly:

-sufficient cleaning of the cold part was very difficult
-warm parts assembly on module is 'dirty'
-couplers loose partially the processing effect

processing:

-two main multipacting levels were seen during processing (~60 kW and ~120 kW)
-strong outgassing during processing
-processing takes too long time

3.2. Requirements for Improvement

Design:

-consideration of actual results of multipacting analysis
-introduction of a high voltage bias for multipacting suppression
-less bellows
-new RT window

Production:

-easy production, manufacturing technologies
-simplify coupler design
-reduction of price
-ultimate cleanliness of all part during and after production
-more control of materials especially ceramic
-reduction of Hydrogen by furnacing all parts at 1100 °C
-careful checking of copper coating

Handling

-easy to clean parts for class 10 cavity assembly
-store under N_2 to keep the processing effect

4. Design of TTF 2 and TTF 3

TTF 2:

-70 Ohm cold coax line to reduce multipacting
-high voltage bias system to reduce multipacting
-less bellows than TTF 1 and FNAL 1
-Qext tuning is a mixture of DESY and FNAL design
-bigger pumping port on wave guide
-less brazing, more welding
-cold window like DESY design, but improved geometry of ceramic (according to multipacting calculations)
-wave guide doorknob transition like FNAL coupler, but with Kapton isolation for high voltage in the vacuum
-new wave guide window is designed at DESY

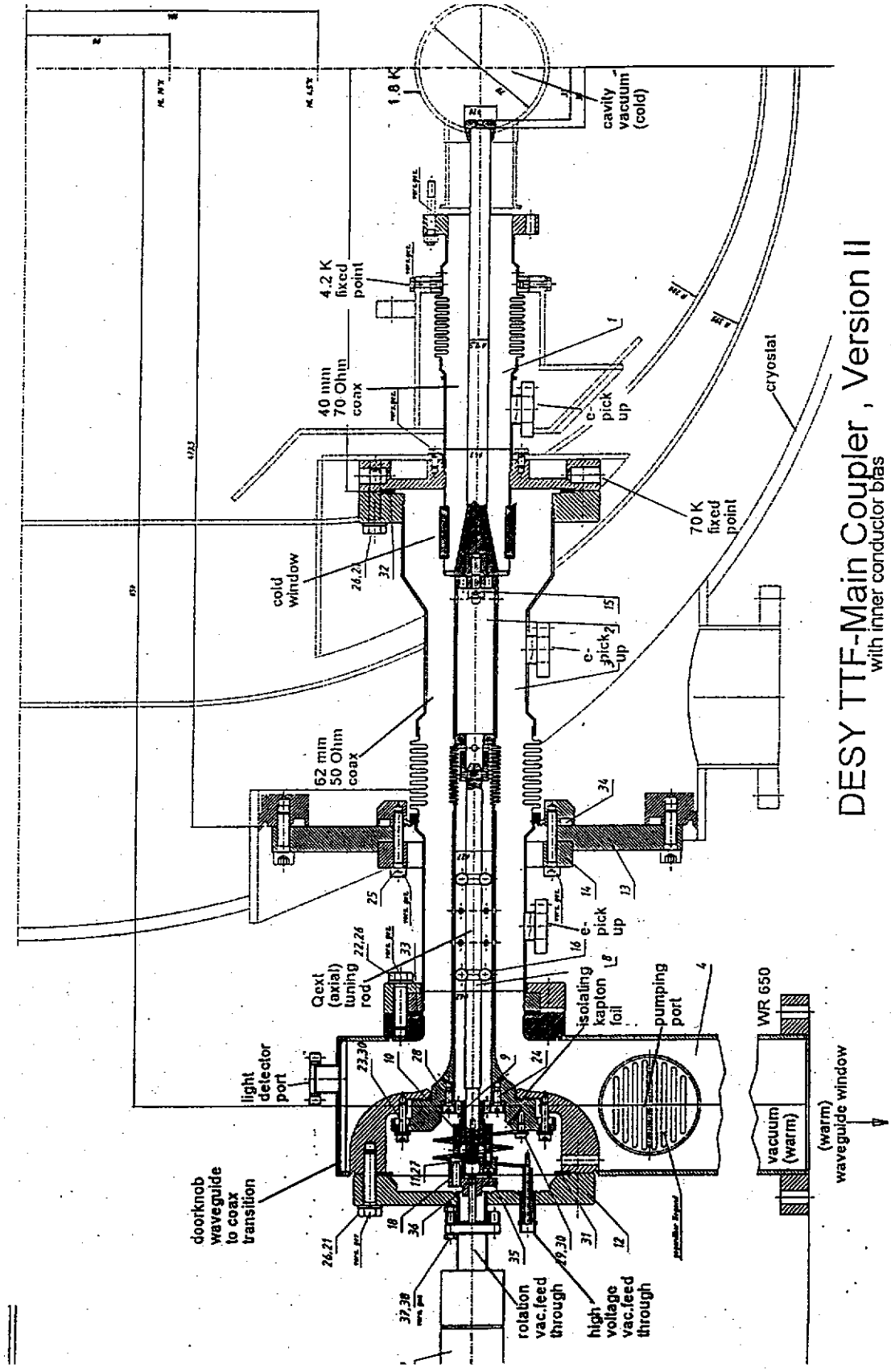

W.D. Möller, TTF coupler meeting, Saclay, October 19-20, 1998

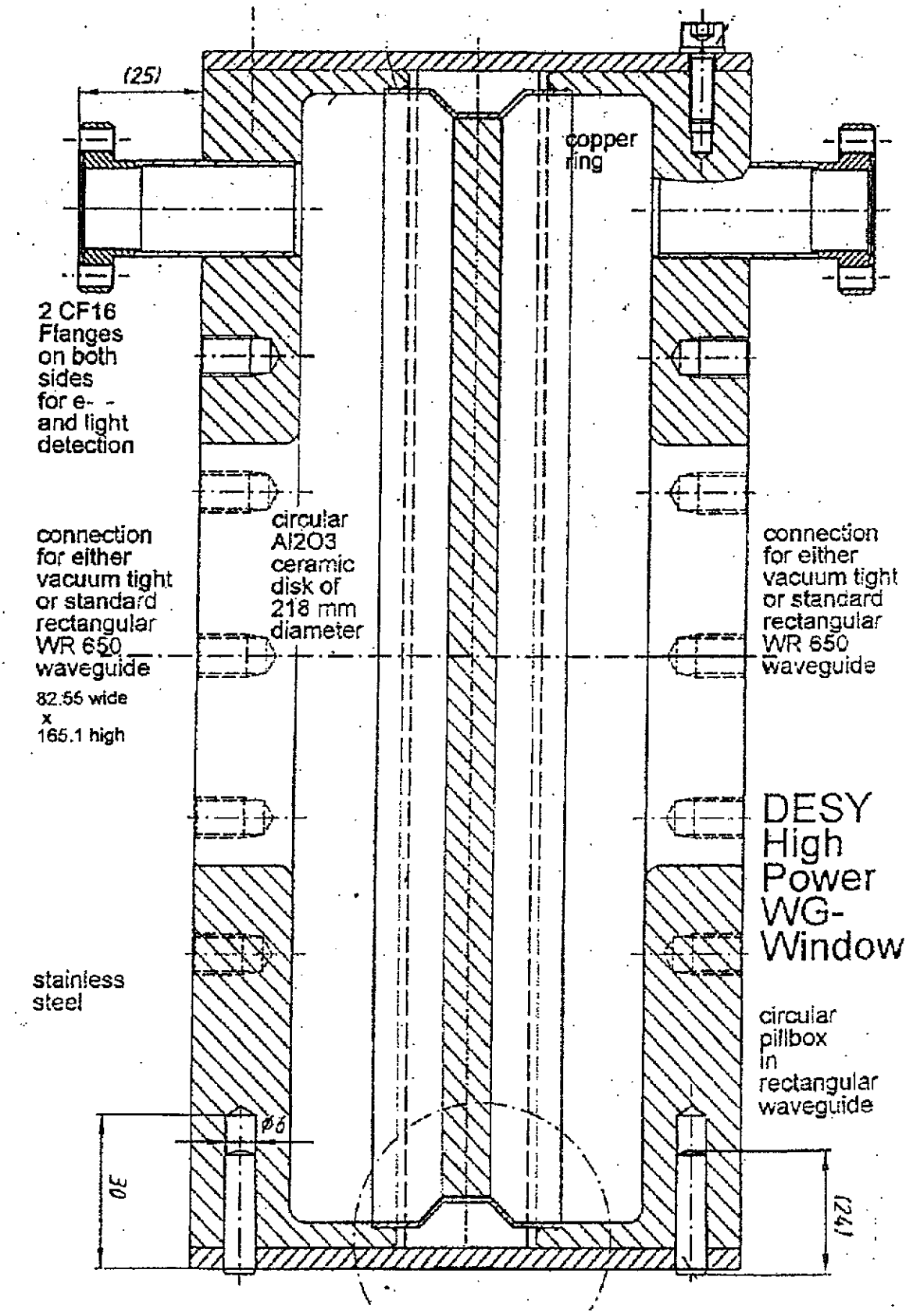
(25)
copper ring
2 CF16 Flanges on both sides for e- - and light detection
connection for either vacuum tight or standard rectangular WR 650 waveguide
82.55 wide
x
165.1 high
circular Al2O3 ceramic disk of 218 mm diameter
connection for either vacuum tight or standard rectangular WR 650 waveguide
DESY High Power WG-Window
stainless steel
circular pillbox in rectangular waveguide
ø6
30
(241)

TTF 3:

-cold part identical to TTF 2
-cylindrical window in the coax to wave guide transition
(no wave guide window, no vacuum wave guide)
-no doorknob but half high wave guide
-Kapton insulation not in vacuum and easy to replace
-Qext tuning drive not in the vacuum, no rotary feedthrough (like TTF 1)

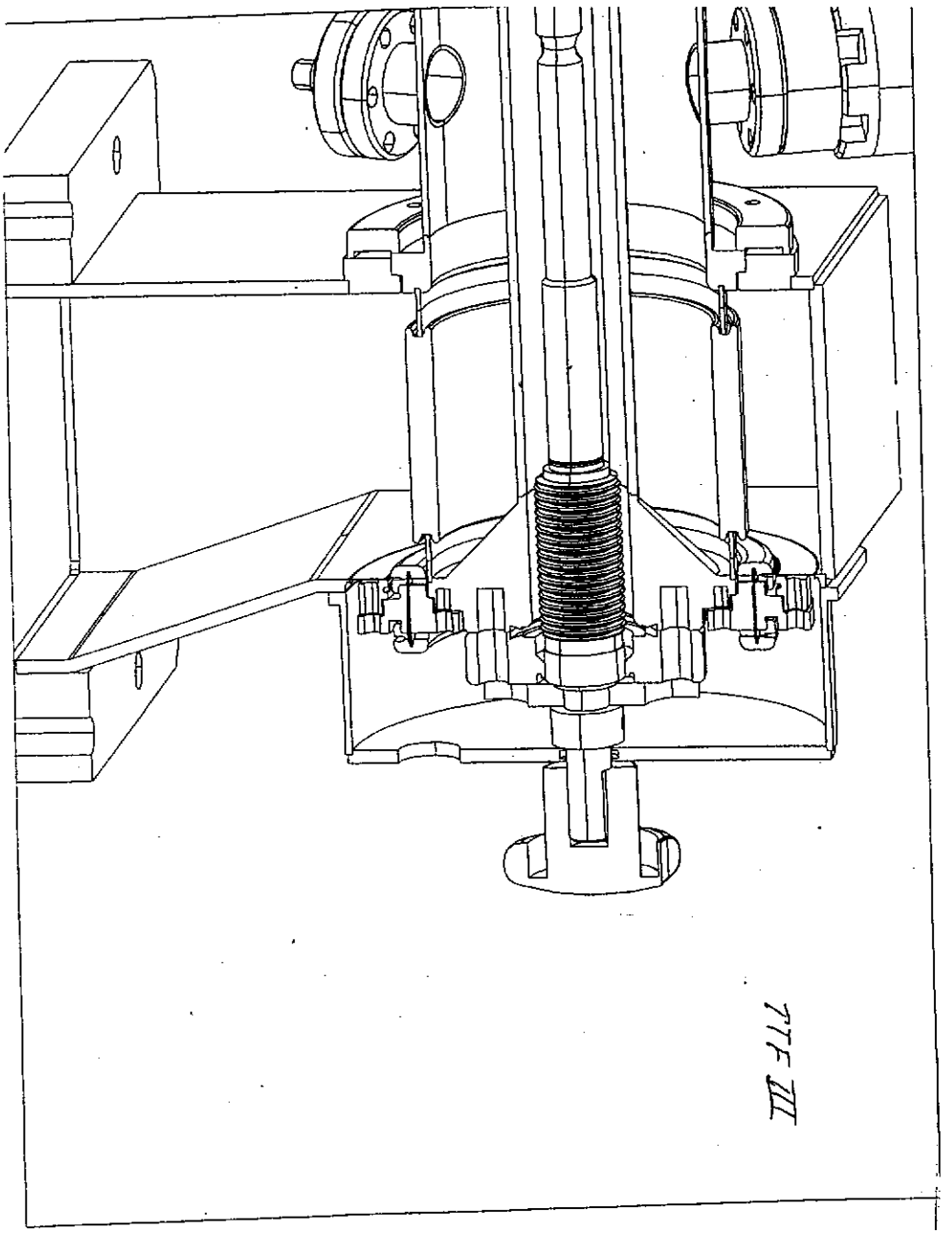

5. Test Results of TTF 2 Coupler

Two tests are performed so far:

First test of a simplified version of a TTF 2 coupler without bellows and copper coating on the outer coax

-*Without high voltage 1* MW at 1.3 μsec pulse length in traveling wave was achieved
-No limitation visible
-Multipacting could be processed
-*With high voltage of* 0.5... 3 kV, new mutipacting levels appear
-New processing was necessary and successful

Problems:
-bad antenna match led to 30% power reflection
-Kapton foil in vacuum needed heating (200°C, 1 day) otherwise bad vacuum

Second test of the TTF 2 coupler

-*Without high voltage* 1.8 MW at 1.3 μsec pulse length in traveling wave was achieved
-No limitation visible
-Multipacting could be processed
-Same problems *with high voltage* than at the first test !
-one waveguide window (Philips) was slightly sputtered with metal (50 G0hm/cm^2), but no unnormal heating was seen on the ceramic

6. Problems with TTF 2

Production:
-bellow dimensions not as specified
-copper plating shows 'black spots' after furnacing
-ceramic has to be careful shaded against the evaporation during e-beam welding
-handling causes often scratches and dirt marks on copper plated RF surfaces

Cleaning:
-cold part not easy to clean according to class 10 assembly
-parts are not jet stored under N_2

Operating:
-Kapton outgassing in coupler vacuum
-High voltage bias was not successful on test stand (probably due to the teststand wave guide transition)
-Qext tuning not easy; too much friction in the thread in vacuum
-high outgassing during processing
-new waveguide windows not jet tested under vacuum

7. Production Status

Pos.	Type	Warm Parts	Cold Parts	Status	Remarks
1	TTF 2	*5 + 5*	*5 + 5*	under RF test	Module 3
2	TTF 2	10	10	under fabrication	Module 4
3	TTF 3	10		under fabrication	Handling and RF tests, next module
4	TTF 3		10	order requested	Complete Pos. 3
5	TTF 3	10	10	order requested	Next modules
6	WG window	20		under fabrication	Module 3

Waveguide Transformers for Superconducting Cavities

B.Dwersteg

DESY

B.Dwersteg, TTF coupler meeting, Saclay, October, 19-20, 1998

B.Dwersteg

(File WGTraf)

Waveguide Transformers for Superconducting Cavities

Waveguide transformers can be used for matching superconducting cavities to a high power transmitter or waveguide system and at the same time providing phase adjustment for proper phasing of the bunch passage.
This is done at the DESY/HERA cavities since many years.

The price for matching by a waveguide transformer and not by a variable input coupler consists of standing waves between waveguide transformer and cavity.

Pure phase shifting can be done without producing standing waves.

This is why in the following it will be tried to show a more or less complete analysis of only the standing wave phenomena occuring at different operation modes of cavities, couplers and waveguide transformers.

A waveguide transformer as discussed here consists simply of three cylindrical metallic plungers which are inserted at the middle of the wide side into a rectangular waveguide.

Waveguide Transformer -- Deduction of S-Parameters
Example : Load match , ßLoad=3

Dw121098

a) Resistance transformer of ratio ßT=3 with matched lines on both sides

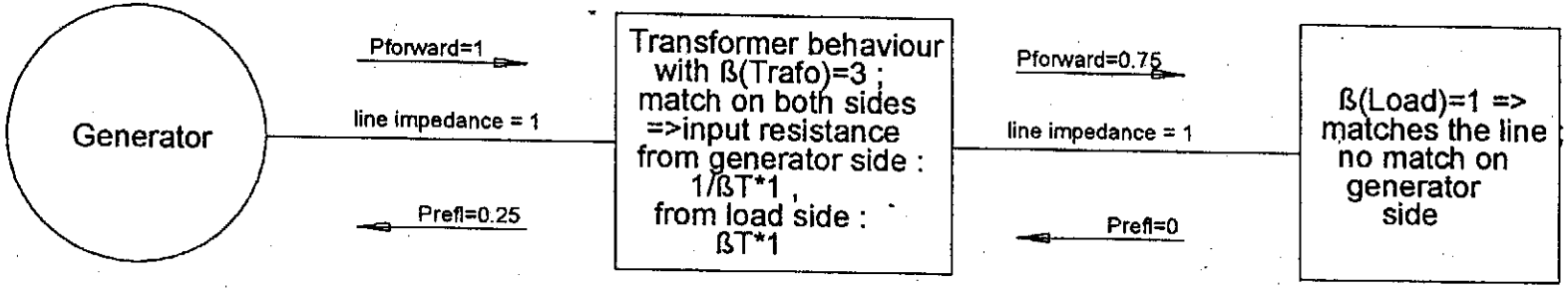

The pure transformer input resistance on the generater side leads to
S11=(1/ßT-1)/(1/ßT+1) => /S12/=(1-S11^2)^(0.5) => S12^2=0.75

The pure transformer input resistance from the load side leads to
S22= (ßT-1)/(ßT+1) => /S21/=(1-S22^2)^(0.5) => S21^2=0.75

=> S11=-0.5 ; S12=0.75^(0.5) ; S22=+0.5 ; S21=S12 ; (These are valid S-Parameters of a purely real Matrix.) -> S11^2=S22^2=0.25

b) Matching a load of ßLoad=3 to the generator by the transformer

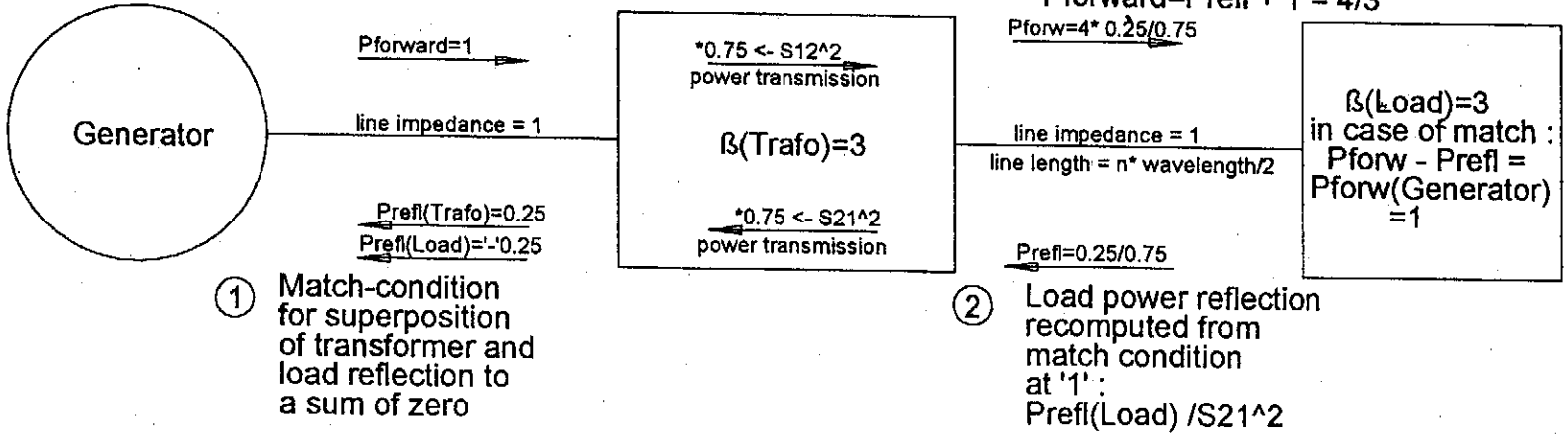

The comments in sequence of 1 , 2 , 3 explain what the transformer does. The deduced power flow values correspond to results from S-matrix computations.

Waveguide transformer with transformation factor ßT=2 + Scaling laws at real load (Cavity on resonance)

DW151098

(all voltages normalized to transmitter/generator forward voltage (ßT->Resistance transformation)
Power computation : Generator forward power*Voltage^2)

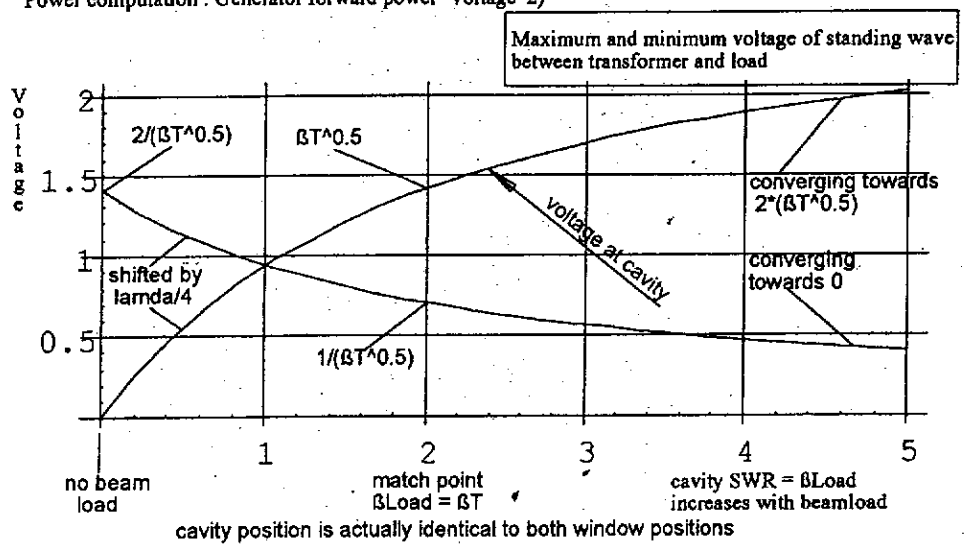

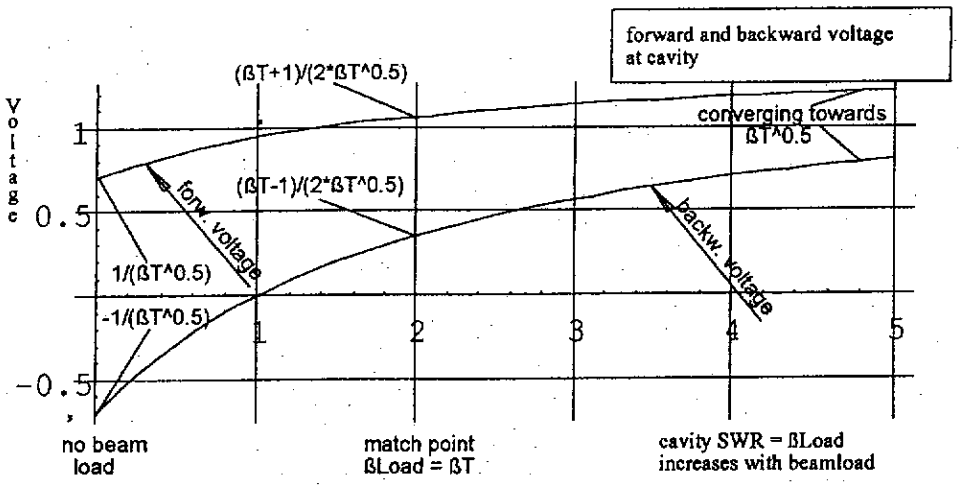

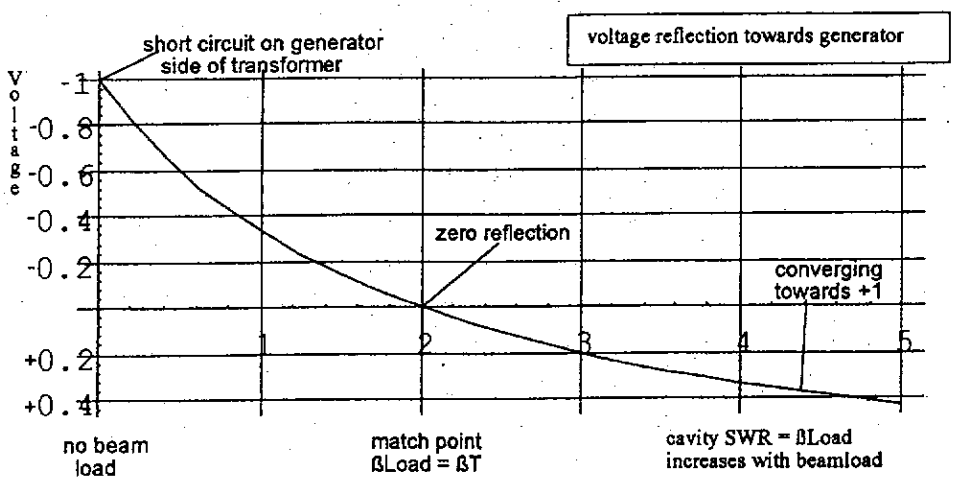

B.Dwersteg, TTF coupler meeting, Saclay, October, 19-20, 1998

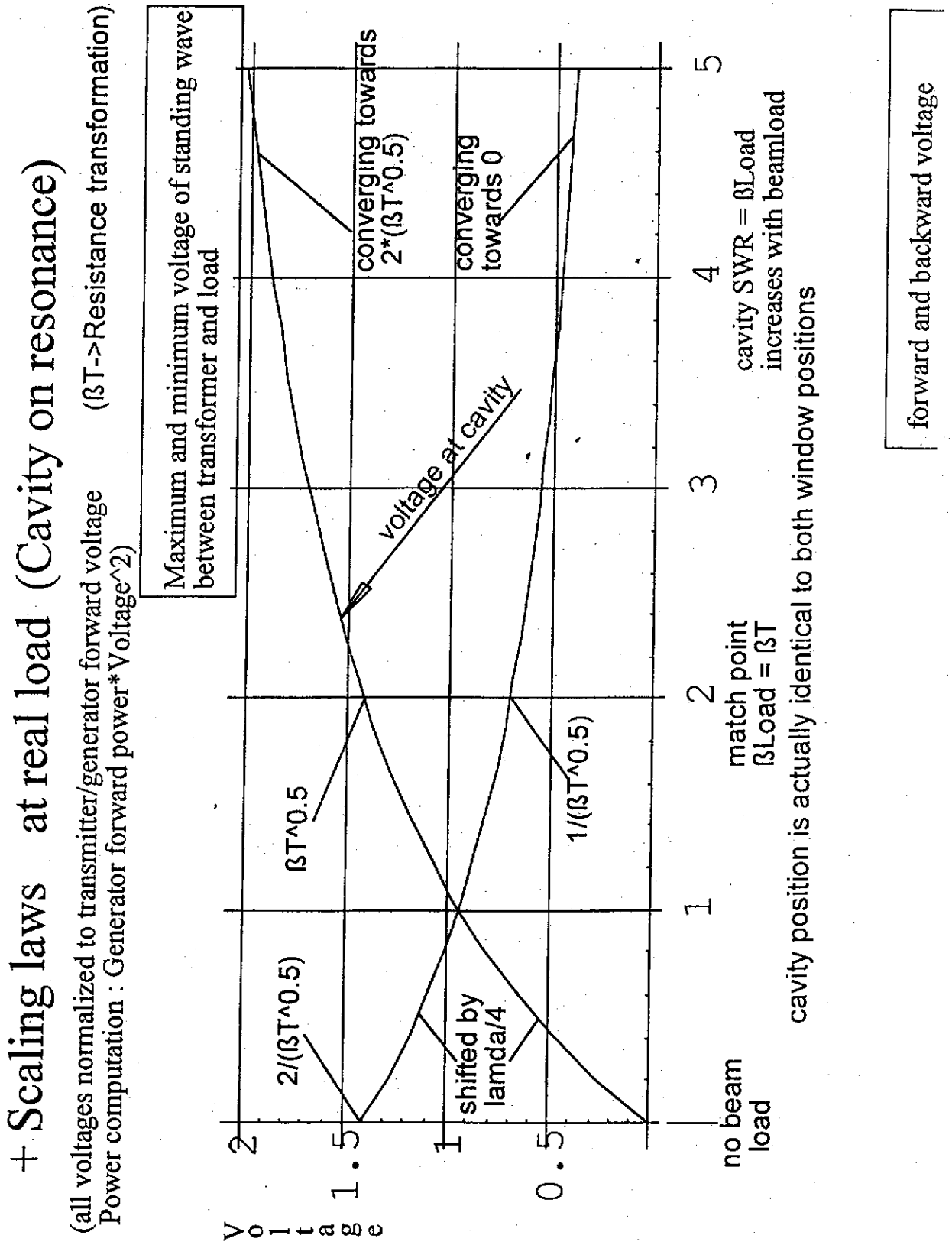
+ Scaling laws at real load (Cavity on resonance)
(all voltages normalized to transmitter/generator forward voltage
Power computation : Generator forward power*Voltage^2)
(ßT->Resistance transformation)
Maximum and minimum voltage of standing wave between transformer and load
converging towards 2*(ßT^0.5)
converging towards 0
voltage at cavity
ßT^0.5
2/(ßT^0.5)
shifted by lamda/4
1/(ßT^0.5)
Voltage
2
1.5
1
0.5
1
2
3
4
5
no beam load
match point ßLoad = ßT
cavity SWR = ßLoad increases with beamload
cavity position is actually identical to both window positions
forward and backward voltage

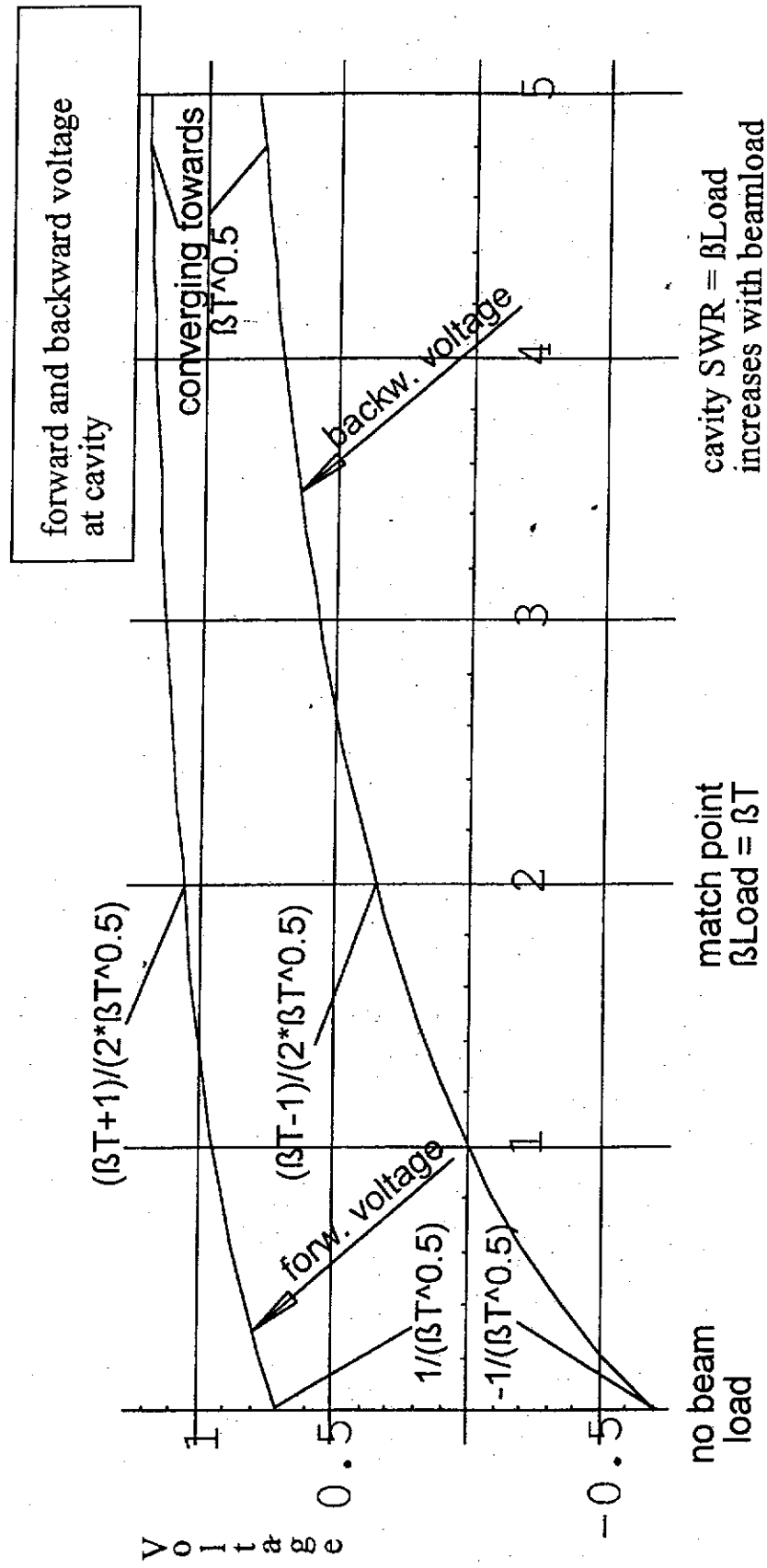

B.Dwersteg, TTF coupler meeting, Saclay, October, 19-20, 1998

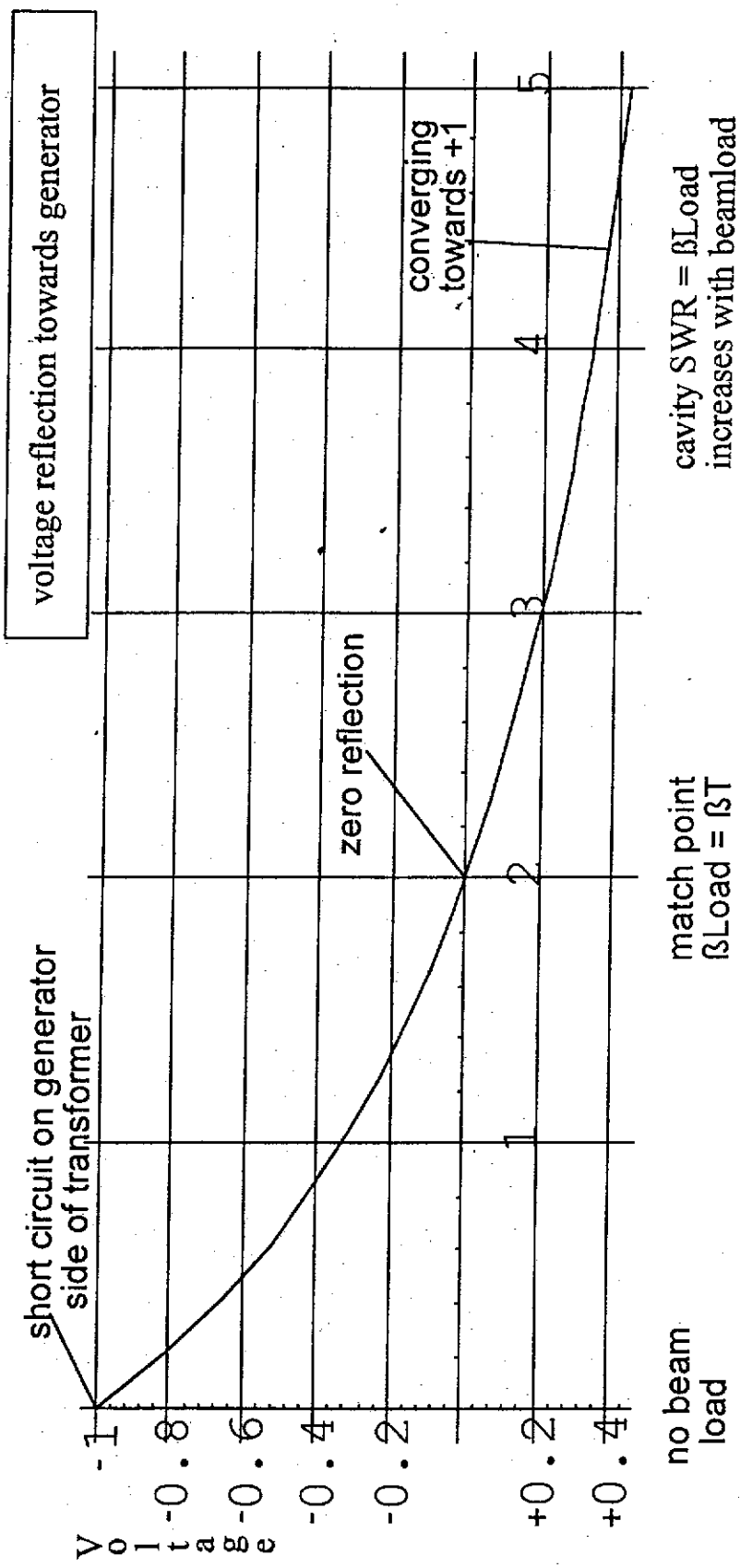

B.Dwersteg, TTF coupler meeting, Saclay, October, 19-20, 1998

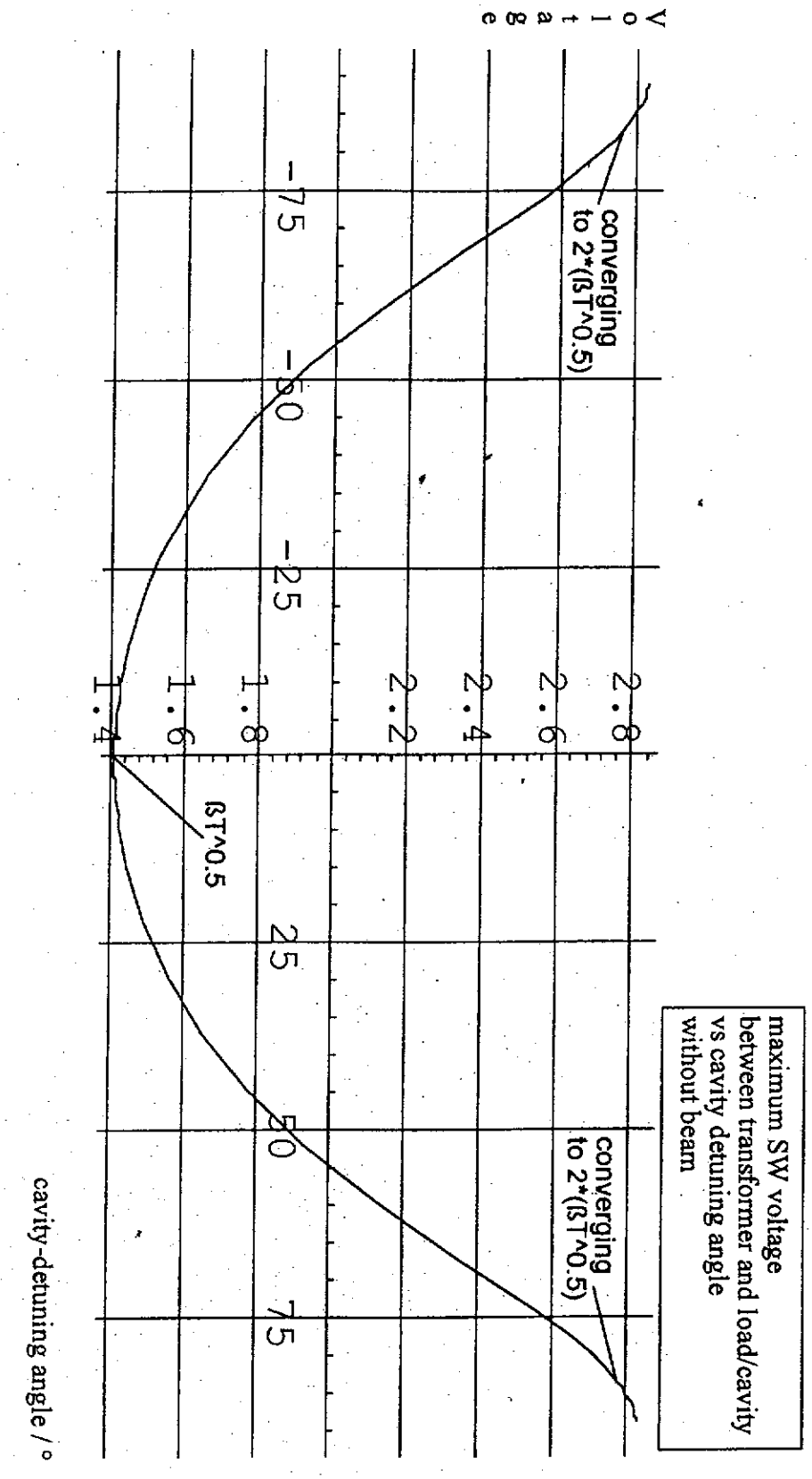

B.Dwersteg, TTF coupler meeting, Saclay, October, 19-20, 1998

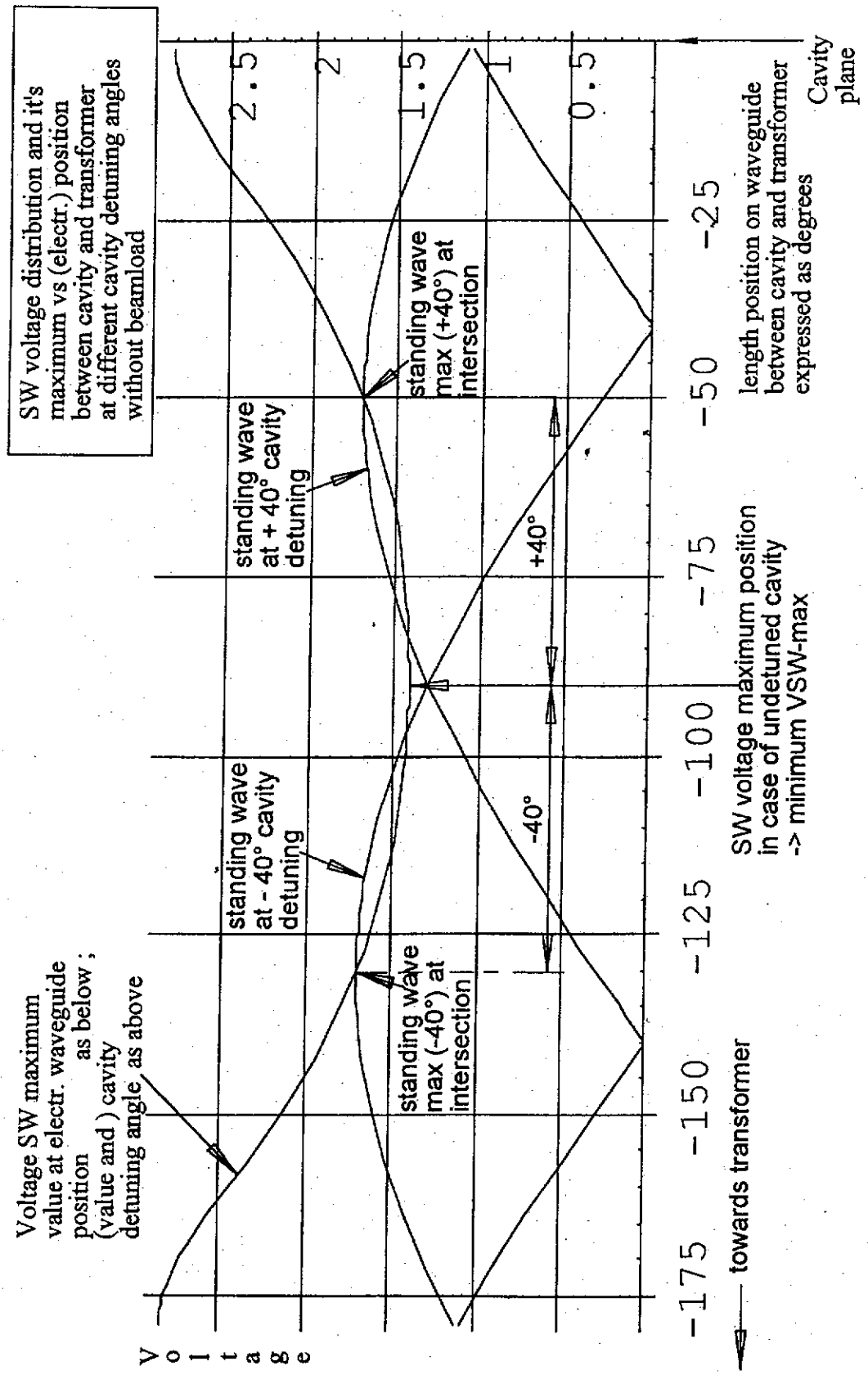

The above ' maximum SW voltage ' curve describes the maximum voltage values enveloppe of all standing waves achievable by detuning the cavity between +90° and -90°. The degree distance of the SW maxima from the -90° (lamda/4) position is the cavity detuning angle at the same time.

Waveguide transformer with ßT=0.2 .. 5 with cavity load matched , unloaded , detuned

DW161098

(Voltages normalized to generator forward voltage
Power computation : Generator forward power*Voltage^2)

Maximum and minimum voltage of standing wave between cavity and transformer in matched case

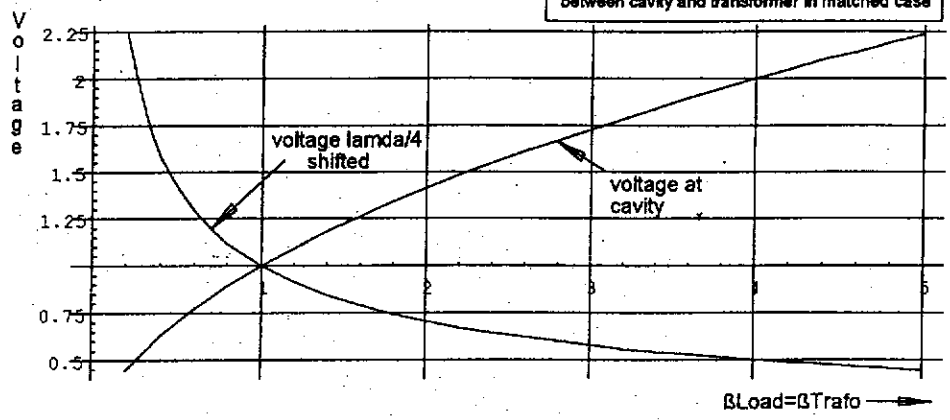

The cavity voltage doubles in case of totally detuned cavity and reduces to 0 in case of no beamload.
The voltage lamda/4 before the cavity reduces to 0 at total detuning and doubles in case of no beamload.
(Total detuning -> open circuit , no beamload -> short circuit)

Forward and backward wave at the cavity in always matched case vs ßT=ßL

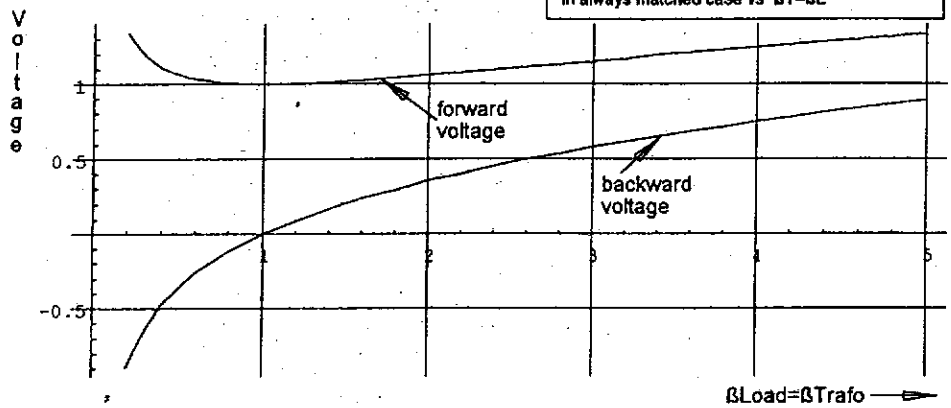

Forward and backward wave at the cavity in case of total detuning and in case of no beam

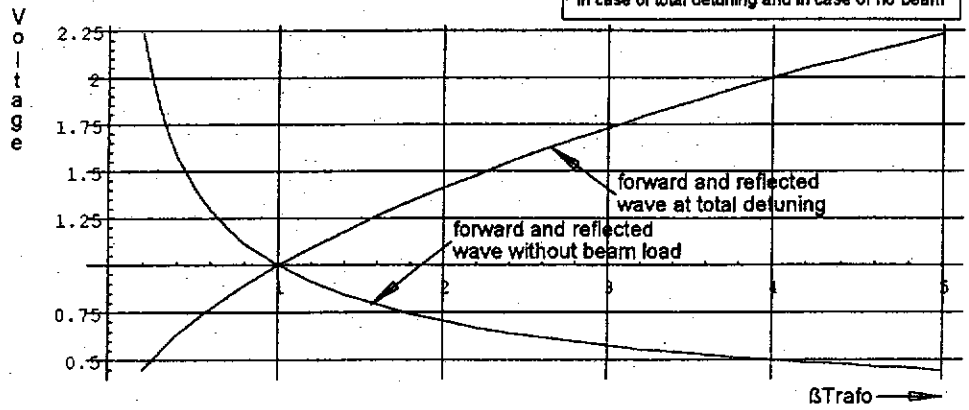

(Total detuning -> open circuit , no beamload -> short circuit)

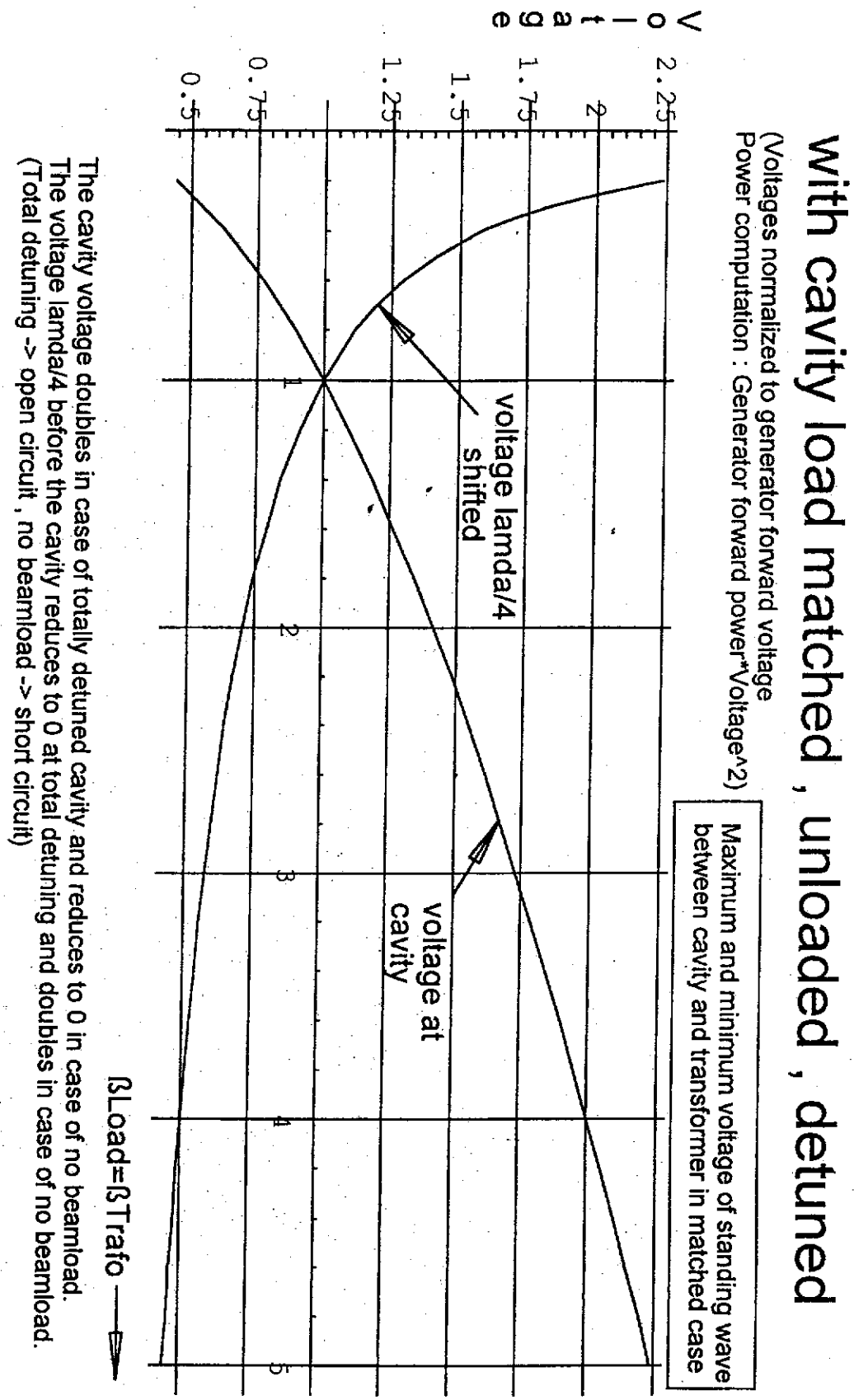

B.Dwersteg, TTF coupler meeting, Saclay, October, 19-20, 1998

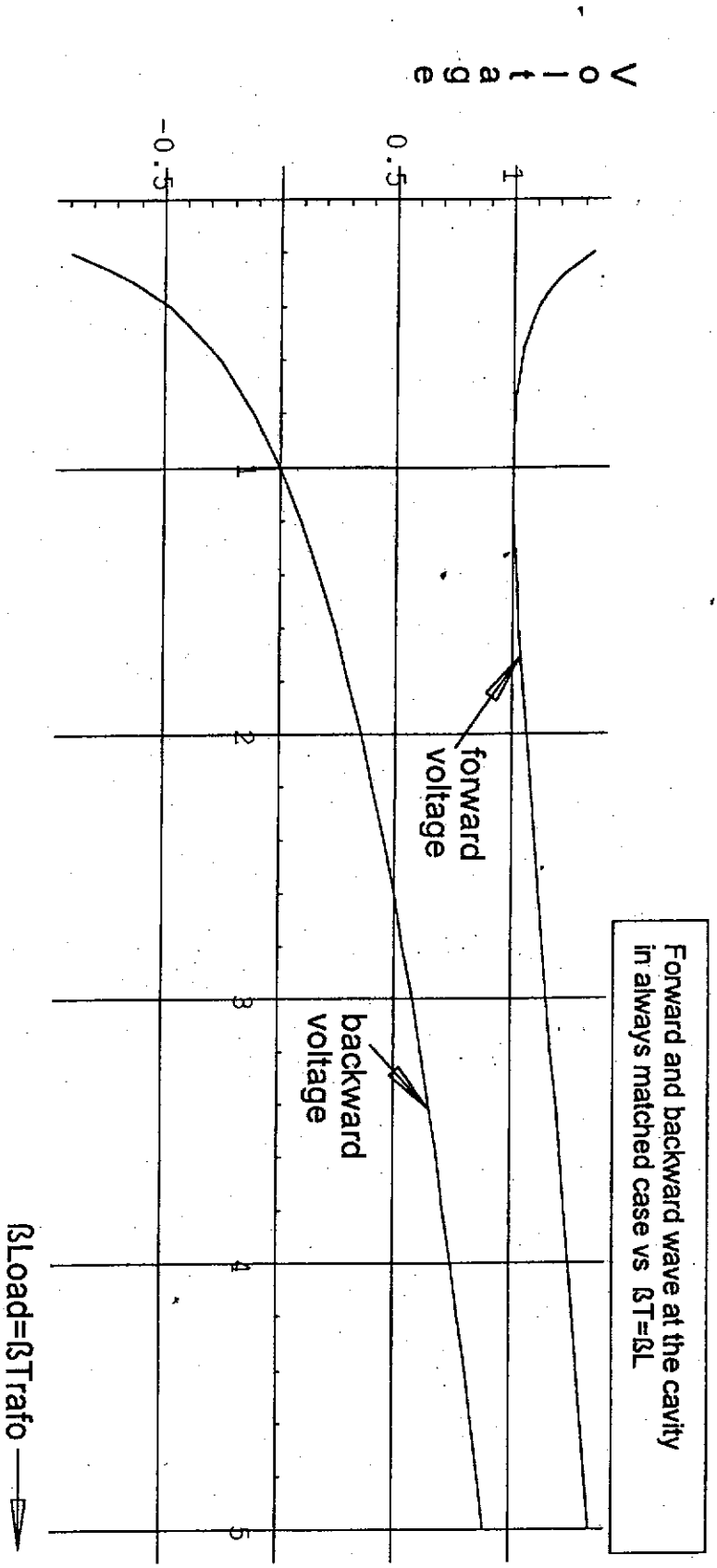

B.Dwersteg, TTF coupler meeting, Saclay, October, 19-20, 1998

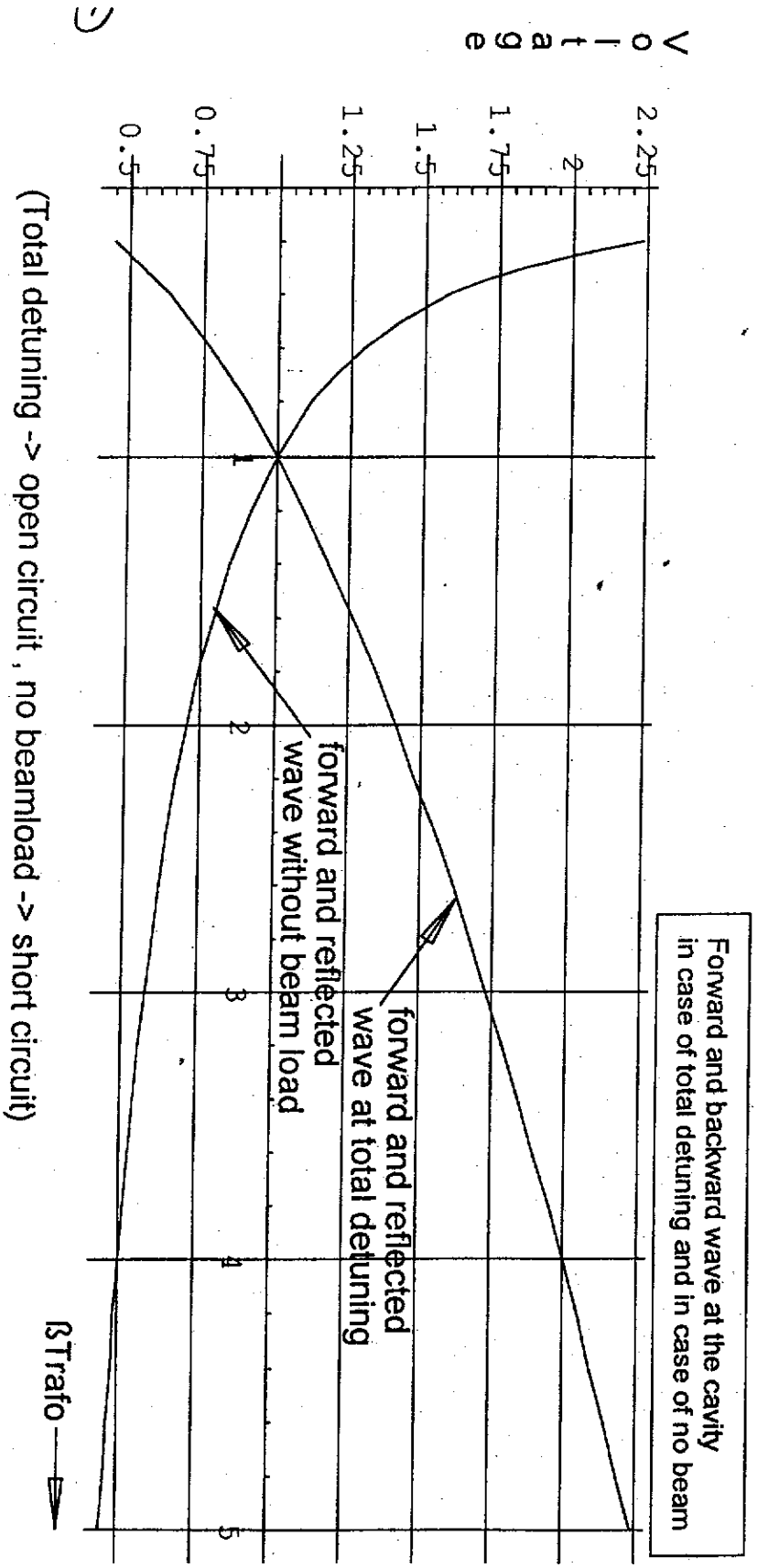

B.Dwersteg, TTF coupler meeting, Saclay, October, 19-20, 1998

New Cryostat Development

Carlo Pagani
INFN Milan

C. Pagani, TTF coupler meeting, Saclay, October, 19-20, 1998

Coupler workshop
Saclay, October 19-20, 1998

New Cryostat Development

Carlo Pagani

Three Cryostat Generations

* **Cryomodule #1** Prototype - Expensive

  - **Shields connected with** screws and **cooled by** copper braids
  - **Difficult to** align - **New Assembling Tools**

* **Cryomodules # 2 & # 3** 50% Cost Cutting

  - **Shields connected and cooled by "finger welding"**
  - **Improved** alignment and tolerances

* **Cryomodules # 4 to # 8** Thinking to TESLA **500**

  - Reduced **size of the Vacuum Vessel**
  - **Compatible with** "rigid coupler" **and** "Super-structures"
  - Stiffer **against external forces acting on the HeGRP**

Carlo Pagani
INFN Milano - **LASA**

3rd Generation Cryostat

Thinking to TESLA 500

- Reduce the Cross Section **and use a** standard "pipeline" tube
  - Redistribute the internal components
  - Reduce the distances to the minimum

- **Compatible with** "rigid coupler" **and** "Superstructures"
  - Position of the active elements longitudinally free

- Improve the connection **of the active elements to the HeGRP**

  - Poor in the present scheme

- Reduce alignment sensitivity **to the forces on the HeGRP edges**

  - Move the external posts closer to the edges

- **Further** simplify the assembling procedure
  - Simplify coupler cones and braids
  - Reduce by a factor two the shield components

- **System thought for** mass production cost cutting
  - Tolerances reduced to the required ones
  - Simpler components and standard tubes wherever possible

Carlo Pagani
INFN Milano - **LASA**

3rd Generation Cryostat

Cross section on Coupler

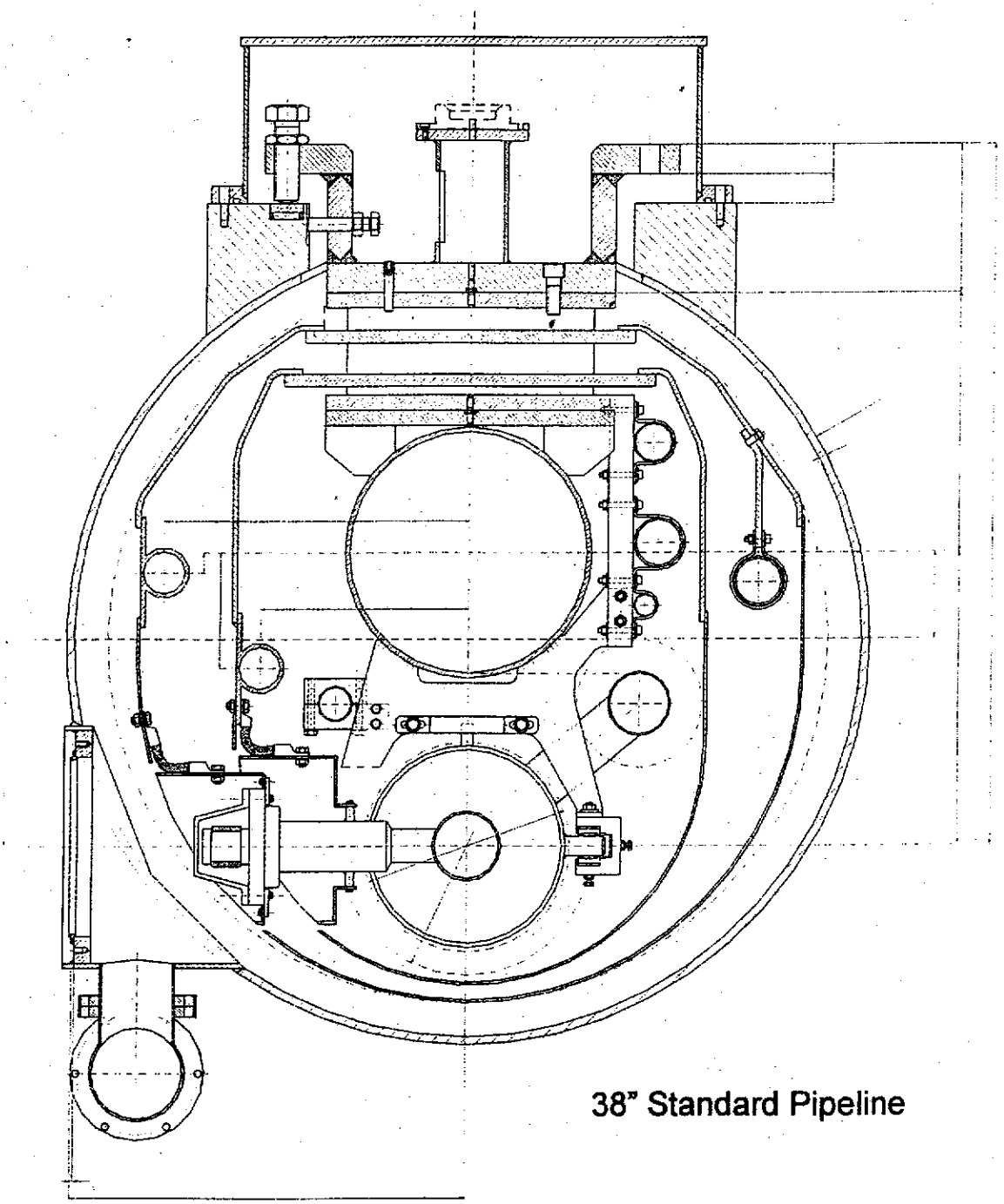

Carlo Pagani
INFN Milano - LASA

3rd Generation Cryostat

Cross section on Cavity - Sliding fixture detail

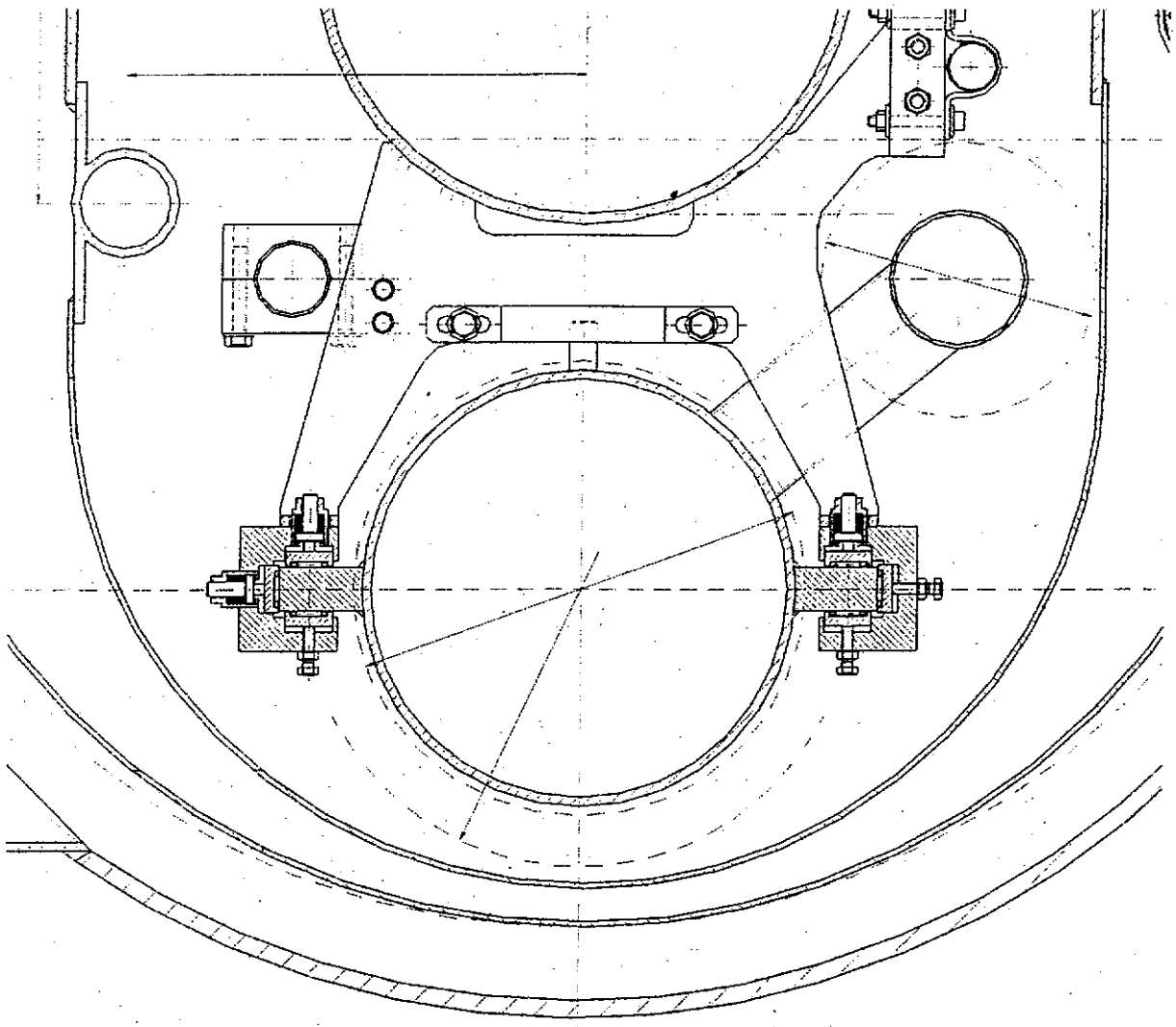

Carlo Pagani
INFN Milano - LASA

3rd Generation Cryostat

Cross section on Cavity - Sliding fixture detail

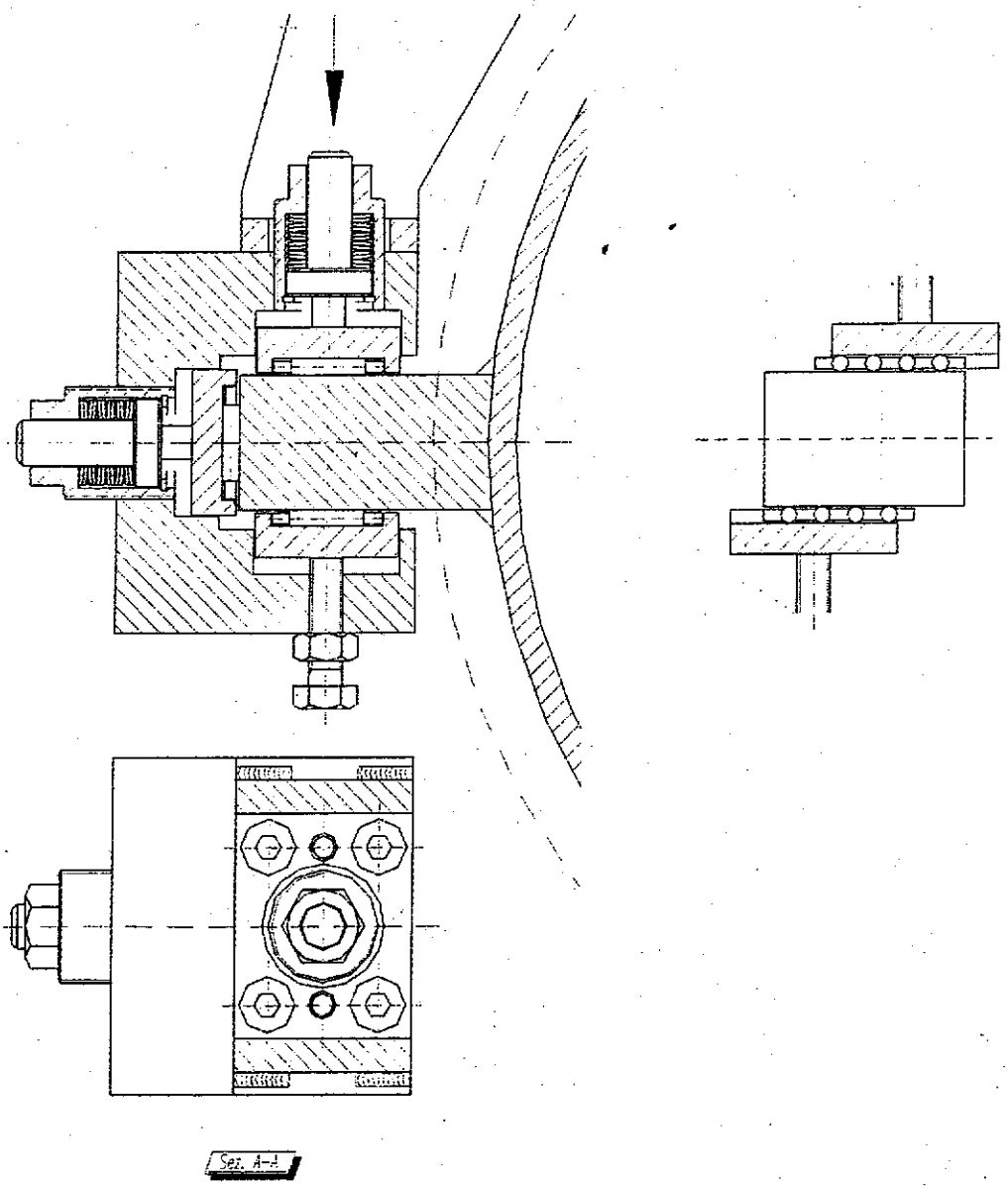

Carlo Pagani
INFN Milano - LASA

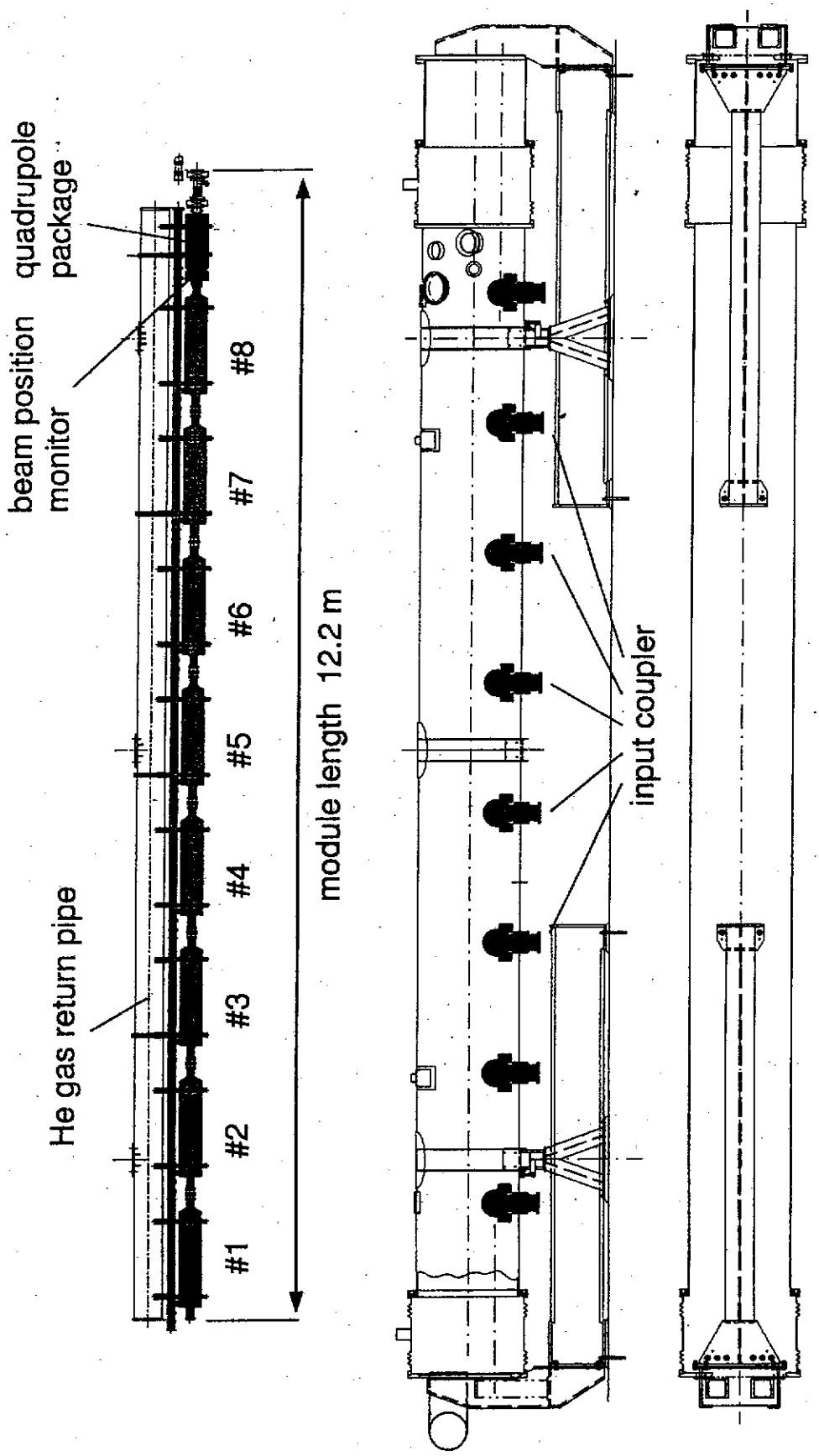

C. Pagani, TTF coupler meeting, Saclay, October, 19-20, 1998

Status of waveguide coupler activity at DESY

V. Kaljuzhny
DESY

Rectangular Wave Guide Coupler for Two 4×7-cells Supercavities

M.Dohlus, A.Gamp, H.Hartwig, N.Holtcamp,
A.Jostingmeier, C.Martens, M.Marx, C.Pagani,
J.Weisend, V.Kaljuzhny, K.Jin, A.Zavadtsev, S.Yarigin

● General Advantages of RWG Coupler

- 2×4×7-cells → 1.327 MW at 25 MV/m
- Space (longitudinal)
- E_m→750.96 - 409.8 kV/m, Losses → 1.85 - 2.50 W/m
  (Travelling wave)
- Less parts, less materials, less steps in the assembly
- Behaviour with multipactor (V_{max}=22.53-45 kV)

● Layout of RWG Coupler

- Coupler Design
- Transmission Line Components
- One Cell Copper Test Cavity Design
- (Feeding circuit)

I.

Parameters of two 4×7-cells supercavities

SUPERCAVITY
two 4*7-cells cavities

$E_{acc\,eff}$, V/m	f_{op}, HZ	T_{RF}, sec	N_{cell}
2.500E+7	1.300000000E+9	1.330000000E-3	56

K_{loss}/N_{cell}, V/C	K_{loss}, V/C	f_{op}/f_b	N_{be}
2.13071E+11	1.19320E+13	9.20000E+2	3.63000E+10

τ_{op}, sec	τ_{op}/T_{RF}	f_b, HZ
8.231068204E-4	6.18877E-1	1.413043478E+6

Q_{ext}	$Q_{ext\,(1+1)}$	q_b, C
3.361626242E+6	1.200580801E+5	5.815947E-9

t_1, sec	t_1/T_{RF}	I_b, A	P_{gen}, W
5.705341719E-4	4.28973E-1	8.218186E-3	1.326635E+6

$$Q_{ext} = \frac{\pi E_{acc\,eff} N_{cell} c}{4K_{loss} N_e e f_b}; \quad \tau = \frac{E_{acc\,eff} N_{cell} c}{4K_{loss} N_e e f_b f_{op}}$$

$$t_1 = \tau \ln 2; \qquad P_{gen} = \frac{E_{acc\,eff} N_{cell} c N_e e f_b}{2 f_{op}}$$

$$c = 2.99792458 \times 10^8 \text{ m/sec}$$

$$e = 1.6021892 \times 10^{-19} \text{ C}$$

$$\frac{K_{loss}\left(\frac{V}{pC}\right)}{N_{cell}} = 0.2131$$

Rectangular Waveguide Coupler For Two 4×7-cells Supercavities

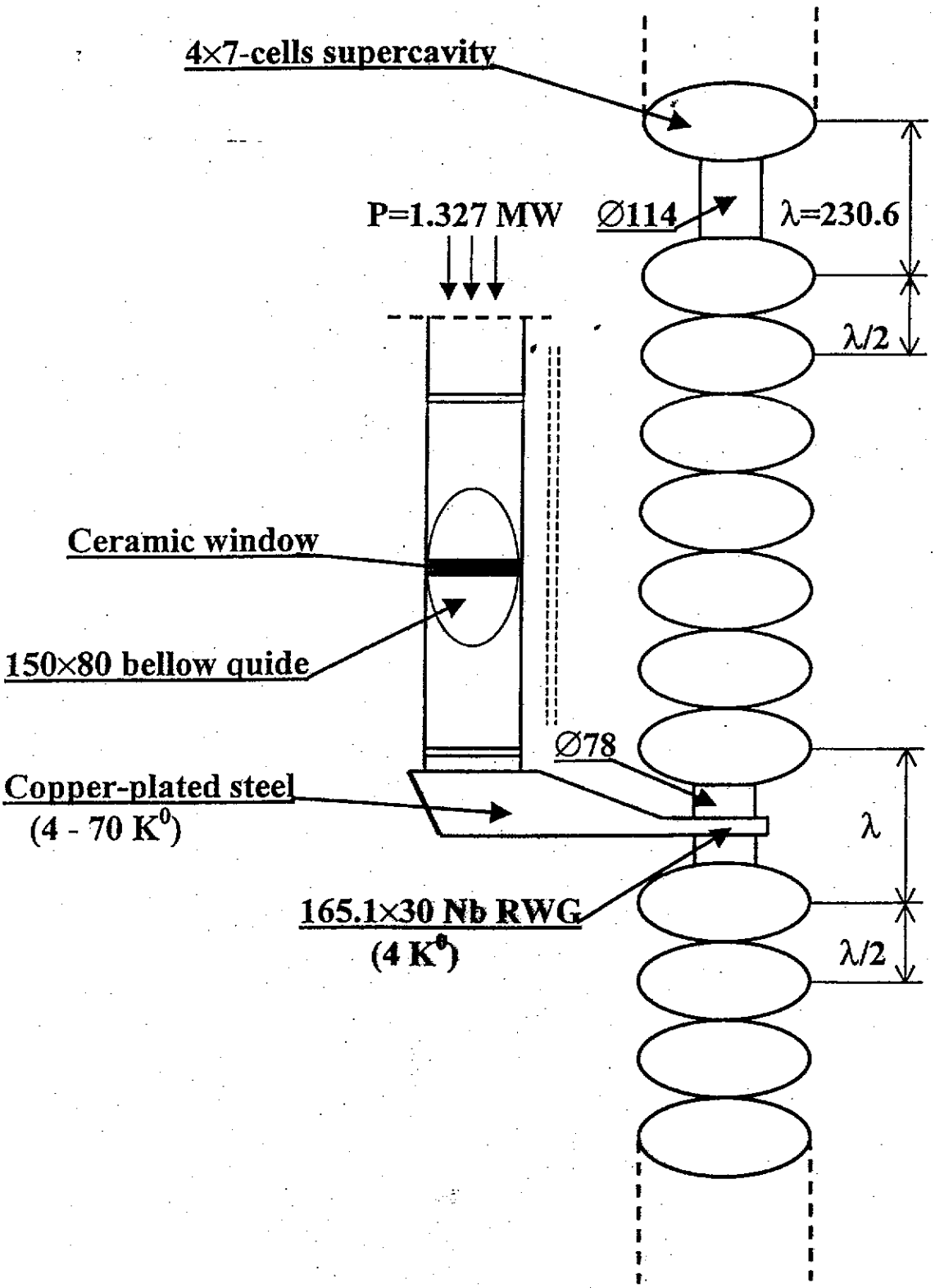

Q_{ext} as function of α

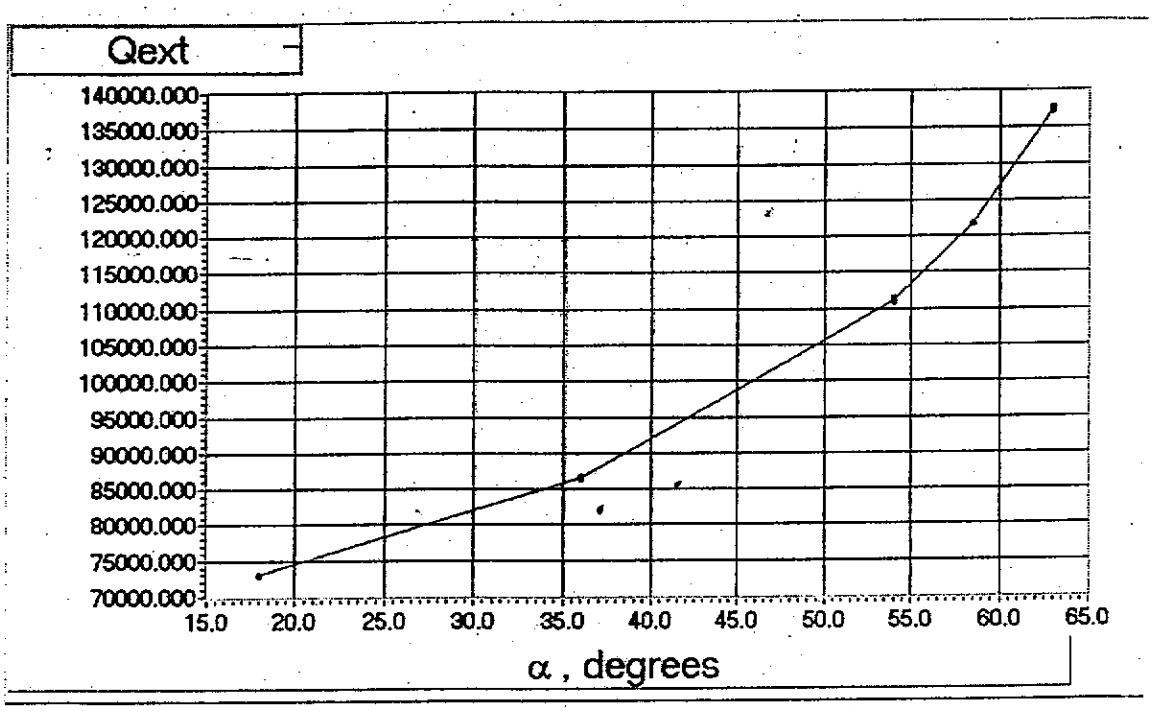

Short-circuiting surface view

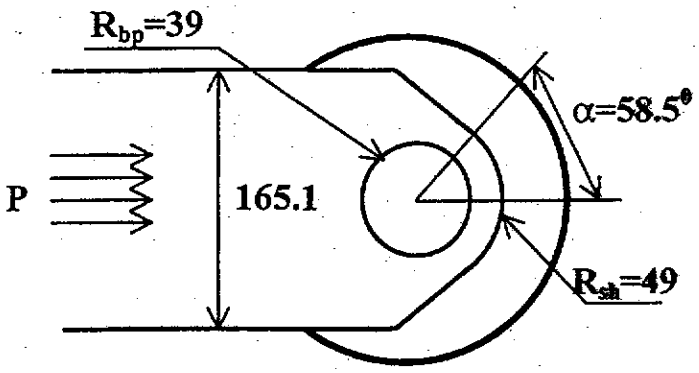

TESLA - HF - Koppler

(Hollkamp - FNW)

13.10.98

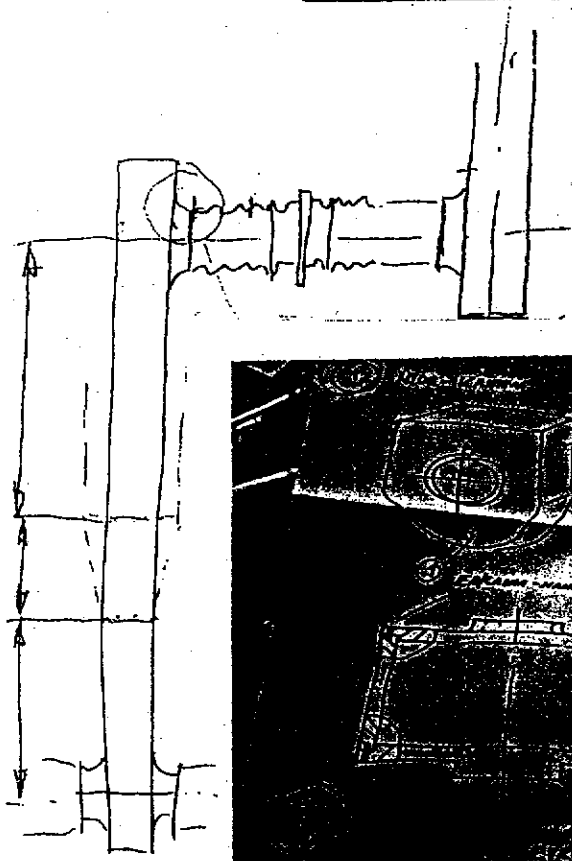

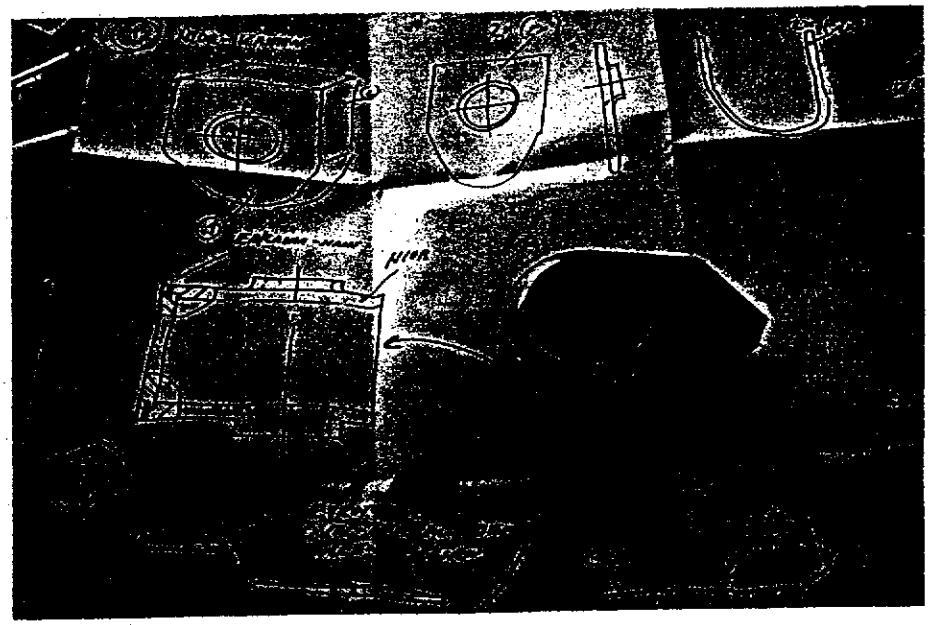

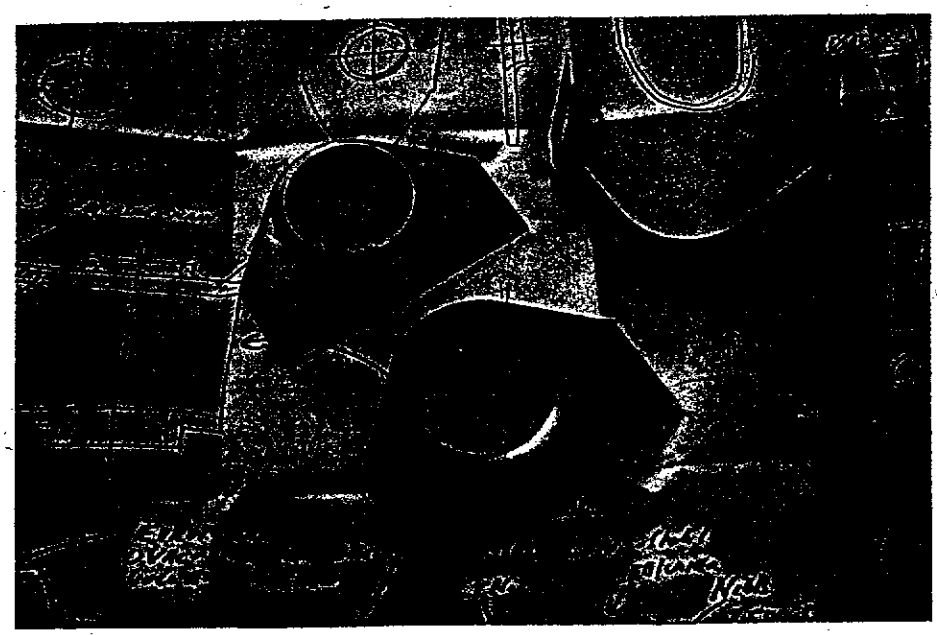

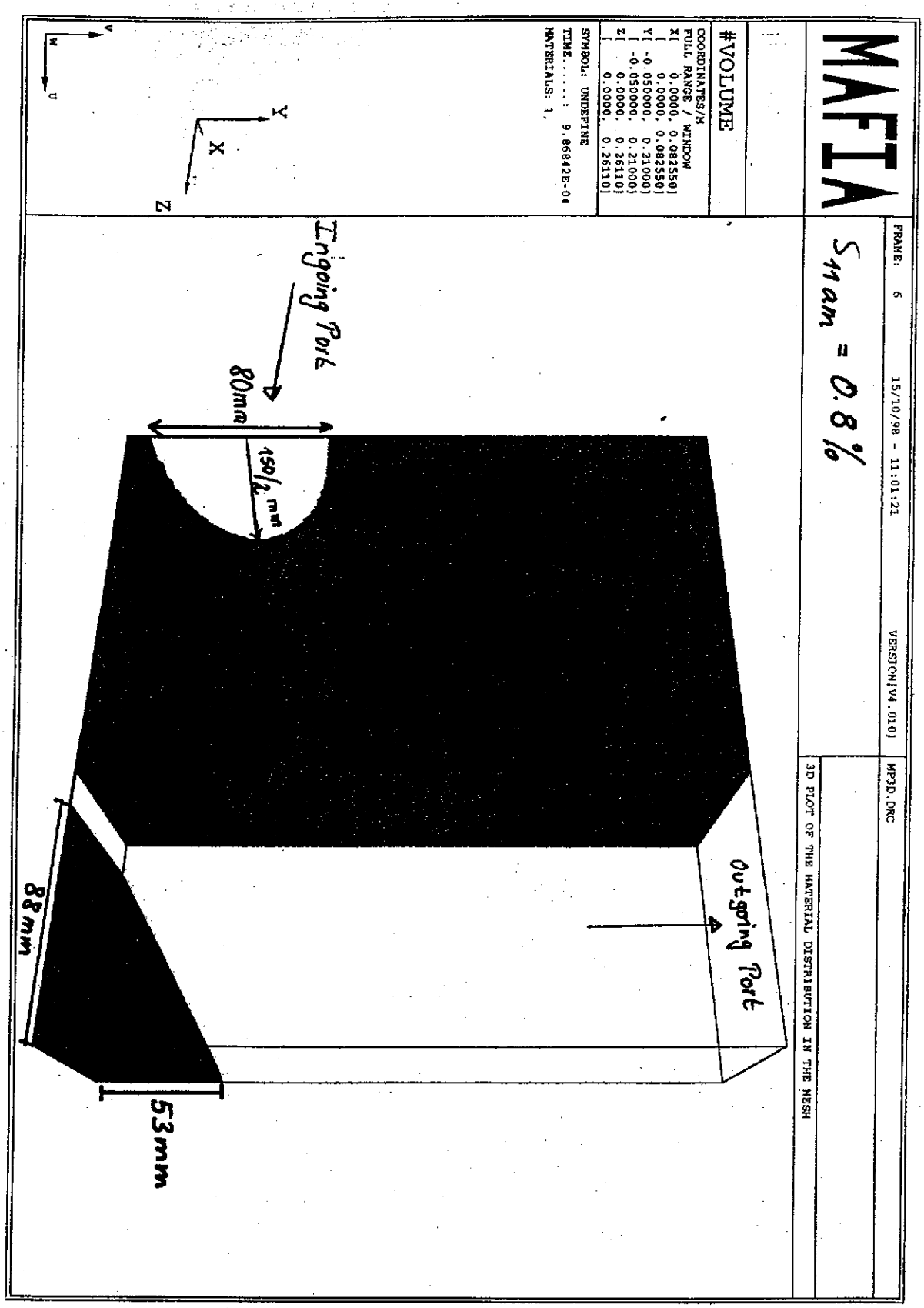
MAFIA
S_{11am} = 0.8 %
FRAME: 6
15/10/98 - 11:01:21
VERSION[V4.010]
MP3D.DRC
3D PLOT OF THE MATERIAL DISTRIBUTION IN THE MESH
#VOLUME
COORDINATES/M
FULL RANGE / WINDOW
X[0.0000, 0.082550]
[0.0000, 0.082550]
Y[-0.050000, 0.21000]
[-0.050000, 0.21000]
Z[0.0000, 0.26110]
[0.0000, 0.26110]
SYMBOL: UNDEFINE
TIME.....: 9.86842E-04
MATERIALS: 1,
Ingoing Port
80mm
150/2 mm
Outgoing Port
88mm
53mm
Y
X
Z
V
W
U

Losses and Field Strength In the RWGs and Coaxial Lines

Travelling wave: P=1.327 MW, f=1.3 GHz, T_{RF}=0.00133 sec, f_{rep}=3 Hz
Duty factor=250.626
COPPER

RWG 165.1*30 mm, E=750.96 kV/m, $H_{x,z}$=1426.7 - 1392.1 A/m

T, K	Losses, dB/m	Losses, W/m
4.000E+0	1.518E-3	1.850E+0
1.000E+1	1.569E-3	1.910E+0
2.000E+1	1.685E-3	2.050E+0
3.000E+1	1.968E-3	2.400E+0
4.000E+1	2.430E-3	2.960E+0
6.000E+1	3.921E-3	4.780E+0
7.000E+1	5.083E-3	6.200E+0
1.000E+2	6.923E-3	8.440E+0
3.000E+2	1.207E-2	1.471E+1

RWG 165.1*101 mm, E=409.28 kV/m, $H_{x,z}$=777.5 - 758.7 A/m

T, K	Losses, dB/m	Losses, W/m
4.000E+0	6.119E-4	7.450E-1
1.000E+1	6.319E-4	7.700E-1
2.000E+1	6.788E-4	8.270E-1
3.000E+1	7.927E-4	9.660E-1
4.000E+1	9.790E-4	1.190E+0
6.000E+1	1.580E-3	1.930E+0
7.000E+1	2.048E-3	2.500E+0
1.000E+2	2.789E-3	3.400E+0
3.000E+2	4.863E-3	5.920E+0

P, W 1.327000E+6

Coaxial line	R2, m	R1, m	E, V/m	H, A/m	Zw, Ohm
40/12.5 mm>>>	2.000000E-2	6.250000E-3	1.872096E+6	4.965888E+3	6.978905E+1
62/27 mm>>>	3.100000E-2	1.350000E-2	1.625213E+6	2.719462E+3	4.987785E+1

Behaviour with multipactor
(V_{max}=22.53-41.3 kV → P=1.327 MW)

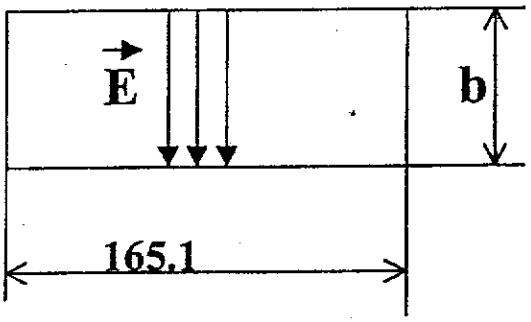

$V_m = 511 \times 4\pi \times (b/\lambda)^2$ kV

λ=230.61 mm

b=30 mm → V_m= 108.67 kV

b=101 mm → V_m= 1231.73 kV

One Cell Copper Test Cavity

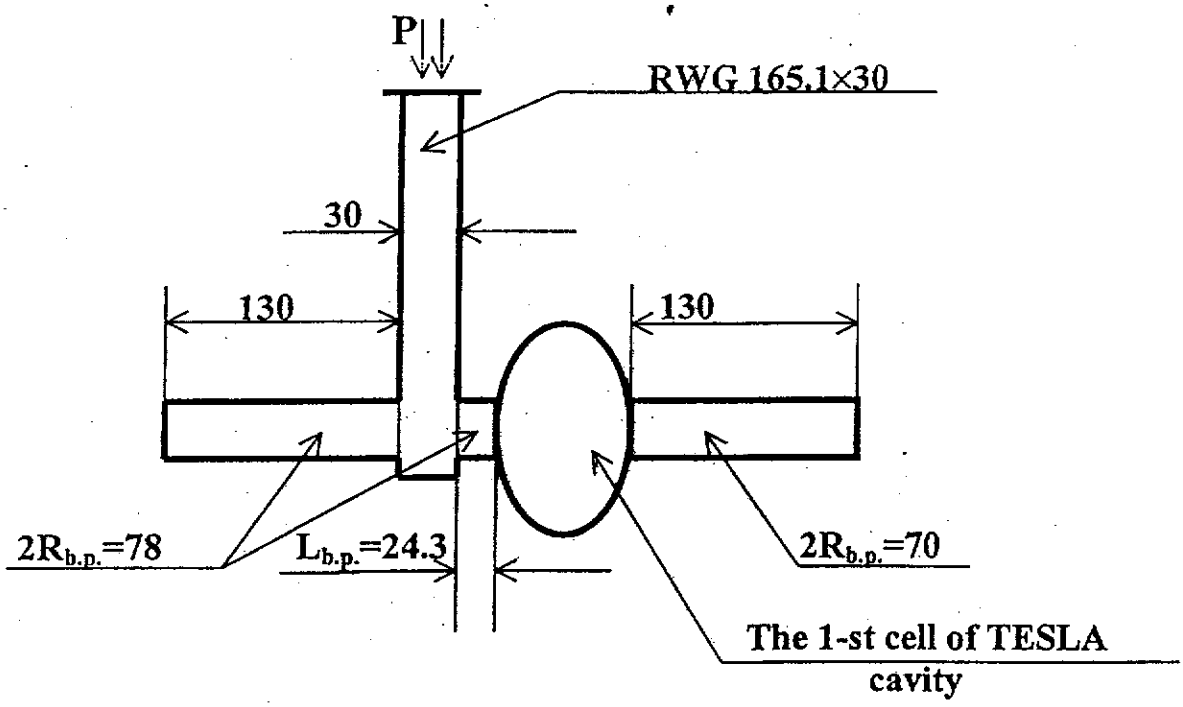

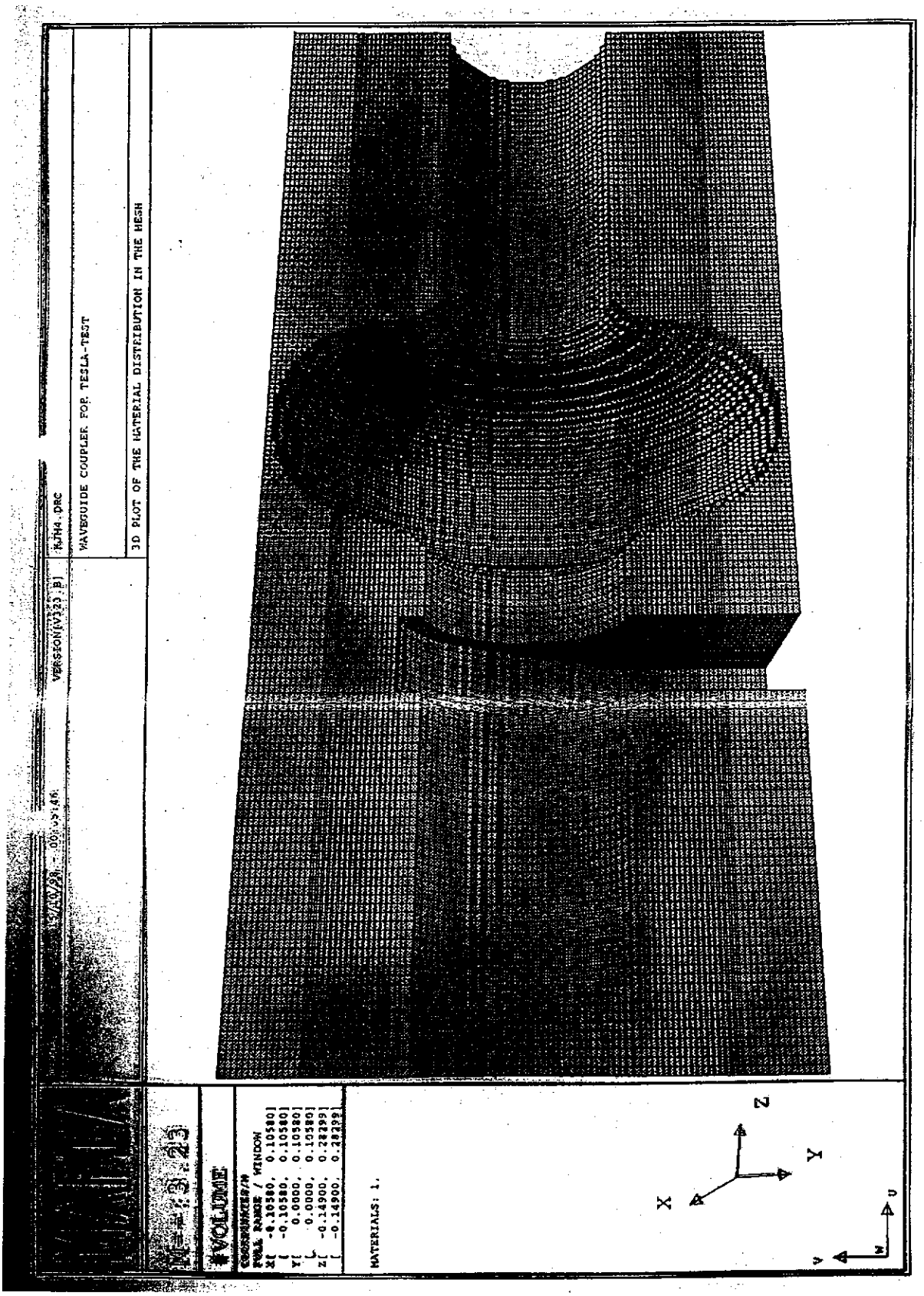
3D PLOT OF THE MATERIAL DISTRIBUTION IN THE MESH
WAVEGUIDE COUPLER FOR TESLA-TEST
VERSION(V323).B]
RJH4.DRC
#VOLUME
COORDINATES/W
FULL RANGE / WINDOW
MATERIALS: 1.
Z
Y
X
U
V
W

New idea for waveguide coupler window

A. Zavadtsev
DESY

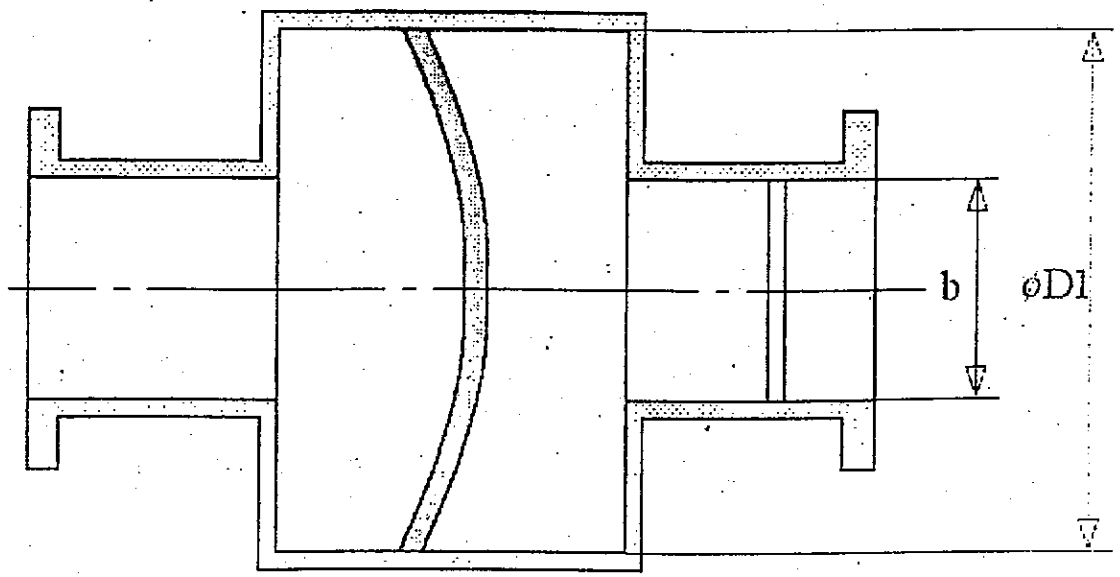

TE111-mode cavity

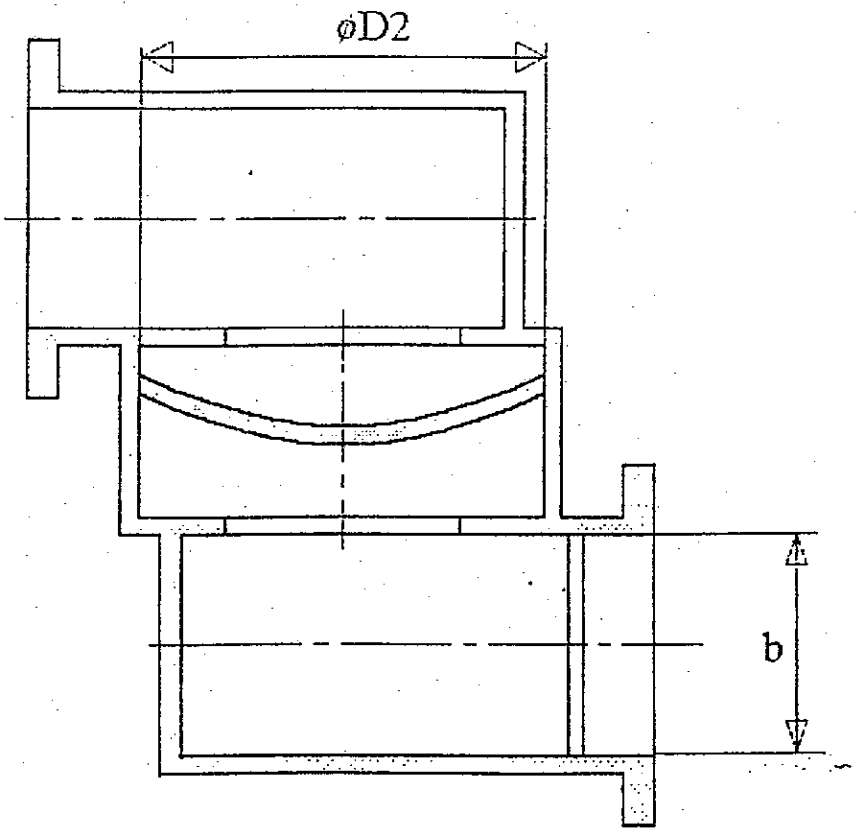

TM010-mode cavity

Alexandre Zavadtsev

Coaxial Coupler for Superstructures

D. Proch
DESY

D. Proch

Coaxial Coupler for Superstructures

Assumptions :

Fix point of cryostat

No mechanical adjustment of coupling strength

Present design :

1 coupler / cavity

no-fix point, up to 15 mm z-mouvement

adjustable coupling 1/10 .. 10

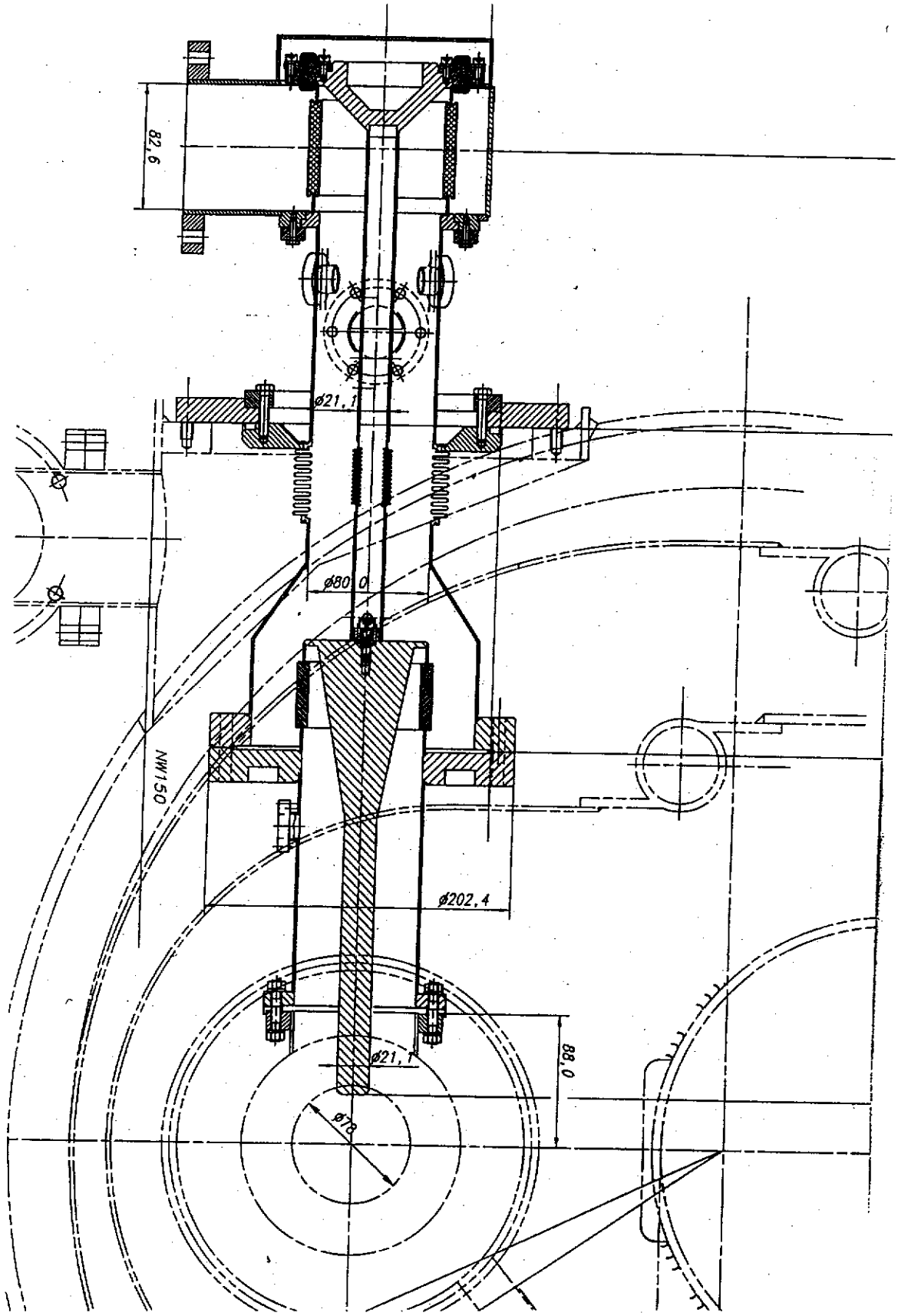
82,6
ø21,1
ø80,0
NW150
ø202,4
88,0
ø21,1
ø70

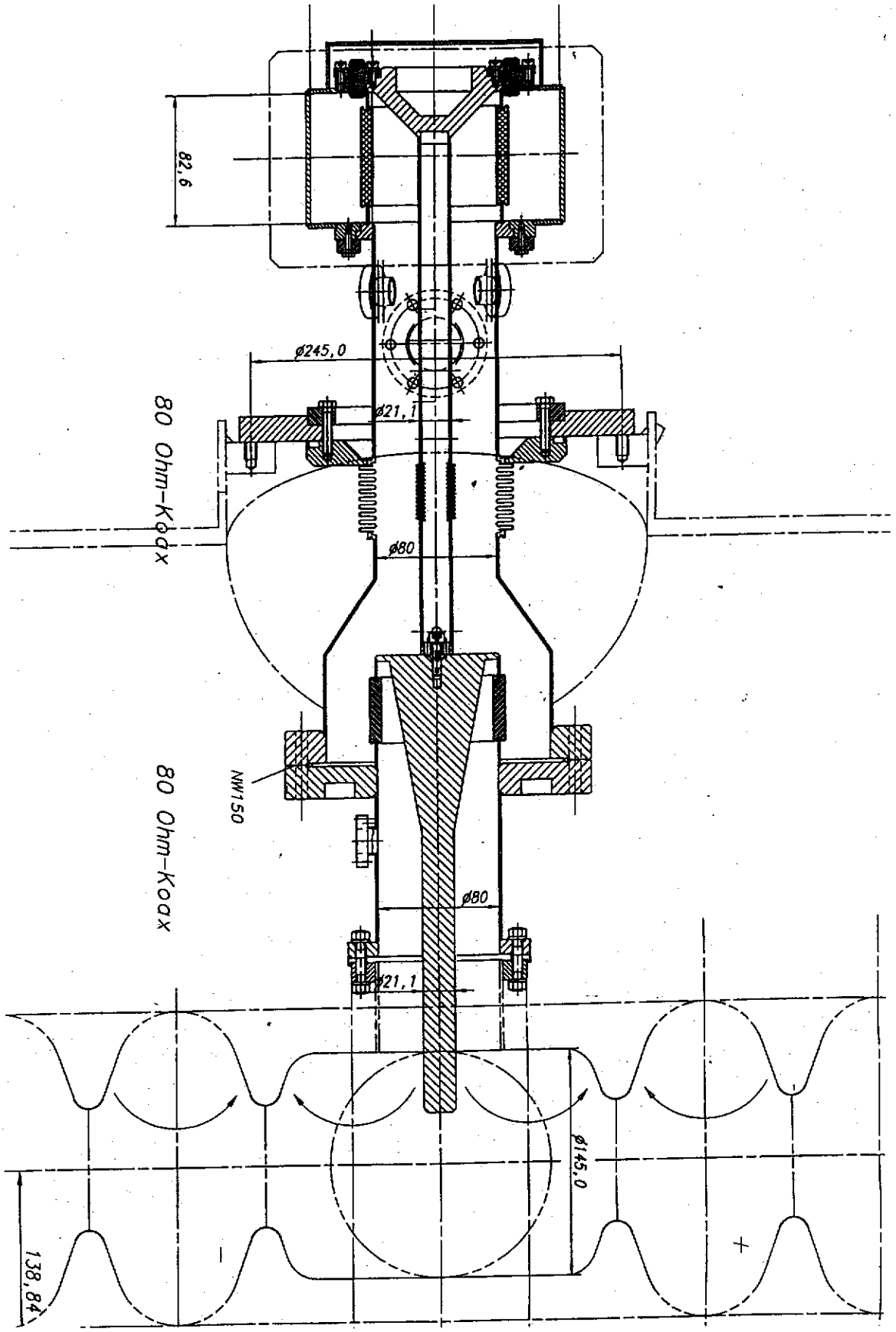
82,6
ø245,0
ø21,1
80 Ohm-Koax
ø80
NW150
80 Ohm-Koax
ø80
ø21,1
ø145,0
138,84
-
+

	loss / cm / K V2A	V_p at 1 MK
	$1.7 \cdot 10^{-4}$	20 kV
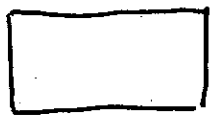	$8 \cdot 10^{-5}$	32 kV
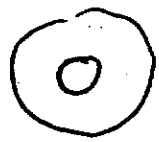	inner Ø: $1 \cdot 10^{-4}$ outer: $4.2 \cdot 10^{-5}$	10 kV

50Ω 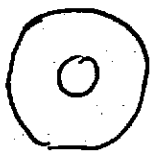

50Ω 

Pro's

· Well understood multipacting scaling in coax lines

with large outer diameter no multipacting

· Well calculated cold window design
no danger of multipacting

· First calculation of warm window
no hint of multipacting

· small radial extension after closing the beam vacuum

- round flanges welded connections

· lower RF loss on outer conductor as compared to rectangular WG

· lower peak voltage as compared to rectangular WG

Status of superstructure studies

J. Sekutowicz
DESY MHF-SL

J. Sekutowicz, TTF coupler meeting, Saclay, October, 19-20, 1998

Status of superstructure studies

J. Sekutowicz
DESY MHF-SL

1. The copper model of the 4x7-cell superstructure

2. Can we feed 2 superstructure with one FM coupler ?

3. FM coupler for the proposed 4x7-cell superstructure: RF requirements

1. The copper model of the 4x7-cell superstructure

The first set of four 7-cell cavities should be ready by the end of October.

There is almost two months of delay because:

- brazing was replaced by electron beam welding,
- cutting of cups caused that equator plane was not parallel to the iris plane, new cutting tool had to be constructed.

Status:

- all cups for the first superstructure are ready for welding,
- all interconnecting tubes with ports for HOM couplers, flanges and thread rods for assembly are ready
- tuning systems for each cavity are manufactured,
- welding parameters have been fixed.
- HOM coupler model has been prepared

Comments:

- RF measurements showed that shape of cups is well reproducible, final frequency corrections are done by trimming on the equator as it is done for Nb cavities.
- we hope to start RF measurements mid November.

2. Can we feed 2 superstructures with one FM coupler ?

The second set of four 7-cell cavities has been ordered to find out experimentally if one can couple <u>8 x 7-cell</u> structures.

↓

This can be answered when RF-measurements will show that we can couple 4 x 7-cell structures !

Two layouts have been proposed:

a) 4 x 7-cell ⟵ WG/Coax. Coupler ⟶ 4 x 7-cell

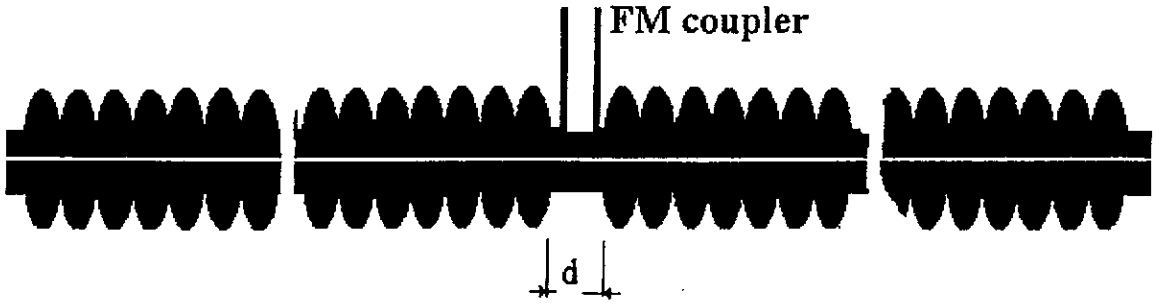

and

b) WG/Coax. **coupler** ⟶ 8 x 7-cell

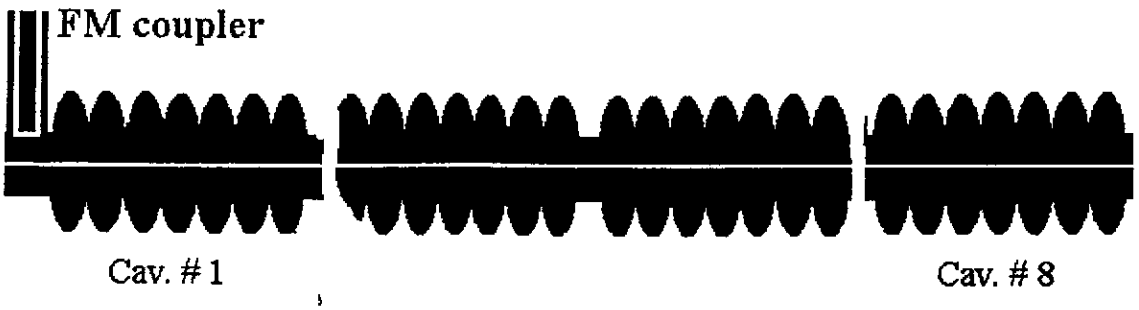

J. Sekutowicz, TTF coupler meeting, Saclay, October, 19-20, 1998

Problems to be investigated:

layout (a)

1) Is there enough field strength at the FM coupler position to get required Qext of ~ 3. 10^6 ?

   To keep synchronism of a beam with the accelerating mode d (length of the interconnection) must be fixed to:

   $d = \lambda/2$ for the WG coupler
   $d = \lambda$ for the Coax. coupler

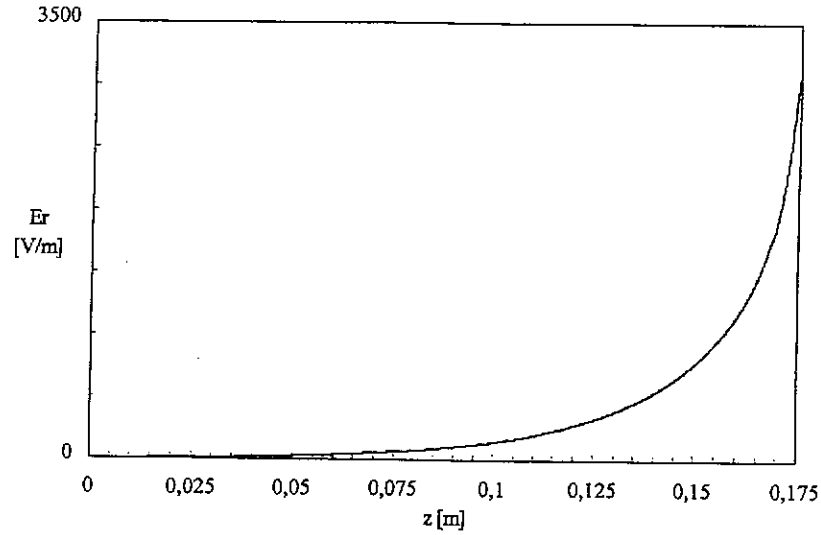

E (z) component at r = 57 mm in the end beam tube. Values computed for the same stored energy.

Scaling: $Qext \sim (E_r)^{-2}$

Conclusion :

TTF coupler placed $\lambda/2 = 115$ mm from the end cell can provide :

$$Qext \sim 3.\ 10^8$$

For the WG coupler this is not a problem since the distance to end cell is $\lambda/4 = 57$ mm. k

2) What is a consequence of the coupling between two superstructures ?

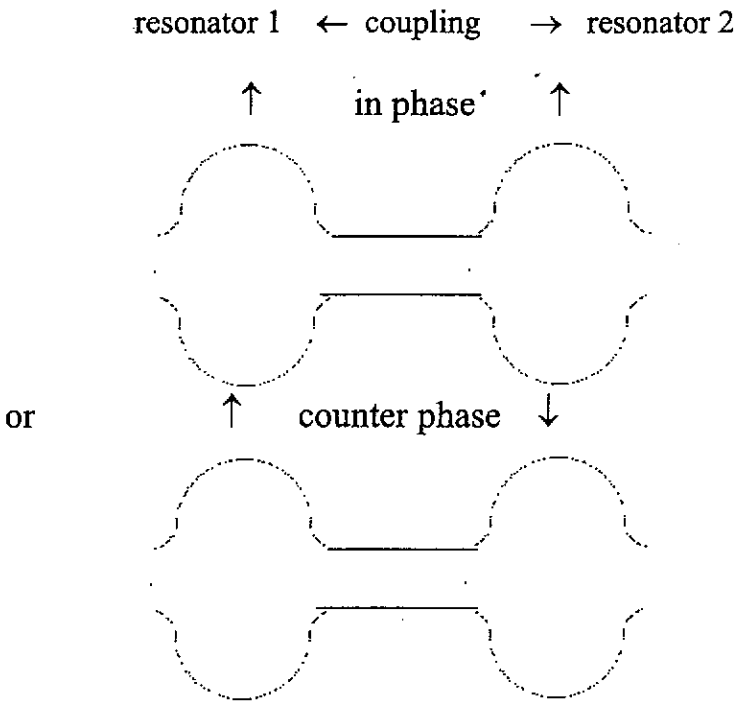

WG coupler couples good to the in phase mode and bad to the counter phase mode: $d = \lambda/2$ is OK

Coax. coupler couples good to the counter phase mode and bad to the in phase mode: $d = \lambda$ is OK

J. Sekutowicz, TTF coupler meeting, Saclay, October, 19-20, 1998

But both couplers couple good only to one mode, it means that mode with bad coupling has high Qext and when (R/Q) # 0 beam impedance can be high.

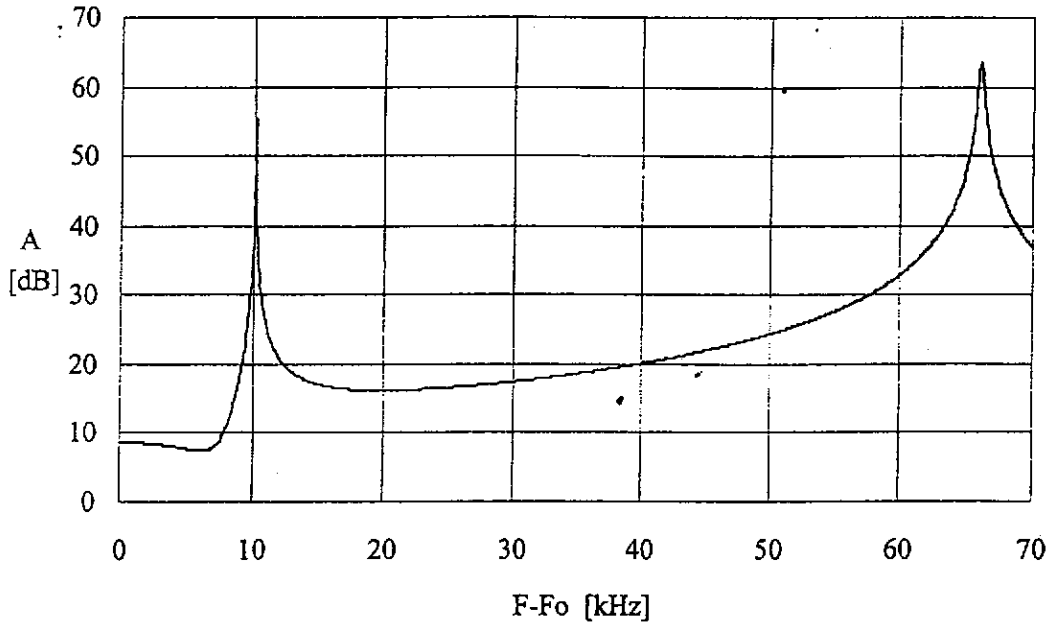

layout (b)

Here both couplers are possible.

But we do not know about:

- transient state and energy flow,
- field flatness,
- HOMs

3. FM coupler for the proposed 4x7-cell superstructure: RF requirements

Normal operation at 25 MV/m

Total voltage in superstructure for the nominal accelerating field of 25 MV/m

$$\mathbf{V} = 25\ \text{MV/m} * 4*0.807\ \text{m} = \mathbf{80.7\ MV}$$

when I_{beam}= **8 mA**

$$Z = (80.7\ \text{MV}) / 8\ \text{mA} = \mathbf{10.088}\ \text{G}\Omega$$

and

$$\mathbf{Q_{ext}} = Z/(R/Q) = (10.088\ \text{G}\Omega)/(2930\ \Omega) = \mathbf{3.44.\ 10^6}$$

Power.

$$\mathbf{P} = 8\ \text{mA} * 80.088\ \text{MV} = \mathbf{640.7\ kW}$$

J. Sekutowicz, TTF coupler meeting, Saclay, October, 19-20, 1998

HPP processing

For a tuned superstructure power needed for the HPP processing is:

$$\mathbf{P_{in} = 4 * P_{TTF} * 7/9 = 3.1\ P_{TTF}}$$

when P_{TTF} is the power needed for 9-cell TTF cavity.
In this case :

$$\mathbf{P1 = P2 = P3 = P4}$$

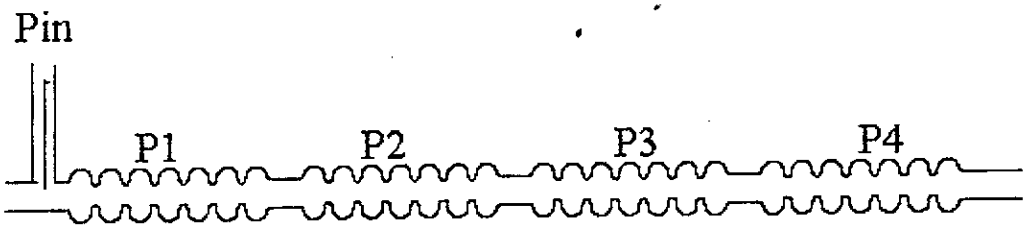

Can be this power reduced by the proper detuning of sub-units?

The problem is not solved yet.
Some examples

1. Processing of the first sub-unit:

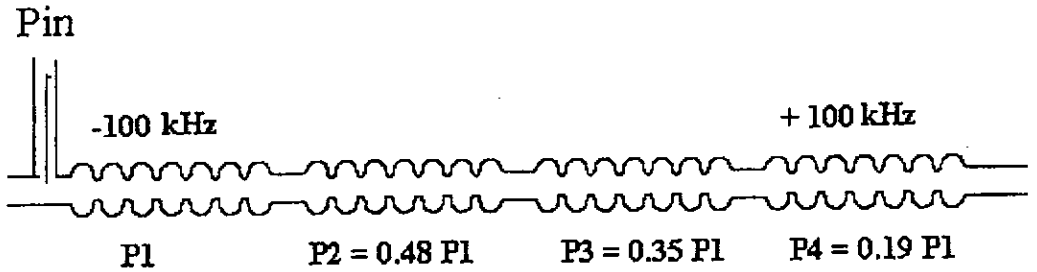

field flatness: sub-unit 1 77%

here power is : $\mathbf{P_{in} = 7/9\ P_{TTF}\ 2.02 = 1.57\ P_{TTF}}$

J. Sekutowicz, TTF coupler meeting, Saclay, October, 19-20, 1998

2. Processing of the second sub-unit:

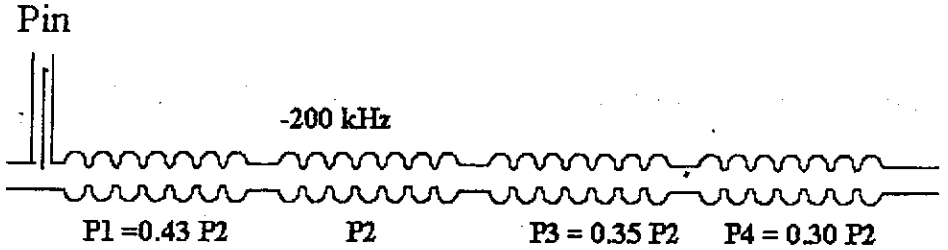

field flatness : sub-unit 2 14 %

required power is : $\mathbf{P_{in} = 7/9\ P_{TTF}\ 2.08 = 1.6\ P_{TTF}}$

3. Processing of the third sub-unit:

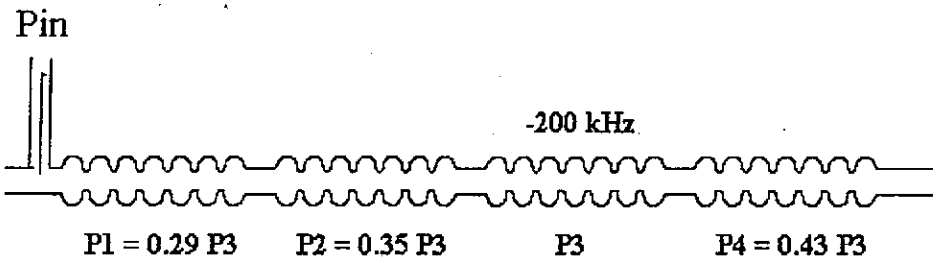

field flatness: sub-unit 3 14 %

required power is : $\mathbf{P_{in} = 7/9\ P_{TTF}\ 2.07 = 1.6\ P_{TTF}}$

4. Processing of the fourth sub-unit:

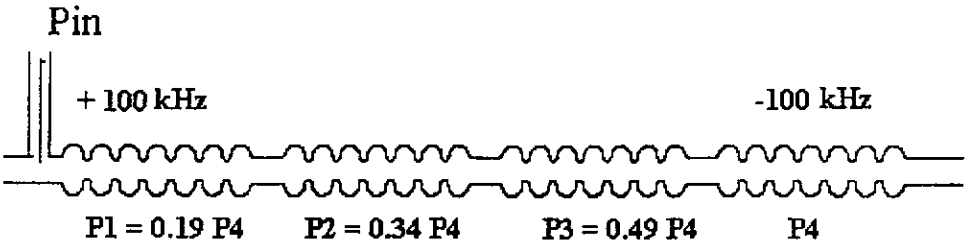

field flatness: sub-unit 4 77%

required power is : $\mathbf{P_{in} = 7/9\ P_{TTF}\ 2.02 = 1.57\ P_{TTF}}$

J. Sekutowicz, TTF coupler meeting, Saclay, October, 19-20, 1998

Conclusion :

we can reduce P_{in} from

$$3.1\ P_{TTF} \text{ to } 1.6\ P_{TTF}$$

but we pay with the field flatness in the processed sub-unit.

Saclay/Orsay test stand

M. Desmons
CEA Saclay

COMMISSARIAT À L'ÉNERGIE ATOMIQUE
DSM - DAPNIA
DIRECTION DES SCIENCES DE LA MATIÈRE

M.DESMONS

11 / 10 / 1998

DEPARTEMENT D'ASTROPHYSIQUE, DE PHYSIQUE DES PARTICULES,
DE PHYSIQUE NUCLÉAIRE ET DE L'INSTRUMENTATION ASSOCIÉE
SERVICE D'ÉTUDE DES ACCÉLÉRATEURS

HP3 test stand

RF lines description

Klystron characteristics

Modulator

RF control system

Measurements and Acquisitions

M.DESMONS

11 / 10 / 1998

COMMISSARIAT À L'ÉNERGIE ATOMIQUE

DSM - DAPNIA

DIRECTION DES SCIENCES DE LA MATIÈRE

DEPARTEMENT D'ASTROPHYSIQUE, DE PHYSIQUE DES PARTICULES,
DE PHYSIQUE NUCLÉAIRE ET DE L'INSTRUMENTATION ASSOCIÉE
SERVICE D'ÉTUDE DES ACCÉLÉRATEURS

1st line

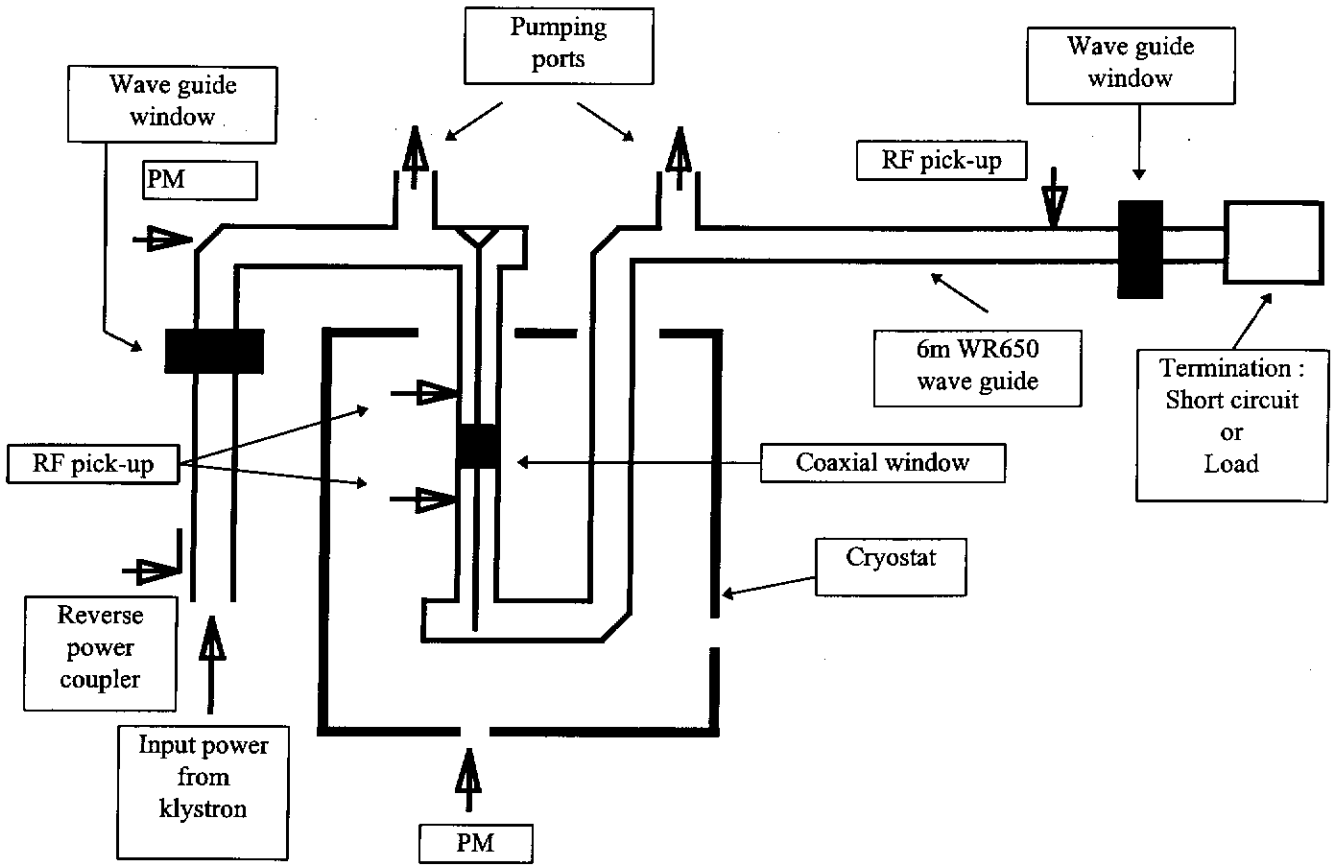

MEASUREMENTS :

Direct input power Reflected power Transmitted power Upstream pick-up RF power Downstream pick-up RF power	RF detection diodes + voltage amplifiers (rise time = 3us)
Upstream pick-up electron current Downstream pick-up electron current	current to voltage amplifiers (1mA/V rise time = 3us)
Upstream waveguide to coaxial transition PM Downstream waveguide to coaxial transition PM	current to voltage amplifiers (rise time = 3us)
Upstream vacuum Downstream vacuum	current to voltage amplifiers (rise time = 1ms)

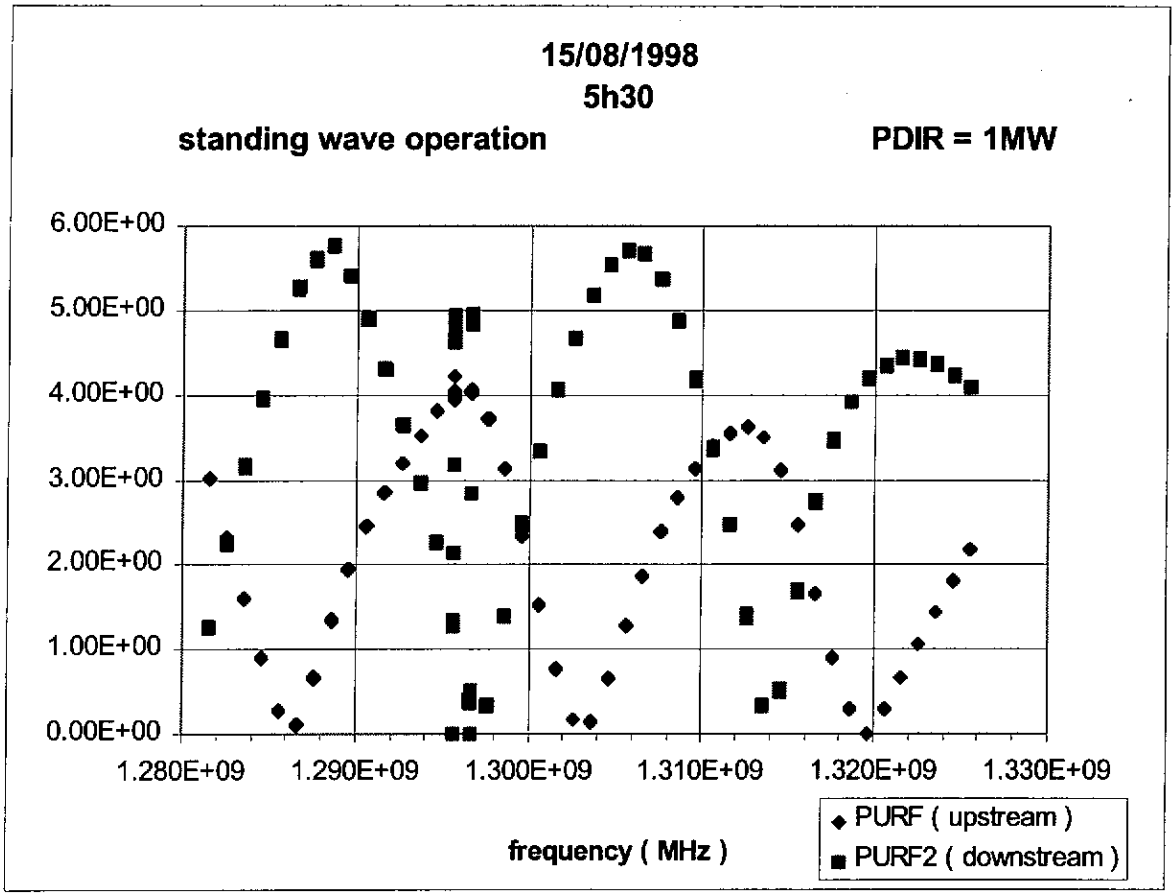

COMMISSARIAT À L'ÉNERGIE ATOMIQUE
DSM - DAPNIA
DIRECTION DES SCIENCES DE LA MATIÈRE

M.DESMONS

11 / 10 / 1998

DEPARTEMENT D'ASTROPHYSIQUE, DE PHYSIQUE DES PARTICULES,
DE PHYSIQUE NUCLÉAIRE ET DE L'INSTRUMENTATION ASSOCIÉE
SERVICE D'ÉTUDE DES ACCÉLÉRATEURS

2nd RF LINE

Test of RF components at room temperature :

- Biased wavegide to coaxial transition
- Coaxial line at atmospheric pressure
- Coaxial windows with atmospheric pressure on one side and vacuum on the other side

Measurements :

RF measurements	Detection diodes + voltage amplifiers
• Direct power	(3 us rise time)
• Reflected power	
• Transmitted power	
• Upstream pick-up	
• Downstream pick-up	
Electron measurement	
• vacuum side pick-up	Current to voltage amplifier (3 us rise time)
Vacuum measurement	
• ionic pump current	Current to voltage amplifier (1 ms rise time)

RF line N°2

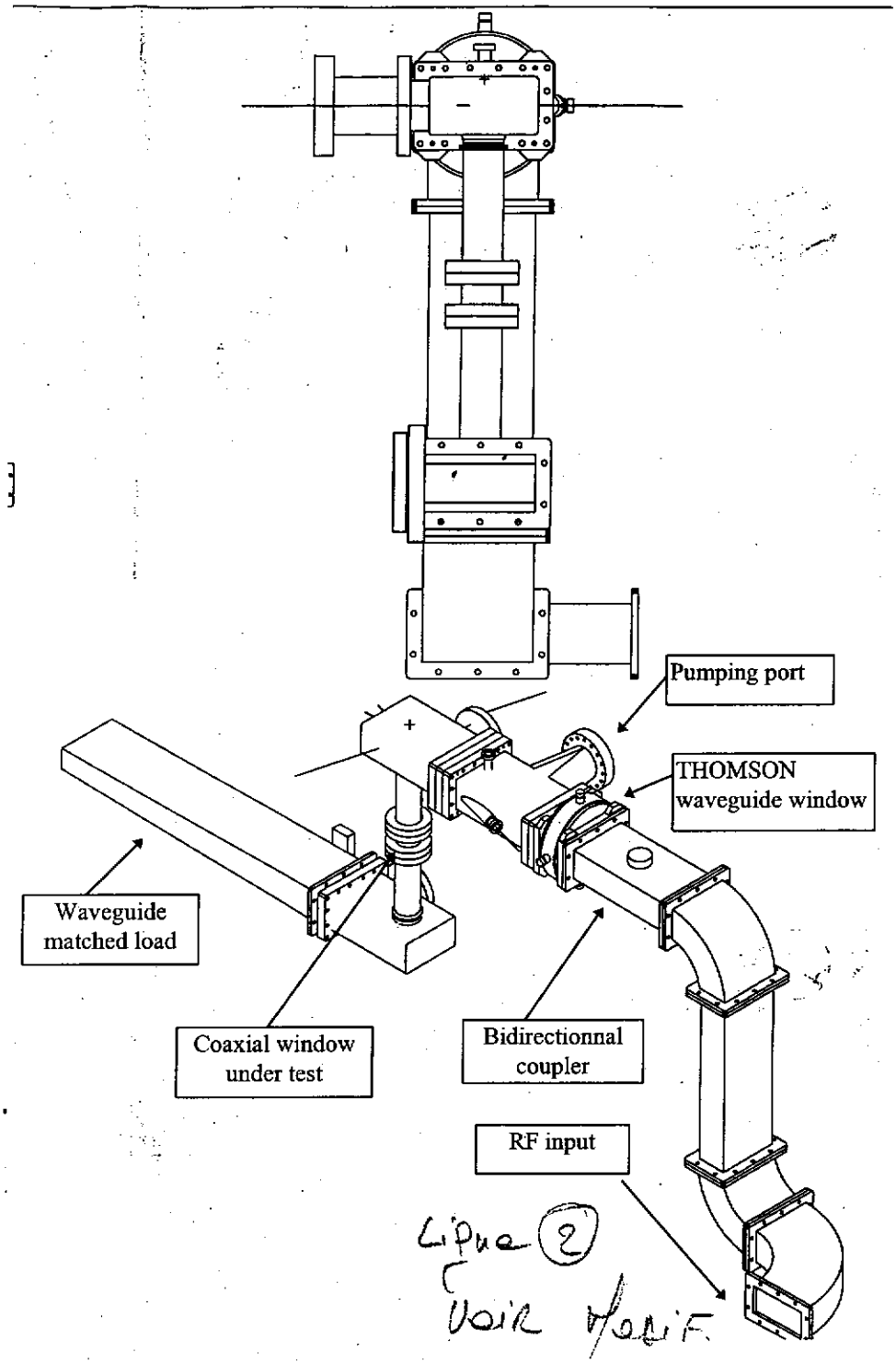

COMMISSARIAT À L'ÉNERGIE ATOMIQUE
DSM - DAPNIA
DIRECTION DES SCIENCES DE LA MATIÈRE

M.DESMONS

11 / 10 / 1998

DEPARTEMENT D'ASTROPHYSIQUE, DE PHYSIQUE DES PARTICULES,
DE PHYSIQUE NUCLÉAIRE ET DE L'INSTRUMENTATION ASSOCIÉE
SERVICE D'ÉTUDE DES ACCÉLÉRATEURS

Operation at full power on each line

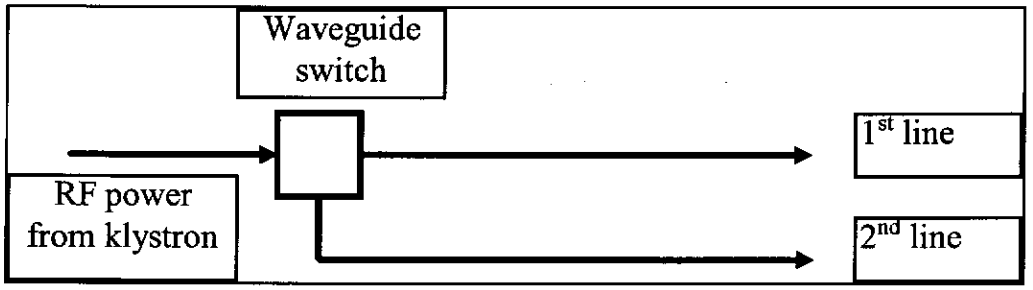

Operating the two lines at the same time

- first line in standing wave mode at half power.
- second line in traveling wave mode at full power.

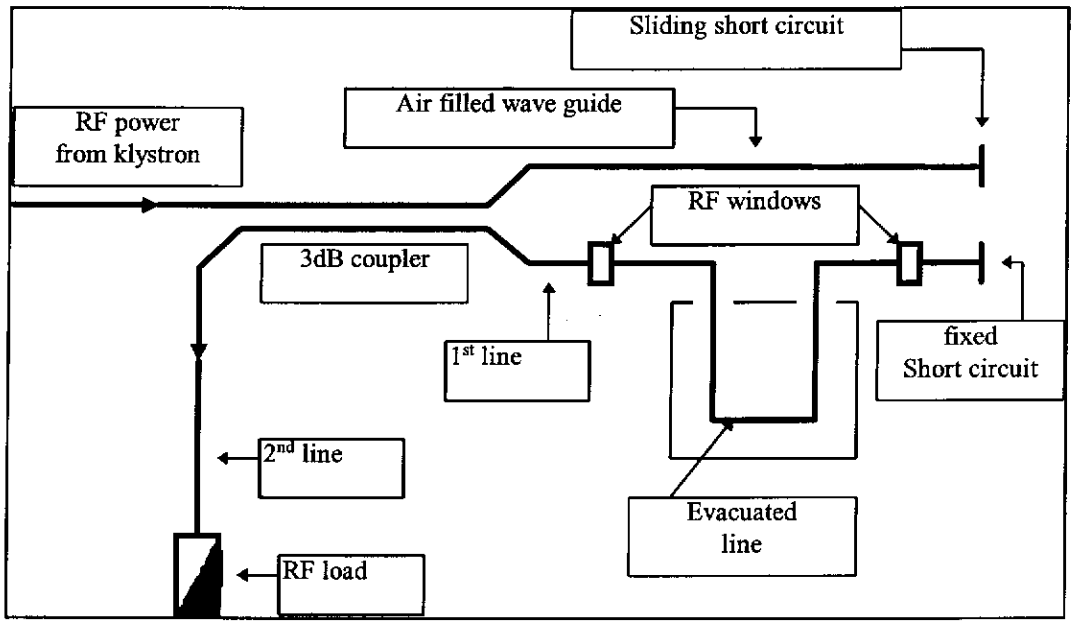

KLYSTRON CHARACTERISTICS

THOMSON klystron TH2086A

5 cavities with mecanical tuning

Output circuit : WR650 wave guide

frequency		1230 to 1330	MHz
bandwidth	(-1 dB)	20	MHz
peak output	500 ms pulse width	0.6	MW
power	250 ms pulse width	1.0	MW
	short pulse	4.5	MW
drive power		30	W
gain		42	dB
efficiency		37	%
perveance		2.3	$uA/V^{3/2}$
solenoïd current		13	A
SWR max		1.5	
phase shift	vs cathode voltage	-10	°/kV
	vs drive power	4	°/dB
cooling	collector	1500	liters/min
water flow	body	8	liters/min
	solenoïd	8	liters/min
weight		120	kg
height		2300	mm

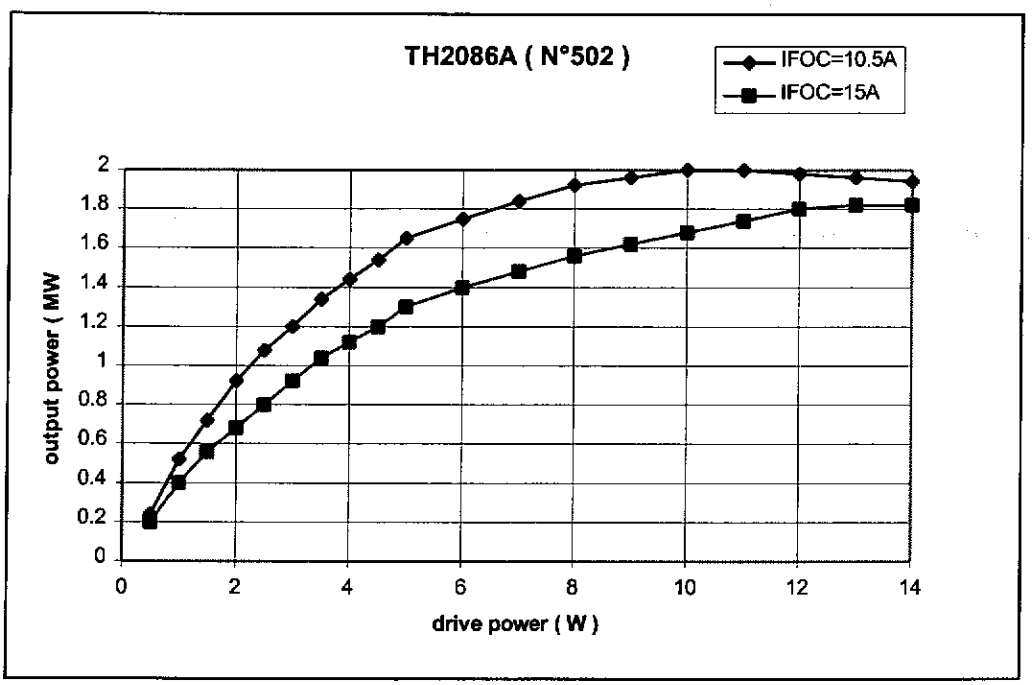
TH2086A (N°502)
IFOC=10.5A
IFOC=15A
output power (MW)
drive power (W)
0
0.2
0.4
0.6
0.8
1
1.2
1.4
1.6
1.8
2
0
2
4
6
8
10
12
14

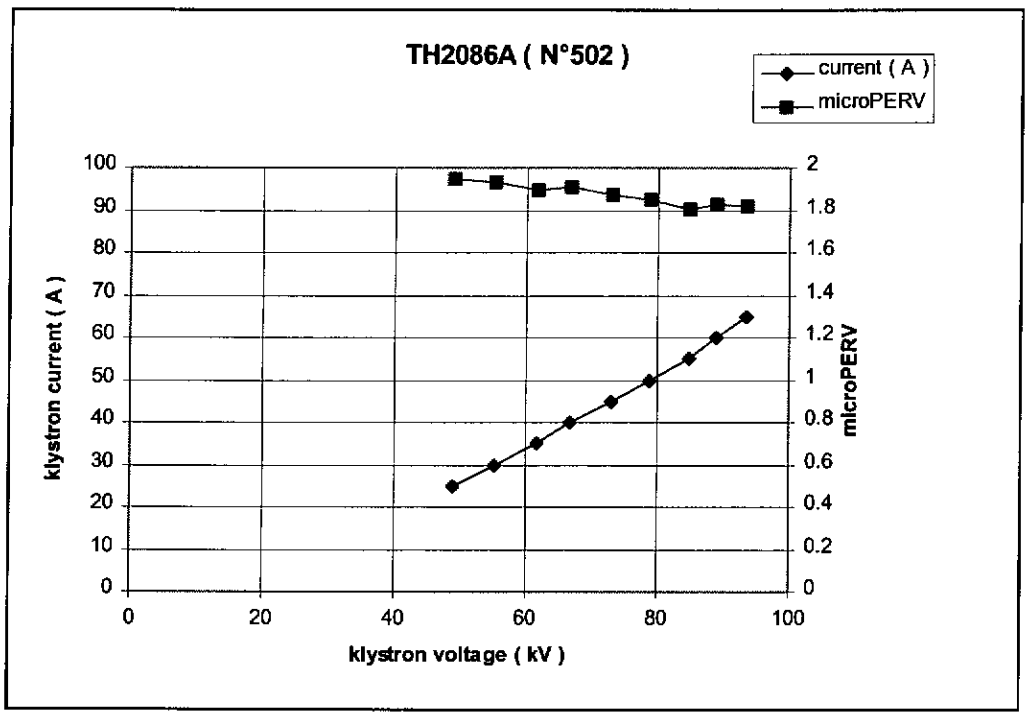
TH2086A (N°502)
current (A)
microPERV
klystron current (A)
microPERV
klystron voltage (kV)
0
10
20
30
40
50
60
70
80
90
100
0
0.2
0.4
0.6
0.8
1
1.2
1.4
1.6
1.8
2
0
20
40
60
80
100

HP3 MODULATOR

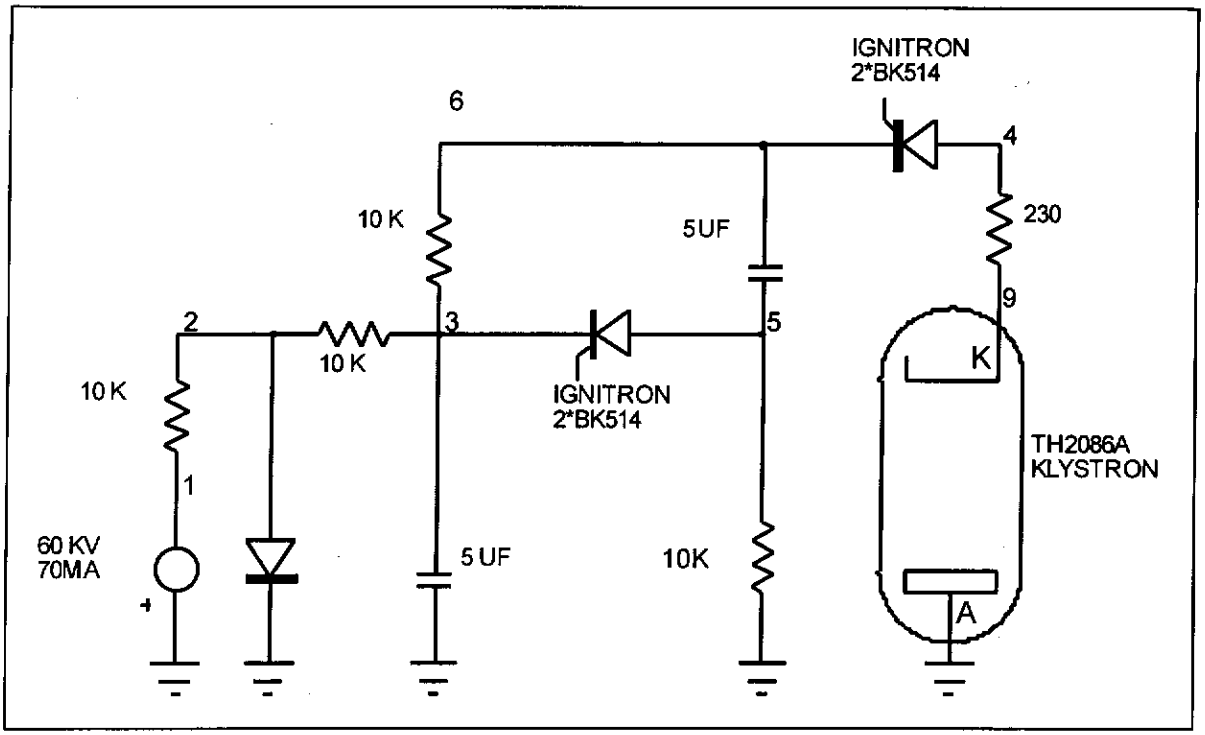

electrical diagram

COMMISSARIAT À L'ÉNERGIE ATOMIQUE
DSM - DAPNIA
DIRECTION DES SCIENCES DE LA MATIÈRE

M.DESMONS

11 / 10 / 1998

DEPARTEMENT D'ASTROPHYSIQUE, DE PHYSIQUE DES PARTICULES,
DE PHYSIQUE NUCLÉAIRE ET DE L'INSTRUMENTATION ASSOCIÉE
SERVICE D'ÉTUDE DES ACCÉLÉRATEURS

HP3 MODULATOR

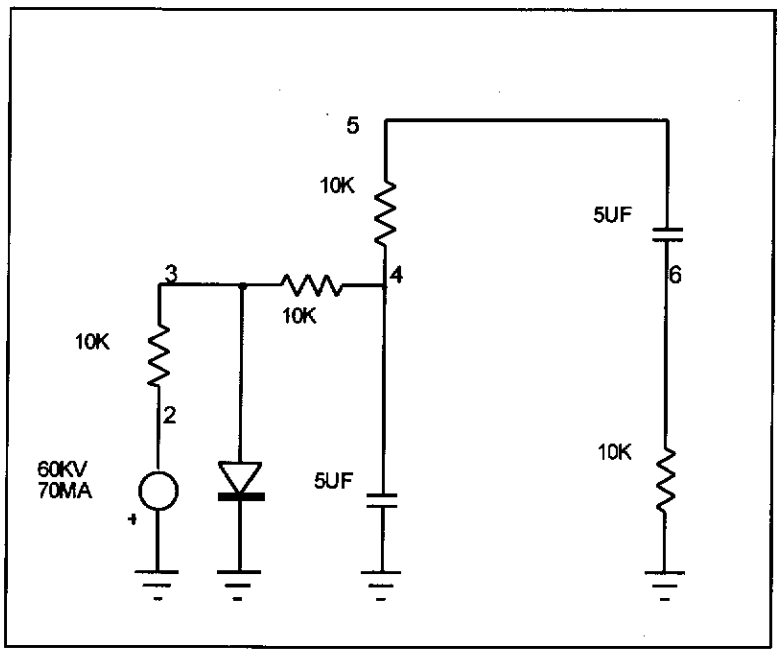

CHARGING PHASE

ignitrons switched off

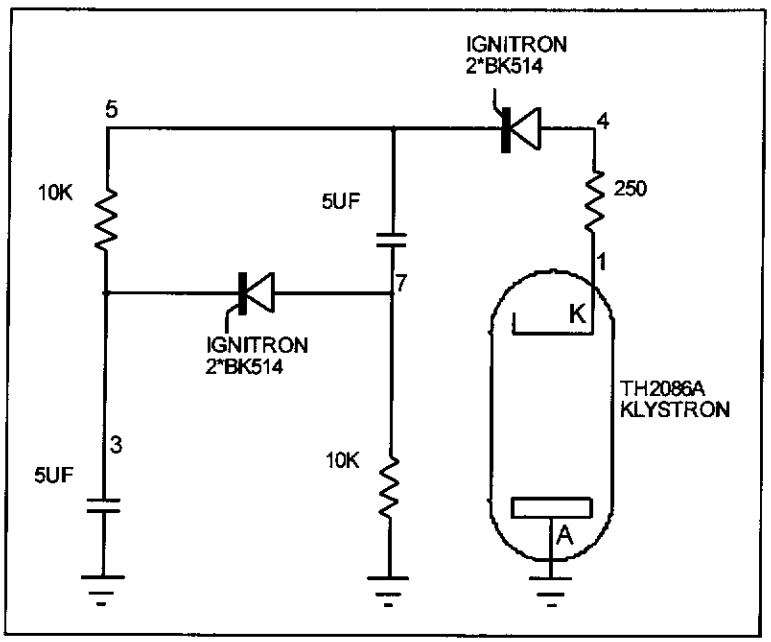

PULSE PHASE

ignitrons switched on

M.DESMONS

11 / 10 / 1998

DEPARTEMENT D'ASTROPHYSIQUE, DE PHYSIQUE DES PARTICULES,
DE PHYSIQUE NUCLÉAIRE ET DE L'INSTRUMENTATION ASSOCIÉE
SERVICE D'ÉTUDE DES ACCÉLÉRATEURS

HIGH VOLTAGE AND RF PULSES

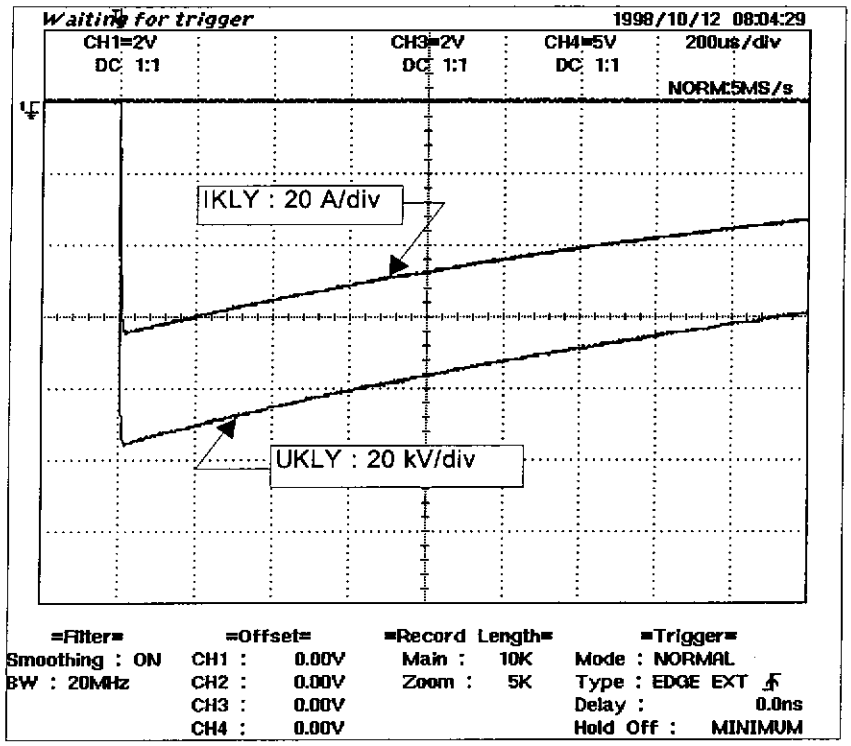

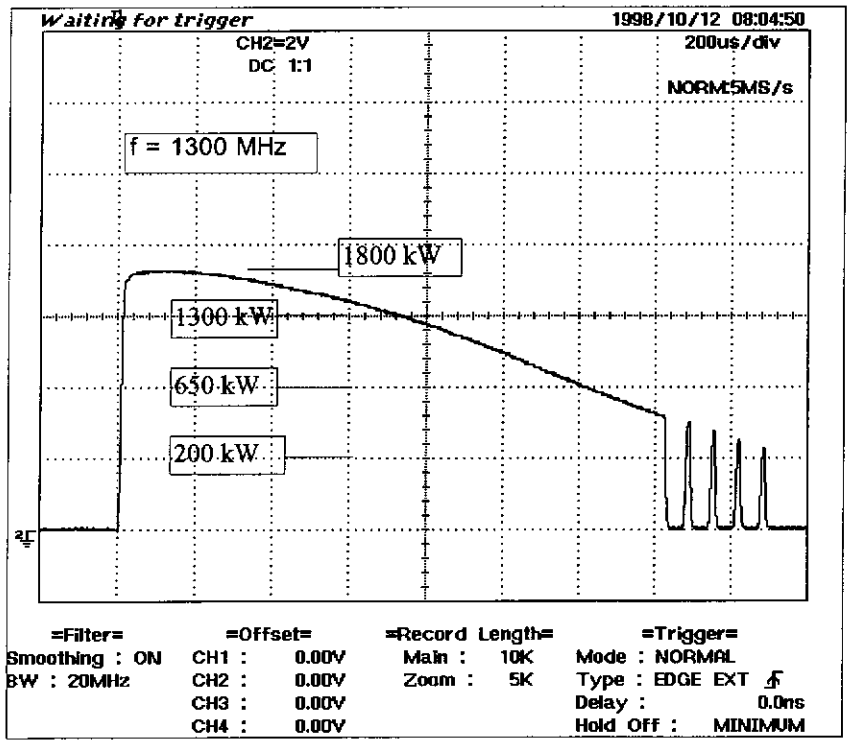

M.DESMONS

DEPARTEMENT D'ASTROPHYSIQUE, DE PHYSIQUE DES PARTICULES,
DE PHYSIQUE NUCLÉAIRE ET DE L'INSTRUMENTATION ASSOCIÉE
SERVICE D'ÉTUDE DES ACCÉLÉRATEURS

RF CONTROL SYSTEM

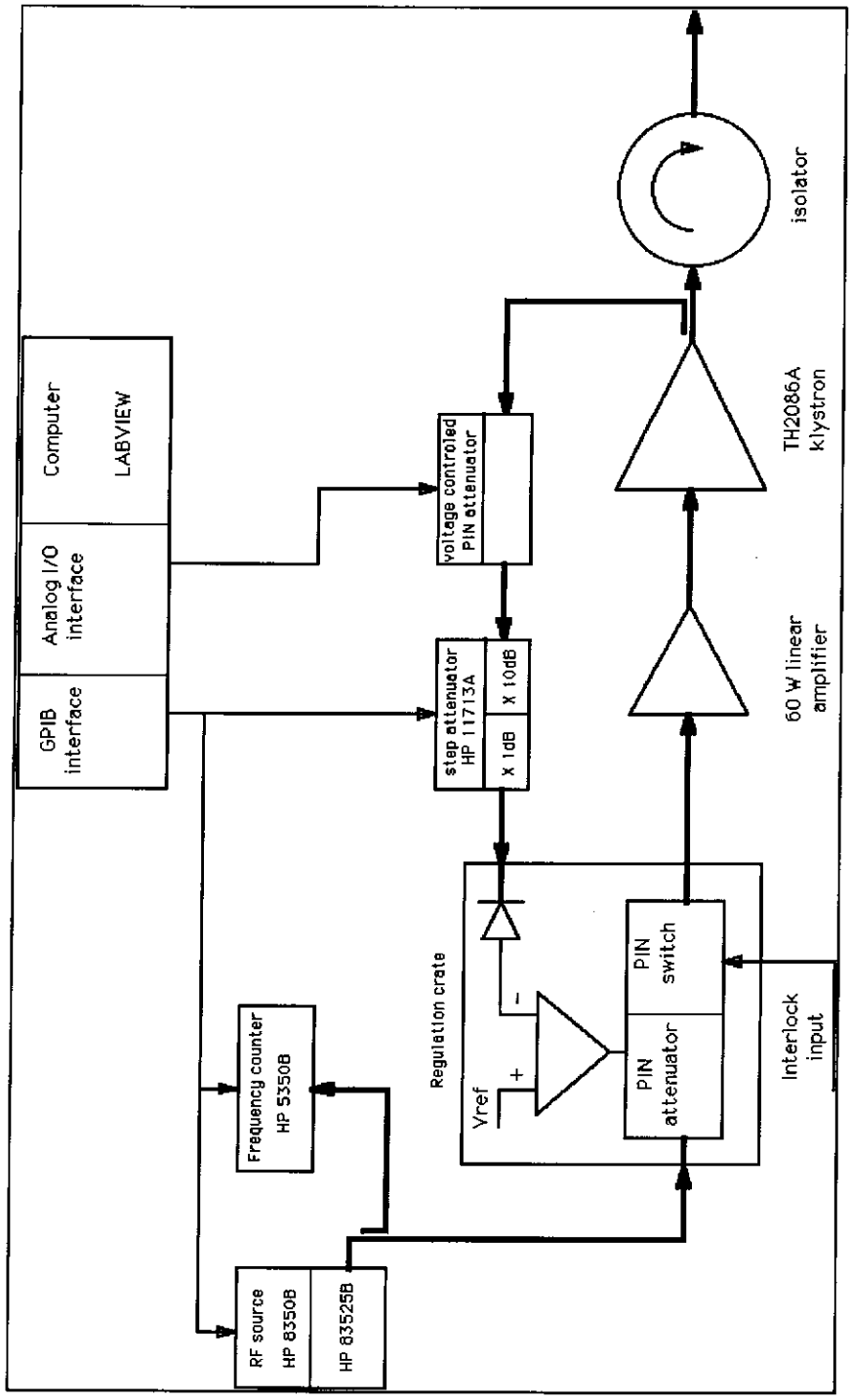

COMMISSARIAT À L'ÉNERGIE ATOMIQUE
DSM - DAPNIA
DIRECTION DES SCIENCES DE LA MATIÈRE

M.DESMONS

11 / 10 / 1998

DEPARTEMENT D'ASTROPHYSIQUE, DE PHYSIQUE DES PARTICULES,
DE PHYSIQUE NUCLÉAIRE ET DE L'INSTRUMENTATION ASSOCIÉE
SERVICE D'ÉTUDE DES ACCÉLÉRATEURS

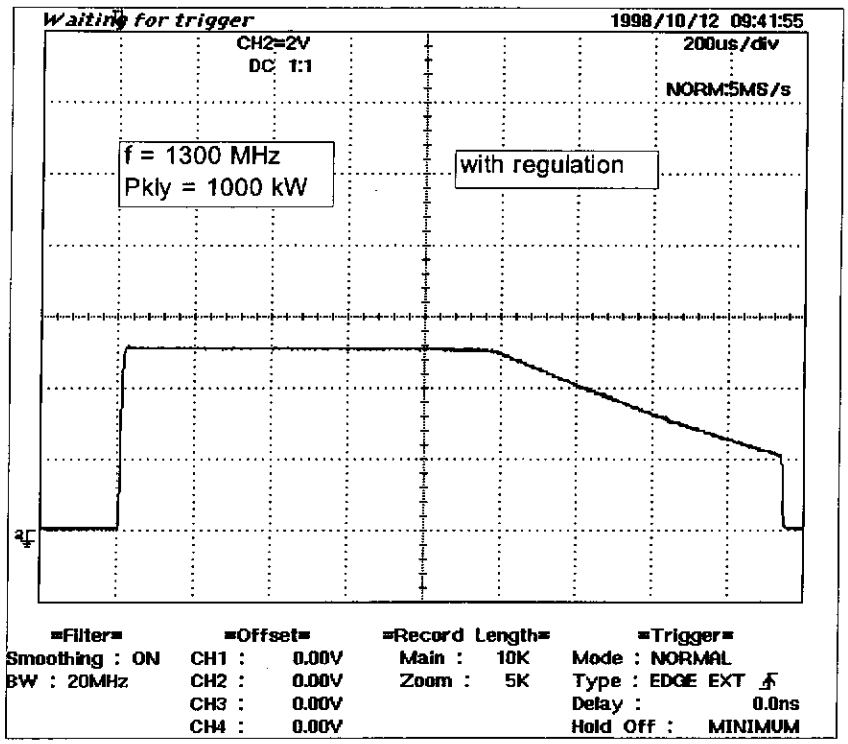
Waiting for trigger
1998/10/12 09:41:55
CH2=2V
DC 1:1
200us/div
NORM:5MS/s
f = 1300 MHz
Pkly = 1000 kW
with regulation
=Filter=
Smoothing : ON
BW : 20MHz
=Offset=
CH1 : 0.00V
CH2 : 0.00V
CH3 : 0.00V
CH4 : 0.00V
=Record Length=
Main : 10K
Zoom : 5K
=Trigger=
Mode : NORMAL
Type : EDGE EXT
Delay : 0.0ns
Hold Off : MINIMUM

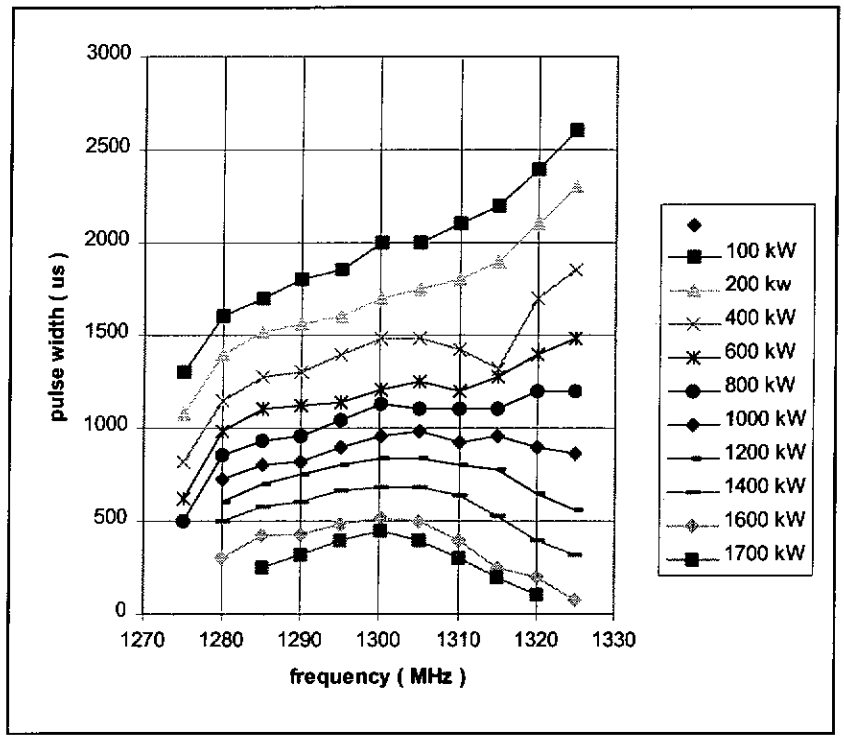
3000
2500
2000
1500
1000
500
0
pulse width (us)
1270
1280
1290
1300
1310
1320
1330
frequency (MHz)
100 kW
200 kw
400 kW
600 kW
800 kW
1000 kW
1200 kW
1400 kW
1600 kW
1700 kW

INTERLOCKS

Fast RF switch off (10 us delay) :

- over electron current in pick-up
- over signal on PM
- Transmitted power too low compared to klystron power
- Arc detection on the klystron window
- Output klystron power too low compared to the drive power

Slow RF switch off (10 ms delay) :

- Vacuum value > 10^{-6}mbar

Exemple of trip caused by over electron current

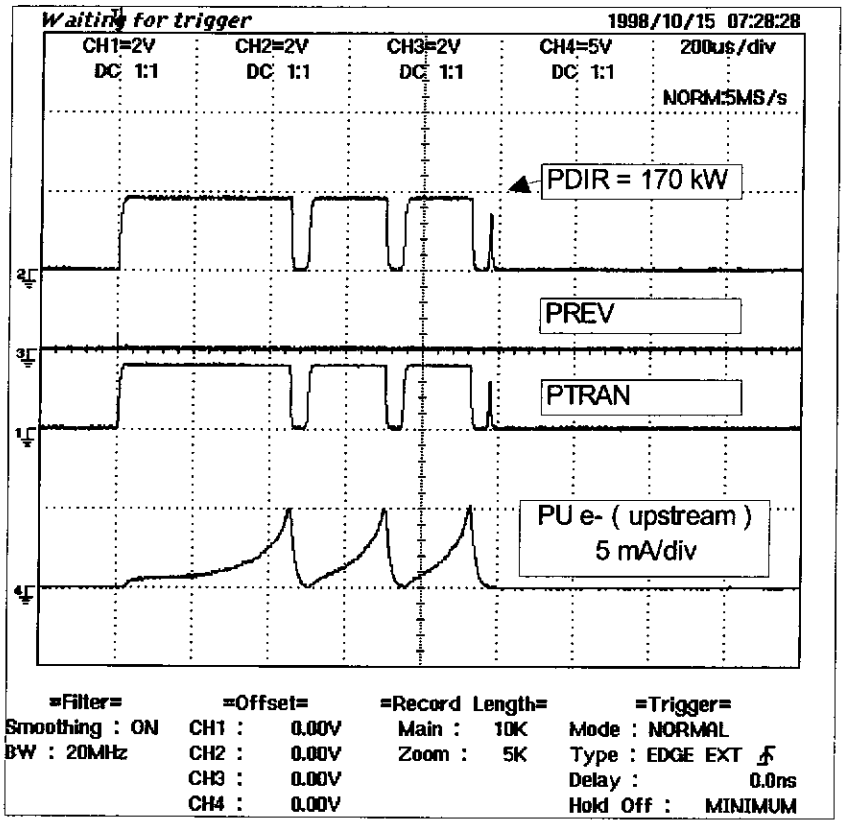

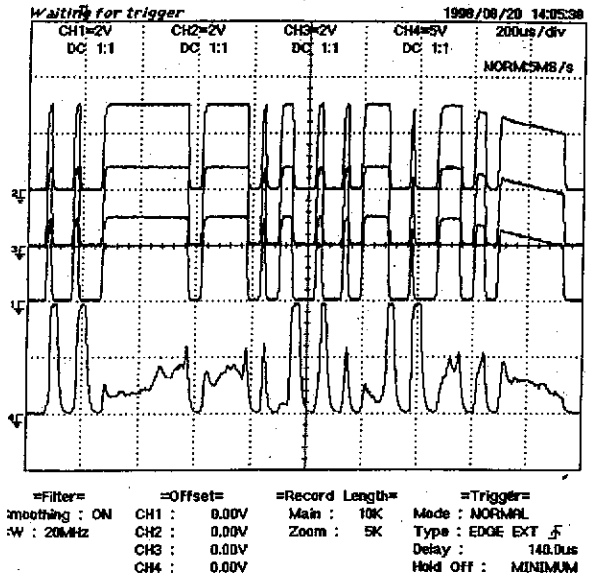
Waiting for trigger
1998/08/20 14:05:38
CH1=2V
DC 1:1
CH2=2V
DC 1:1
CH3=2V
DC 1:1
CH4=5V
DC 1:1
200us/div
NORM:5MS/s
=Filter=
moothing : ON
W : 20MHz
=Offset=
CH1 : 0.00V
CH2 : 0.00V
CH3 : 0.00V
CH4 : 0.00V
=Record Length=
Main : 10K
Zoom : 5K
=Trigger=
Mode : NORMAL
Type : EDGE EXT
Delay : 140.0us
Hold Off : MINIMUM

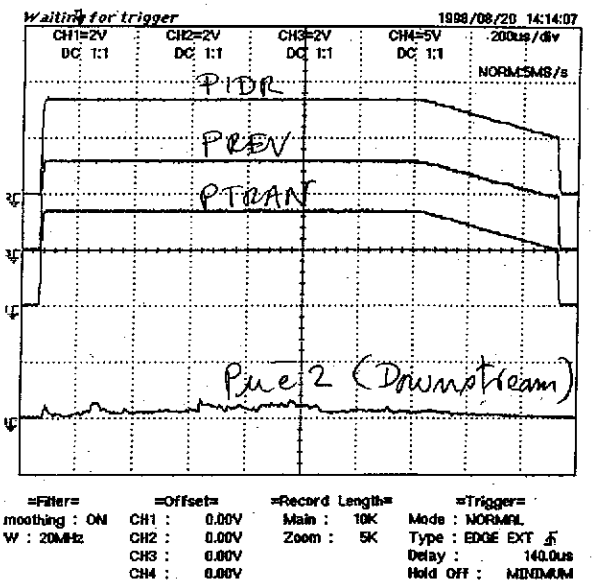
Waiting for trigger
1998/08/20 14:14:07
CH1=2V
DC 1:1
CH2=2V
DC 1:1
CH3=2V
DC 1:1
CH4=5V
DC 1:1
200us/div
NORM:5MS/s
PIDR
PREV
PTRAN
Pipe 2 (Downstream)
=Filter=
moothing : ON
W : 20MHz
=Offset=
CH1 : 0.00V
CH2 : 0.00V
CH3 : 0.00V
CH4 : 0.00V
=Record Length=
Main : 10K
Zoom : 5K
=Trigger=
Mode : NORMAL
Type : EDGE EXT
Delay : 140.0us
Hold Off : MINIMUM

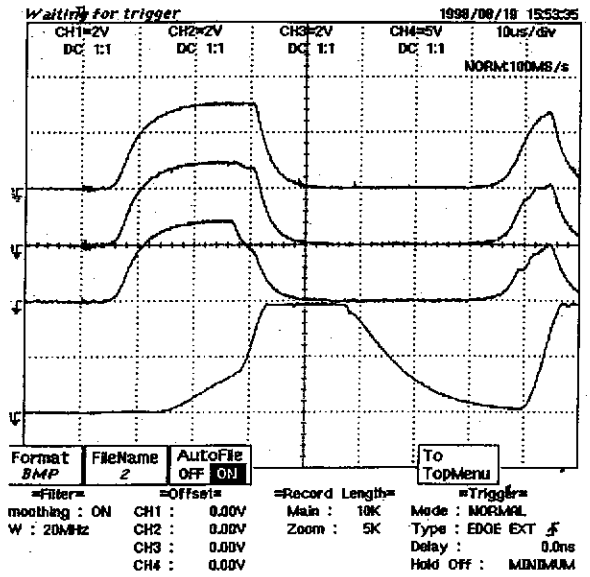
Waiting for trigger
1998/08/19 15:53:35
CH1=2V DC 1:1
CH2=2V DC 1:1
CH3=2V DC 1:1
CH4=5V DC 1:1
10us/div
NORM:100MS/s
Format BMP
FileName 2
AutoFile OFF ON
To TopMenu
=Filter= moothing : ON W : 20MHz
=Offset= CH1 : 0.00V CH2 : 0.00V CH3 : 0.00V CH4 : 0.00V
=Record Length= Main : 10K Zoom : 5K
=Trigger= Mode : NORMAL Type : EDGE EXT Delay : 0.0ns Hold Off : MINIMUM

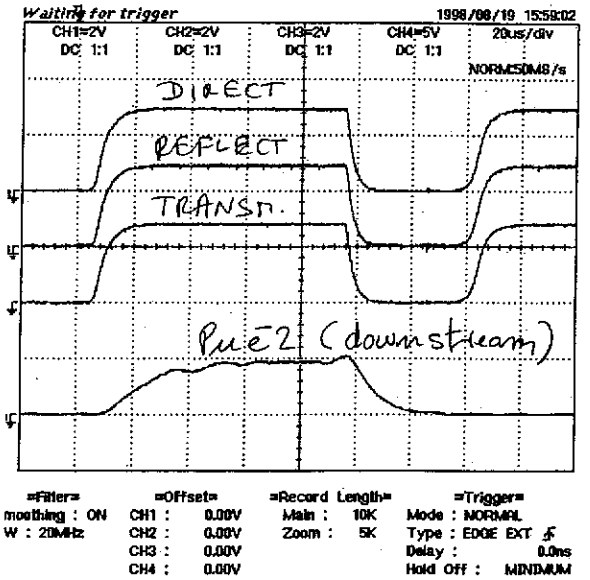
Waiting for trigger
1998/08/19 15:58:02
CH1=2V DC 1:1
CH2=2V DC 1:1
CH3=2V DC 1:1
CH4=5V DC 1:1
20us/div
NORM:50MS/s
DIRECT
REFLECT
TRANSM.
PuE2 (downstream)
=Filter= moothing : ON W : 20MHz
=Offset= CH1 : 0.00V CH2 : 0.00V CH3 : 0.00V CH4 : 0.00V
=Record Length= Main : 10K Zoom : 5K
=Trigger= Mode : NORMAL Type : EDGE EXT Delay : 0.0ns Hold Off : MINIMUM

ACQUISITIONS

Analog inputs :

Fast signals (RF, PM, electron currents):

2 National Instrument analog inputs devices (ATMIO 16 E 1)
10 us sample period, 2 ms acquisition length
5 values/parameter stored into files :

- Maximum value
- Minimum value
- Average value
- Pulse rising-edge time
- Pulse falling-edge time

Slow signals (vacuum):

1 National Instrument analog inputs device (ATMIO 16 E 10)
10 ms sample period, 1 s acquisition length
2 values/parameter stored into files :

- Initial value
- Maximum value

Temperature measurements :

1 HP voltmeter and GPIB interface

Frequency measurement :

1 HP RF counter and GPIB interface

Tests results

Christian Travier
CEA Saclay

Tests results

C. Travier

DSM/DAPNIA/SEA Saclay

- Data analysis
- List of tested components
- $\lambda/2$ window detailed results
  - SW@300 K
  - TW@300 K
  - SW@80 K

Recorded data

For each RF pulse, the following information is stored in a file

- RF power (input, transmitted, reflected)
- Field at window (upstream, downstream)
- Vacuum (upstream, dowstream) before pulse and max during pulse
- Electron and PM signals
- Temperatures
- Frequency, time

For each type of signal, one records

- the maximum value during the pulse
- the minimum
- the average
- the integral
- the beginning
- the end

Alltogether, 77 parameters are recorded for each pulse

Data analysis

For a typical run, one has to deal with:

300000 pulses * 77 data = 23 millions
= 100 Mo

~8 hours @10 Hz (~1 month @ 0.1 Hz)

Too big to be treated with EXCEL type softwares

We use PAW (Physics Analysis Workstation)
used at CERN for high energy physics

A Fortran program reads the data files, and put them into Column Wise Ntuples through HBOOK library. The datas are then viewed with PAW++, in a interactive way, with the following possibilities:

- plot any data vs. any other data (2 or 3 D)
- histogram of any data
- cuts, fits, etc..

List of tested components

Waveguide to coax transition

tested 04/1997	**• 4 stubs transition (Φ40)**	OK 1 MW
tested 04/1997	**• doorknob transition**	OK 1 MW
tested 11/1997	**• antenna transition**	OK 1 MW
to be tested	**• polarized doorknob transition**	

Cold windows

tested 07/1997	**• FERMI conical window**	OK 1 MW @300K
tested 08/1998	**• λ/2 window**	OK 1 MW @300K and 80 K
to be tested	**• travelling wave window**	

Other components

tested 05/1997	**• ϕ60-ϕ40 tapered transition**	not OK multipactor for P<500 kW
to be tested	**• λ/2 RF trap**	
to be fabricated	**• ϕ60-ϕ40 step transition**	

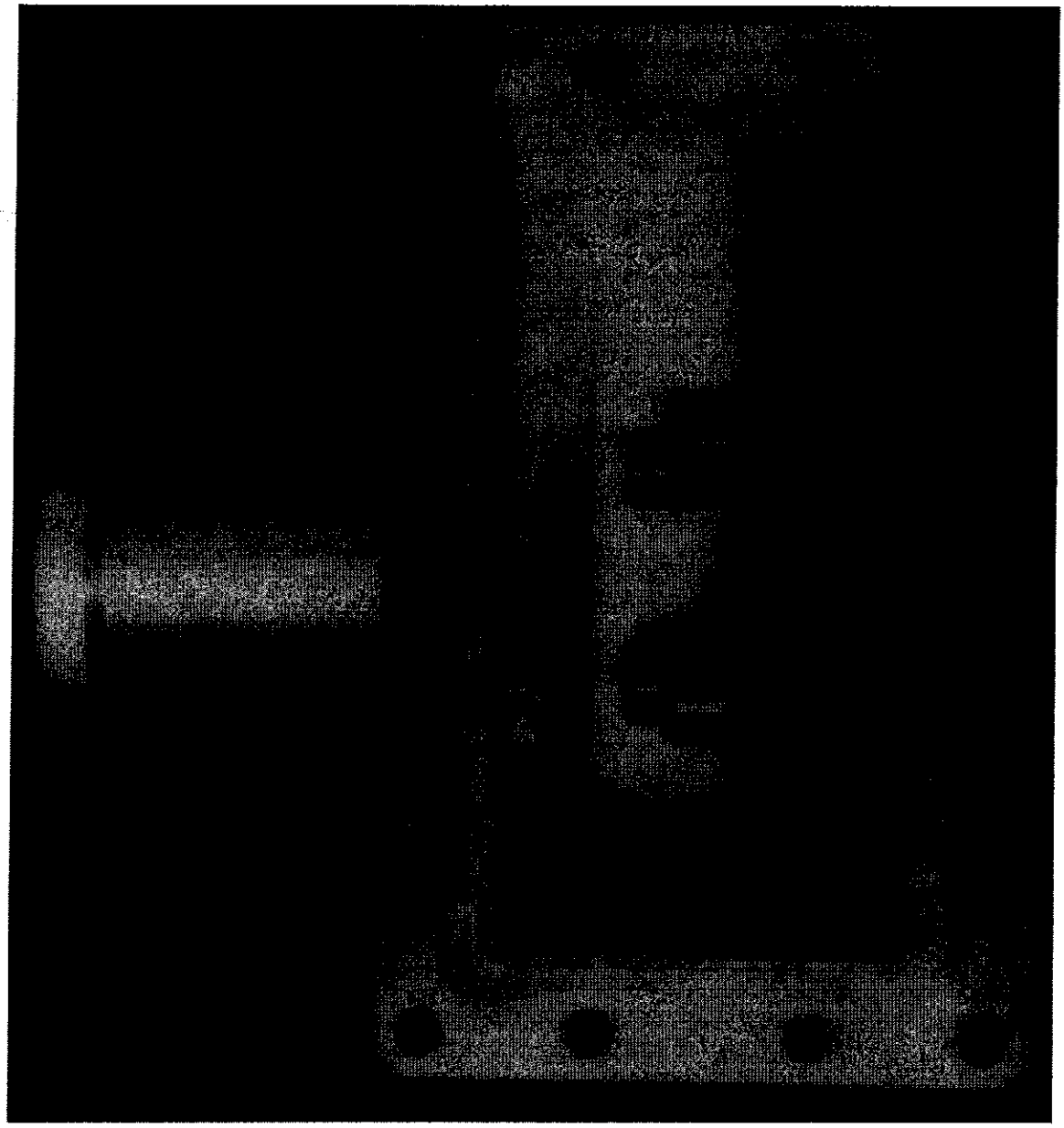

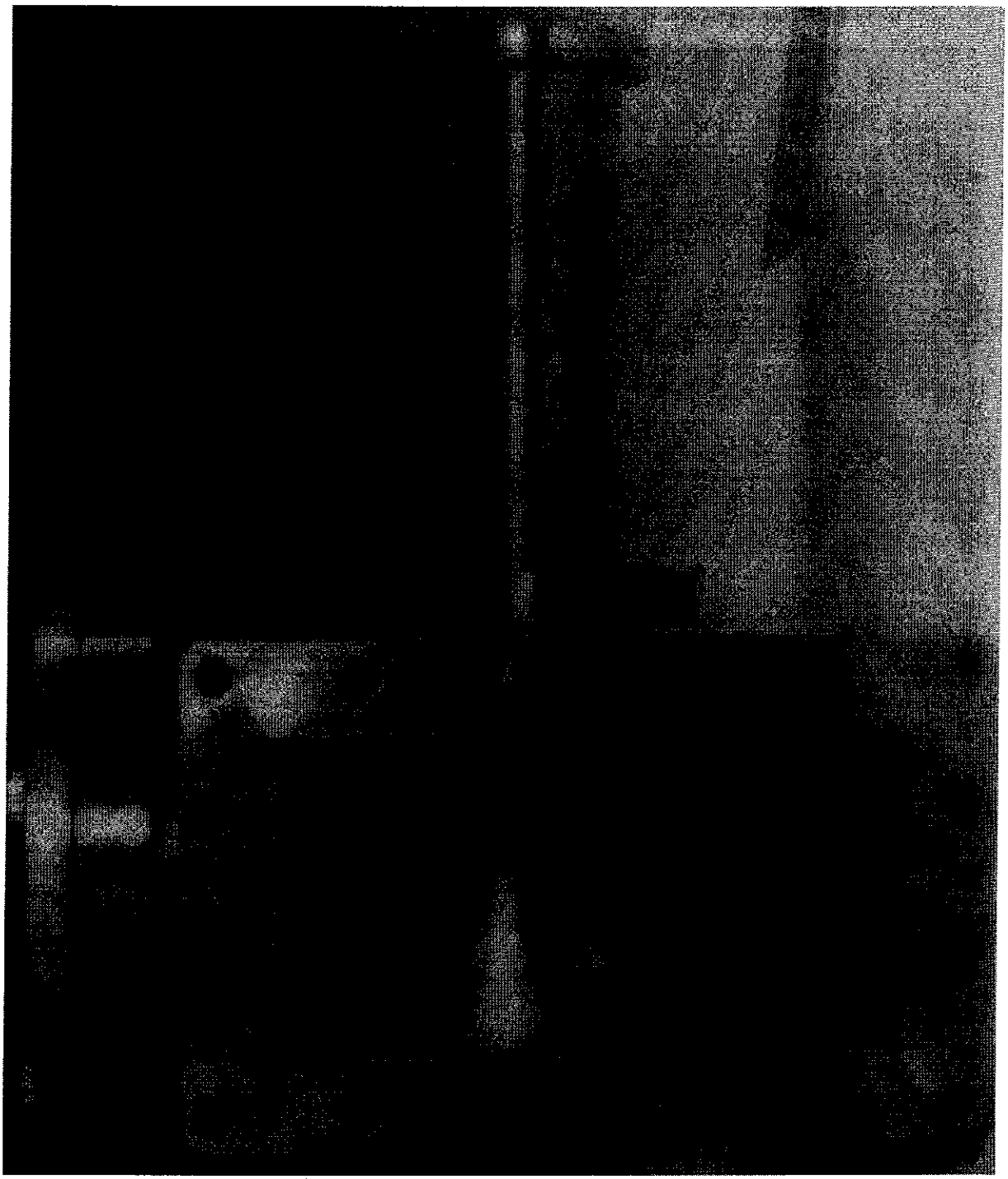

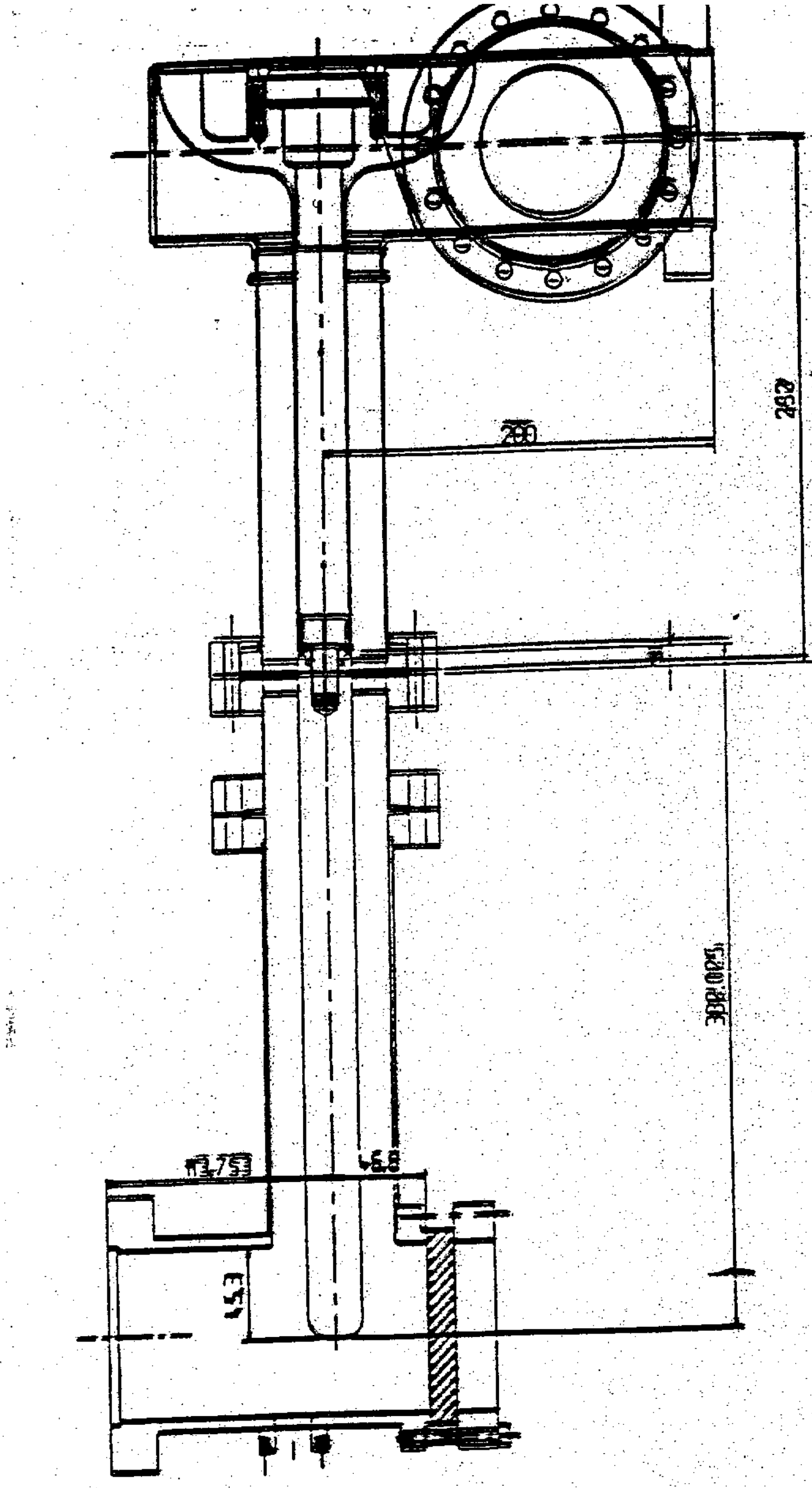

λ/2 window

Advantages	Drawbacks
•easiest concept	•maximum field
•low cost	at brazing point
•robustness	•high dielectric losses
•E field parallel to ceramic	•direct view of
➡ no multipactor	cavity electrons

Fabricated by SICN

ceramic: Wesgo Al300
+ TiN coating
inner conductor: copper
outer conductor: kovar +
copper coated SS

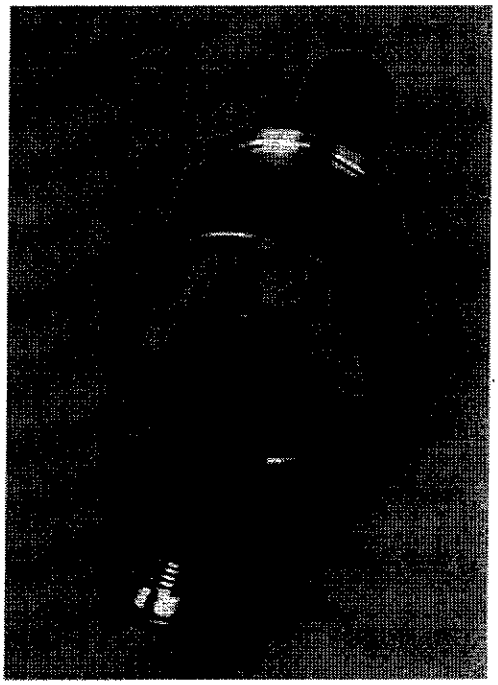

λ/2 window experiment

1) Conditionning at 300 K, Standing wave (SW)

from august 10 to september 25: 338000 pulses

2) Conditionning at 300 K, Travelling wave (TW)

from september 25 to september 28: 28000 pulses

3) Losses measurements at 300 K, 1 MW, SW

from september 28 to october 9: 97000 pulses

4) Conditionning at 80 K, SW

from october 12 to october 15: 20000 pulses

5) Conditionning at 80 K, TW

from october 15 to now:

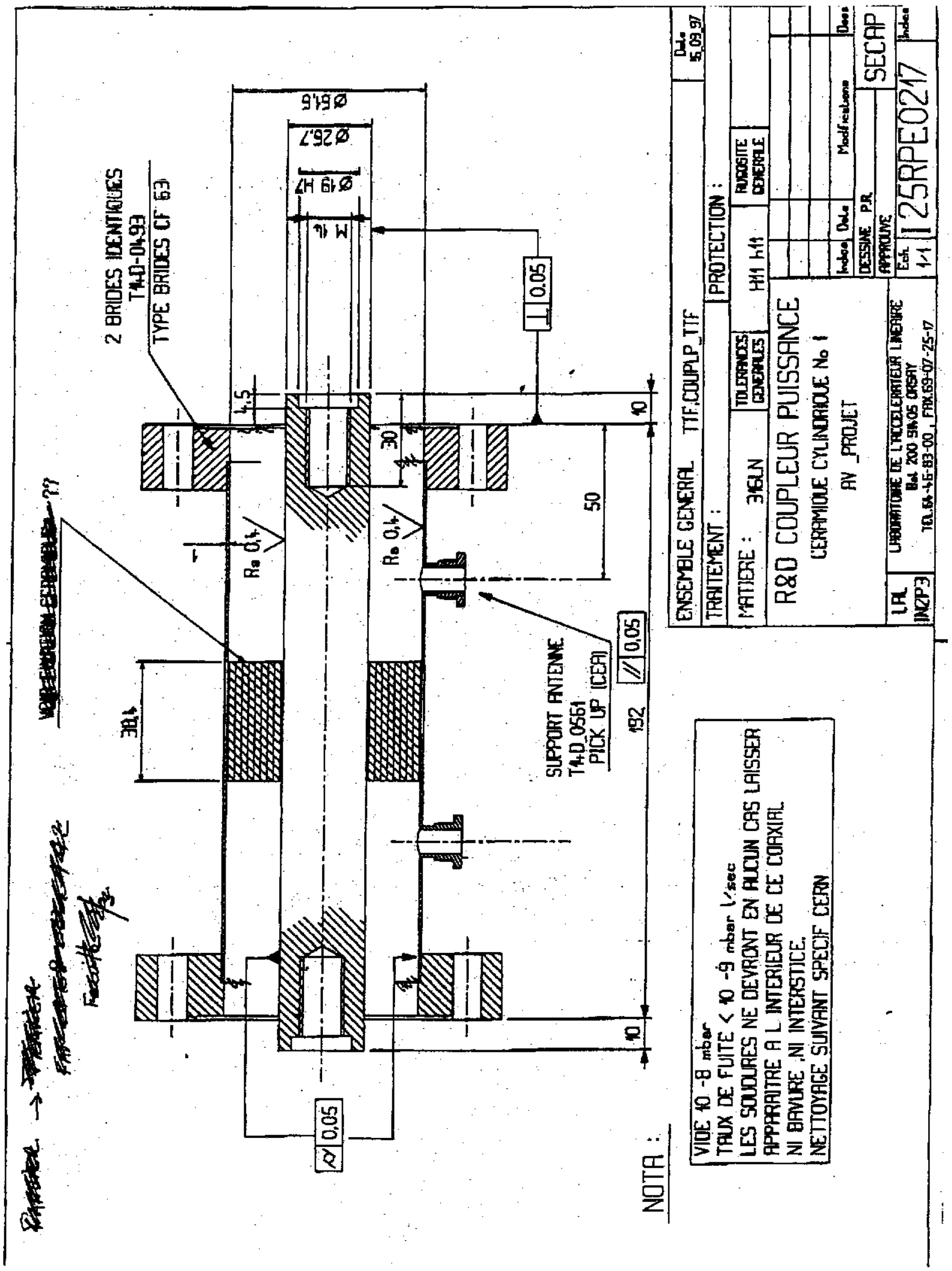
2 BRIDES IDENTIQUES
T4D-0493
TYPE BRIDES CF 63
Ø61,6
Ø26,7
Ø19 H7
M 4
0,05
4,5
10
30
50
Ra 0,4
38,1
SUPPORT ANTENNE
T4D_0561
PICK UP (CEA)
0,05
192
NOTA :
VIDE 10 -8 mbar
TAUX DE FUITE < 10 -9 mbar l/sec
LES SOUDURES NE DEVRONT EN AUCUN CAS LAISSER
APPARAITRE A L INTERIEUR DE CE COAXIAL
NI BAVURE ,NI INTERSTICE.
NETTOYAGE SUIVANT SPECIF CERN
ENSEMBLE GENERAL TTF.COUPLP_TTF
TRAITEMENT :
PROTECTION :
MATIERE : 316LN
TOLERANCES GENERALES
H11 h11
RUGOSITE GENERALE
R&D COUPLEUR PUISSANCE
CERAMIQUE CYLINDRIQUE No 1
AV_PROJET
LAL
IN2P3
SECAP
125RPE0217
Ech. 1/1
DESSINE P.R.
APPROUVE
Date 15.09.97

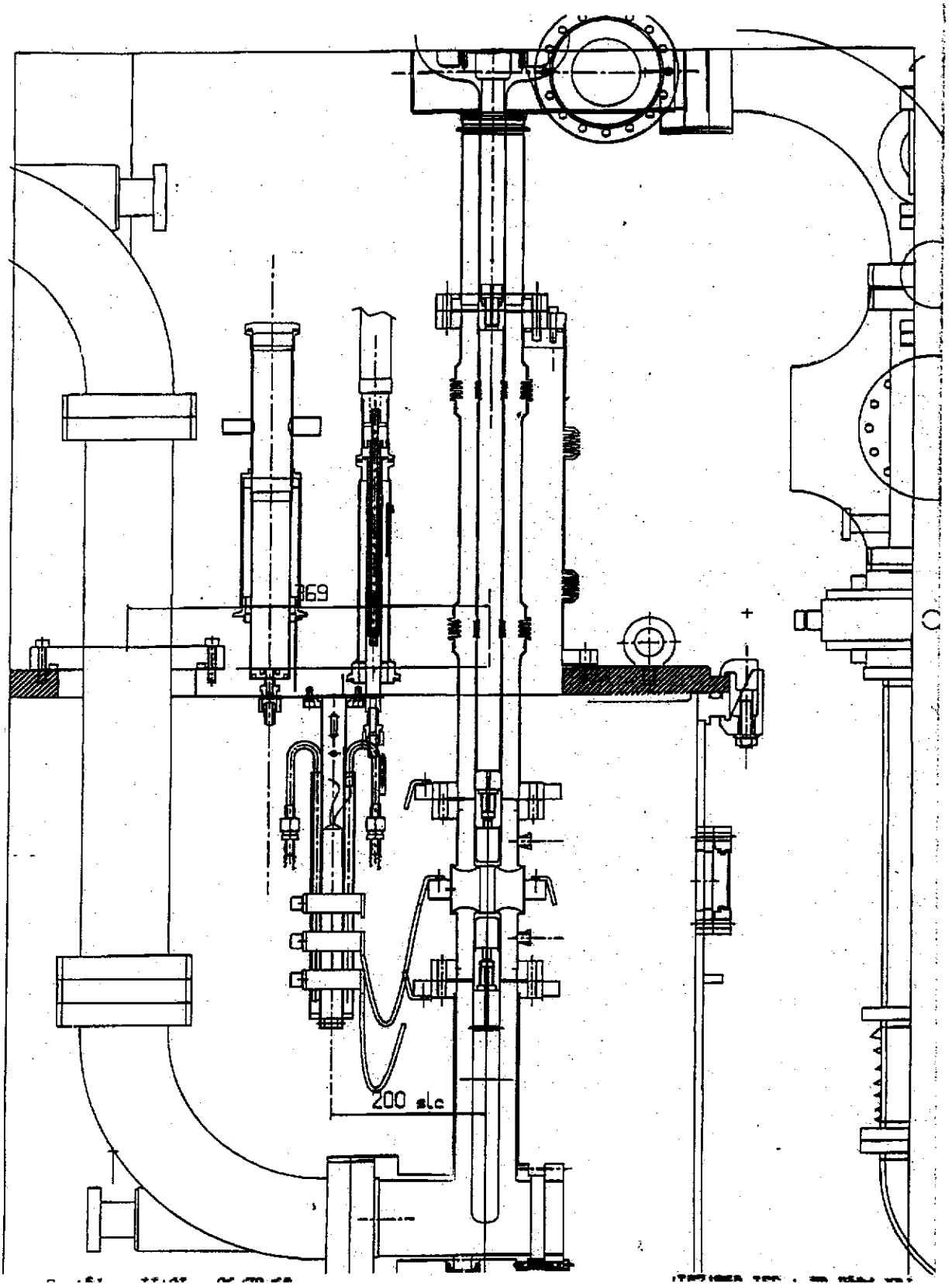
369
200 slc

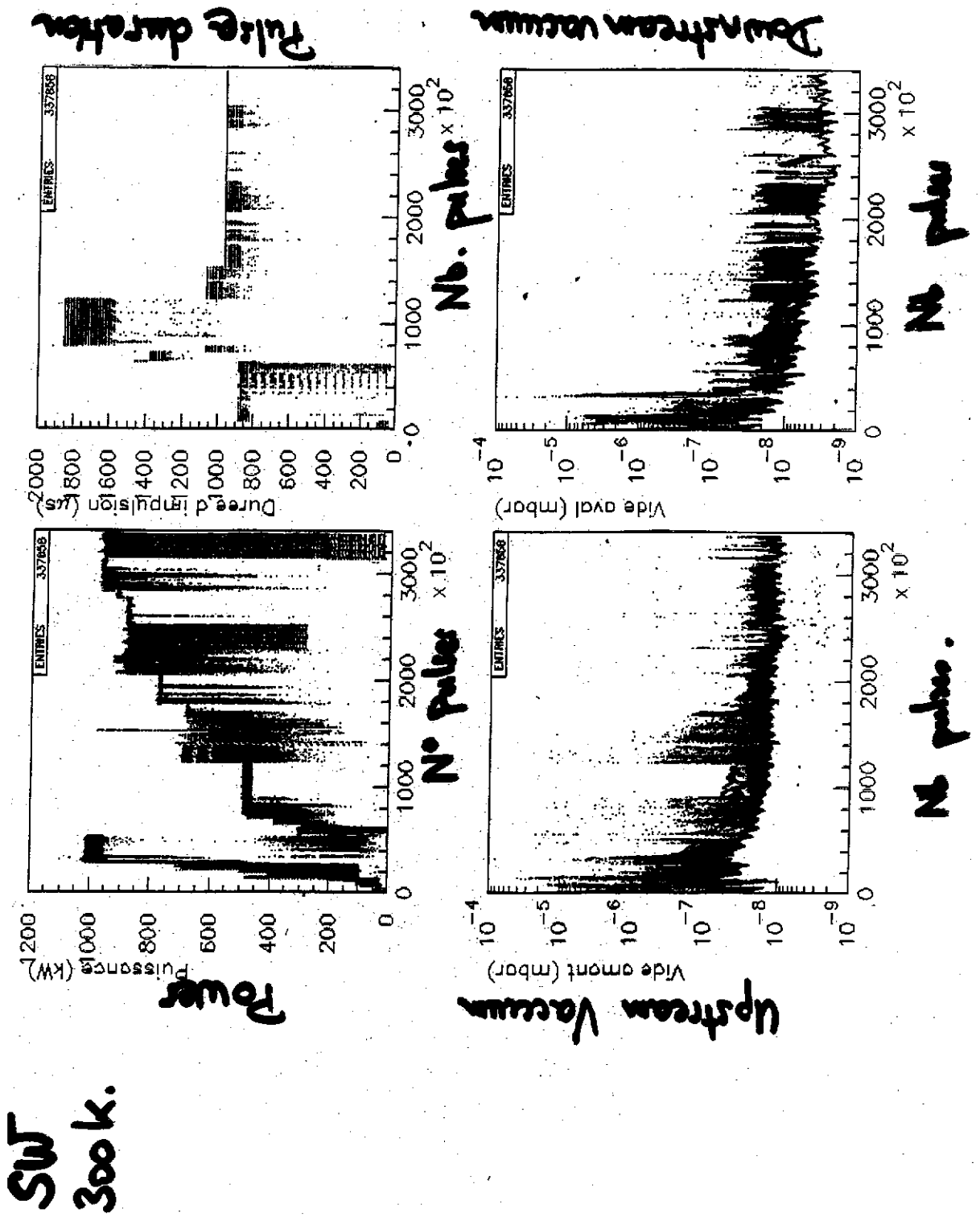
SW 300 k.
Upstream Vacuum
Vide amont (mbar)
ENTRIES 3378568
N° Pulse
Power
Puissance (kW)
Pulse duration
Durée d'impulsion (µs)
Downstream vacuum
Vide aval (mbar)
Nb. Pulses

SW 300 k

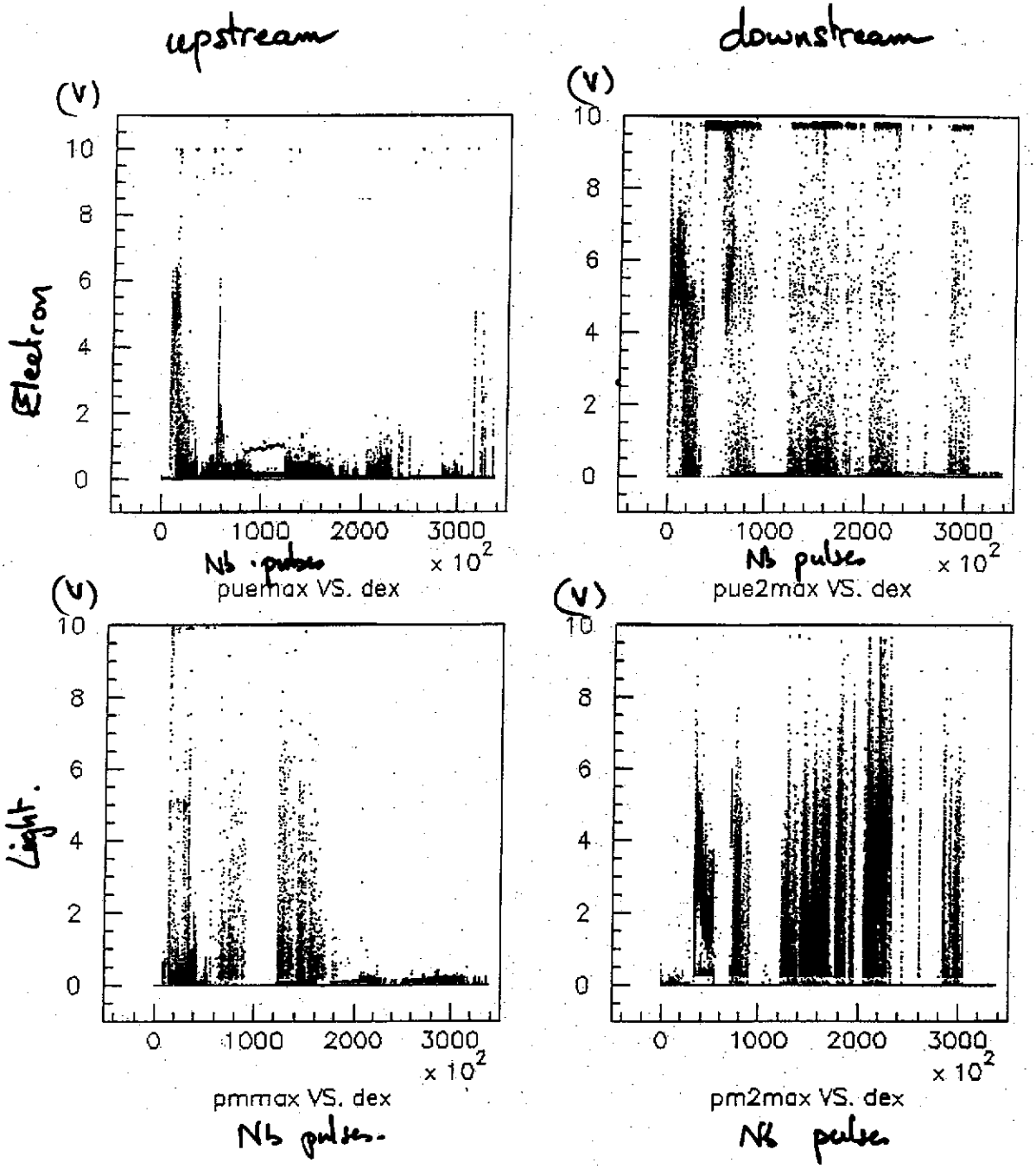
upstream
downstream
(V)
Electron
10
8
6
4
2
0
0
1000
2000
3000
x 10^2
Nb pulses
puemax VS. dex
pue2max VS. dex
Light.
pmmax VS. dex
pm2max VS. dex
Nb pulses

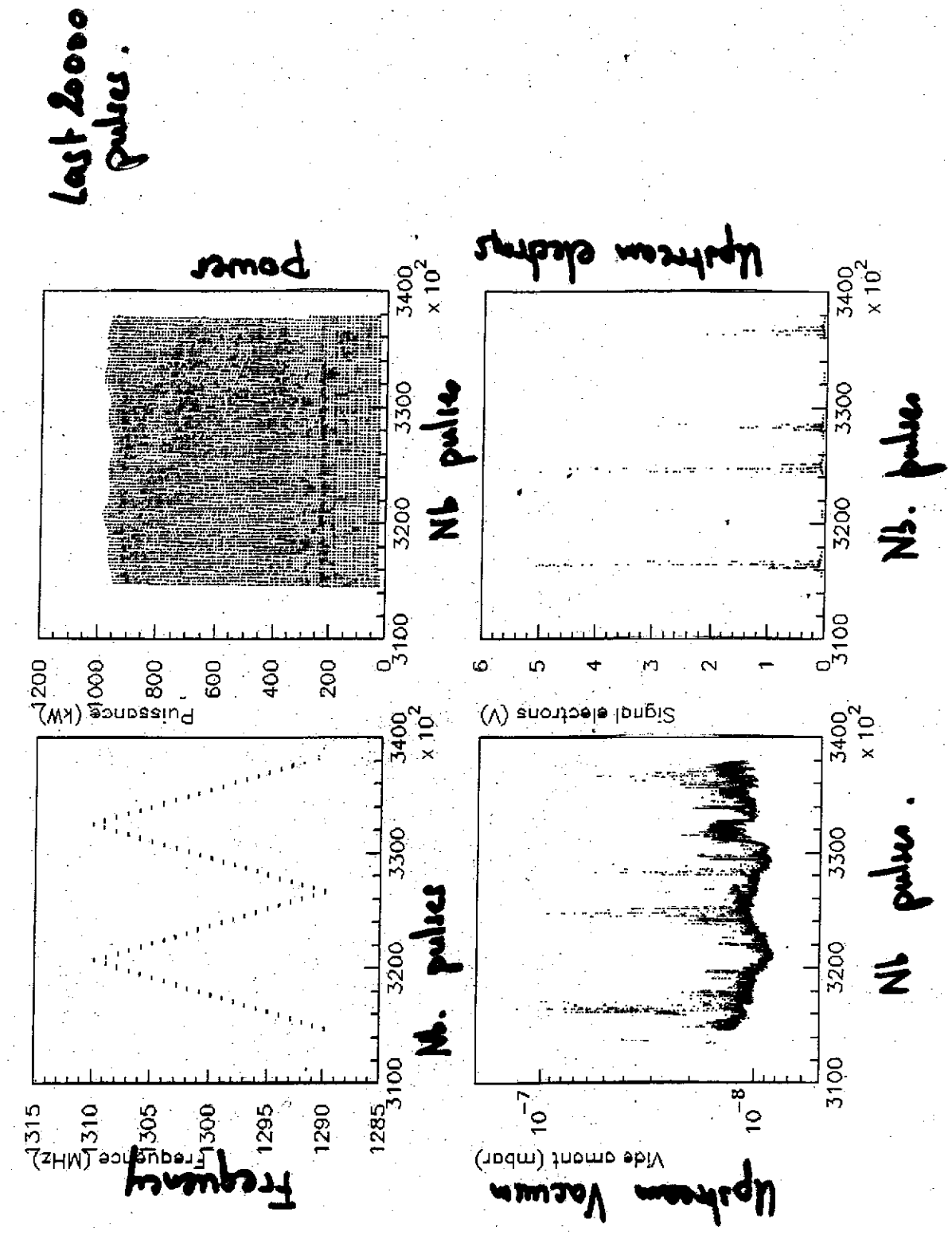
Last 2000 pulses.
Power
Nb pulse
Klystron electrons
Nb. pulse
Puissance (kW)
Signal électrons (V)
Nb. pulses
Nb pulse.
Frequency
Klystron Vacuum
Fréquence (MHz)
Vide amont (mbar)
SW 300K

Nombre impulsions
Frequence (MHz)
Puissance (kW)
Nombre impulsions
Frequence (MHz)
Puissance (kW)

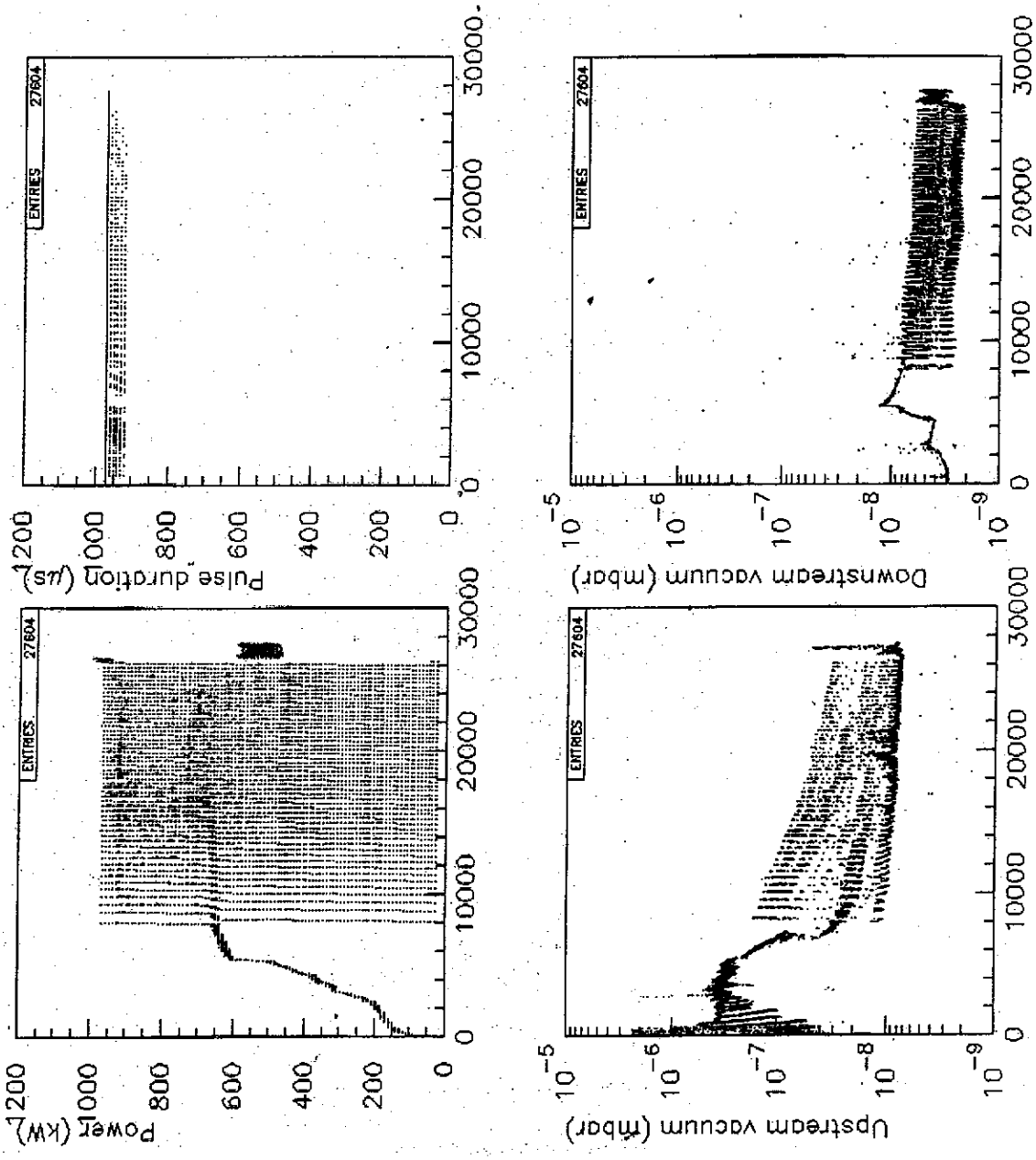
Power (kW)
Pulse duration (μs)
Upstream vacuum (mbar)
Downstream vacuum (mbar)
ENTRIES 27604

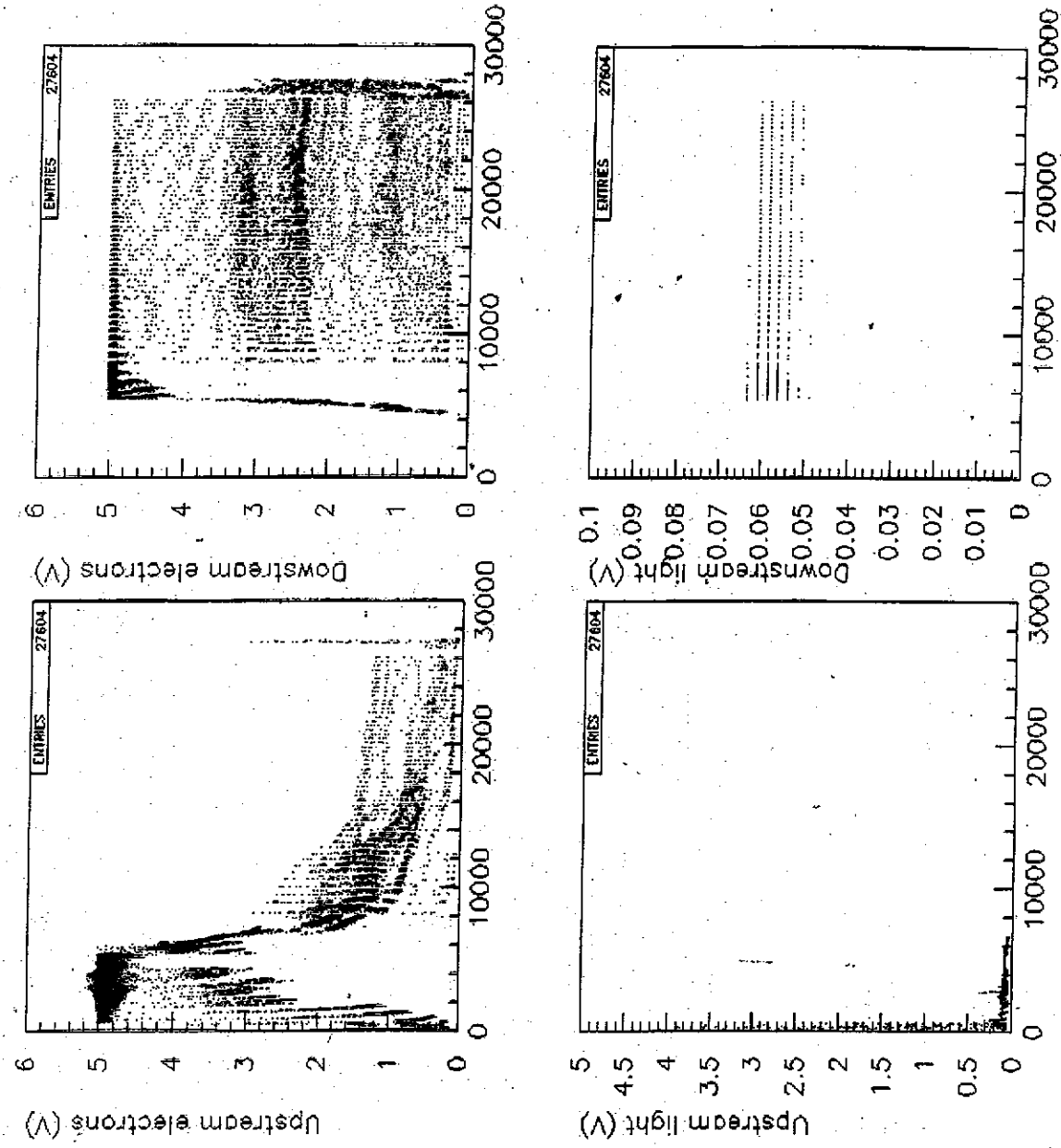
Upstream electrons (V)
Downstream electrons (V)
Upstream light (V)
Downstream light (V)
ENTRIES
27604

TW 300K

TW 300k

10000 pulses.

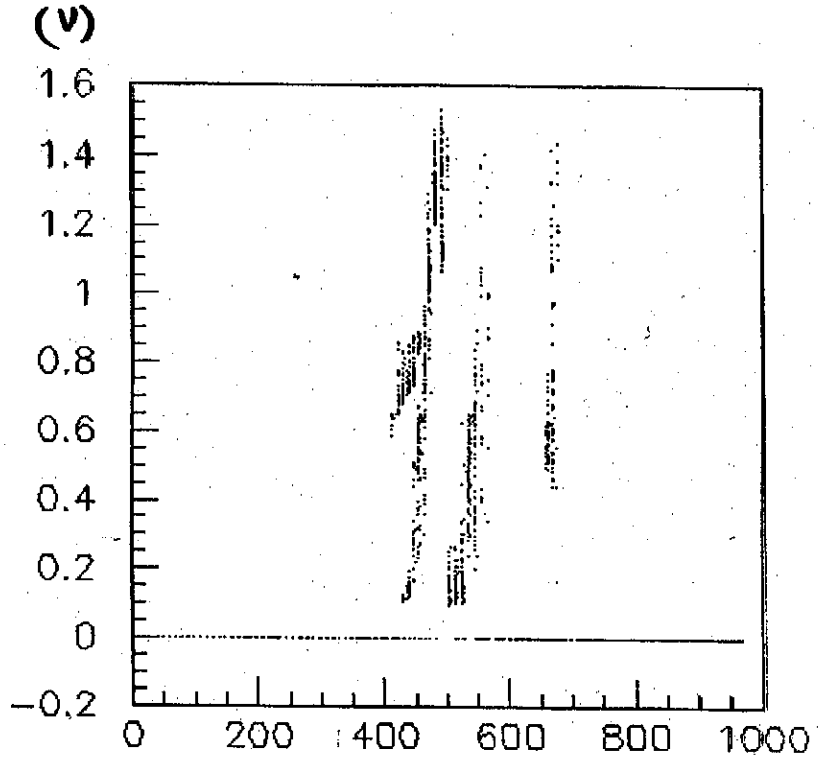

puemax VS. pdirmax

upstream electrons vs Power (kW)

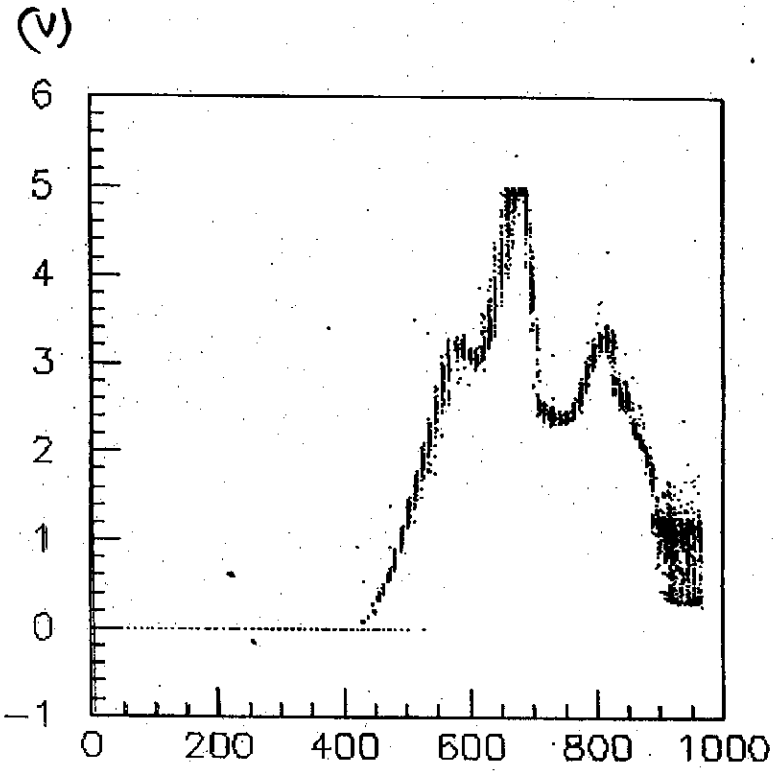

pue2max VS. pdirmax

downstream electrons vs. Power (kW)

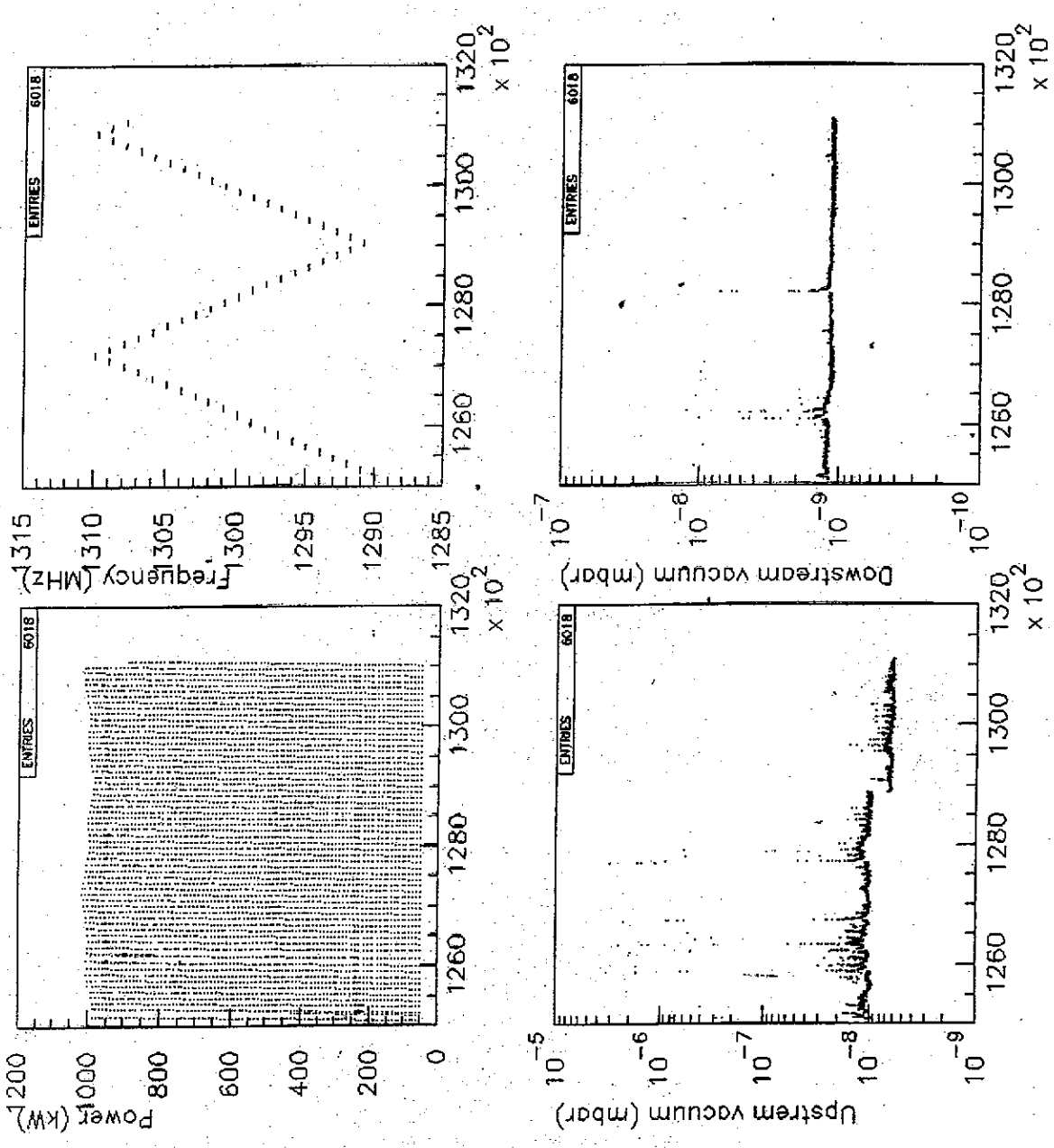
Power (kW)
Frequency (MHz)
Upstream vacuum (mbar)
Downstream vacuum (mbar)
ENTRIES
6018
x 10^2

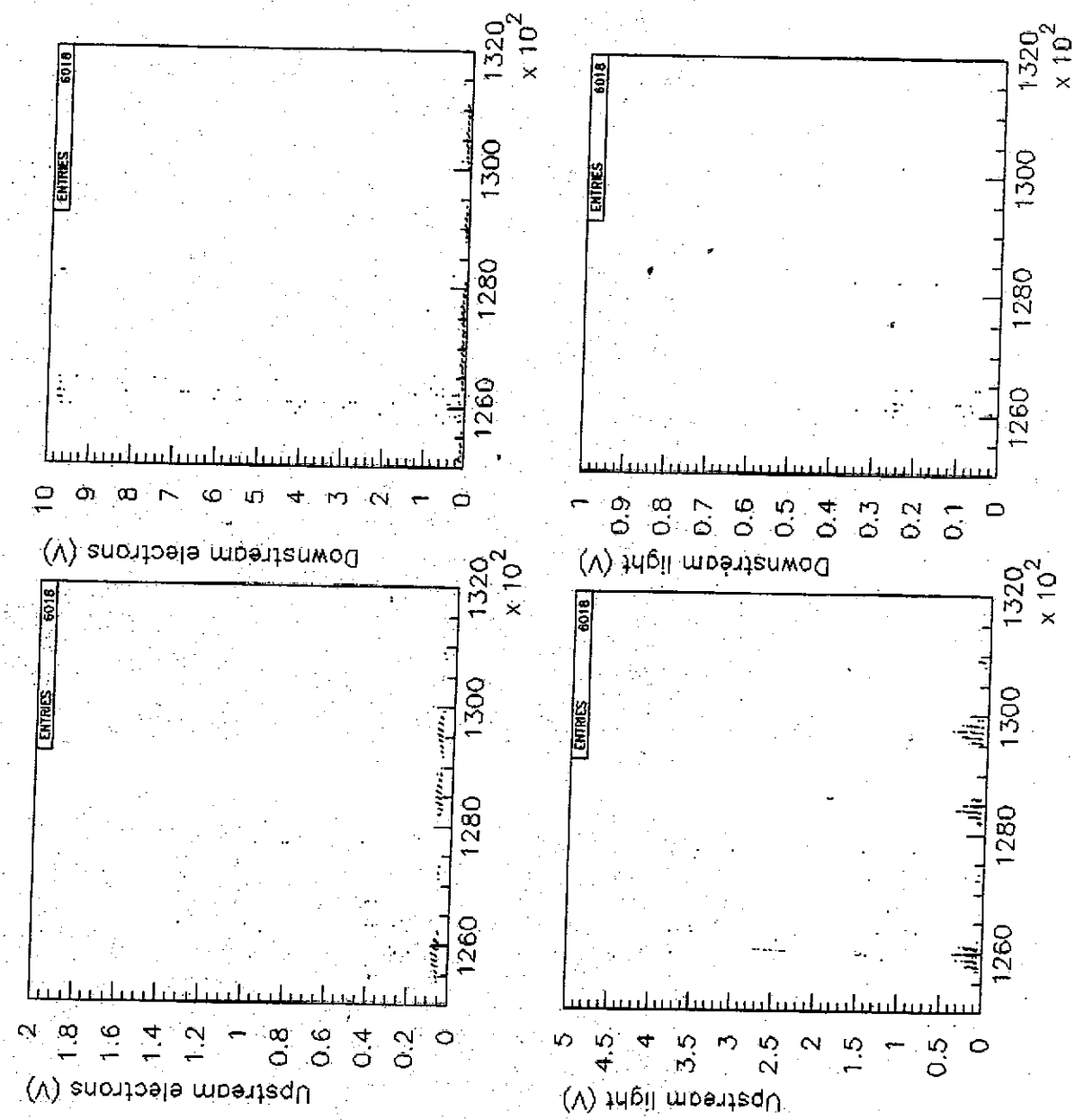
Upstream light (V)
Downstream light (V)
Upstream electrons (V)
Downstream electrons (V)
ENTRIES
6018
x 10²
1260
1280
1300
1320

C. Travier, TTF coupler meeting, Saclay, October 19-20, 1998

PROBLEMS WITH DATA ANALYSIS.

- Real local field not known.

  Due to mismatches, it is very difficult to know exactly what is the field value at each point of the system.

  ↳ this messes up the multipacting barrier analysis.

- Difficulty to localize multipacting events

  In principle, the frequency pattern of electrons or light signals indicates where multipactor is happening.

  in reality, it is difficult due to:

  - a lack of precision. (waveguide is too short).
  - difficulty to simulate precisely (mismatch)

- Low repetition rate limits the number of experiments needed to confirm hypothesis.

Dielectric losses. ½ window

1 MW, 1 ms, 0,1 Hz

1 W SW @ max field
0,1 W SW @ min field
0,3 W TW

With TESLA numbers:

0,2 MW
5 Hz
500 µs TW
800 µs SW

→ 3 W.

CONCLUSION ON λ/2 WINDOW

(1) It can be fabricated

brazing ceramic to outer and inner conductors over 3.84 cm is possible

(2) Max Field at brazing location not a problem

assuming brazing is done correctly.

(3) It stands 1 MW, 1 ms (SW and TW) both at 300 k and 80 k.

(4) High dielectric losses

0.8-1W @ 1MW, 0,5 Hz (SW case)

↑ calculated ↑ measured including resistive losses

(5) Behaviour at 10 Hz to be checked.

This experiment showed than MEGO parameters are not correct.

$\varepsilon = 9 \longrightarrow 9.6$

$\tan\delta = 3.10^{-4} \longrightarrow 4\text{-}5\ 10^{-4}$

to be confirmed

Window design

Christian Travier
CEA Saclay

Window design

C. Travier

DSM/DAPNIA/SEA Saclay

- Window RF design tool
- Window comparison criteria
- Travelling wave window design
- Mechanical simulations
- Coupler design

Windows RF studies

RF studies are done with SUPERFISH

- run on a PC
- allow good definition (small mesh size
  0.5 mm -> 400 k mesh -> 5 minutes)
- good plotting facilities
- simulation of TW
- FORTRAN codes to calculate SWR,
  do automatic matching, calculate bandwidth

Cold window comparison

Criteria to compare windows:

- maximum field on ceramic, at brazing location
- bandwidth
- multipactor (normal E field at ceramic)
- ghosts modes
- dielectric losses
- exposure to cavity electrons and X-rays
- mechanical and thermal properties
- mechanical tolerances
- number of braze or weld
- fabrication process (price)
- easiness to clean
- .....

Window comparison

good bad

	Conical	Cylindrical	Lambda/2	Concave	TW	Double coax	Double coax 2	Stair
Ceramic thickness (mm	3	4	38,4	38,4	20	10	10	20
Bandwidth (MHz) (S11<0,2)	> 1000	> 1000	131	390	340	120	170	220
Emax/Ecoax ϕ60	1,2	3	1	1,6	2,2	2,6	2,4	2,4
Emax brazing/ Ecoax F60	0,4	1,5	1	0,1	0,6	0,2	0,2	0,2
Emax ceramic/ Ecoax F60	1	2,9	1	0,6	0,6	0,2	0,2	0,2
Dielectric power loss /Conical window power loss	1	1,3	13,6	10,2	7,7	1,6	2,4	5,2
Multipactor	- -	-	+ +	+	++	++	++	++
Exposure to electrons impact	- -	++	- -	- -	-	++	++	+
Fabrication (price)	- -	- -	+ +	+	+	+	+	++

difficulty to estimate precisely the maximum field

C. Travier, TTF coupler meeting, Saclay, October 19-20

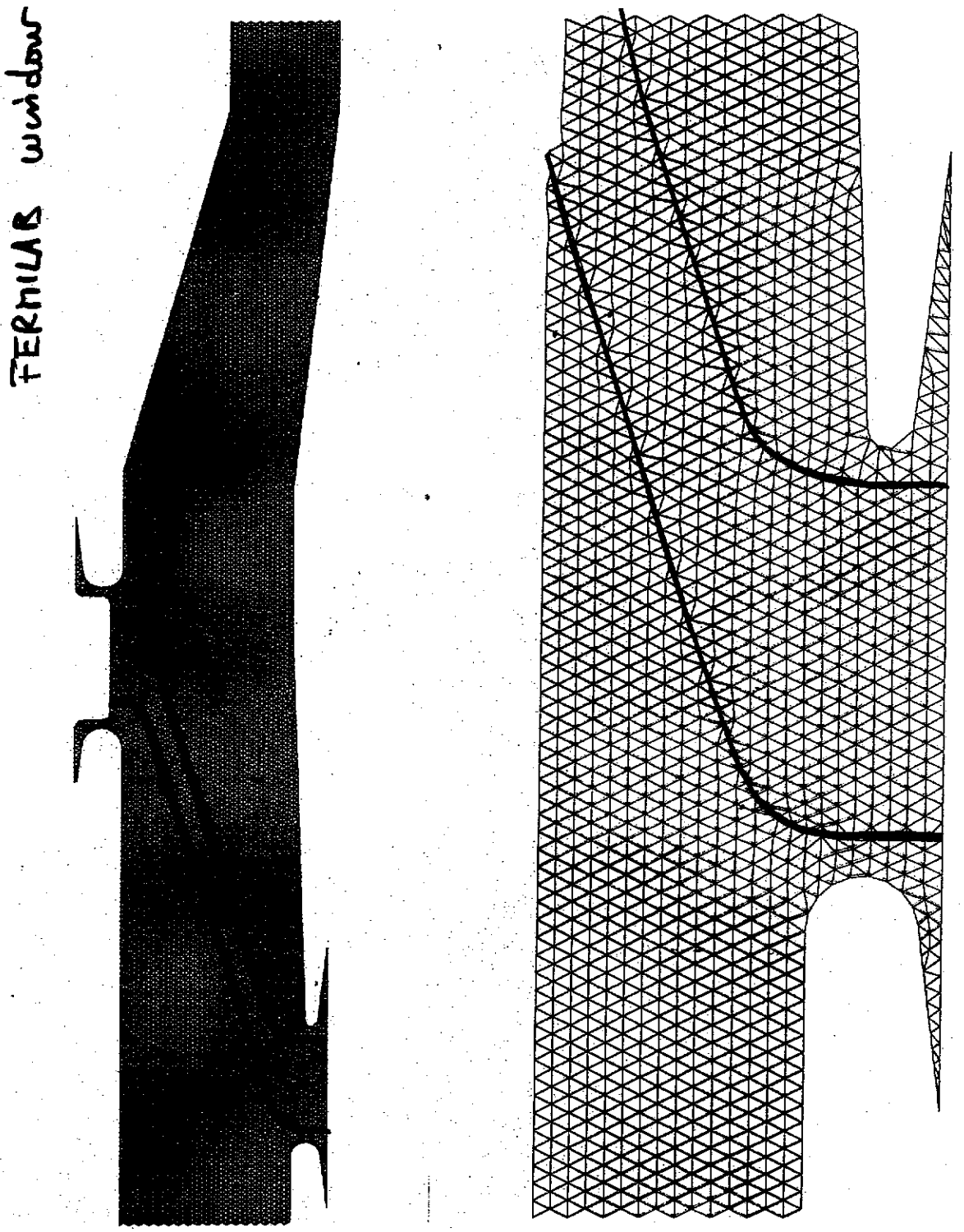

C. Travier, TTF coupler meeting, Saclay, October 19-20

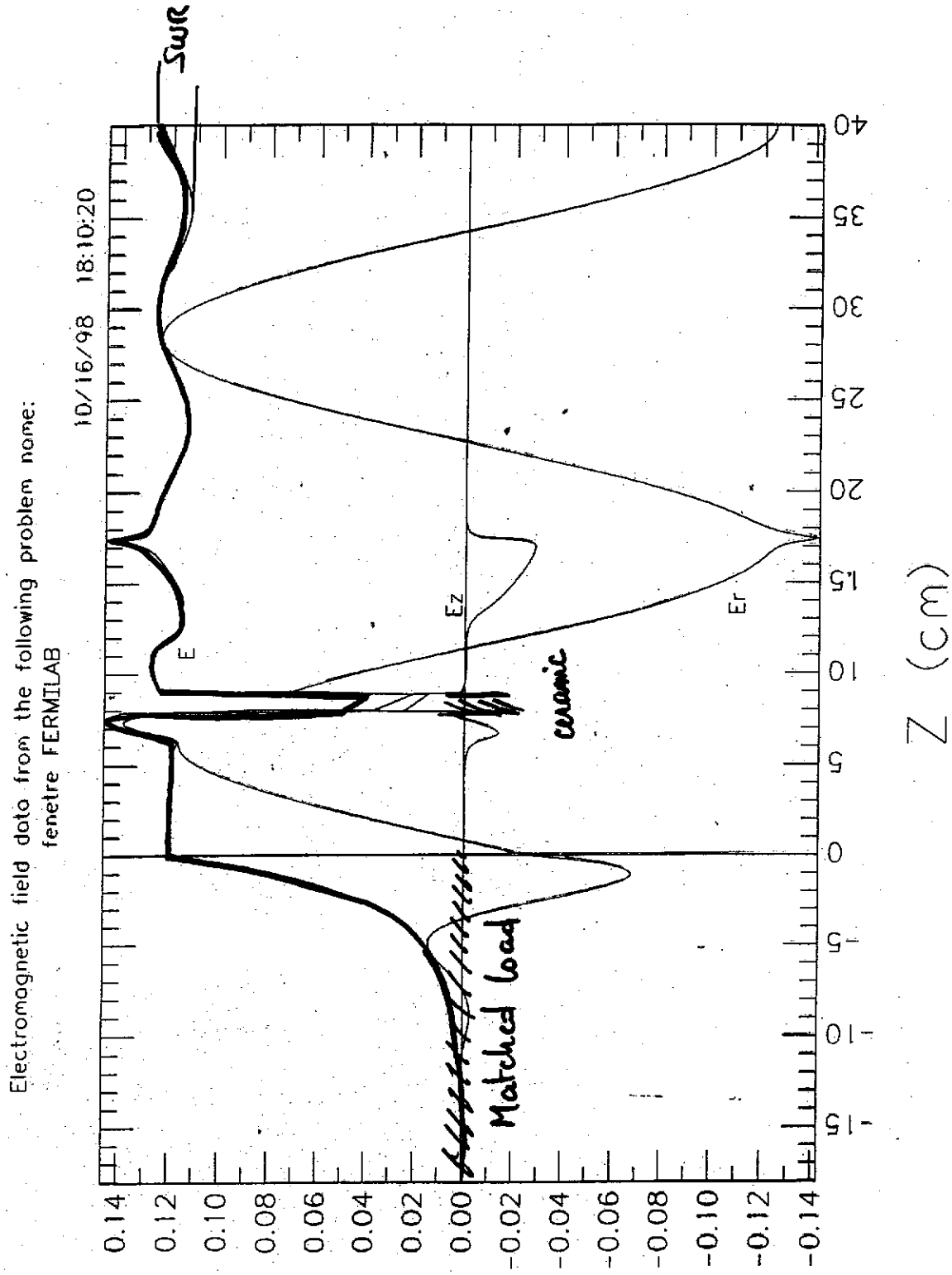

C. Travier, TTF coupler meeting, Saclay, October 19-20

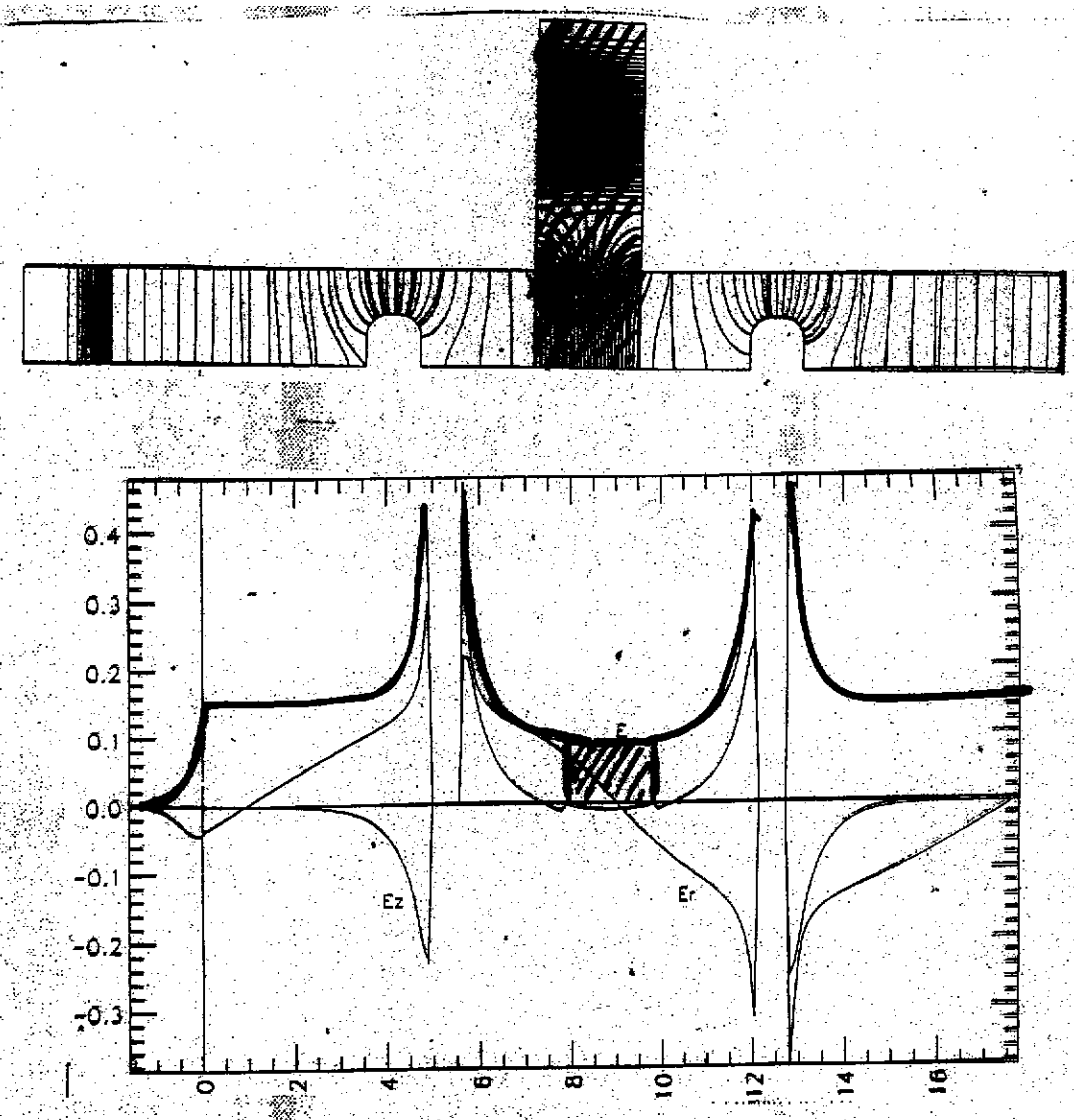

TW window (A. Mosnier design).

Advantages: - pure travelling wave inside ceramic (lower field).
- no ⊥ field → no multipactor.

Drawbacks of this particular design.
- higher field at matching disks.
- direct view of cavity e^-
- no easy to fabricate.

C. Travier, TTF coupler meeting, Saclay, October 19-20

Travelling Wave Window (Stair like)

Advantage : - no direct view of cavity e⁻
- easy to fabricate.
- can be optimized analytically (MATHEMATICA)

Drawbacks : - high field
- very long (25 cm)

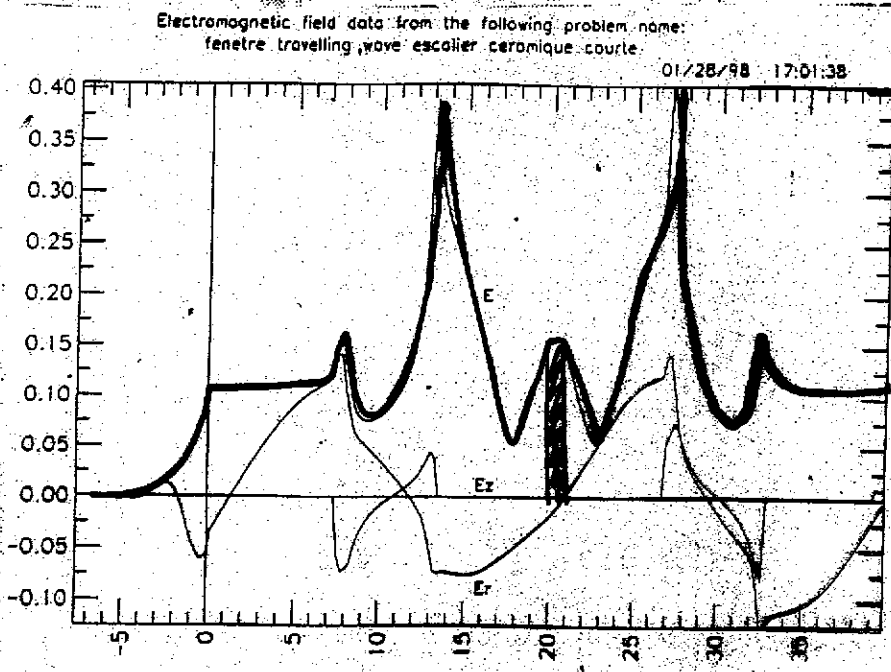

C. Travier, TTF coupler meeting, Saclay, October 19-20

Travelling wave window

Advantages

- pure TW in ceramic
- no direct view of cavity electrons
- low field at brazing point
- low dielectric loss
- great flexibility in parameter choice
- moderate cost
- E field parallel to ceramic

➡ no multipactor

Drawbacks

- large diameter
- high field on noses
- cavity electrons difficult to clean

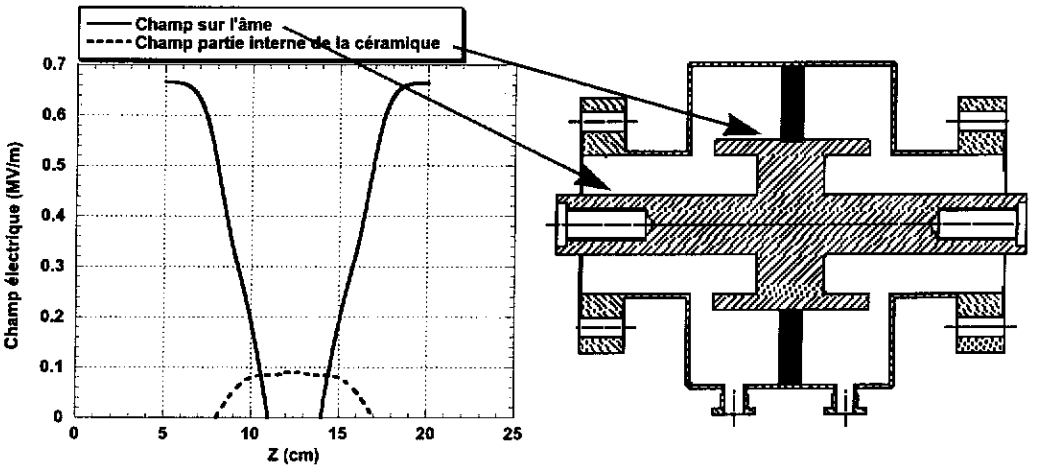

C. Travier, TTF coupler meeting, Saclay, October 19-20

Travelling wave window

Ceramic: WESGO Al300

Inner conductor: copper

Outer conductor:

Two fabrication options are considered:

copper and titanium

Ordered to SICN

Should be ready by end of year

MECHANICAL CALCULATIONS.

Mechanical and thermo-mechanical calculations made with ANSYS, PRELUDE- ANALYSIS.

Goal:
- estimate residual constraints after brazing.
- estimate window behaviour under several kind of constraints.

in order to compare windows designs.

Difficulties

- How to simulate brazing?
- What are copper properties at 800°C?
- material data over 80k - 1000k.
- availability of good, complete codes.

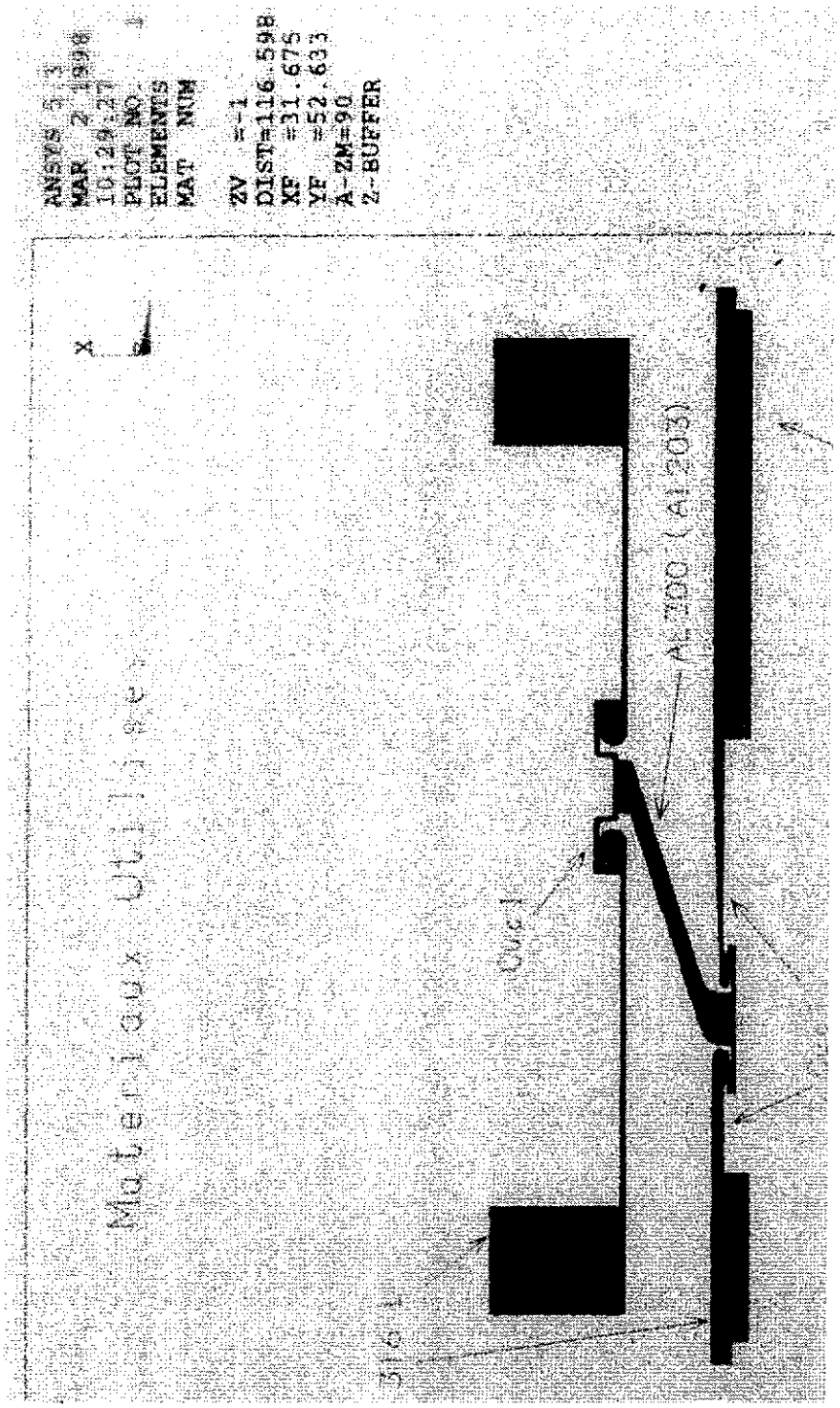

C. Travier, TTF coupler meeting, Saclay, October 19-20

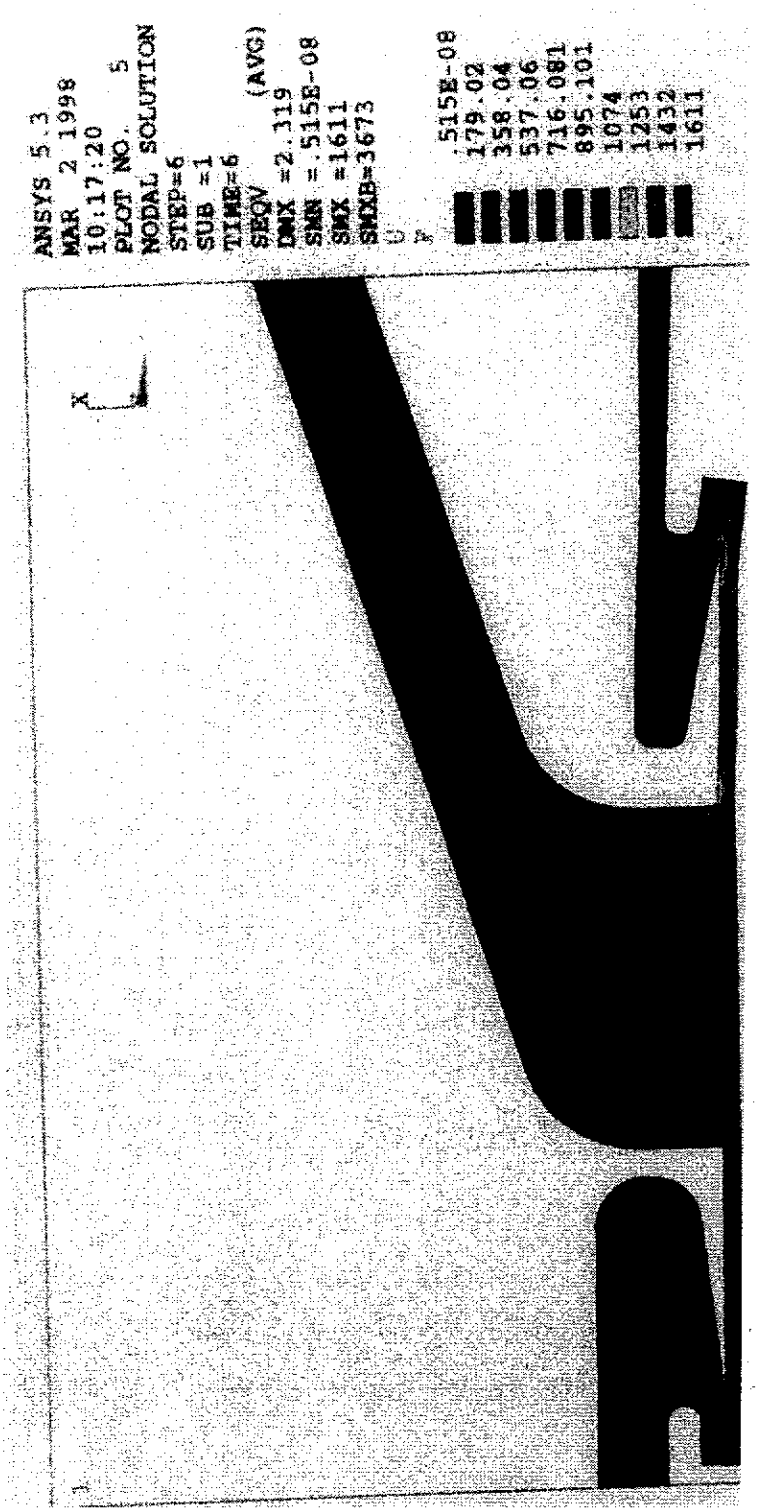

C. Travier, TTF coupler meeting, Saclay, October 19-20

Coupler design

Not yet systematic design made

Ideas persued to reduce cost are the following:

- use two identical coax windows, preferably TW window
- use atmospheric pressure waveguide to coax transition
- use RF trap for conduction barrier (avoid Cu coated bellows)

COUPLER

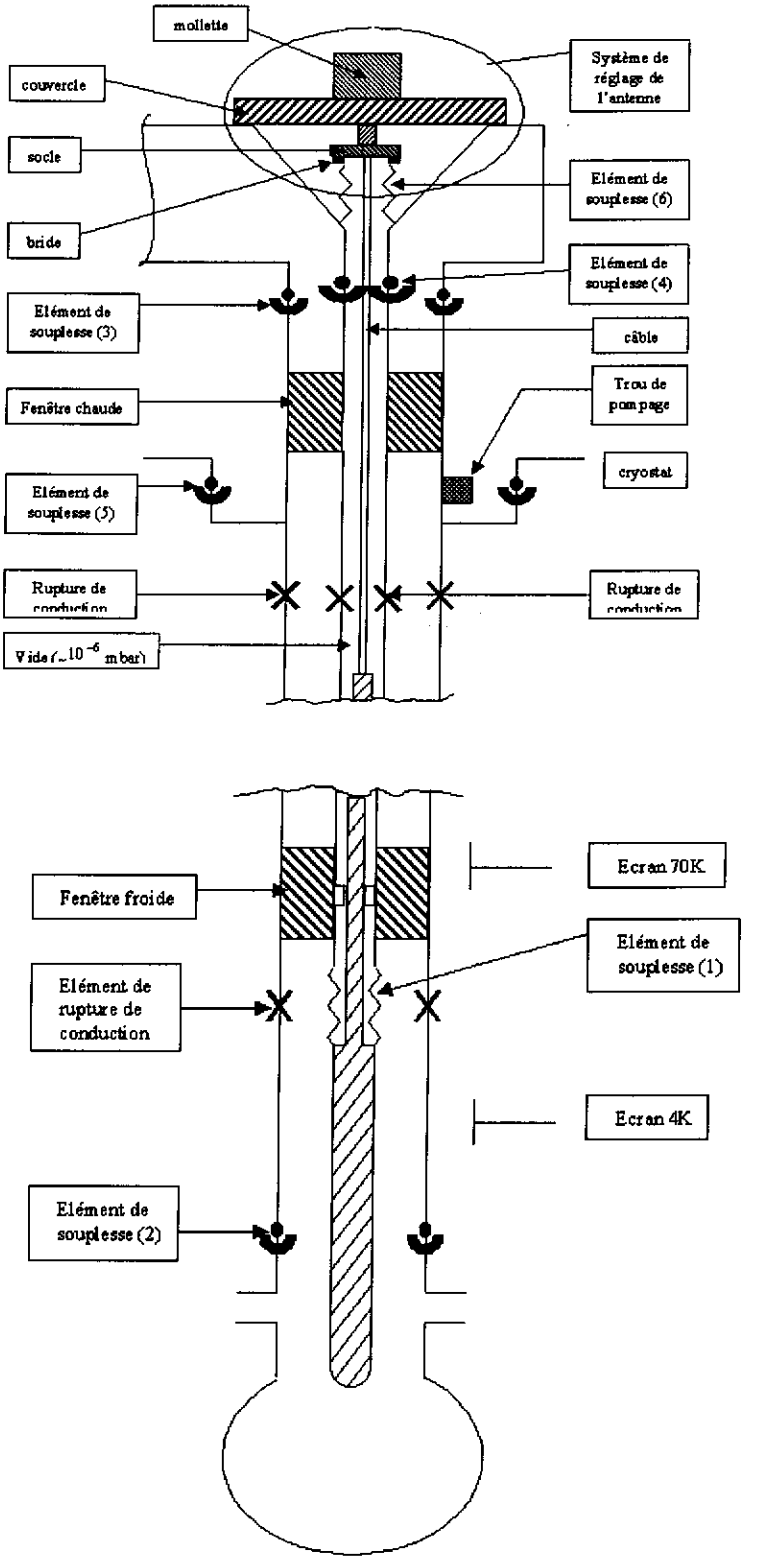

C. Travier, TTF coupler meeting, Saclay, October 19-20

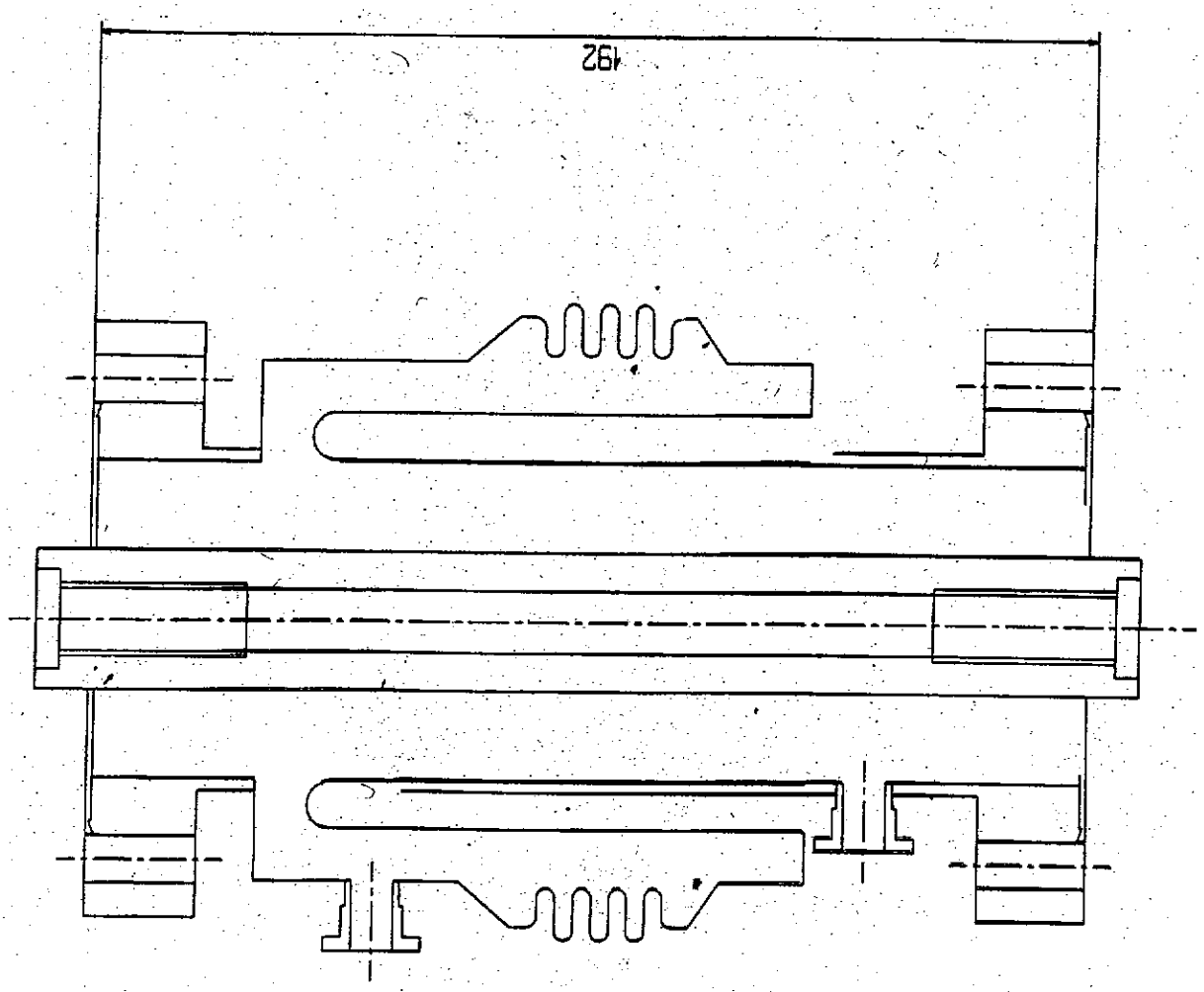

Polarized transition

P. Lepercq

C. Travier, TTF coupler meeting, Saclay, October 19-20

LAL, Orsay

RF studies for the power coupler

l/ Polarised doorknob transition (to be tested)
2/ Bellow in RF trip (to be realised)
3/ Alternative transition

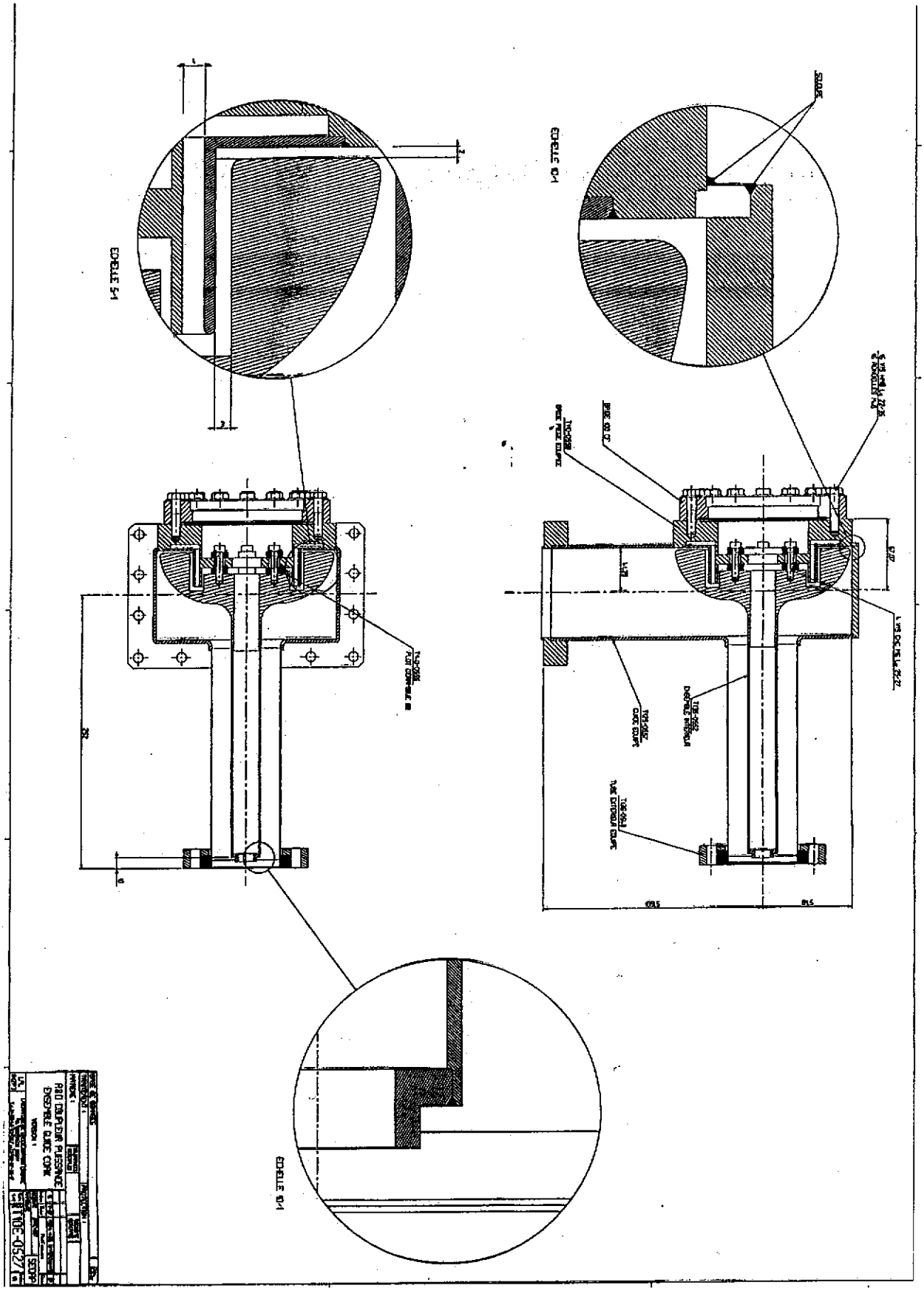

P.Lepercq, TTF coupler meeting, Saclay, October 19-20 , 1998

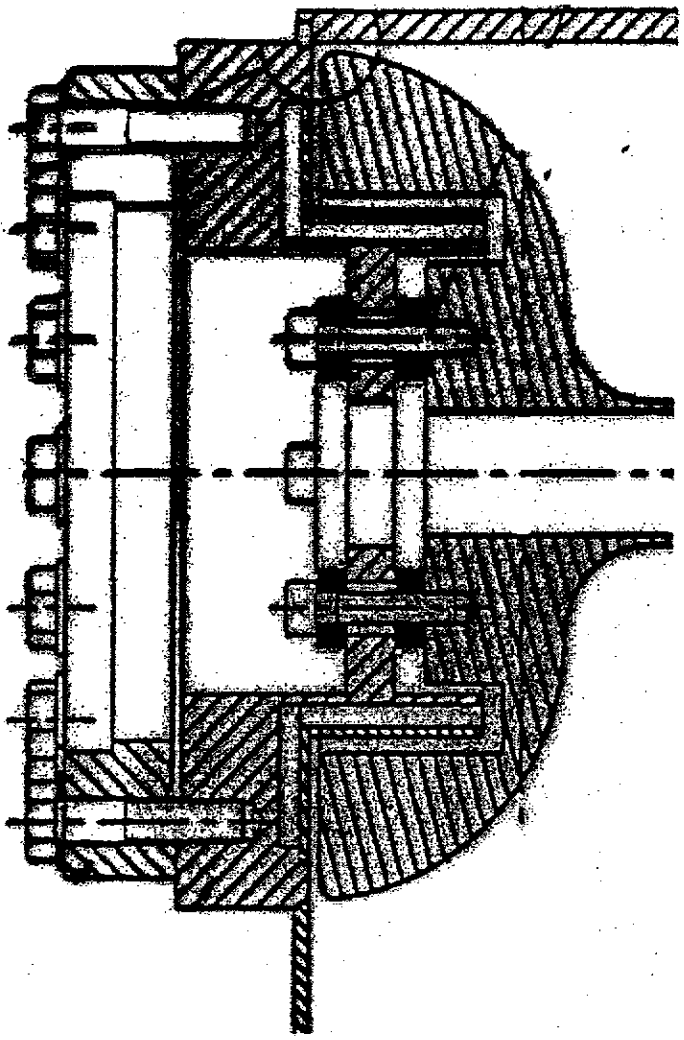

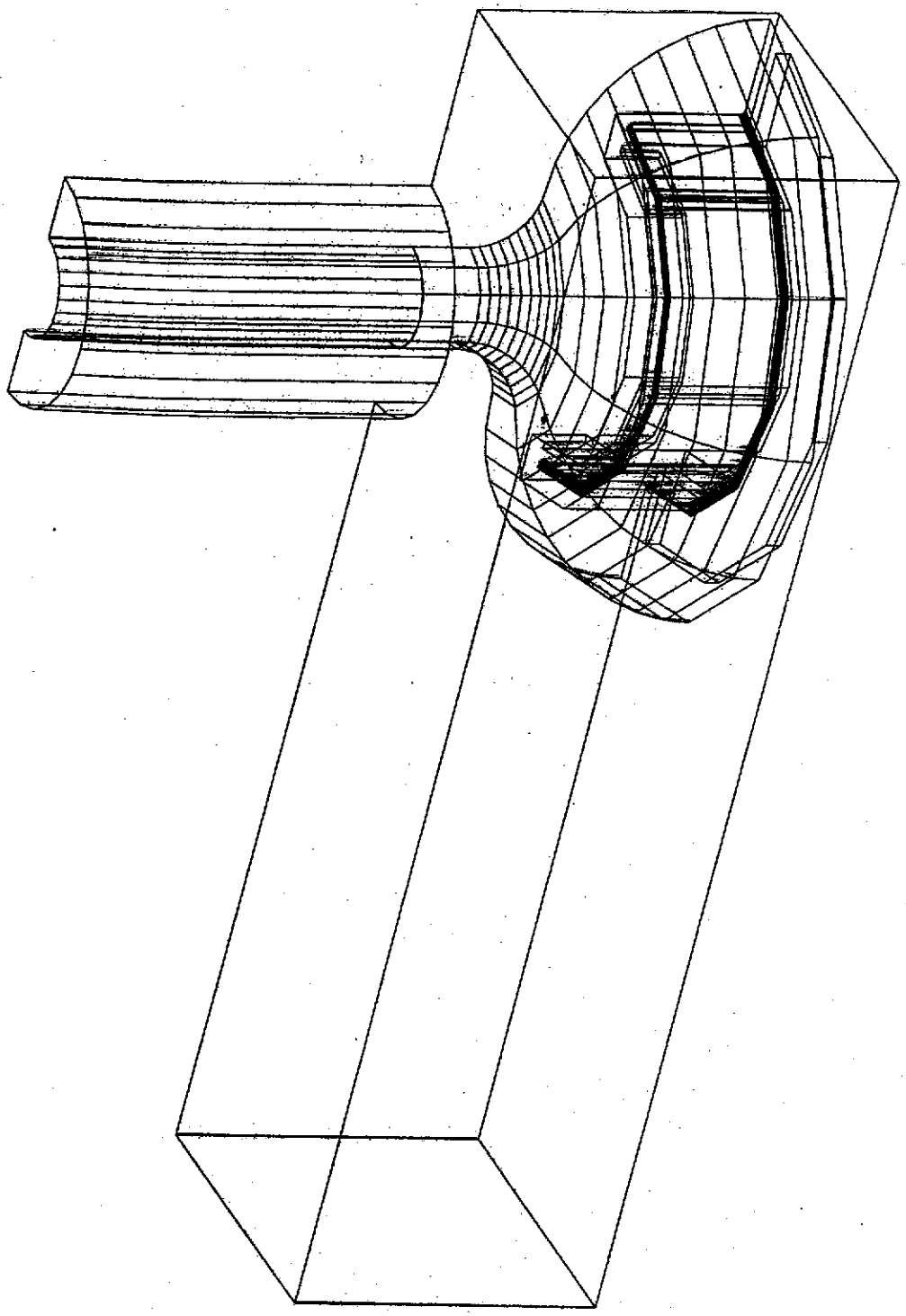

P.Lepercq, TTF coupler meeting, Saclay, October 19-20 , 1998

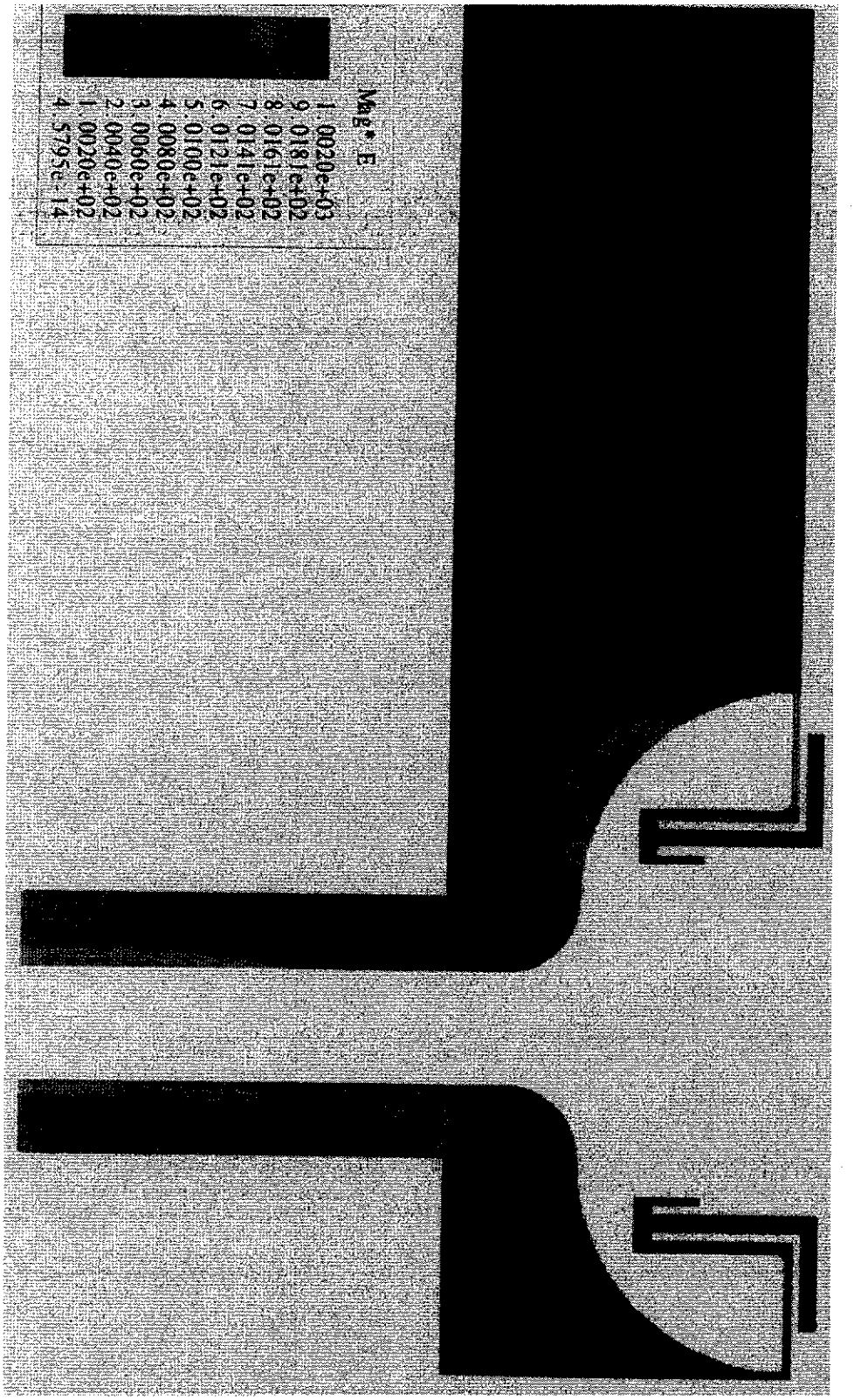

P.Lepercq, TTF coupler meeting, Saclay, October 19-20 , 1998

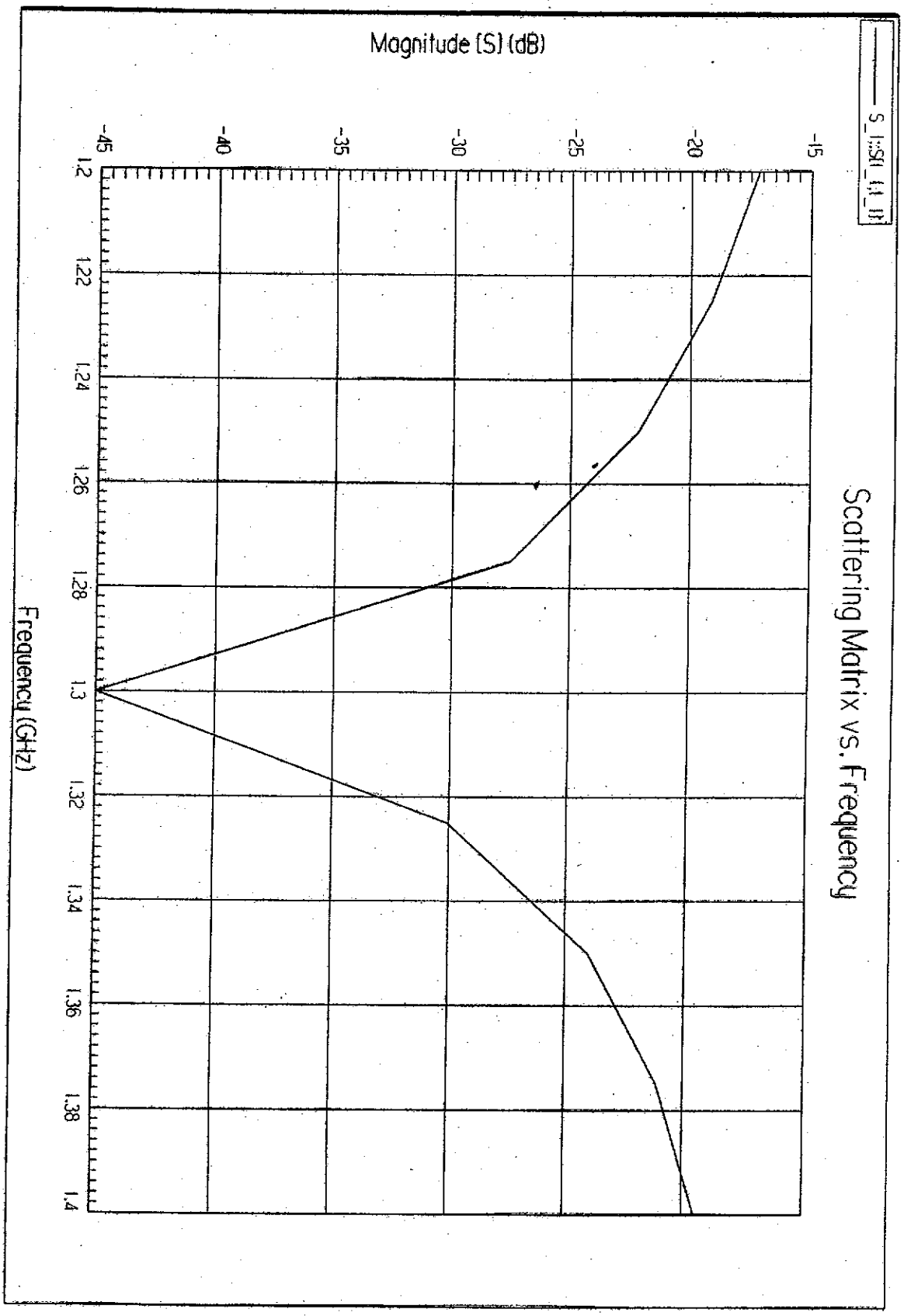

P.Lepercq, TTF coupler meeting, Saclay, October 19-20 , 1998

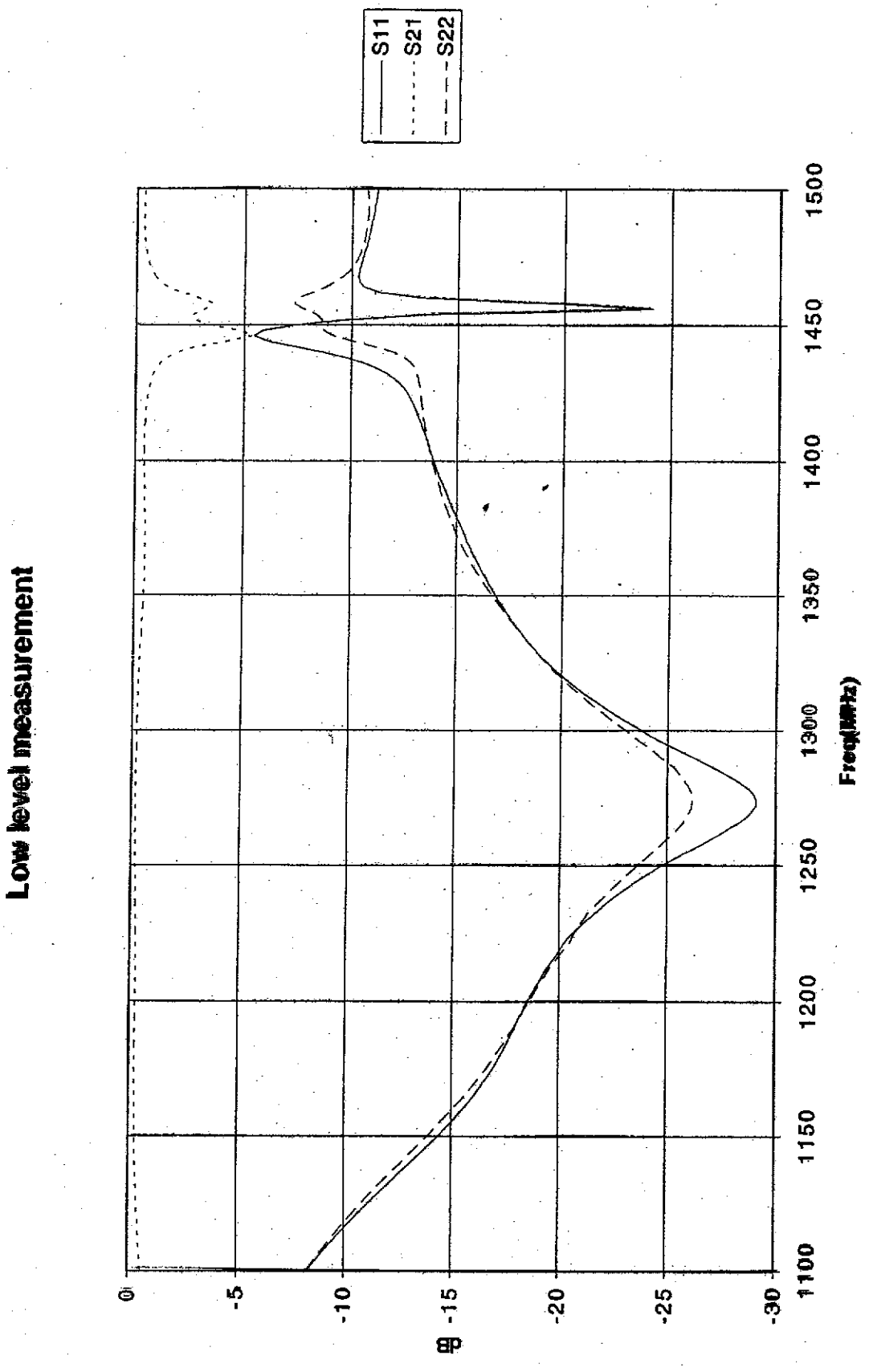

P.Lepercq, TTF coupler meeting, Saclay, October 19-20 , 1998

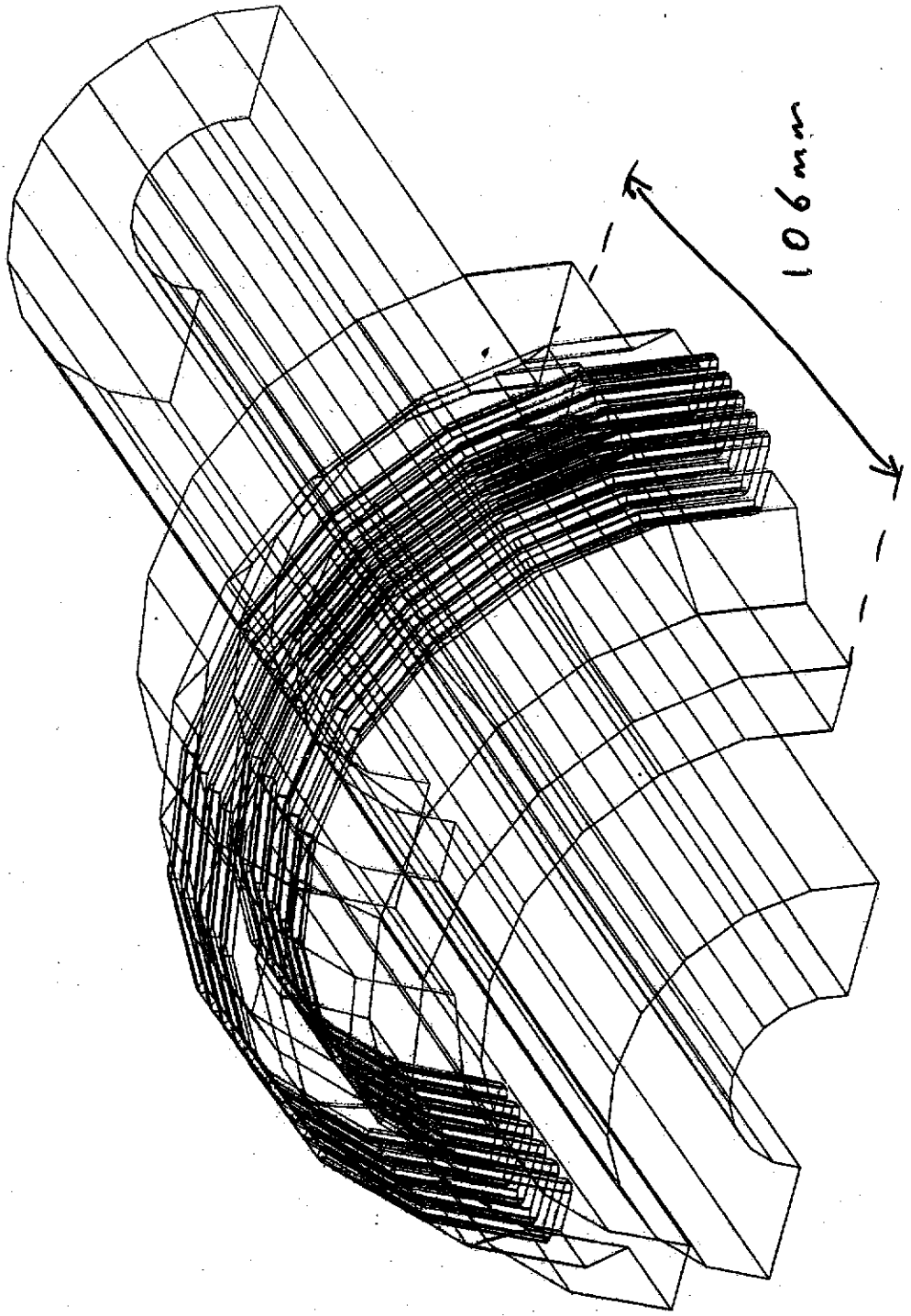
106mm

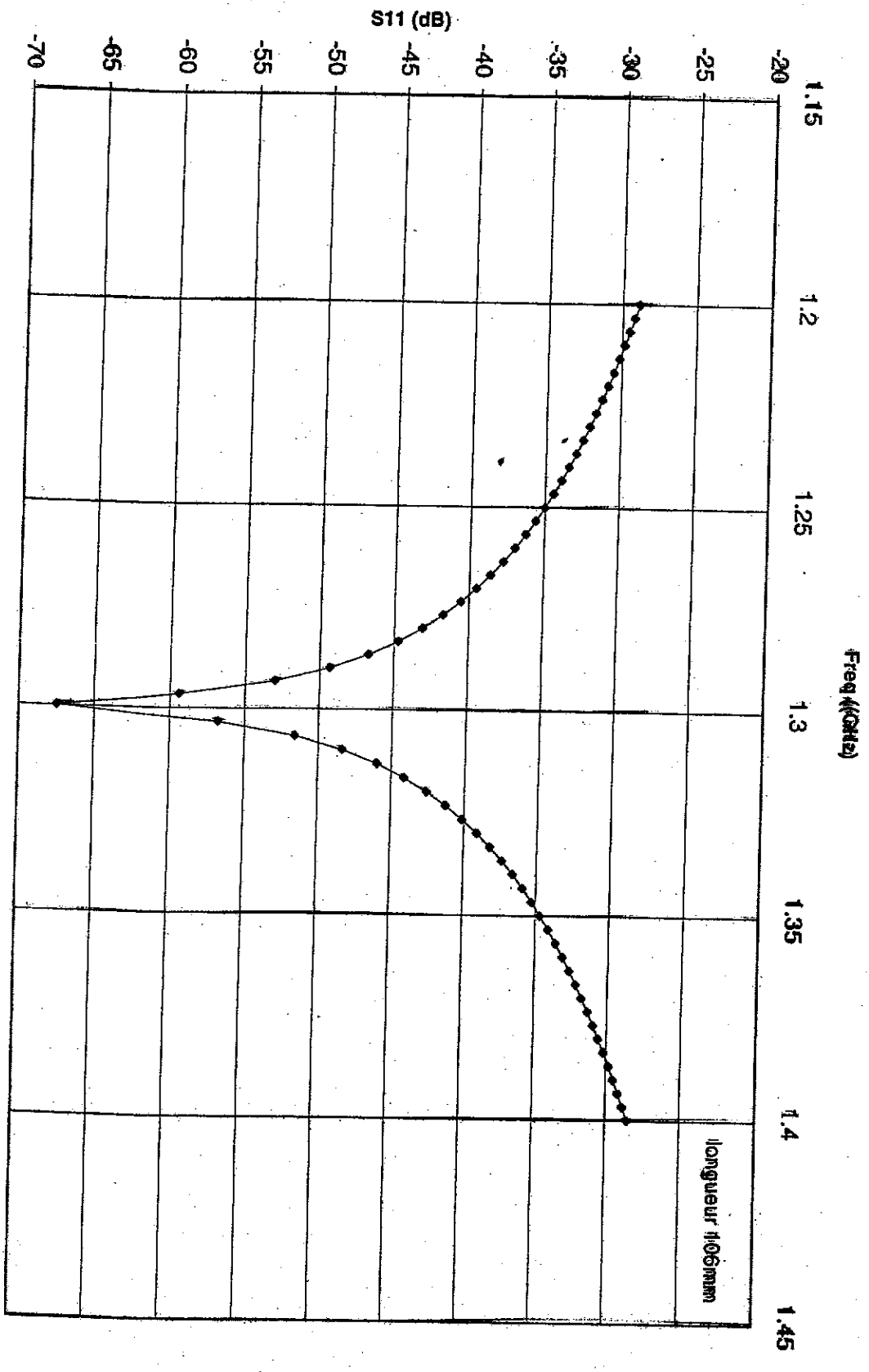

P.Lepercq, TTF coupler meeting, Saclay, October 19-20 , 1998

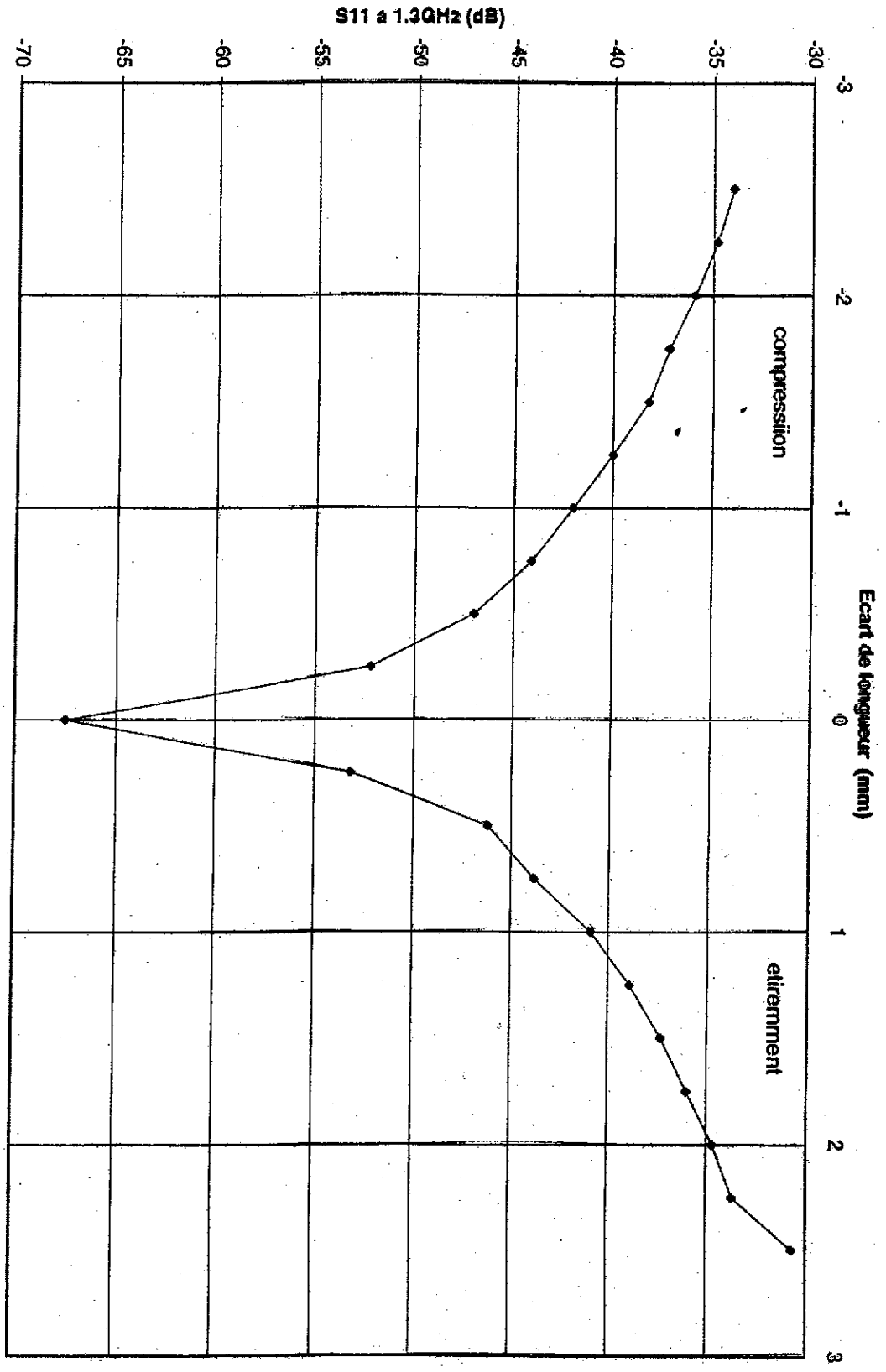

P.Lepercq, TTF coupler meeting, Saclay, October 19-20 , 1998

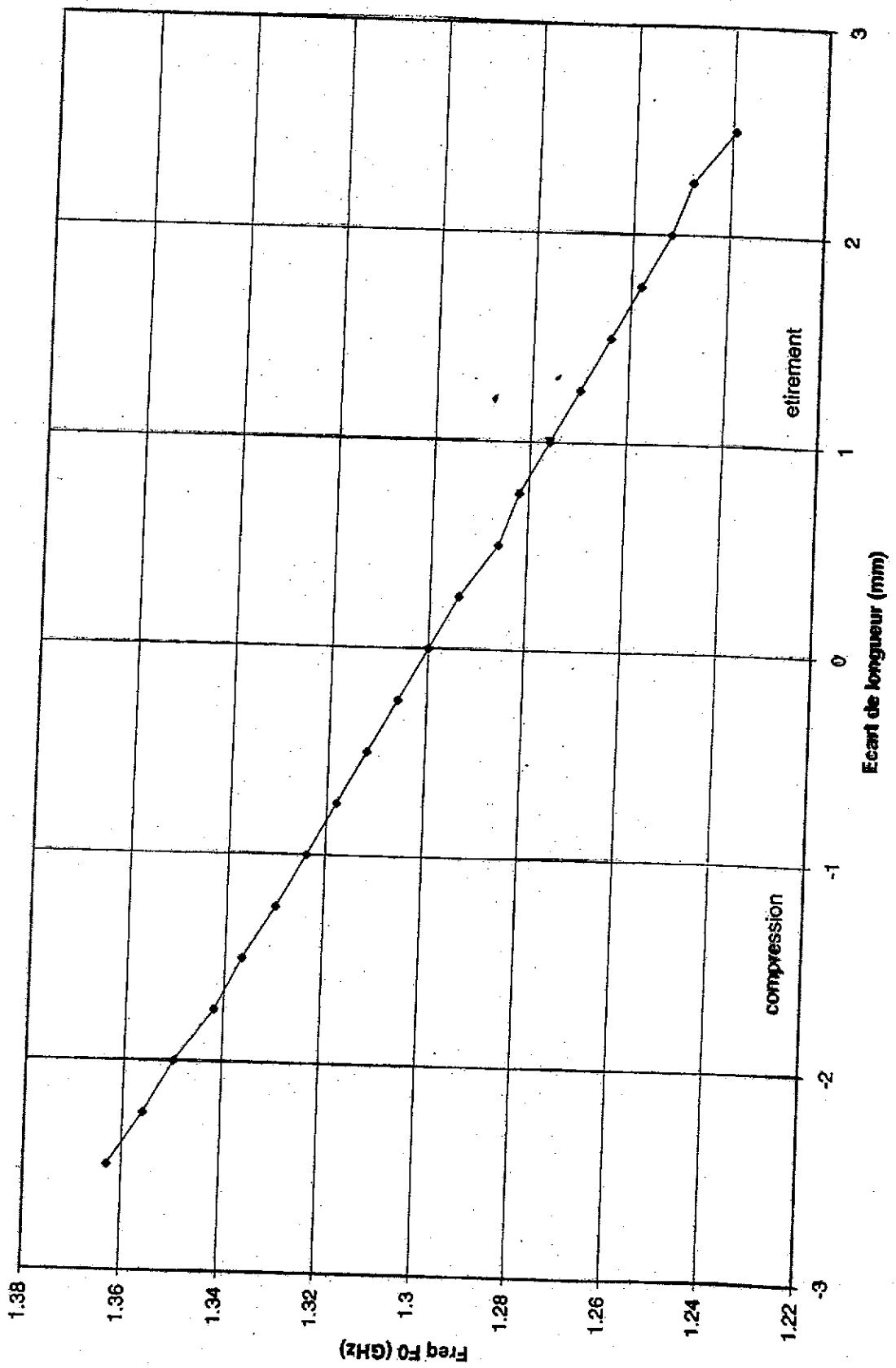

P.Lepercq, TTF coupler meeting, Saclay, October 19-20 , 1998

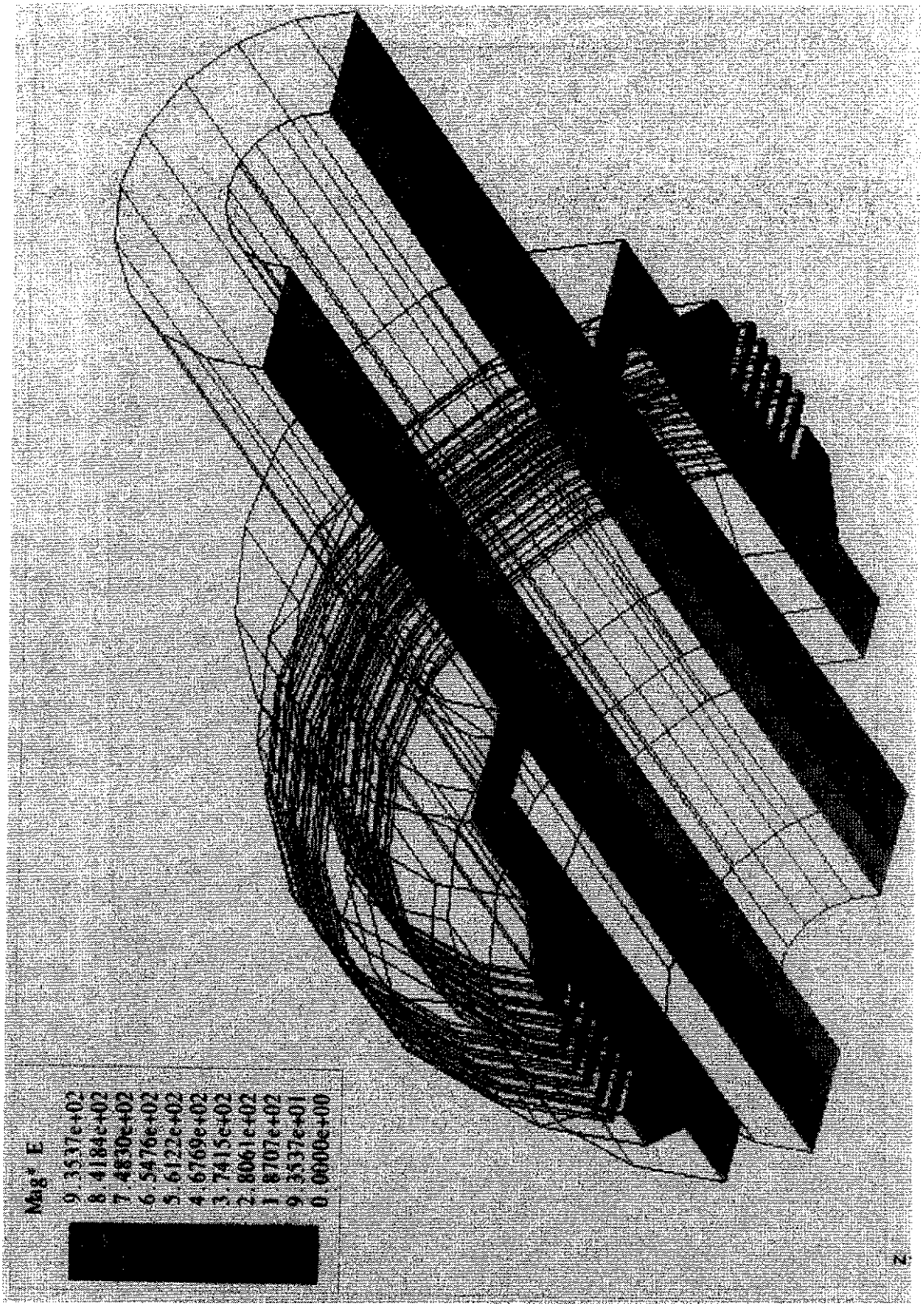

P.Lepercq, TTF coupler meeting, Saclay, October 19-20 , 1998

Alternative transition

Goal: working under air or neutral gas pressure (instead of vacuum)

study electric field

tolerance on dimensions

leadsto realisation is easier

lower cost

TESLA Report 1998-28

Multipactor simulations

D. Proch
DESY

Multipactor Simulations

D.Proch

Report about investigations of Prof. Sarvas and co-workers, Department of Mathematics, Rolf Nevanlinna Institute, University of Helsinki

I Introduction

II Results of multipacting simulations in:

- A, Coax-lines: Traveling & standing waves
- B, Coax lines with DC bias
- C, Windows in coax lines: tapered and cylindrical ceramics
- D, Cylindrical windows in coax lines with complex reflection factors
- E, Cylindrical windows in transition from coax to rectangular wave-guide

II Investigation of Multipacting in rectangular wave-guides (ESTEC, ESA)

III Conclusions

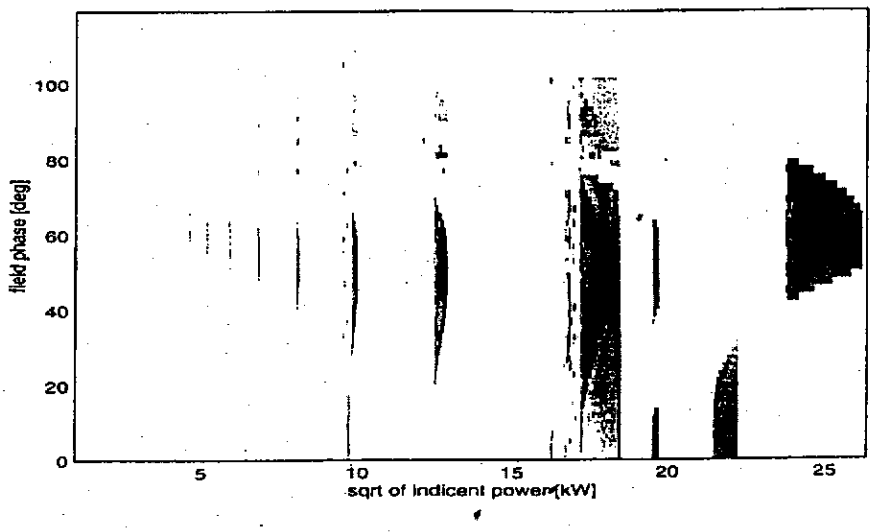

FIGURE 8 The gray scale contour plot of the distance function d_{30} when the primary electron emission is restricted to the maximum of the electric field. The darkest shading corresponds to the minima. Initial phases corresponding to electron trajectories that end up to the shadow are marked with white. Same geometry as in Figure 6. The horizontal axis gives the square root of the incident power in kW and the vertical axis gives the field phase in degrees.

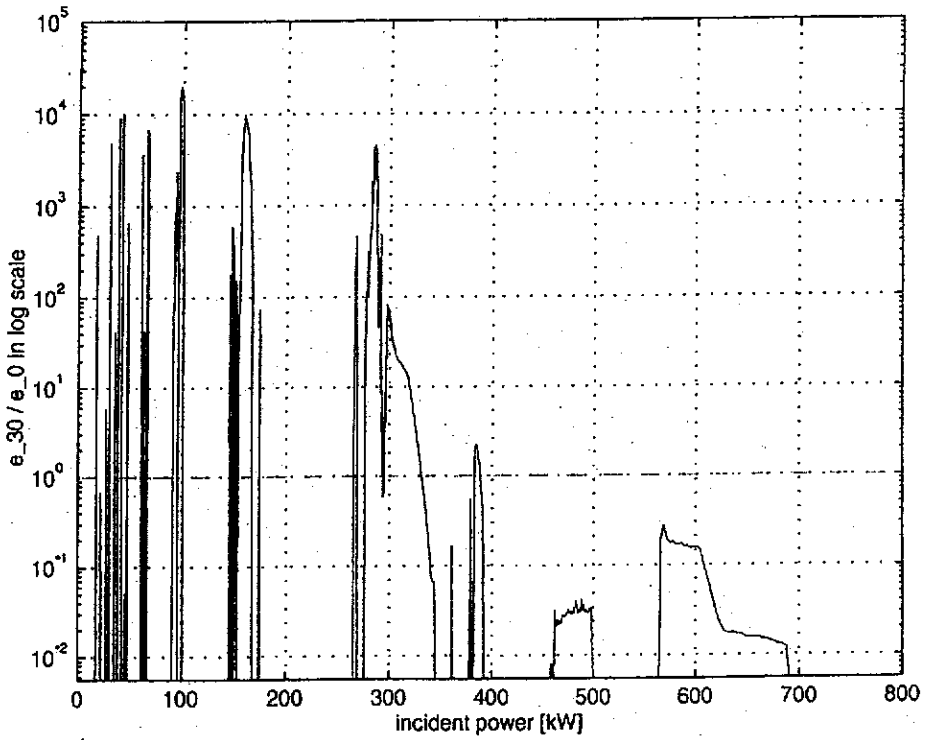

FIGURE 9 Relative enhanced counter function in the logarithmic (base 10) scale restricted to E_{max}, same geometry as in Figure 6. Note that when multipacting occurs, the relative enhanced function (in the logarithmic scale) is greater than one, i.e., the number of the electrons is increased.

Particle Accelerators, Vol. 59, pp. 107–141
Reprints available directly from the publisher
Photocopying permitted by license only

COMPUTATIONAL METHODS FOR ANALYZING ELECTRON MULTIPACTING IN RF STRUCTURES

ERKKI SOMERSALO [a], PASI YLÄ-OIJALA [b,*], DIETER PROCH [c] and JUKKA SARVAS [b]

[a] *Department of Mathematics, Helsinki University of Technology, Finland;* [b] *Rolf Nevanlinna Institute, University of Helsinki, P.O. Box 4 (Yliopistonkatu 5) FIN-00014, Finland;* [c] *Deutsches Elektronen-Synchrotron DESY, Hamburg, Germany*

(Received 15 September 1997; In final form 9 January 1998)

Electron multipacting can cause loss of the field level in resonators or it can break the high power rf components like couplers and windows. This phenomenon starts if certain resonant conditions for electron trajectories are fulfilled and if the impacted surface has a secondary yield larger than one. A general cure against multipacting is to avoid the resonant conditions. Therefore, we investigated the dynamics of the electron trajectories in order to find rules for these resonances. We developed new computational methods which combine the standard trajectory calculations with advanced searching and analyzing methods for multipacting resonances. In numerical experiments we consider different coaxial structures. We are able to find those rf incident power levels at which the multipacting occurs and, thereafter, to locate and identify different multipacting processes. We characterize multipacting behavior in straight and tapered lines, and for the straight coaxial line we give simple scaling laws for the multipacting power bands with respect to the diameter, impedance and frequency. Furthermore, the present analysis method turns out to be a powerful tool for optimizing different methods to suppress multipacting. Here, in particular, the biasing DC voltage method is considered.

Keywords: Multipacting; rf structures; Superconducting cavities; Dynamical systems

* Corresponding author. Tel.: +358 9 191 22775. Fax: +358 9 191 22779.
E-mail: Pasi.Yla-Oijala@RNI.Helsinki.FI.

- counter function C_{30} :

  number of e^- after 30 impact, $\delta = 1$

- enhanced counter function e_{30} :

  number of e^- after 30 impact, $\delta \geq 1$

- distance function d_n

$$d_n = \left(|x_0 - x_n|^2 + \gamma (\phi_0 - \phi_n)^2 \right)^{1/2}$$

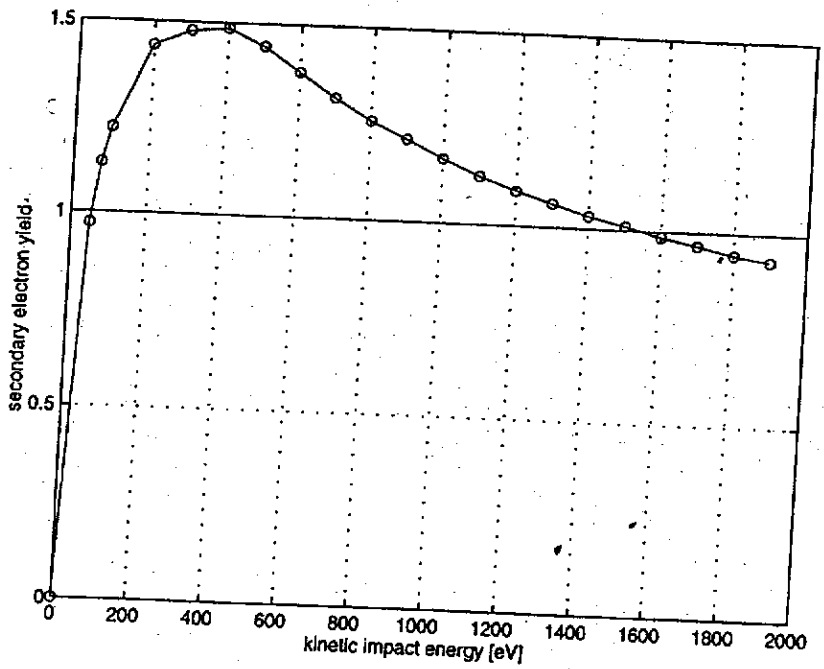

FIGURE 1 The secondary electron yield at different impact energies (in eV) for a niobium surface baked at 300°C.

Considering the full discrete trajectory, the number of secondary electrons due to one single electron starting at p after n impacts is

$$\alpha_n(p) = \prod_{j=0}^{n-1} \alpha(R^j(p)), \quad p \in G. \tag{13}$$

Now the second condition (2) for multipacting can be written in the terms of the multiplicity function by

$$\alpha_n(p) > 1, \quad p \in G. \tag{14}$$

2.2 Counter and Distance Functions

Our aim is to develop methods by which we can, on one hand, find those EM field levels at which the electron multipacting may occur, and, on another hand, analyze the mechanism of the process at the found multipacting field levels. Especially, we want to find the location of the multipacting process in the phase space, and also, to compute the multipacting trajectories and find their kind (one-point, two-point, etc.) and order.

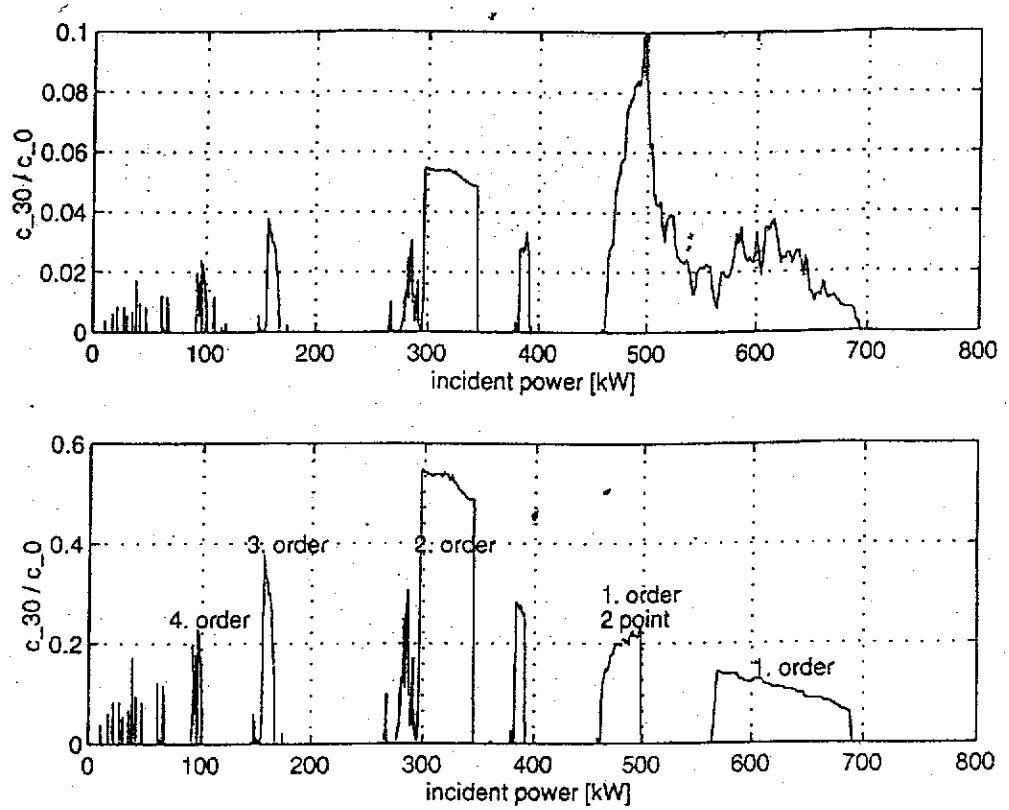

FIGURE 6 Relative electron counter functions after 30 impacts. The computation was done with a 50 Ω line with inner and outer radii $a = 22.4$ mm, $b = 51.5$ mm, respectively, at the frequency 500 MHz. In the top frame, electrons from $\lambda/4$ (maximum electric field) to $\lambda/2$ (maximum magnetic field) were tracked, and in the bottom frame, the initial electrons were restricted to the maximum of the electric field only. The differences showing in these plots (from 450 to 690 kW) are due to the first order two-point process. Note the different scaling of the figures.

rf power is chosen from one of the multipacting bands. A further demonstration of the phase focusing is seen in Figure 8, where we have plotted the distance $|\varphi - \varphi_n|$, i.e., the difference between the original and final phases after n impacts for each incident power. Here, the electron trajectories are initiated only at the maximum of the electric field. The darkest areas are the attracting phases, and the shaded areas around them are the focused phases.

Basically two different dominant multipacting types can be recognized. First, there are one-point multipacting processes of different order on the outer conductor of the line. Secondly, there are two-point processes from the outer conductor to the inner one and back. In addition, we were able to find some more complicated processes that show up only on relatively narrow power bands that are usually overlapping with the more prominent one- and two-point bands. An

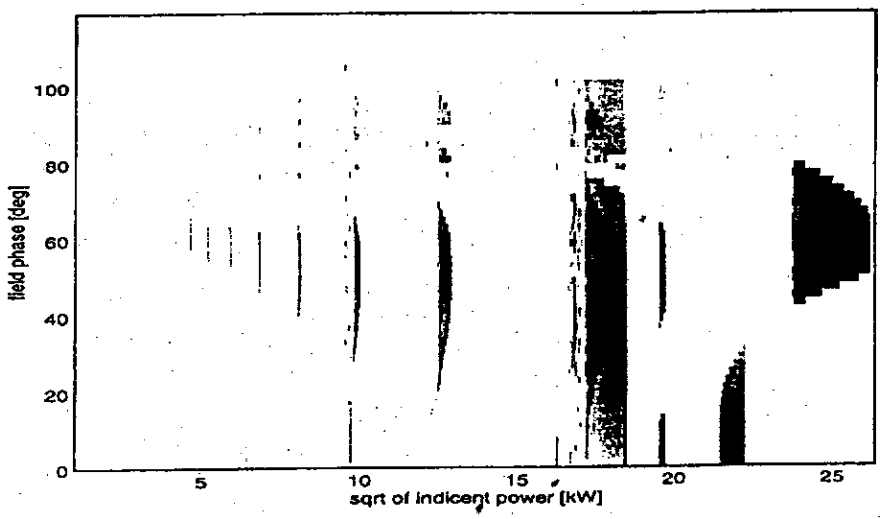

FIGURE 8 The gray scale contour plot of the distance function d_{30} when the primary electron emission is restricted to the maximum of the electric field. The darkest shading corresponds to the minima. Initial phases corresponding to electron trajectories that end up to the shadow are marked with white. Same geometry as in Figure 6. The horizontal axis gives the square root of the incident power in kW and the vertical axis gives the field phase in degrees.

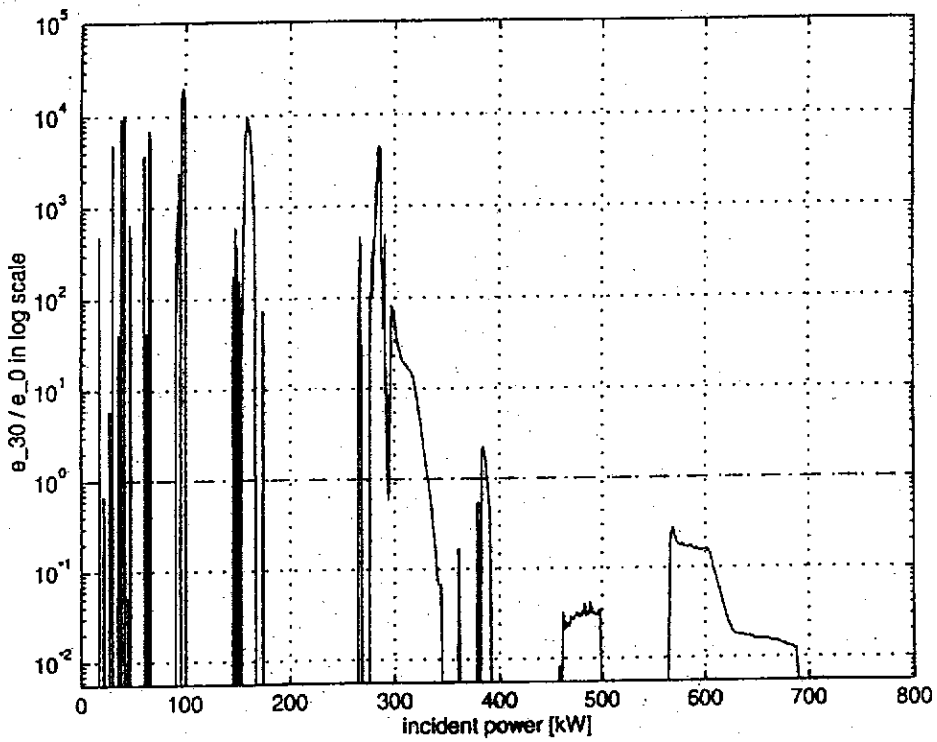

FIGURE 9 Relative enhanced counter function in the logarithmic (base 10) scale restricted to E_{max}, same geometry as in Figure 6. Note that when multipacting occurs, the relative enhanced function (in the logarithmic scale) is greater than one, i.e., the number of the electrons is increased.

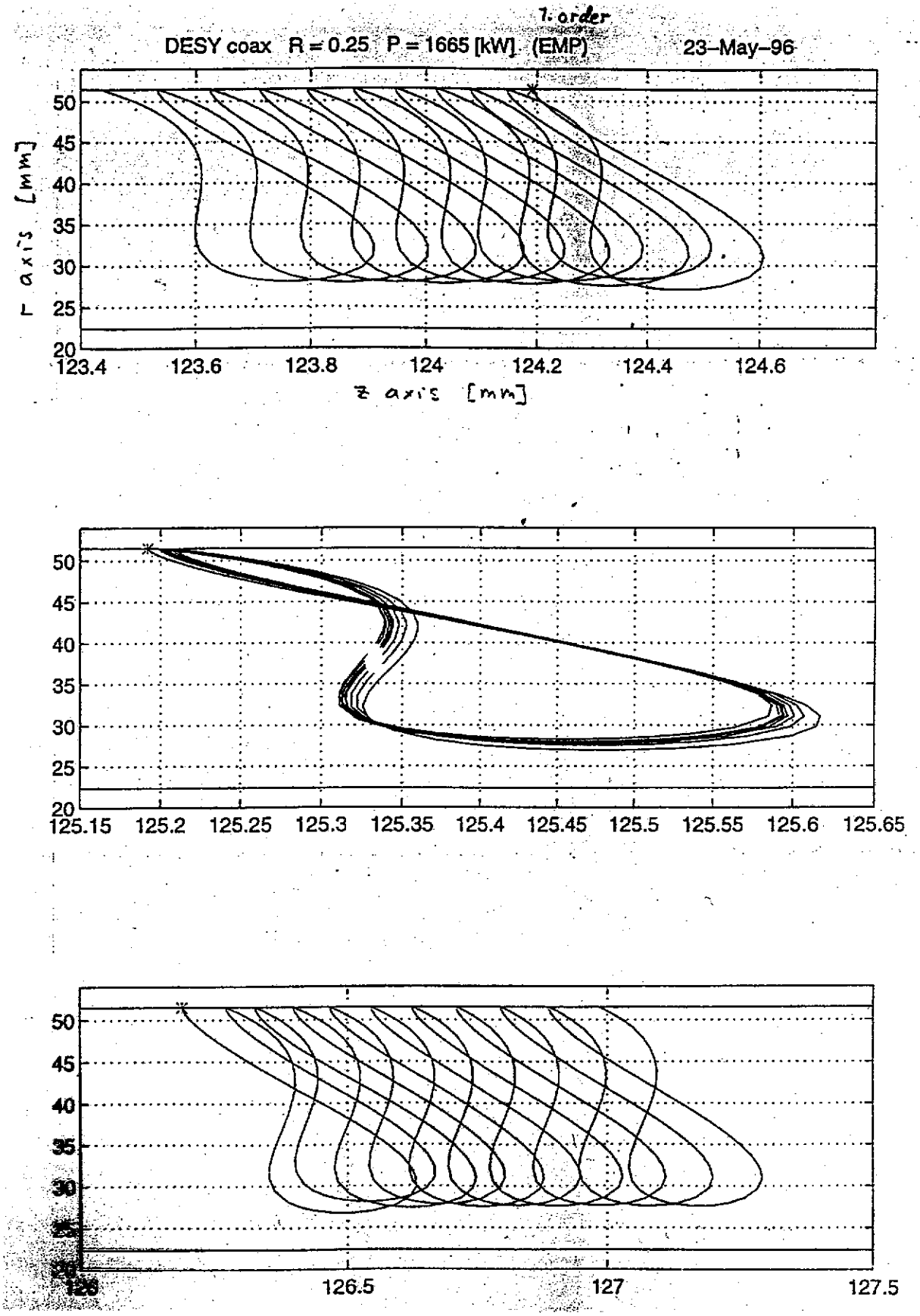
1. order
DESY coax R = 0.25 P = 1665 [kW] (EMP) 23–May–96
r axis [mm]
z axis [mm]
50
45
40
35
30
25
20
123.4
123.6
123.8
124
124.2
124.4
124.6
125.15
125.2
125.25
125.3
125.35
125.4
125.45
125.5
125.55
125.6
125.65
126.5
127
127.5

3. COAXIAL LINE

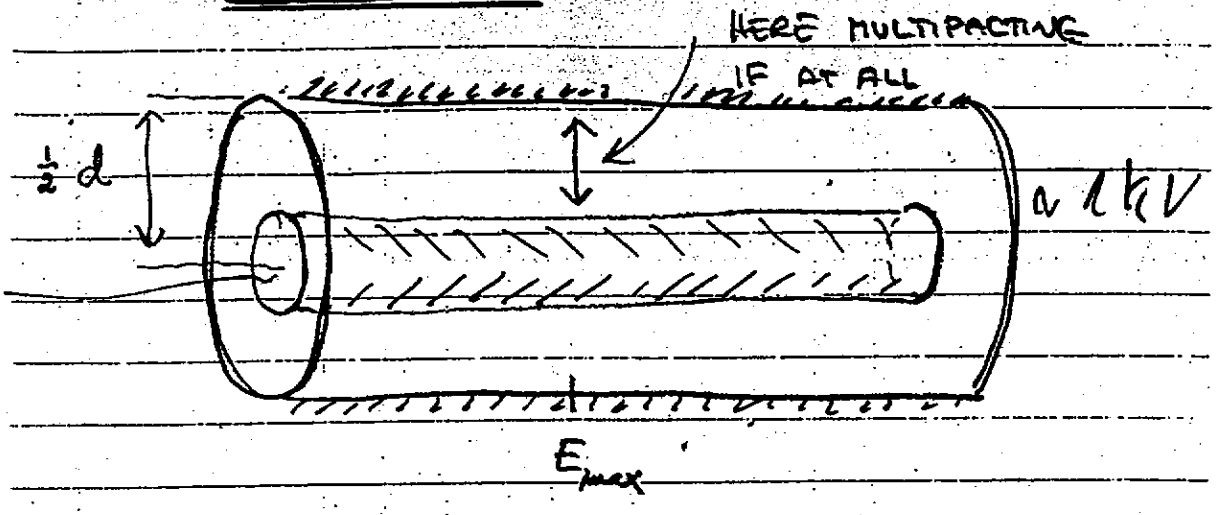

Standing wave : Multipacting occurs at max of E with certain field powers

Scaling laws :

$$P_{\text{one-point}} \sim (fd)^4 Z$$

$$P_{\text{two-point}} \sim (fd)^4 Z^2$$

Travelling wave :

$$P_{TW} = 4 P_{SW}$$

Mixture of SW and TW : Not as expected

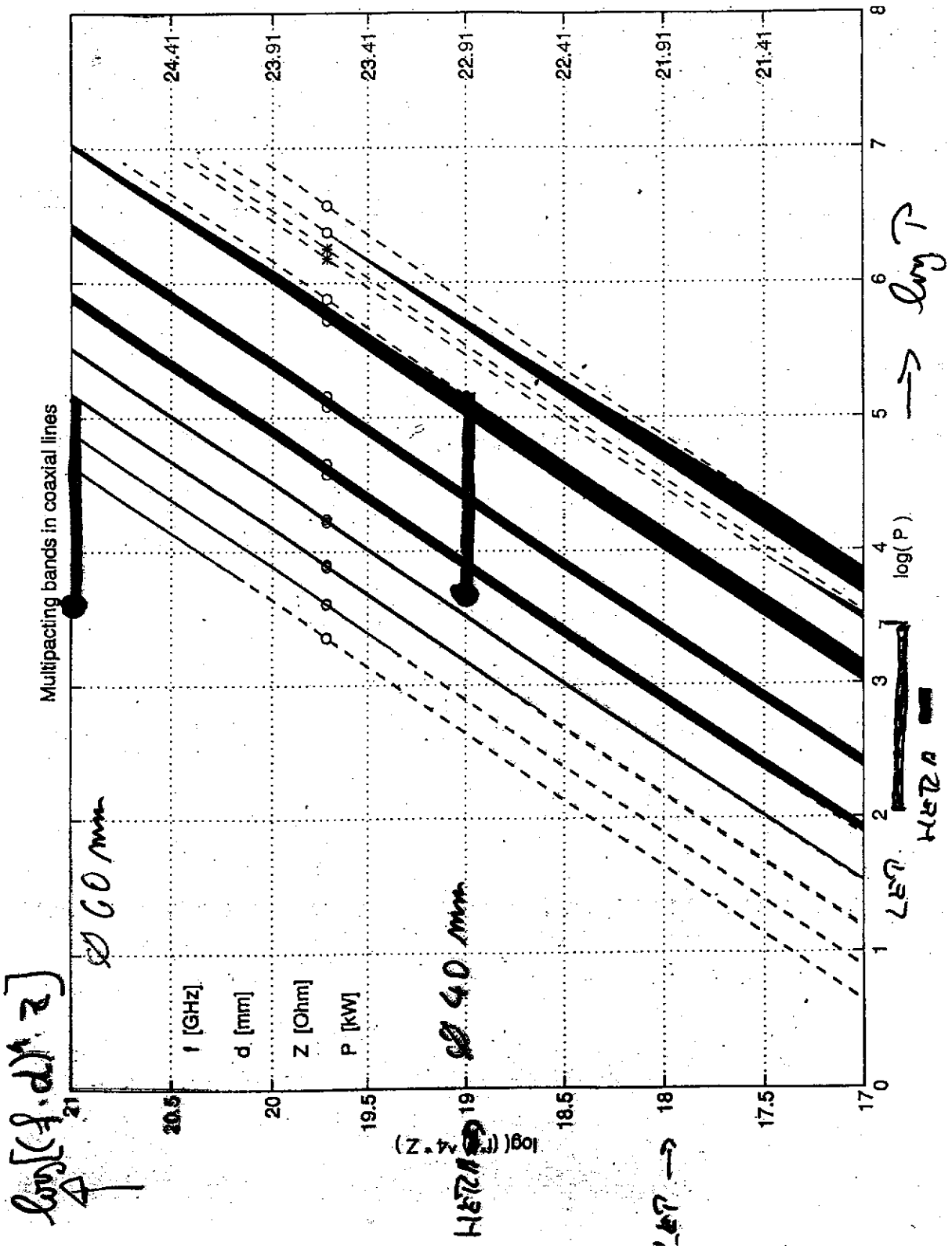
Multipacting bands in coaxial lines
f [GHz]
d [mm]
Z [Ohm]
P [kW]
24.41
23.91
23.41
22.91
22.41
21.91
21.41
log(P)

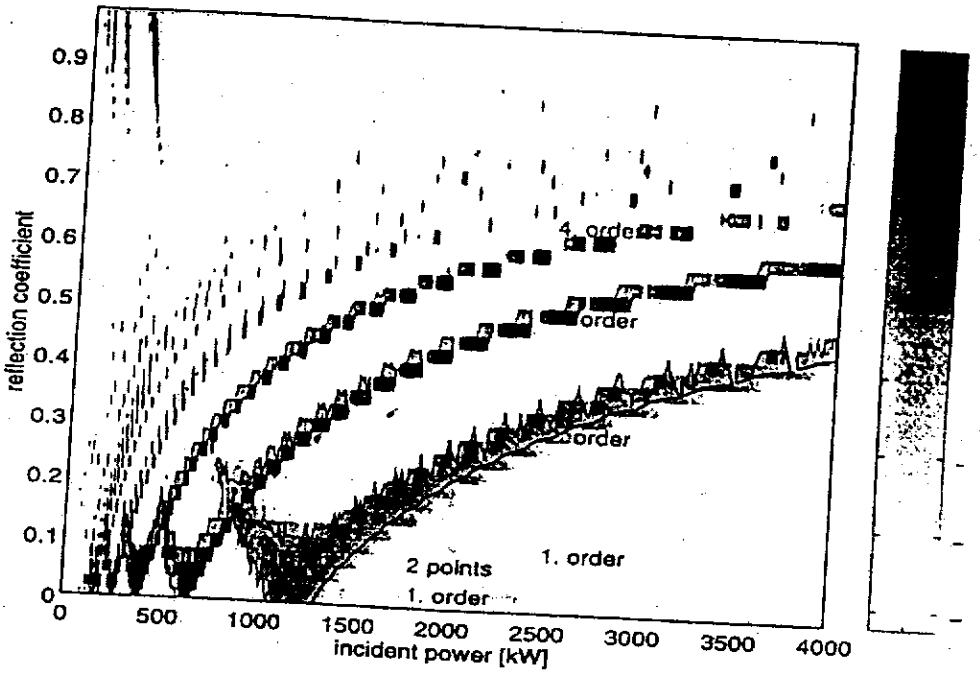

FIGURE 14 The gray scale plot of the 10 base logarithmic of the enhanced cou function e_{30} as a function of the incident power (horizontal axis) in kW and reflec coefficient (vertical axis). In the figure, all positive values of the counter func correspond to the multipacting processes of different order and type. This zero lir indicated in the plot. The outer diameter of the line is 103 mm, frequency is 500 M and the impedance is 50.

coefficient increases, the processes of different nature split into elect and magnetic processes. The dependence of the electric multipacti powers on the reflection coefficient can be described approximately i the formula

$$P_R^{\text{electric}} \sim \frac{1}{(1+R)^2} P_{\text{TW}} = \frac{4}{(1+R)^2} P_{\text{SW}}. \qquad (2$$

A heuristic physical explanation for this rule is similar as for the rul relating the SW and TW operations: For given R, the peak voltage i $(1+R)$ times the corresponding peak voltage of the traveling waves However, the behavior of the magnetic multipacting bands are differ ent. As R increases, the multipacting power levels increase very rapidly A logarithmic scale plot shows that the increase is faster than poly- nomial with respect to R.

A closer analysis of electron trajectories shows an important feature. Multipacting in the mixed wave operation is due to certain [illegible]

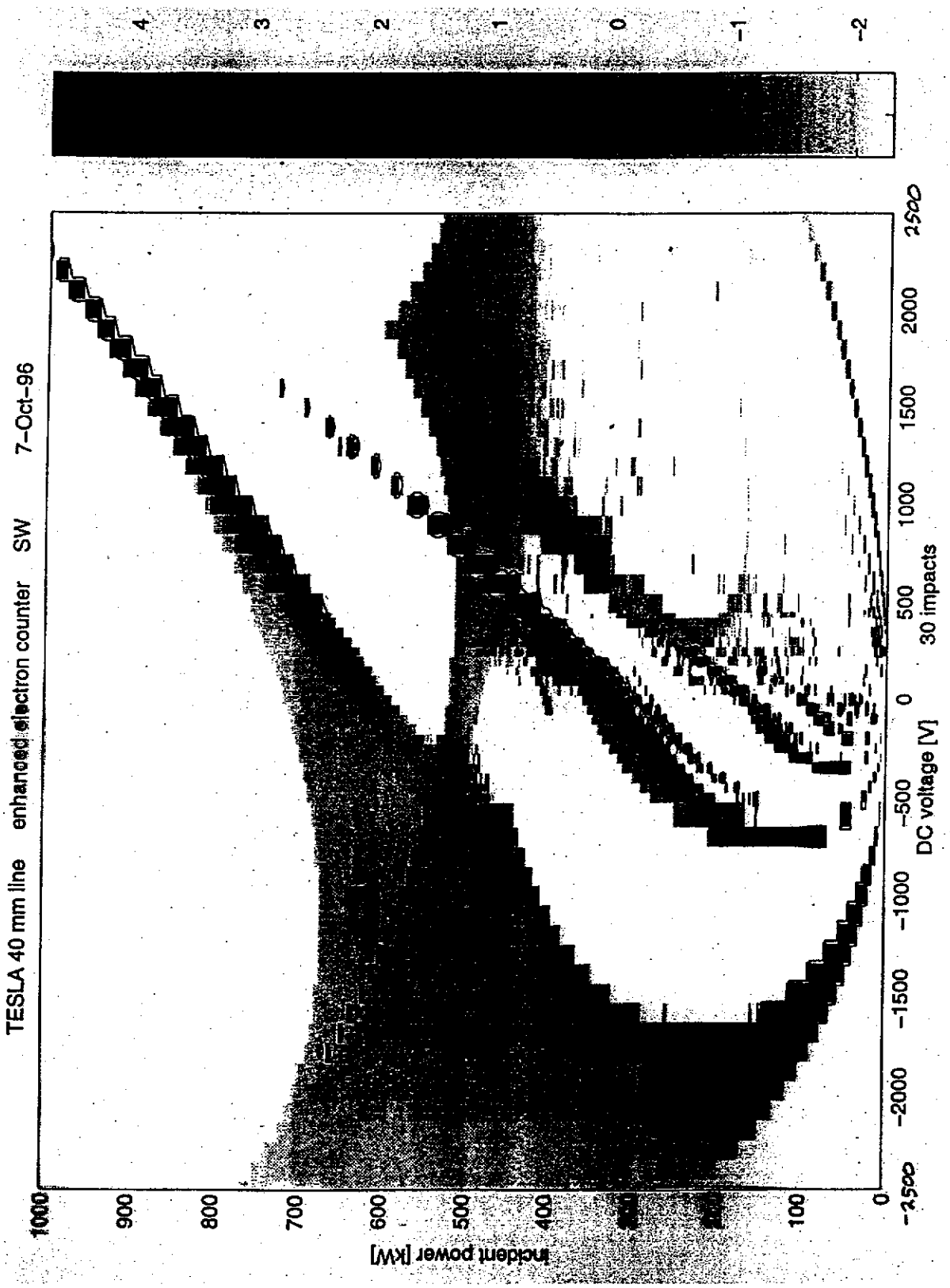
TESLA 40 mm line enhanced electron counter SW 7-Oct-96
Incident power [kW]
DC voltage [V]
30 impacts
4
3
2
1
0
-1
-2
1000
900
800
700
600
500
400
100
0
2500
2000
1500
1000
500
0
-500
-1000
-1500
-2000
-2500

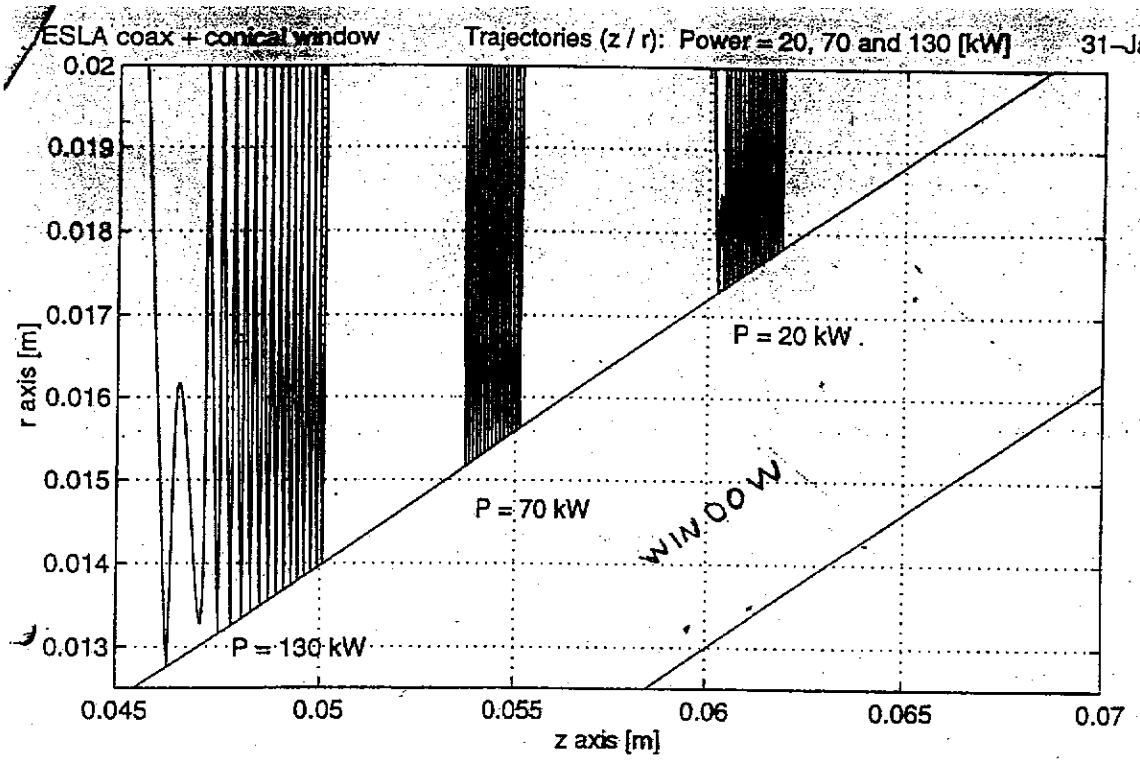
TESLA coax + conical window
Trajectories (z / r): Power = 20, 70 and 130 [kW]
31-Jan-9
r axis [m]
z axis [m]
P = 20 kW
P = 70 kW
P = 130 kW
WINDOW
0.02
0.019
0.018
0.017
0.016
0.015
0.014
0.013
0.045
0.05
0.055
0.06
0.065
0.07

FIGURE 11A

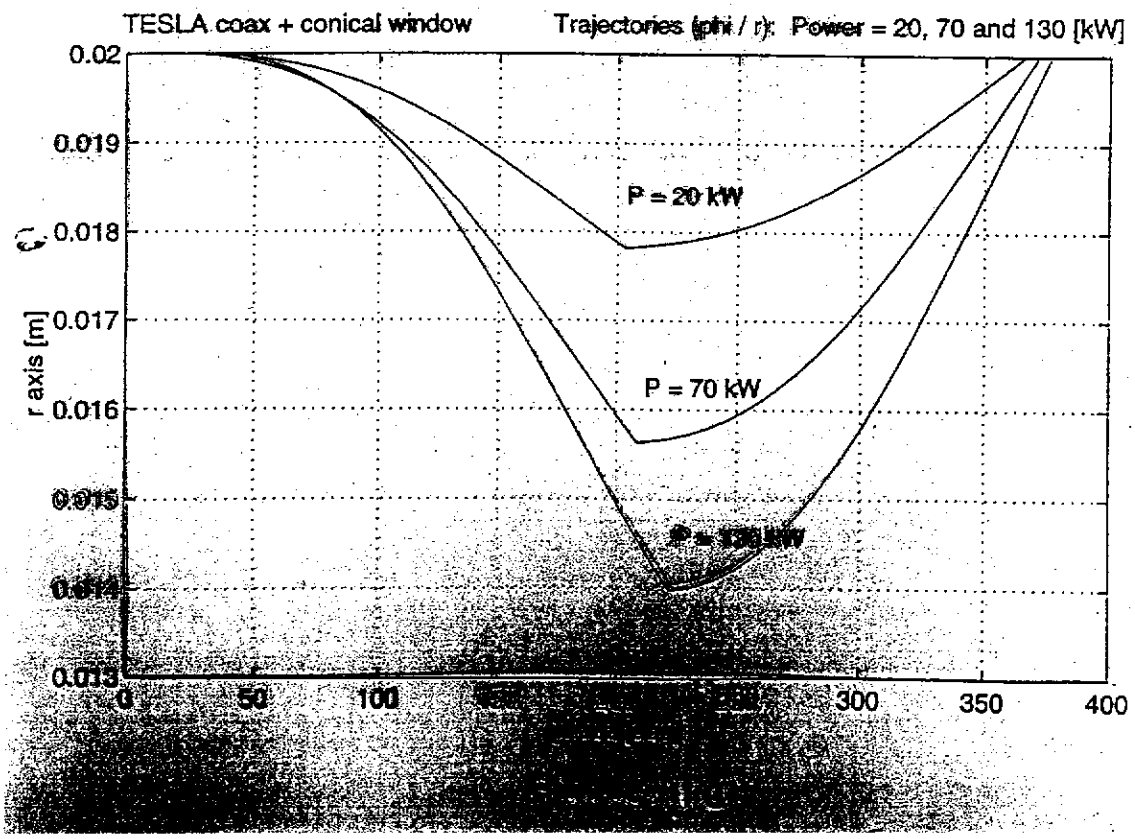
TESLA coax + conical window
Trajectories (phi / r): Power = 20, 70 and 130 [kW]
r axis [m]
P = 20 kW
P = 70 kW
0.02
0.019
0.018
0.017
0.016
0.015
0.014
0.013
0
50
100
300
350
400

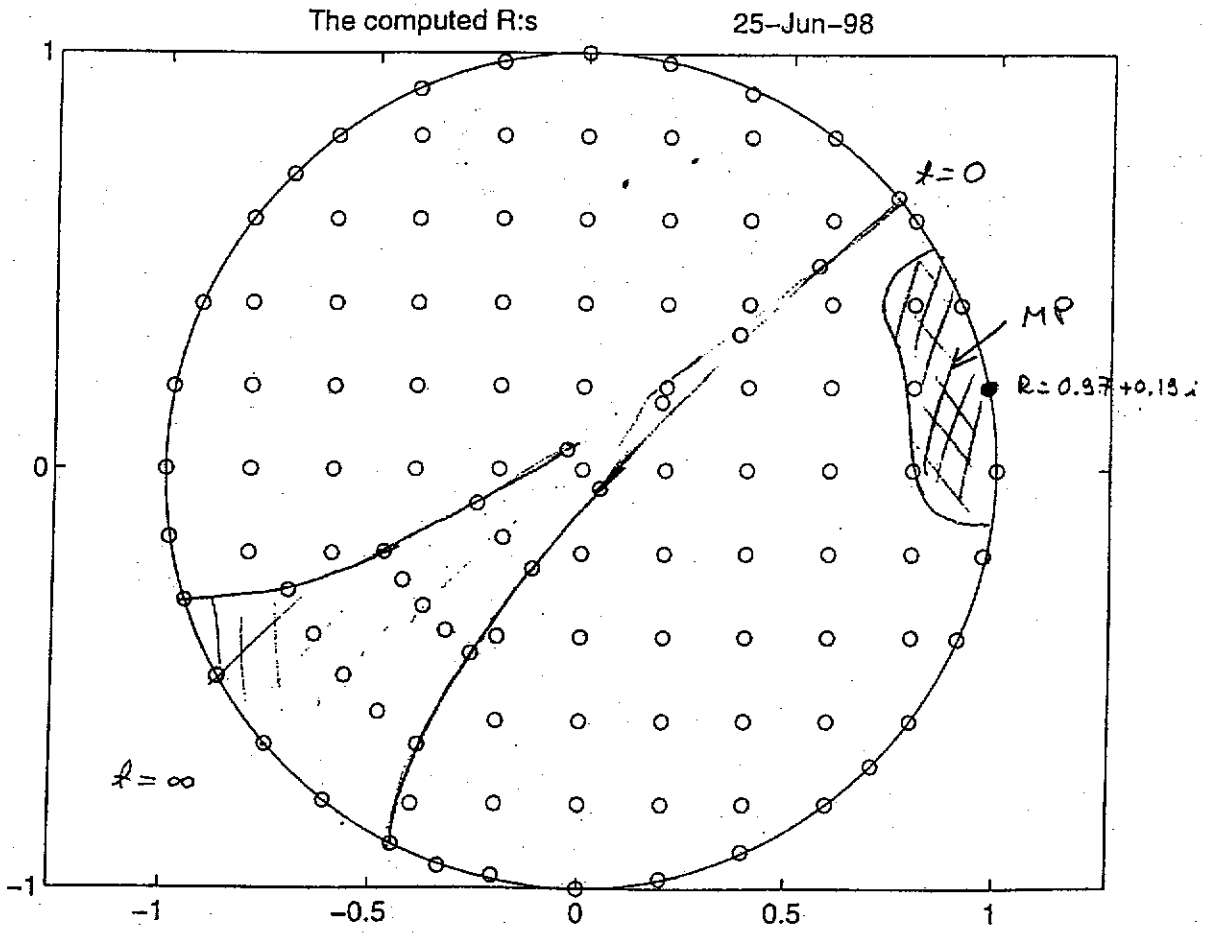
The computed R:s
25-Jun-98
1
0
-1
-1
-0.5
0
0.5
1
ℓ = 0
MP
R = 0.97 + 0.15 i
ℓ = ∞

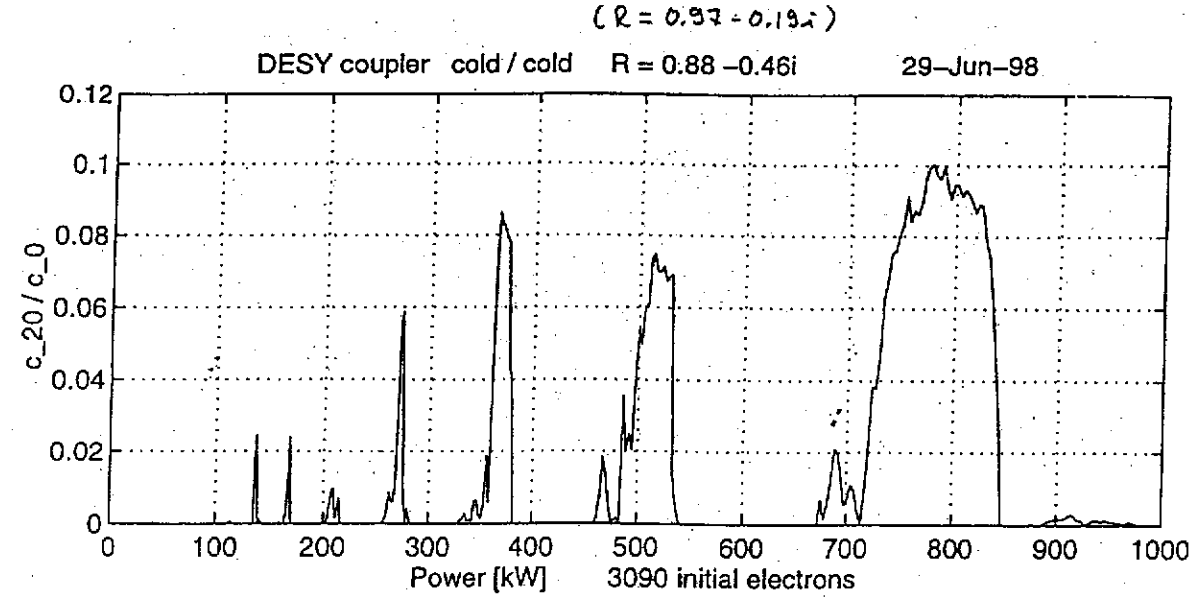
(R = 0.97 - 0.19i)
DESY coupler cold / cold R = 0.88 –0.46i 29–Jun–98
c_20 / c_0
Power [kW] 3090 initial electrons

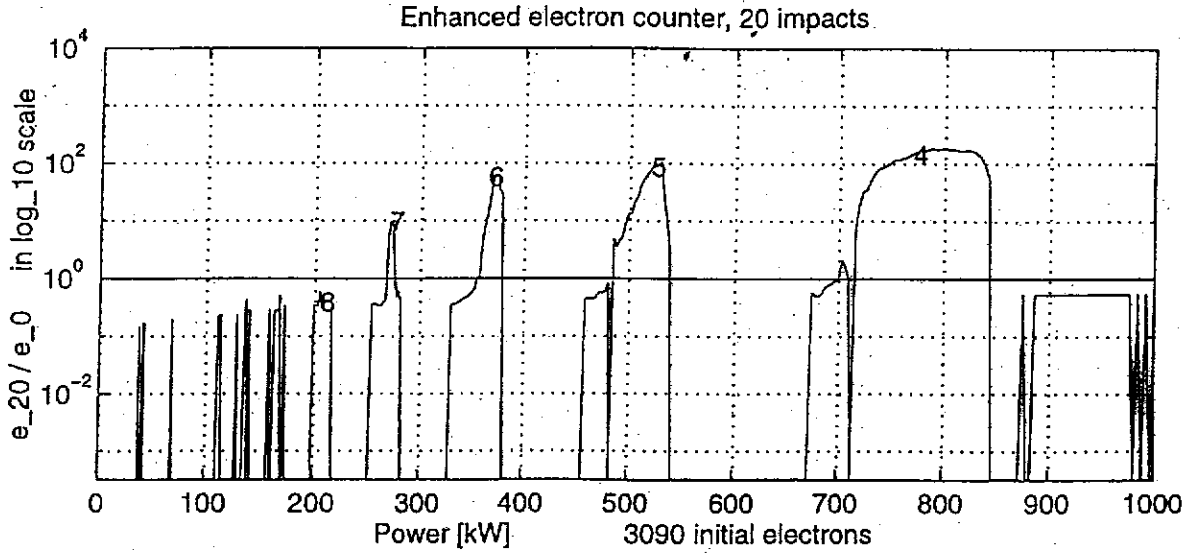
Enhanced electron counter, 20 impacts
e_20 / e_0 in log_10 scale
Power [kW] 3090 initial electrons

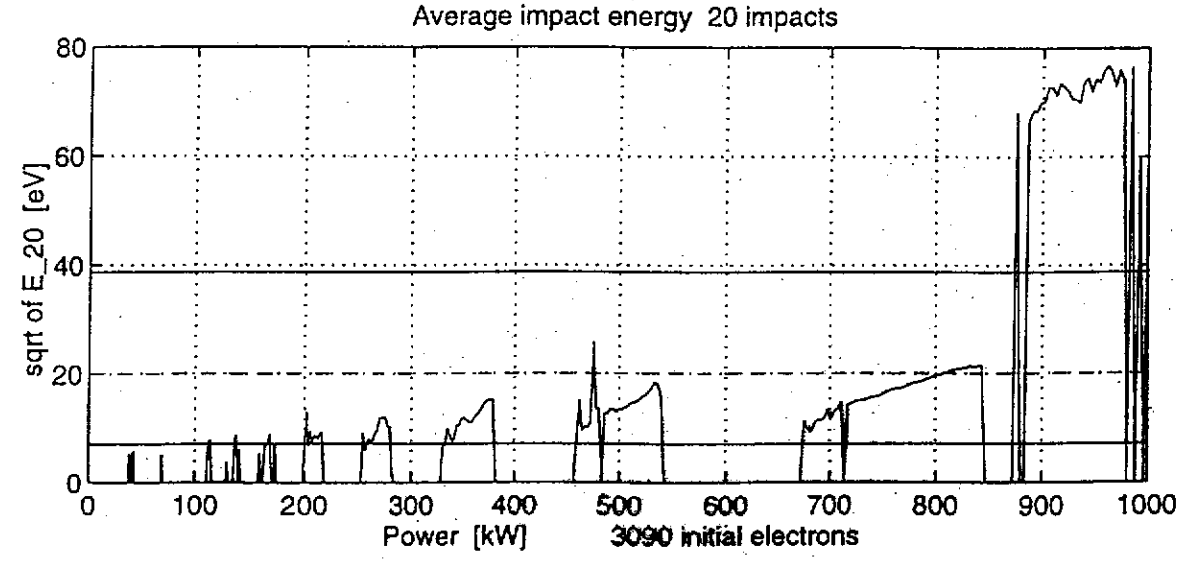
Average impact energy 20 impacts
sqrt of E_20 [eV]
Power [kW] 3090 initial electrons

Electron path at the minimum of the distance map with R = 0.9772+0.1988*i* and P = 271.1kW 25–Jun–9

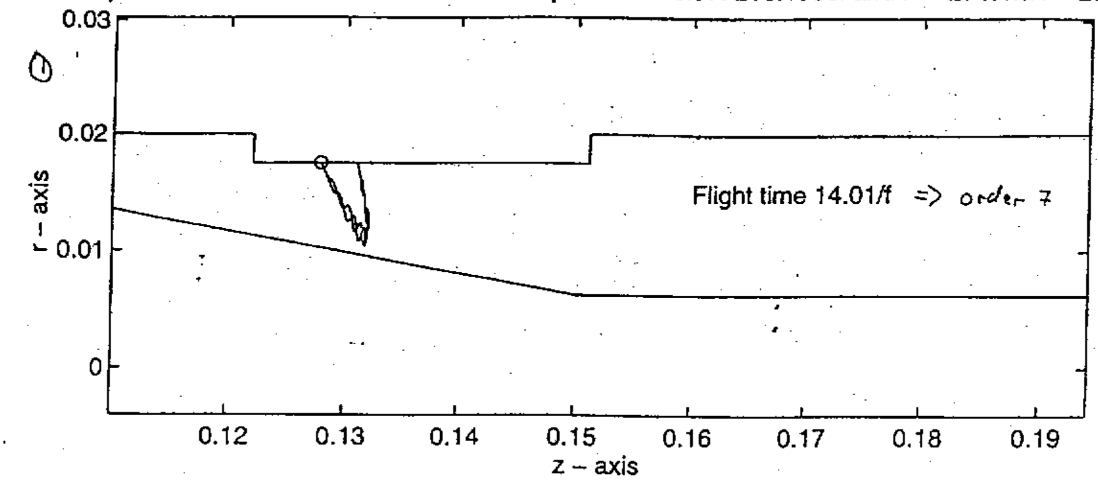

R = 0.9772+0.1988i and P = 374.4kW

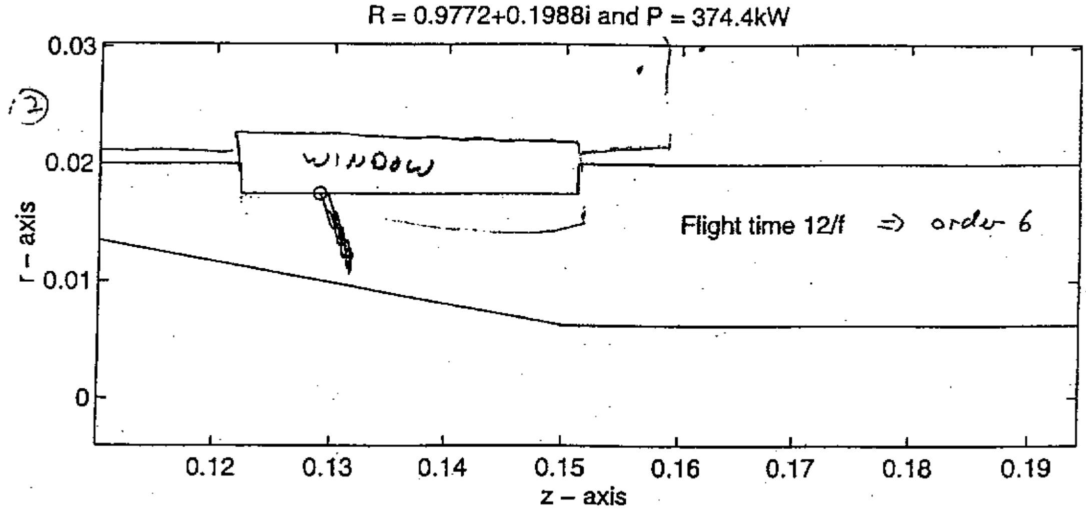

R = 0.9772+0.1988i and P = 530.4kW

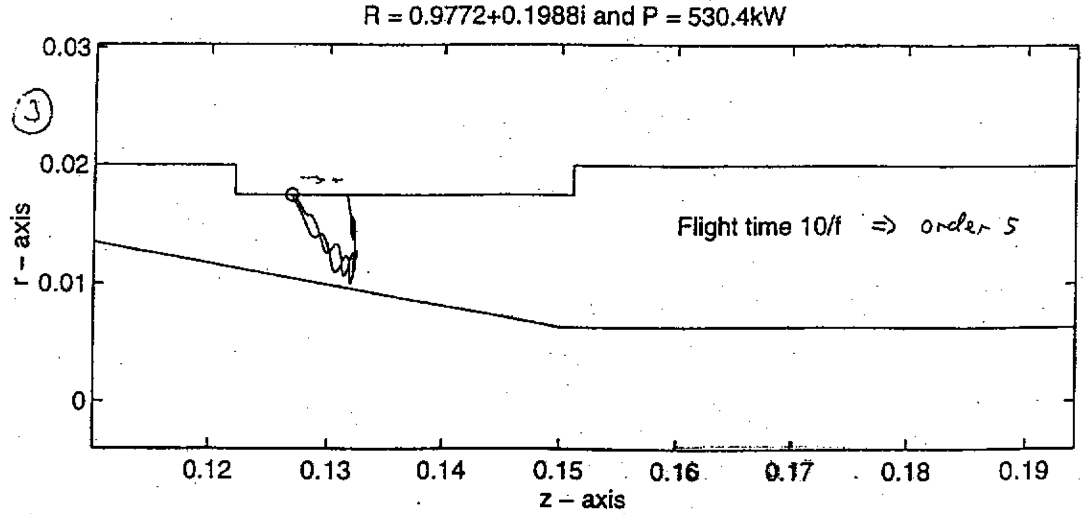

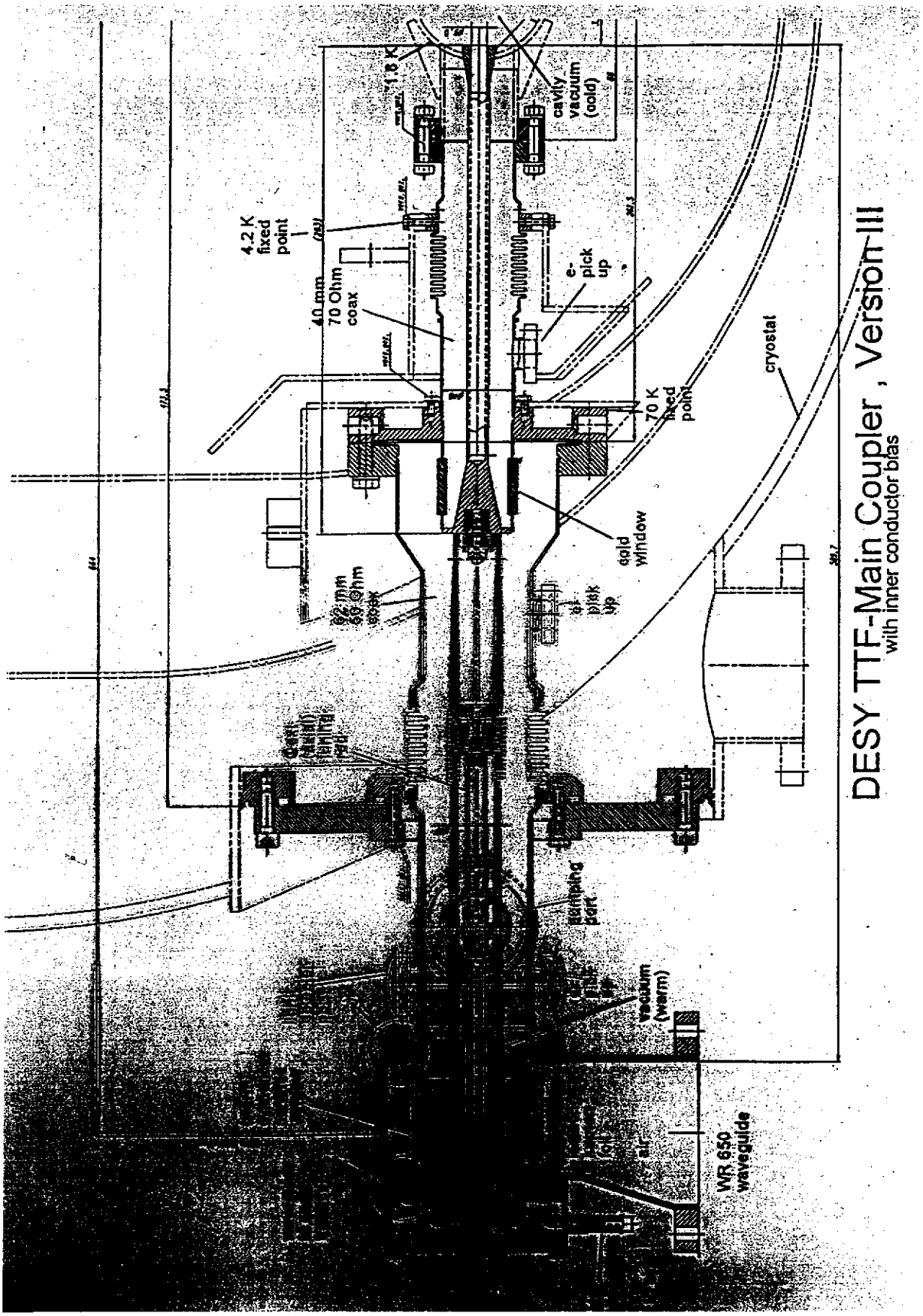
DESY TTF-Main Coupler , Version III
with inner conductor bias
4.2 K fixed point
40 mm 70 Ohm coax
e- pick up
cavity vacuum (cold)
cryostat
70 K fixed point
cold window
e- pick up
vacuum (warm)
WR 650 waveguide
air

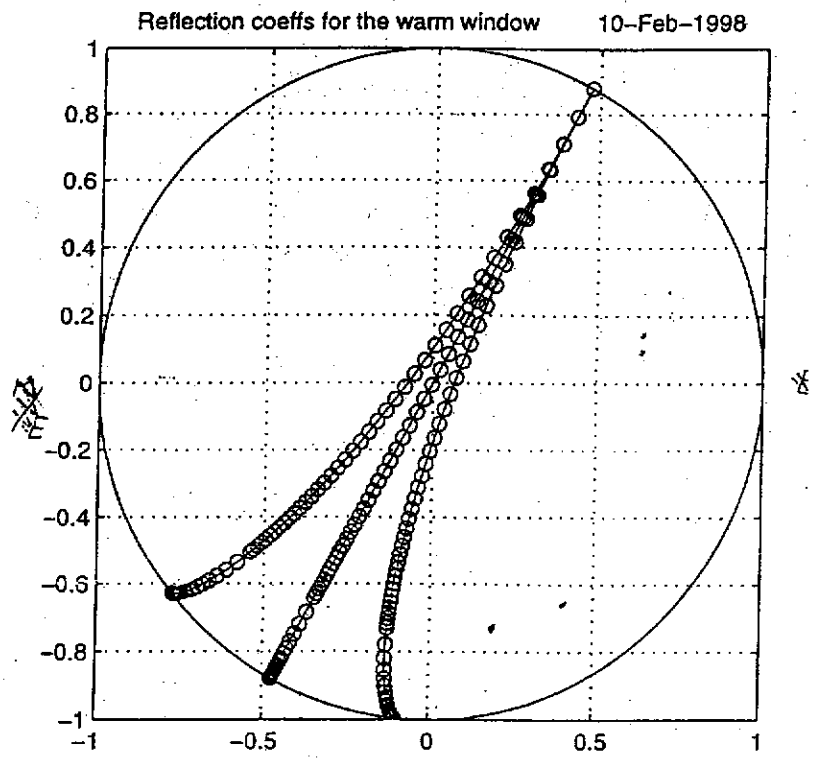

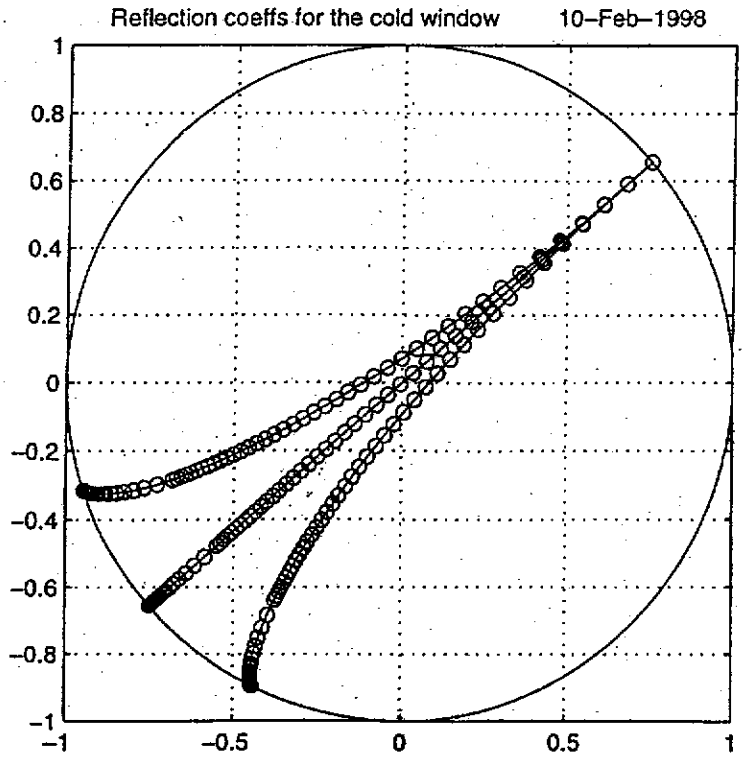

$C\left(e^{ik_z} + Re^{-ik_z}\right)$

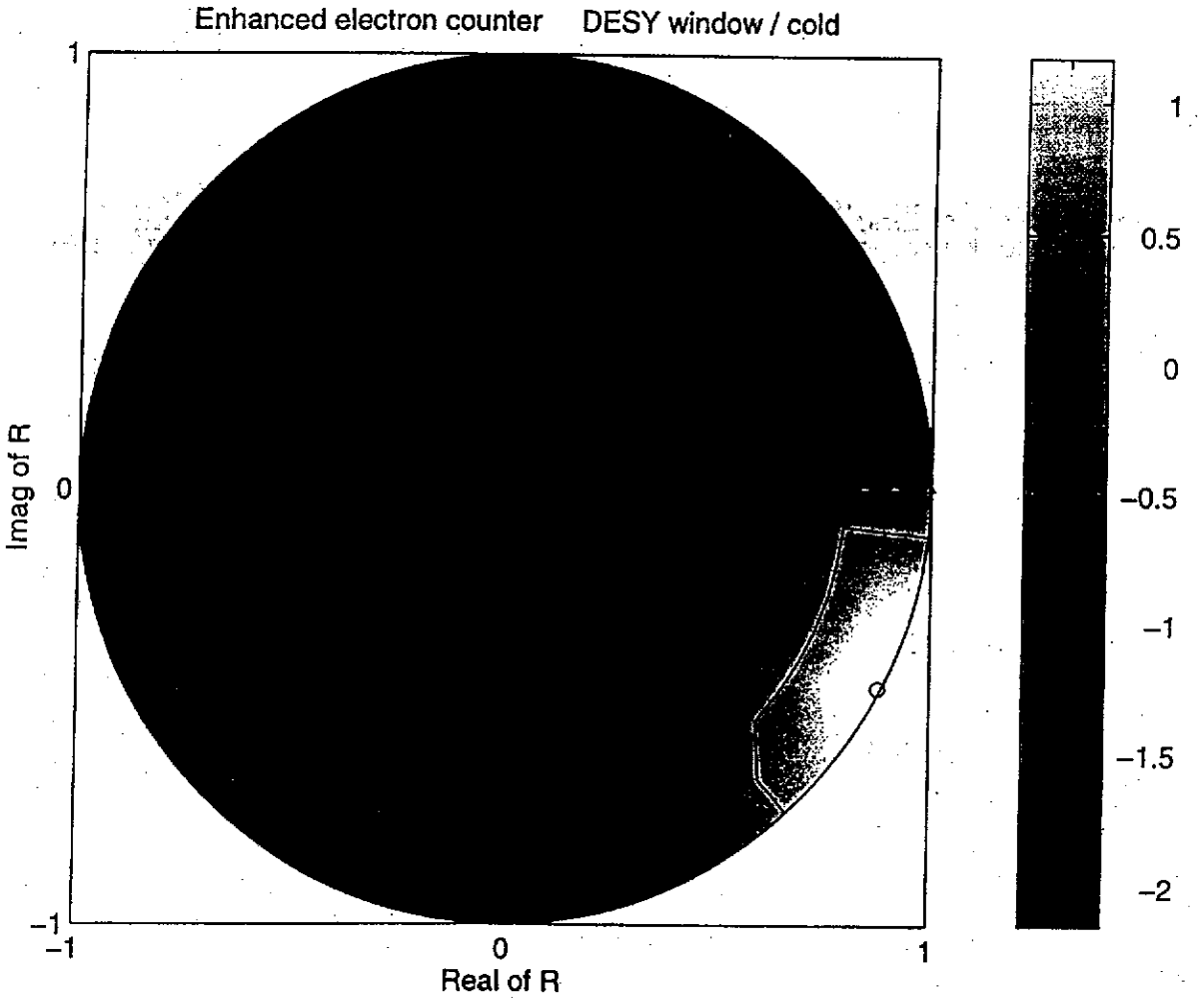
Enhanced electron counter DESY window / cold
Imag of R
Real of R
1
0
−1
−1
0
1
1
0.5
0
−0.5
−1
−1.5
−2

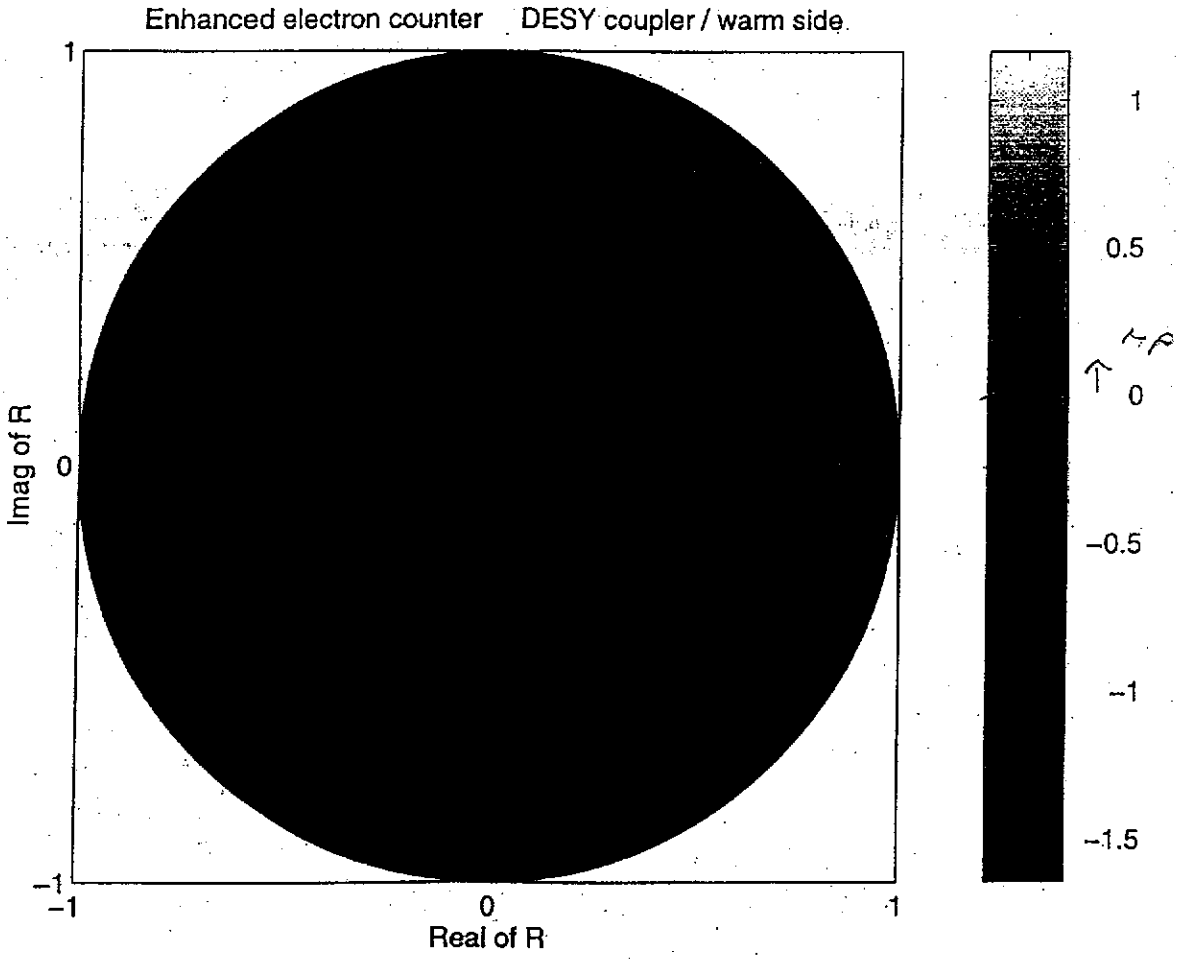
Enhanced electron counter DESY coupler / warm side
Imag of R
Real of R
1
0
−1
−1
0
1
1
0.5
0
−0.5
−1
−1.5

A. Woode & J. Petit
Radio-Frequency Systems Division, ESTEC, Noordwijk, The Netherlands

Investigations into Multipactor Breakdown in Satellite Microwave Payloads

Abstract In parallel with the Agency's ERS-1 satellite multipactor test programme, a study was initiated to examine more closely those factors relevant to multipactor design, component handling and diagnostics. The result has been a much improved understanding of those parameters that are important for achieving a multipactor free, high-power payload. The work has been undertaken using the experience and measurement capabilities at ESTEC and the materials expertise of the Applied Physics Department of the University Autonoma of Madrid.

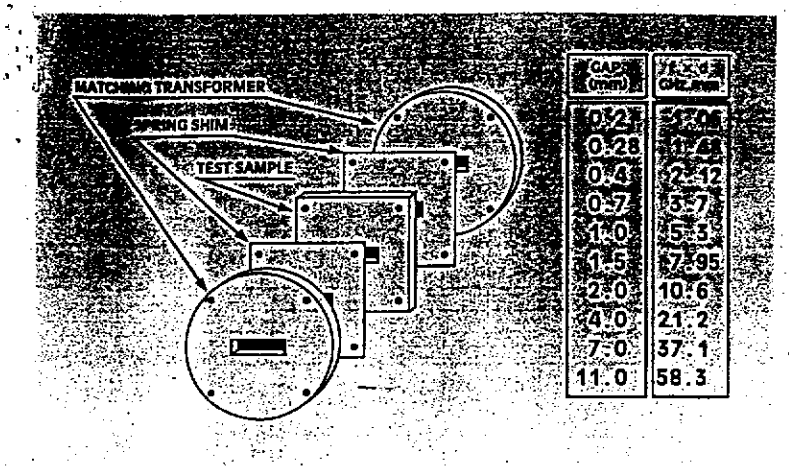

Figure 3. Standard waveguide WR187 multipactor test sample

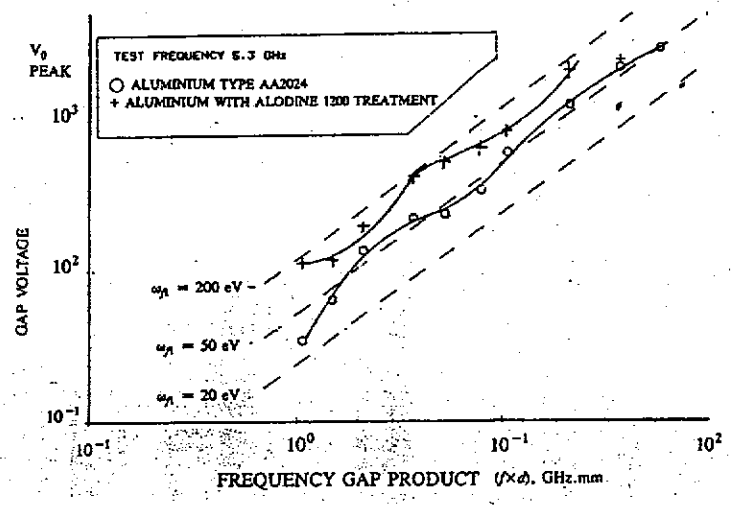

Figure 4. Plot of multipactor threshold as a function of frequency–gap product for waveguide test samples

(Appendix). Later theories were all based on this early work[4,8,11] and the theory of Sombrin[11] was thought to be the most accurate. Sombrin stated that the velocity of ondary electrons leaving the surface (v_s) was a constant, whereas Hatch and Williams made the assumption that the ratio of primary to secondary electron velocity $K=(v_f/v_s)$ was constant.

With the measured results we were able to make comparisons between the different theoretical predictions, and it was found that the theory of Hatch and Williams was a much better fit to measurement than that of Sombrin. It is accepted, however, that the simple theories are incorrect for the region of lowest arrival energy (W_{f1}) for the minimum gap, and the upper energy boundary.

Based on this finding, the theory of Hatch and Williams was used for setting up a simple computer model to match the ESTEC results and to generate sets of multipactor susceptibility design curves. The theory is presented in the Appendix. Matching of the parameters was carried out in an iterative manner, changes being made to the model to match the sets of measured data for the different materials. Results of the simulation for aluminium and aluminium alodine are shown in Figures 5 and 6. General design curves for all the tested materials are shown in Figure 7.

As a separate experiment, a comparison was also made between the value of W_{f1} measured by UAM in their Electron Spectroscopy Chemical Analysis (ESCA) facility and that extracted from the theoretical model matched to the measured data (Appendix, Equation 7). Although a difficult experiment, the measurements largely correlated (Table 1), thus demonstrating that the primary electron energy (W_{f1}) was the major significant factor in establishing the actual multipactor threshold.

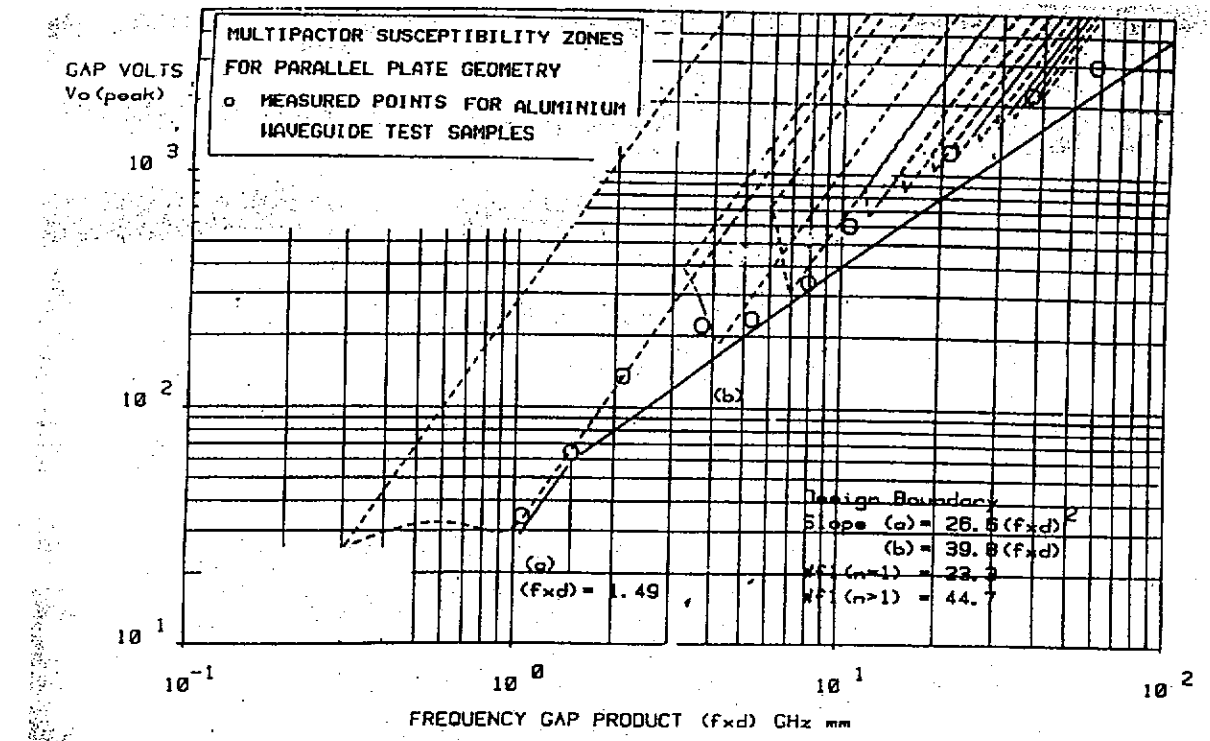
MULTIPACTOR SUSCEPTIBILITY ZONES
FOR PARALLEL PLATE GEOMETRY
o MEASURED POINTS FOR ALUMINIUM
WAVEGUIDE TEST SAMPLES
GAP VOLTS
Vo (peak)
10 3
10 2
10 1
10 -1
10 0
10 1
10 2
(a)
(fxd) = 1.49
(b)
Design Boundary
Slope (a) = 26.6 (fxd)2
(b) = 39.8 (fxd)
Wf1 (n=1) = 23.2
Wf1 (n>1) = 44.7
FREQUENCY GAP PRODUCT (fxd) GHz mm

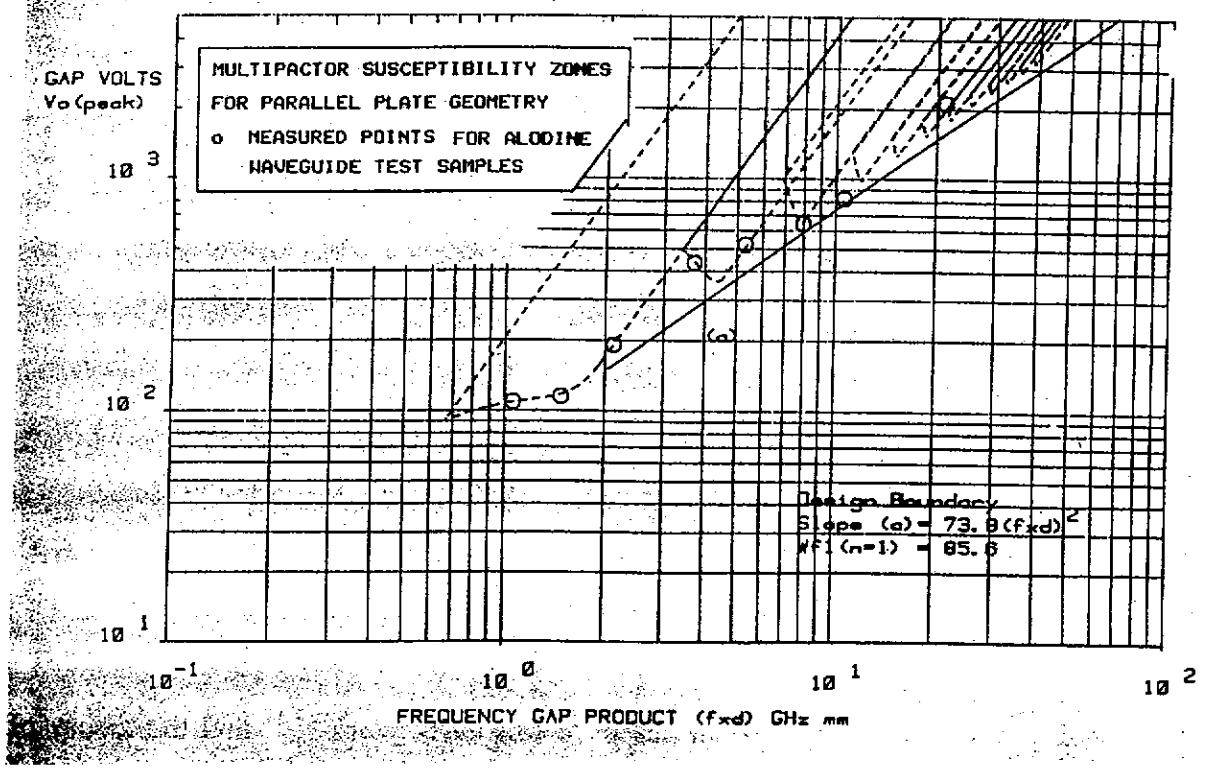
MULTIPACTOR SUSCEPTIBILITY ZONES
FOR PARALLEL PLATE GEOMETRY
o MEASURED POINTS FOR ALODINE
WAVEGUIDE TEST SAMPLES
GAP VOLTS
Vo (peak)
10 3
10 2
10 1
10 -1
10 0
10 1
10 2
(a)
Design Boundary
Slope (a) = 73.8 (fxd)2
Wf1 (n=1) = 85.6
FREQUENCY GAP PRODUCT (fxd) GHz mm

Conclusions

- Multipacting is completely described for coax lines
  - -dominant electric driven one point from the outer conductor
  - -multipacting charts are available for SW, TW and mixed conditions
  - -tapers and steps enhance multipacting
  - -tapered window shows broad band multipacting
  - -cylindrical window is nearly free of multipacting
- Multipacting in rectangular wave-guides
  - -dominant electric driven two point
  - -multipacting chart available (traveling wave)
- 2D MP code is operational and will be made available
- 2.5D code (e.g. window in transition from coax to rectangular wave-guide) is operational
- 3D code (e.g. needed for round windows in rectangular wave-guide) is under development

TiN coating studies

Stéphane Chel

CEA Saclay

from "RF Superconductivity for accelerators" - H. Padamsee

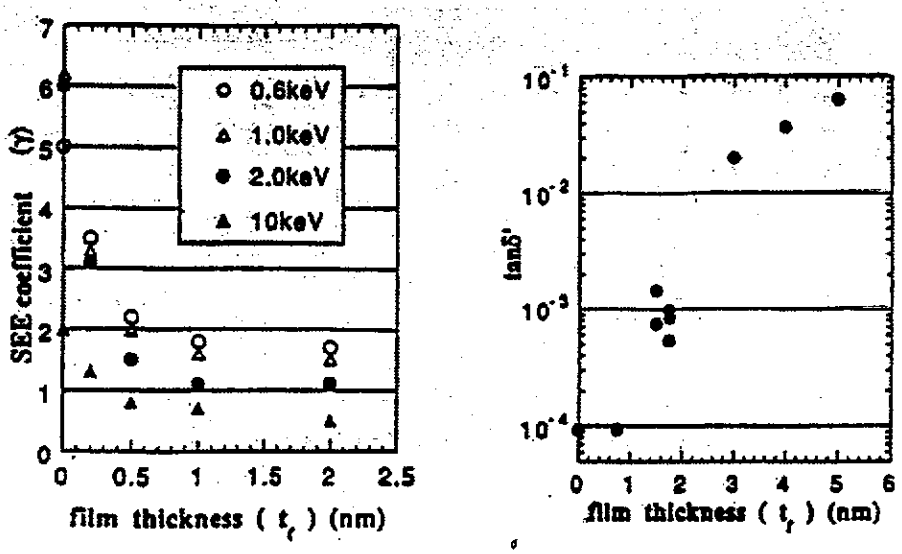

(a) (b)

Figure 18.12: (a) Secondary emission coefficient and (b) loss tangent of TiN layer on an alumina substrate, as a function of coating thickness.

desorption from the ceramic and metal surfaces can degrade the vacuum, leading to a glow discharge, which in turn can cause metal deposition on the ceramic by rf sputtering. This can lead to inhomogenous heating, thermal stress, and cracking of the ceramic.

18.4.1 Antimultipactor Measures

It is essential to reduce the secondary emission coefficient of the ceramic by applying a thin coating of special materials. The most used coating is TiN. Others are TiNO, SiN, Cr_2O_3, copper black, and gold black. If they are slightly conductive, these anti-multipacting coatings also help to provide charge drainage, which reduces the risk of voltage breakdown. The thickness of the coating layer must be carefully controlled because the rf loss of the coating increases the surface losses of windows. Figure 18.12 shows the drop in the secondary yield and the increase of loss tangent with coating thickness. Evidently 1 nm is the optimum thickness for TiN [317].

At CERN the conditioning of couplers has been greatly improved by applying a bias voltage of 2.5 kV between the center and outer conductors [168, 311]. The inner conductor is isolated from the outer conductor at the waveguide to coax transition. The multipactor trajectories are altered by the dc field. After operation for some time, the multipactor levels may reappear, presumably due to gas recondensation, and re-conditioning may be required [318].

TAB. 1 – *Données bibliographiques*

Labo/manip	Type	f (MHz)	(ϕi)-ϕc-(L) (cm)	h (cm)	$\hat{P}$ (MW)	P (kW)	Méthode	δ (nm)	Réf.
CERN (LEP2)	Cylindrique	352	10.3-(12.03)	0.56	0.2	200			[16]
SLAC (PEP II)	Disque	476	25.4	1.9	0.5	500	Sput.		[10, 11, 12]
KEK (TRIST. cavity)	Cylindrique	508	15.2-(19.3)	0.5	0.225	225	DC react. sput.	6	[9]
KEK (TRIST. klystron)	Disque	508			1.2	1200	DC react. sput.	10	[4]
KEK (B-fact)	Coax-Disque	508	(3.8)-16.6	1	0.8	800		10	[17]
KEK (JHP klystron)	Disque	1296	19	0.56	4	113		6-10	[6, 7]
FERMI (TESLA)	Coax-conique	1300	(2.68)-6.16	0.32	0.208	2.8	Evap.	10	[20]
DESY (TESLA)	Cylindrique	1300	4-(3.05)	0.8	0.208	2.8		10	[3, 21]
KEK (linac med.)	Disque	2856	8.8	0.44	5.53	54		8	[8]
KEK (TW)	Disque	2856	8.42	0.759	400	40		1.5	[13]
KEK (PF linac)	Disque	2856	9.2	0.35	30	10	DC react. sput.	0.5-1.5	[22]
SLAC (klystron)	Disque	2856			67	60.3		2.5	[1]
KEK (LC-pill-box)	Disque	11424	2.8	0.15	50	0.1	RF sput.	6	[15]
KEK (LC-TE11)	Disque	11424	5.1	0.412	84	1.5	RF sput.	0.8	[15]
SLAC (LC)	Disque	11400	2.7	0.37	60	3	DC react. sput.	1.8-2	[14]

Ti:N coating (made by SICN)
by: DC sputtering with N_2 gas.

$P = 3\,kW$

N_2 Pressure : $4 \cdot 10^{-3}$ mbar

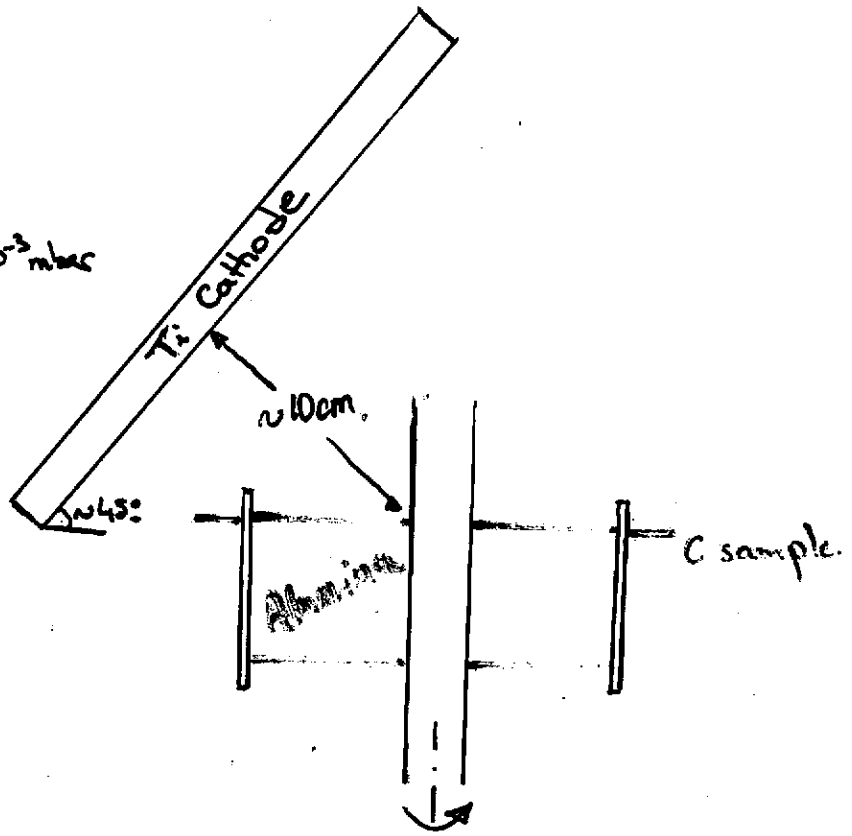

But : Measurement of the ~~thickness~~ resistance (between IC & OC)

⇒ In situ but not continuous

10 nm ⇒ Resistance ?

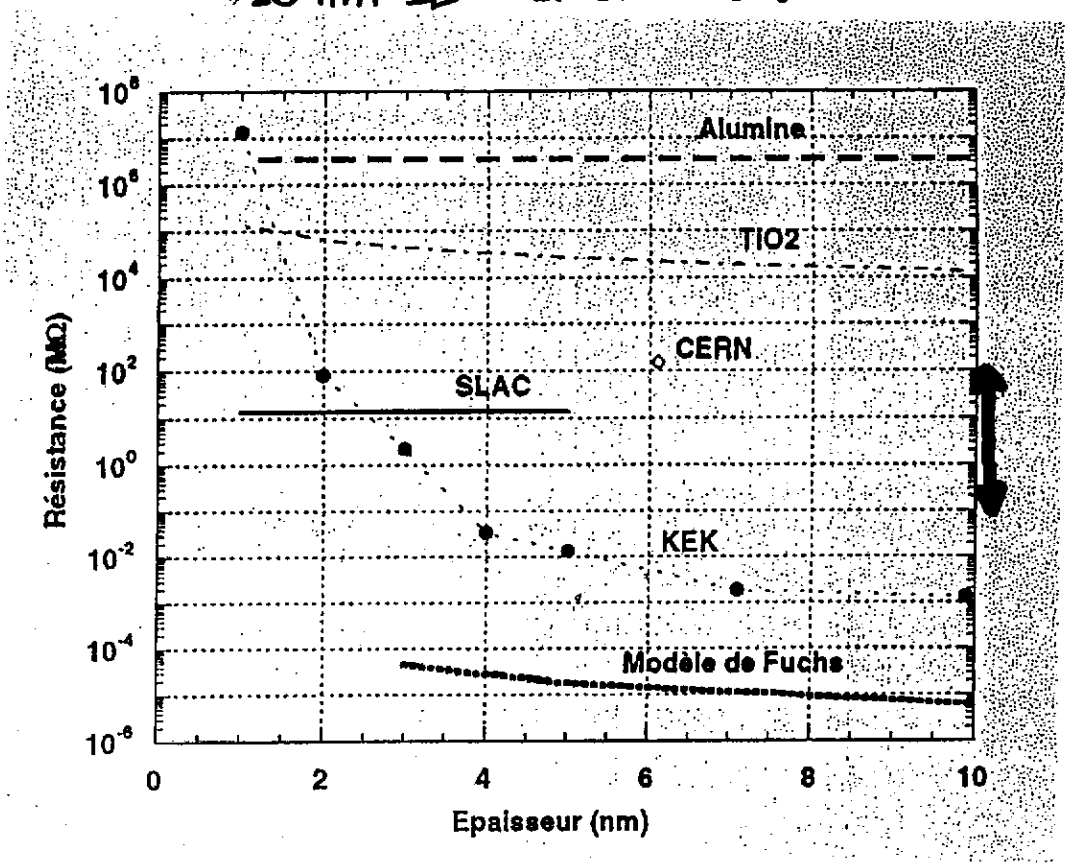

RBS analysis on samples and ceramics (for various resistances: 0,1 to 100 Ω/□).

→ Resistance is not the good parameter.

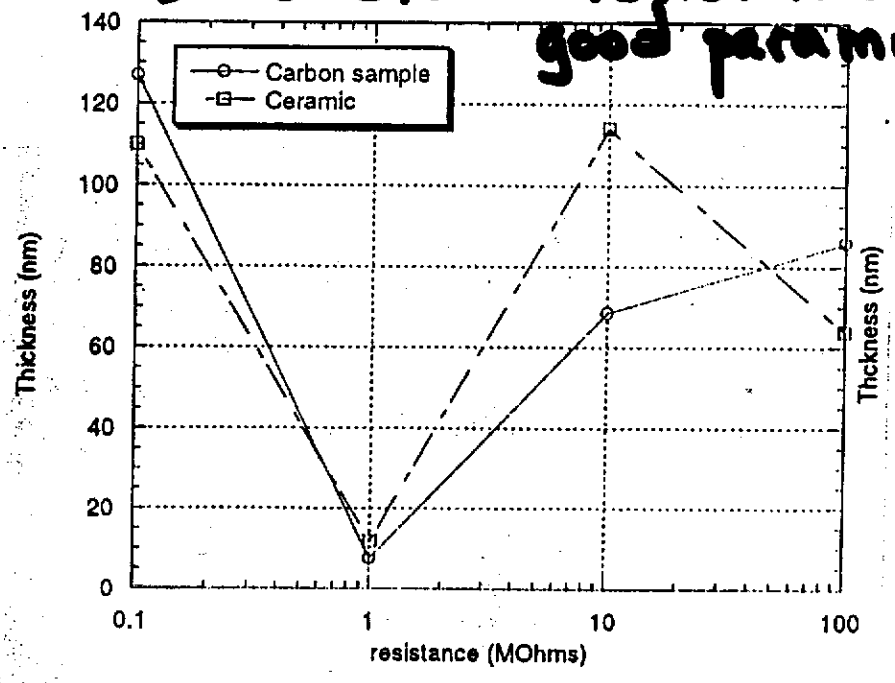

- Contact DC :

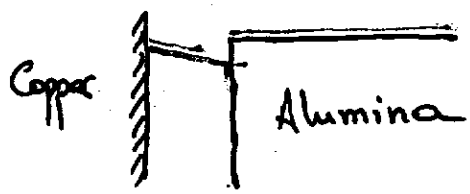

→ higher resistance

- Roughness : ~ 15µm peak to peak

- Porosity : ⇒ desorbtion of O_2
⇒ $\rho_{coating}$ ↗

- Non continuous measurement :

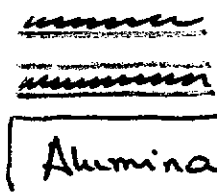

→ O_2 layer (during measurement DC power off).

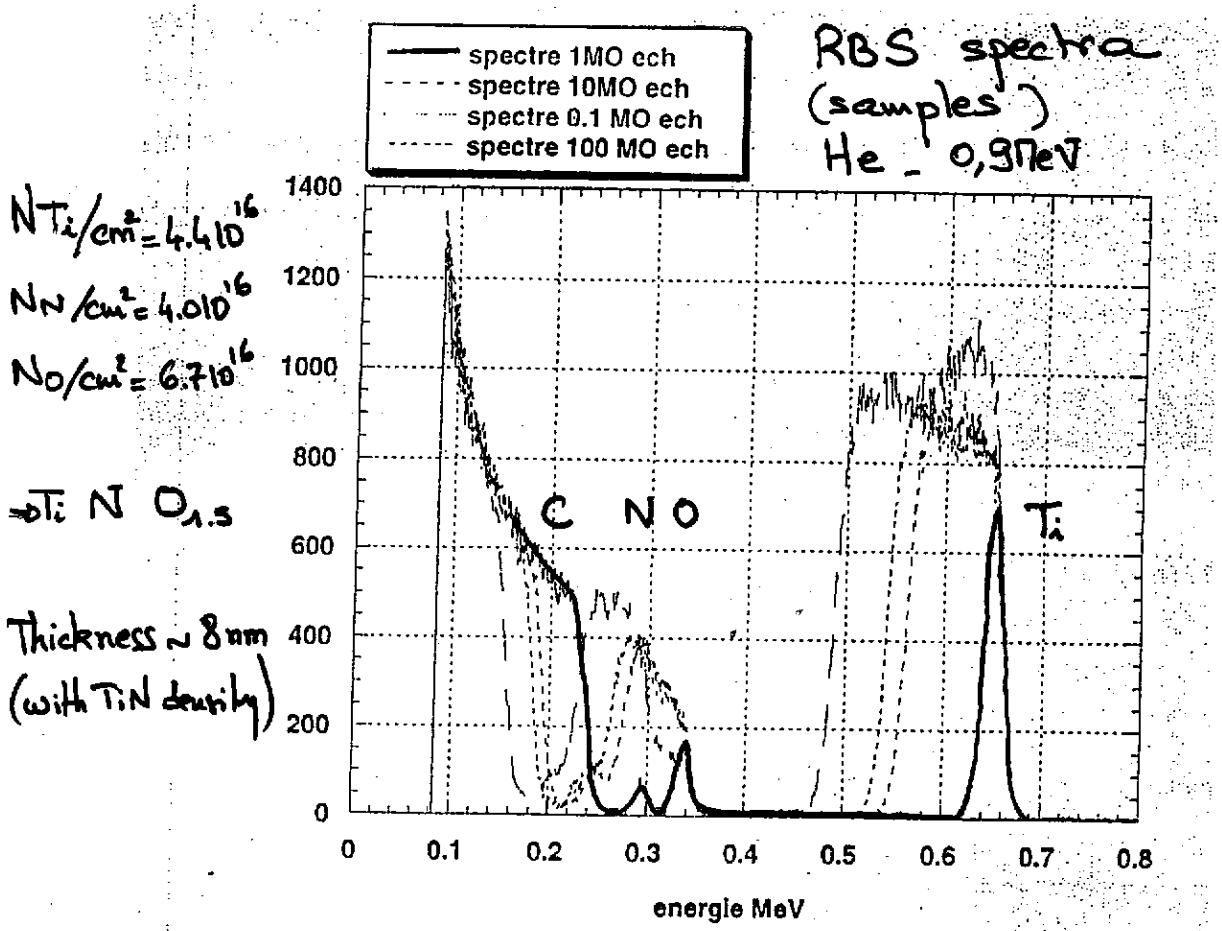
spectre 1MO ech
spectre 10MO ech
spectre 0.1 MO ech
spectre 100 MO ech
RBS spectra (samples) He _ 0,97eV
NTi/cm² = 4.4 10¹⁶
NN/cm² = 4.0 10¹⁶
NO/cm² = 6.7 10¹⁶
⇒ Ti N O1.5
Thickness ~ 8 nm (with TiN density)
C N O
Ti
1400
1200
1000
800
600
400
200
0
0 0.1 0.2 0.3 0.4 0.5 0.6 0.7 0.8
energie MeV

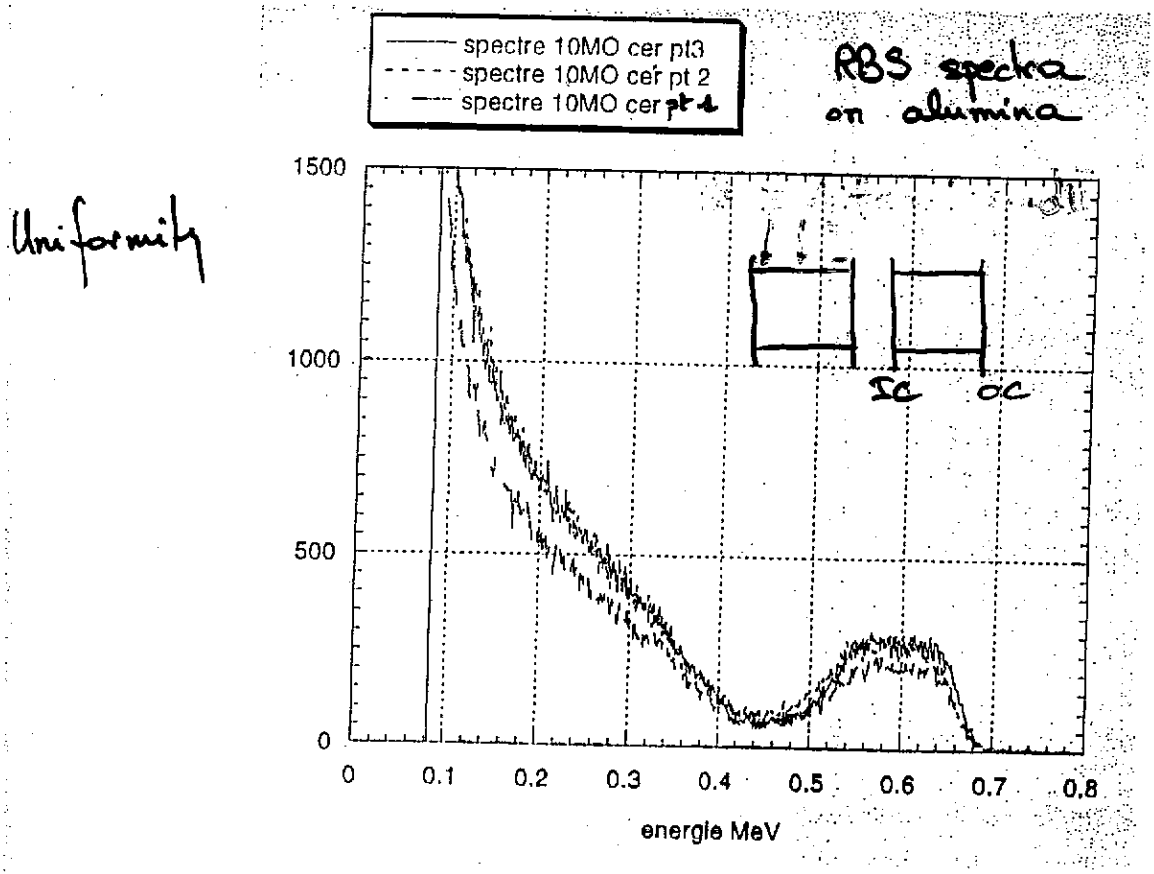
spectre 10MO cer pt3
spectre 10MO cer pt 2
spectre 10MO cer pt 1
RBS spectra on alumina
Uniformity
IC
OC
1500
1000
500
0
0 0.1 0.2 0.3 0.4 0.5 0.6 0.7 0.8
energie MeV

Thickness vs time :
dispersion due to changes in stochiometry
($Ti N O_{1.5}$; $Ti N_{0.3} O_2$; ...)

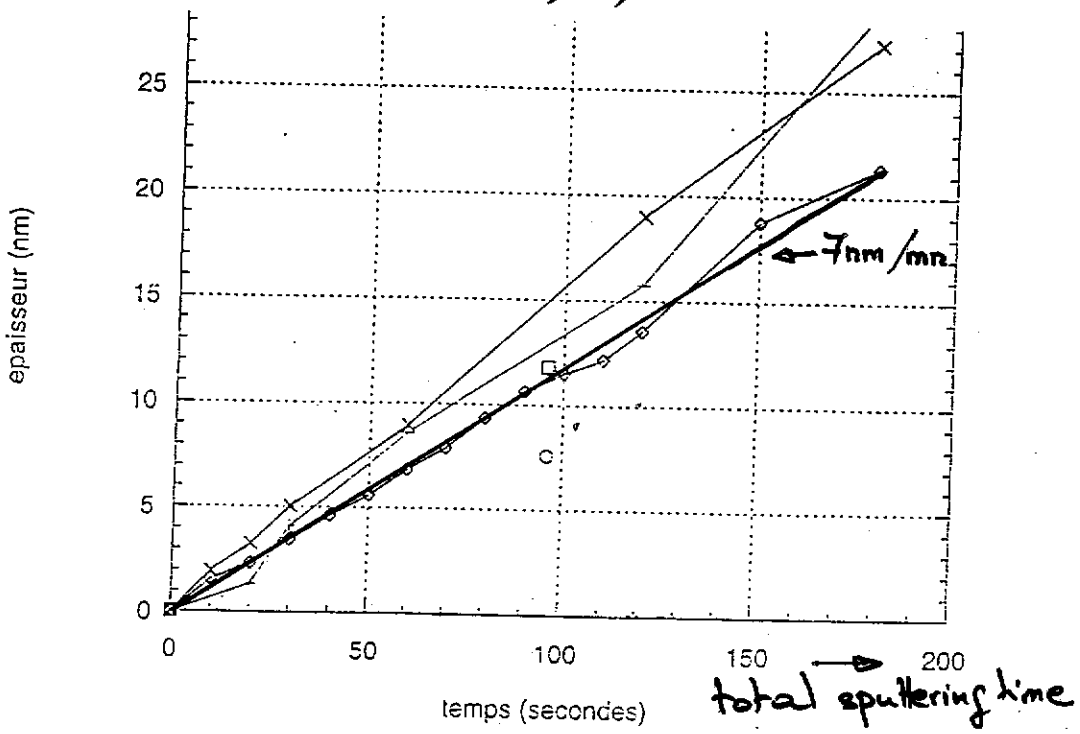

→ Use of a quartz detector to control thickness
→ in situ measurement

sensitivity :
$56 Hz/(\mu g/cm^2)$

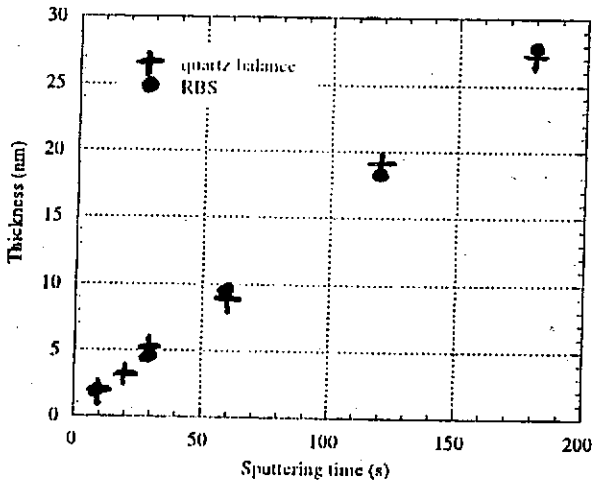

Last results : Stochiometry OK : Ti N (2% of Oxy).
Thickness 40 nm

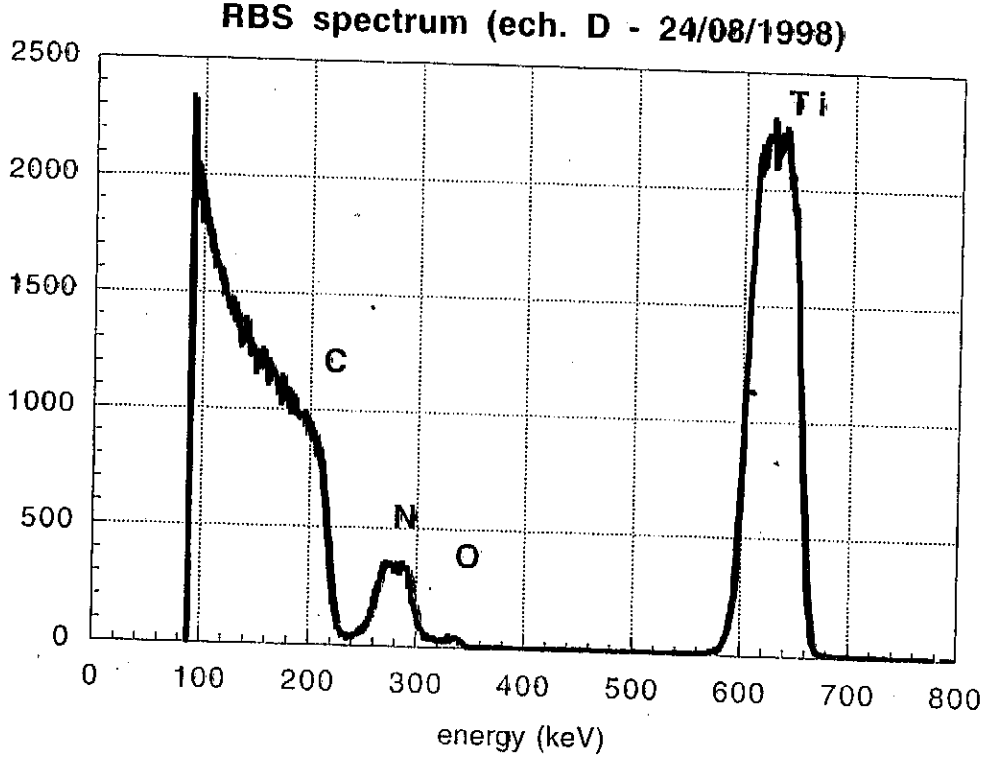

No change (stochio., thick.) after thermal treatment @ 800°C
⇒ possible to make the coating before the brazing.

A	6.02E+23					
q	1.60E-19					
Sig Ti	3.49E-24 MA		47.88			
sig N	3.10E-25		14			
Sig O	4.19E-25		16			
Omega	2.44E-03					
	Surface	A/cm²	g/cm²	TiN [nm]	O/Ti	N/Ti
Ech D-98082402						
Charge	10.02 He		6.26E+13			
Ti	114366	2.14E+17	1.71E-05		0.02	1.02
N	10395	2.19E+17	5.10E-06			
O	318	4.97E+15	1.32E-07			
Total		4.39E+17	2.23E-05	41		
EchD-98082401						
Charge	10 He		6.25E+13			
Ti	122438	2.30E+17	1.83E-05		0.02	1.14
N	12412	2.63E+17	6.11E-06			
O	251	3.93E+15	1.04E-07			
Total			2.45E-05	45		
Ech C-98082413						
Charge	10 He		6.25E+13			
Ti	76970	1.45E+17	1.15E-05		0.07	1.01
N	6920	1.46E+17	3.40E-06			
O	619	9.69E+15	2.57E-07			
Total			1.52E-05	28		
Ech C-980824014						
Charge	10 He		6.25E+13			
Ti	76356	1.43E+17	1.14E-05		0.07	0.93
N	6319	1.34E+17	3.11E-06			
O	653	1.02E+16	2.72E-07			
Total			1.48E-05	27		
Ech B-98082428						
Charge	10 He		6.25E+13			
Ti	123762	2.33E+17	1.85E-05		0.03	1.10
N	12143	2.57E+17	5.97E-06			
O	393	6.15E+15	1.63E-07			
Total			2.46E-05	45		
Ech B-98082427						
Charge	10 He		6.25E+13			
Ti	124361	2.34E+17	1.86E-05		0.00	1.05
N	11555	2.44E+17	5.68E-06			
O	67	1.05E+15	2.79E-08			
Total			2.43E-05	45		
Ech A-98082426						
Charge	10 He		6.25E+13			
Ti	92836	1.74E+17	1.39E-05		0.02	1.06
N	8709	1.84E+17	4.28E-06			
O	258	4.04E+15	1.07E-07			
Total			1.83E-05	34		

5x 10 sec.
P = 6 kW

10x 10 sec
P = 3kW

1x 50 sec.
P = 6kW

1x 100 sec.
P = 3kW

→ Ti N + % O

30-4 nm

→ Fix the parameters for having 10nm of TiN

It could be interesting to obtain thiner coating (≈2nm ?)

→ Verify with a good coating that SEES 1

→ Measurement of the ρ of the layer

→ Use of an other method to measure the thickness

→ Try an other deposition method like Sapor deposition.